THE
LONDON, EDINBURGH, AND DUBLIN
PHILOSOPHICAL MAGAZINE
AND
JOURNAL OF SCIENCE.

[SEVENTH SERIES.]

JULY 1927.

I. *The Storch Equation, a General Dilution Formula, and the Validity of the Law of Mass Action at Limiting Dilutions.* By ALLAN FERGUSON, *M.A., D.Sc.*, and ISRAEL VOGEL, *M.Sc., D.I.C.**

IN the present investigation the authors propose to discuss the application to electrolytes of various types of the Storch equation, either with constant exponent (Storch, *Z. phys. Chem.* 1896, xix. p. 13 ; Bancroft, *ibid.* 1899, xxxi. p. 188), or in a more general form with the exponent (n) considered as a linear function of the concentration.

The Storch equation,

$$\frac{(C\alpha)^n}{C(1-\alpha)} = K, \quad . \quad . \quad . \quad . \quad . \quad . \quad (1)$$

may be written

$$n \log (C\alpha) = \log K + \log C(1-\alpha), \quad . \quad . \quad . \quad (2)$$

and a plot of $\log(C\alpha)$ against $\log C(1-\alpha)$ yields a rectilinear graph only if n be independent of the concentration †. The slope and intercept of the graph determine n and K, and where the law is followed we have found it possible to determine n correct to four significant figures by using large sheets of precision graph paper.

Equation (1) has, apart from its use by Noyes and his colleagues (see papers in J. Amer. Chem. Soc. 1908–13, *cf.* especially J. Amer. Chem. Soc. 1908, xxx. p. 335) and by Bates (*ibid.* 1913, xxxv. p. 519), hardly received the

* Communicated by the Authors.

† α is a symbol for Λ/Λ_0.

attention which it merits. Our own investigations show that for certain electrolytes the simple Storch equation holds almost to normal concentrations. For others, the simple equation is valid up to concentrations of the order of one hundredth normal, at which point a departure from the linear equation is manifested. This departure often becomes apparent for concentrations at which the so-called viscosity correction is assumed to become sensible. For a third type, the linear equation is departed from at a comparatively early stage. For samples of these types we have been able to show that the assumption that n $(=a+bC)$ is a linear function of the concentration brings them satisfactorily into line *, and we are able to exhibit a general method for the calculation of the constants a, b, and K.

We have deemed it well to make the Storch form the starting-point of our investigation, since it seems to us that this form, especially when exhibited by means of a rectilinear plot, serves admirably to test the validity of Ostwald's dilution formula at limiting dilutions. It has been asserted (Washburn, J. Amer. Chem. Soc. 1918, xl. p. 122) that the theoretical basis of Ostwald's formula is such that any dilution formula which does not yield it as a limiting case is to be rejected on that account, and further, that measurements made at the lowest concentrations show results which can be interpreted only in terms of Ostwald's formula. Concerning these dicta, we would merely say that the first encourages a dangerous tendency to force facts to fit theories, and that it is always possible, even in a simple theoretical deduction, to overlook some factor which may profoundly modify our formulæ. With respect to the second (Weiland, J. Amer. Chem. Soc. 1918, xl. p. 131 ; Washburn, *ibid.* 1918, xl. p. 150)—and we refer here particularly to Weiland's very careful measurements on potassium chloride at 18° (*loc. cit.*),—we think that their interpretation is erroneous, as we shall later attempt to show.

When we assert that Ostwald's law is, or is not, true at zero concentration, when we define Λ_0 as the equivalent limiting conductance, what do we mean exactly? Surely no more than this : that if the law followed at finite concentrations be assumed to hold good in the limit, we are then led to limiting values of certain constants given by the expressions mentioned above. Emphatically, we do not assert that we should find these values were it possible, for example, to measure the equivalent conductance of a single

* Iodic acid is the one exception.

molecule in an infinite ocean of solvent. Indeed, the theoretical basis of Ostwald's law, statistical as it is in character, becomes as meaningless in the limit as the expression "temperature of a single molecule." The validity of Ostwald's law at limiting concentrations can, we take it, mean nothing more than that over a limited range of low but *finite* concentration the expression $\frac{(C\alpha)^2}{C(1-\alpha)}$ is a constant quantity.

Now this may be tested either directly by experiment at *low* concentrations or by extrapolating the results obtained at higher concentrations. Weiland's results for potassium chloride are usually quoted as showing directly that the law is followed over the range 0·00002 to 0·00007 normal. His results are exhibited in Table I.

TABLE I.

Potassium Chloride, 18°.

Concentration *.	K_E (Weiland).	K_E (Authors).
$1{\cdot}0\times10^{-5}$	0·02000	0·01921
$2{\cdot}0\times10^{-5}$	0·02002	0·02016
$3{\cdot}0\times10^{-5}$	0·02003	0·01994
$4{\cdot}0\times10^{-5}$	0·02006	0·02002
$5{\cdot}0\times10^{-5}$	0·02014	0·02014
$6{\cdot}0\times10^{-5}$	0·02022	0·02022
$7{\cdot}0\times10^{-5}$	0·02035	0·02033
$8{\cdot}0\times10^{-5}$	0·02050	0·02051
$9{\cdot}0\times10^{-5}$	0·02070	0·02065
$1{\cdot}0\times10^{-4}$	0·02102	0·02103

Now the fundamental criticism of his figures *as they stand* is that over *no* region of finite concentration is the quantity $\frac{(C\alpha)^2}{C(1-\alpha)} = K_E$ constant. This function over the whole range measured is varying continuously with C, although certainly more slowly as the concentration decreases. Unfortunately the variation, owing to errors in Weiland's calculations, is even more pronounced than is indicated in column 2, the values as recalculated by the authors from Weiland's figures

* C will be expressed in gram equivalents per litre throughout this paper.

being given in column 3. The pronounced variation of the quantity K_E over the whole range of concentration completely destroys the value of this, the only direct experimental evidence quoted in support of Ostwald's dilution law for aqueous salt solutions.

Kraus and Parker's experiments (J. Amer. Chem. Soc. 1922, xliv. p. 2429) with iodic acid and Parker's experiments (*ibid.* 1923, xlv. p. 2017) with hydrochloric acid are commonly quoted as affording evidence for the validity of the mass-action law at low concentrations. For iodic acid at 25° we find n equal to 2·000 over a fairly wide range (C=0·00005 to C=0·001 normal). Hydrochloric acid affords an interesting commentary on our views. Taking Parker's figures at 25° and recalculating them, we find the column headed K_{E_1}, in which it will be seen that the constancy is not quite so good as it appears in Parker's original table. In Table II. the value for Λ_0 is, of course, that assumed by Parker, viz. 425·69. If, however, we recalculate Parker's figures, assuming the value for Λ_0 of 425·68 which we have calculated by other methods, we arrive at the column headed K_{E_2}.

TABLE II.

Hydrochloric Acid, 25° C.

Concentration.	K_E (Parker).	K_{E_1}.	K_{E_2}.
$5{\cdot}0\times10^{-5}$	0·105	0·1063	0·1120
$1{\cdot}0\times10^{-4}$	0·105	0·1051	0·1090
$2{\cdot}0\times10^{-4}$	0·105	0·1049	0·1060
$5{\cdot}0\times10^{-4}$	0·1051	0·1049	0·1054
$1{\cdot}0\times10^{-3}$	0·1131	0·1132	0·1137
$2{\cdot}0\times10^{-3}$	0·1421	0·1422	0·1426
$3{\cdot}0\times10^{-3}$	0·1726	0·1727	0·1705

Now Washburn (J. Amer. Chem. Soc. 1918, xl. p. 124) has said :—" Of course it is true that if one starts with the *a priori* assumption that the Mass-action law will never be obeyed, and then proceeds to determine a Λ_0 value in harmony with this assumption, then naturally it might not be difficult with the aid of this to compute values for the Mass-action expression K_E which would not exhibit any pronounced tendency to conform to the Mass-action law. . . ." Quite true ; and *mutatis mutandis* the argument applies if one

assumes the truth of the mass-action law and calculates values of Λ_0 in accordance with that assumption.

Hydrochloric acid admirably illustrates the dangers attendant on any *a priori* assumptions concerning figures obtained at low concentrations. The quantity $(1-\alpha)$ is very nearly zero, and an error of 1 in 10,000 in Λ_0 may burden $(1-\alpha)$ with a systematic 10-per-cent. error, more or less. If, then, one makes *any* assumption whatever with regard to the mass law in calculating Λ_0, it is more than probable that one will see that assumption reflected in the form of the dilution equation deduced. Thus, if instead of tracing the variations of K_E—in itself a process of doubtful validity—we make a logarithmic plot of equation (2), using Parker's figures for the four points of low concentration, we find a good straight line which yields quite definitely the value $n=2{\cdot}00$. If, however, still using Parker's experimental figures, we adopt the number $425{\cdot}68$ for Λ_0, we find that the same four points determine in a perfectly unambiguous way a straight line for which n is $2{\cdot}02$. That is, a change of 1 in 40,000 in the value of Λ_0 produces a change in n of about one per cent.! Clearly quantitative arguments based on low concentration results *alone* are exceedingly dangerous ; and if the argument is weighted with any assumption *pro* or *con*, the result is more or less a foregone conclusion.

It seems to us that the correct procedure in testing the validity or invalidity of Ostwald's dilution formula is to assume a dilution formula which is a simple generalized form of Ostwald's equation, and to see if the constants of this formula determined over as wide a range of concentration as possible are such as to yield Ostwald's formula at limiting concentrations. The correctness of this procedure is further emphasized by making a determination of the constants at "middle" concentrations, plotting functions of α and C which yield a rectilinear graph. If it be then found that all the points for lower concentrations fall automatically on the straight line, we are *fully* justified in an extrapolation to zero concentration. We emphasize this point, since a rectilinear graph shows very markedly whether the law assumed is a *vera causa*, or merely a good approximation. Conversely, the deduction of constants from a curvilinear graph is at best a dangerous expedient, and one not to be adopted if a rectilinear graph can be drawn.

The Storch equation in the form (2) over low and medium —and sometimes indeed up to high—concentrations gives an admirable straight line. Departures from this straight line,

when they exist, are apparent in regions of *high* concentration. If a straight-line graph be established over a region of medium concentration, in every instance which we have examined—and they are some nineteen in number—we find the law automatically followed by the points of lower concentration down to the minimum concentration measured.

It would be difficult, it seems to us, to devise a more indifferent * test of the validity of Ostwald's law. We assume neither its validity nor its invalidity ; our only assumption is that the form of the dilution equation is $\frac{(C\alpha)^n}{C(1-\alpha)} = K$, where n may or may not be constant, and the very form itself is tested by the rectilinearity of the plot based on equation (2). If, then, we find that the plot is rectilinear down to the lowest concentrations measured and shows no signs of wavering, and the slope is such that n is equal to 2, so much the better for Ostwald's law. If not, —. Or, if the results are better fitted by $n=a+bC$, then, for the validity of Ostwald's equation, a must be equal to 2.

But what of the value of Λ_0 used in the calculation of α? Does Washburn's criticism (*ibid.* p. 124) apply here? We do not think so ; for again, in the equation

$$\Lambda_0=\Lambda+BC^{n_0}, \quad . \quad . \quad . \quad . \quad . \quad . \quad (3)$$

which we have used for the computation of Λ_0, we make no assumption whatever as to the validity or invalidity of Ostwald's equation. The rectilinear graphs obtained show that equation (3) is accurately followed over the region of concentration studied, and show—what is of primary importance—that there is no wavering from the law as the concentration falls. Moreover, *the values of* n_0 *and of* B *vary from substance to substance, and in a regular manner for related substances* (Ferguson and Vogel, Phil. Mag. 1925, 1. p. 971). It follows, therefore, that the usual assumption that n_0 is independent of the nature of the electrolyte must lead to values of Λ_0 of doubtful validity †.

Now, equation (3), which we assume to hold good only over low concentrations, is, as it should be to be logically used to furnish values of Λ_0 for use with the Storch equation, a limiting case of that formula.

* We use the word in its old sense.

† This remark is not without importance in view of the fact that the Debye-Hückel theory leads to a value of n equal to 0·5.

For, putting $\alpha = \Lambda/\Lambda_0$, equation (1) becomes

$$K\Lambda_0^{n-1}(\Lambda_0 - \Lambda) = C^{n-1}\Lambda^n,$$

$$\Lambda_0 = \Lambda + \frac{\Lambda^n}{K\Lambda_0^{n-1}} C^{n-1}.$$

For low values of C the second term on the right-hand side is small. Putting in this small term the approximate value Λ_0 for Λ, we obtain

$$\Lambda_0 = \Lambda + \frac{\Lambda_0}{K} C^{n-1},$$

taking the form (3) with n_0 *approximately* equal to $n-1$ and B *approximately* equal to Λ_0/K. The degree of agreement is shown in Table III. below, in which are exhibited

TABLE III.

Electrolyte.	n_0.	$1+n_0$.	n.
NaCl	0·4431	1·4431	1·4763
KCl	0·4520	1·4520	1·4867
LiCl	0·4364	1·4364	1·4612
$NaNO_3$	0·4458	1·4458	1·4484
KNO_3	0·4796	1·4796	1·4916
$LiNO_3$	0·4253	1·4253	1·4465
$NaIO_3$	0·4551	1·4551	1·4877
KIO_3	0·4604	1·4604	1·4566
$LiIO_3$	0·4422	1·4422	1·4715
$Ca(NO_3)_2$ ...	0·4196	1·4196	1·4312
$Sr(NO_3)_2$ ...	0·4582	1·4582	1·4916
$Ba(NO_3)_2$ ...	0·5120	1·5120	1·5436
$CuSO_4$	0·5711	1·5711	1·6429
$CdSO_4$	0·5511	1·5511	1·6487
HIO_3	0·9687	1·9687	2·0000
HCl	0·9672	1·9672	2·0158

the values of n_0 (deduced from equation (3)) and of n_0+1 and of n.

The acceptance of equation (3) as an accurate representation of the facts down to the lowest observed concentrations has important consequences. For if Ostwald's law be valid over any of the regions studied, or be approached as a more or less limiting case, we shall have n_0 constant at a value

Fig. 1.

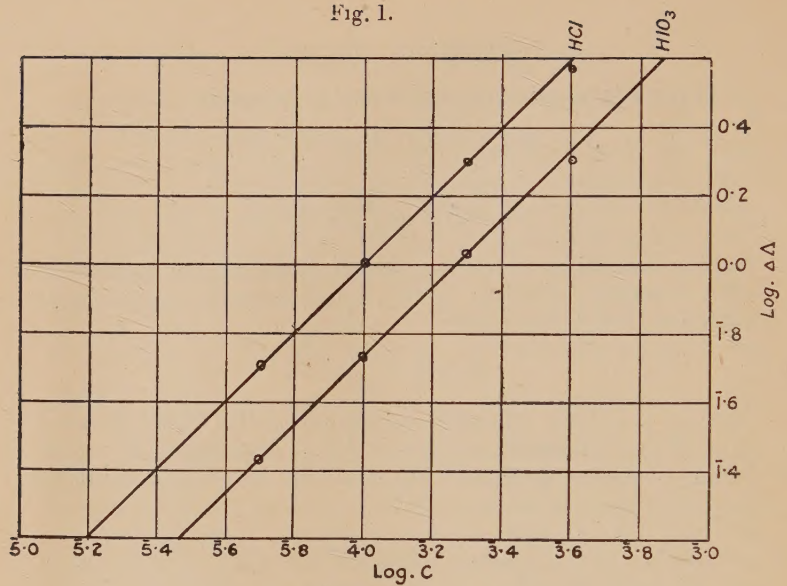
HCl
HIO3
0·4
0·2
0·0
1̄·8
1̄·6
1̄·4
Log. Δ
5̄·0
5̄·2
5̄·4
5̄·6
5̄·8
4̄·0
3̄·2
3̄·4
3̄·6
3̄·8
3̄·0
Log. C

Fig. 2.

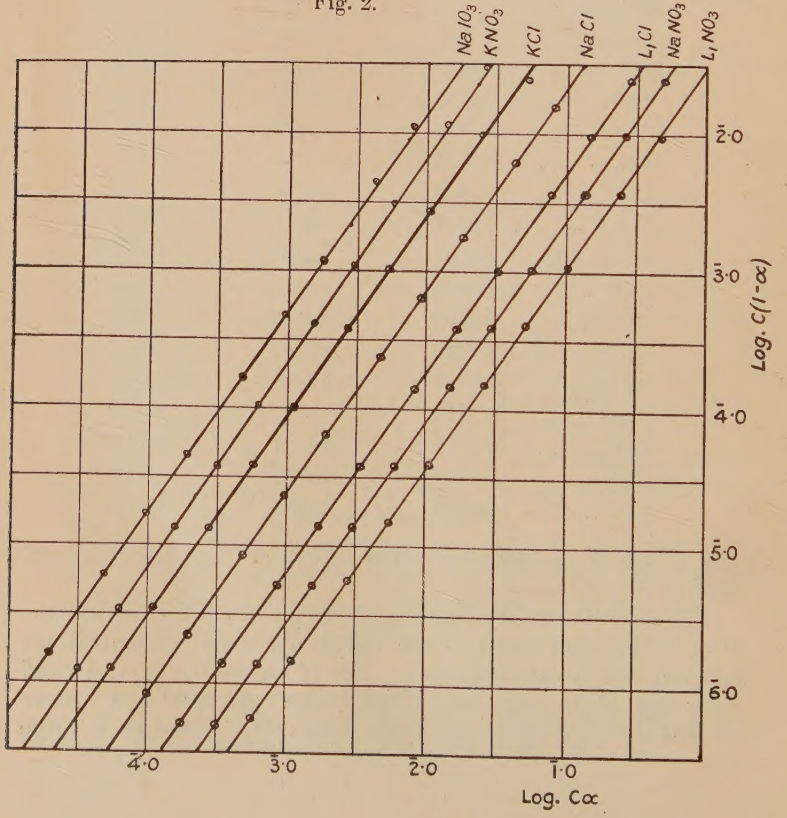
NaIO3
KNO3
KCl
NaCl
L1Cl
NaNO3
L1NO3
2̄·0
3̄·0
4̄·0
5̄·0
6̄·0
Log. C(1-α)
4̄·0
3̄·0
2̄·0
1̄·0
Log. Cα

approximating to unity, or variable and approaching unity as a limiting value. These facts show that n_0 is constant within the range of experimental error, and Table III. shows that for iodic and hydrochloric acids only is the exponent in the neighbourhood of unity. The rectilinear graphs for these two acids are shown in fig. 1.

We now proceed to test the validity of the simple Storch equation by the logarithmic plot of equation (2). Figs. 2, 3, and 4 exhibit graphically the results for all the

Fig. 3.

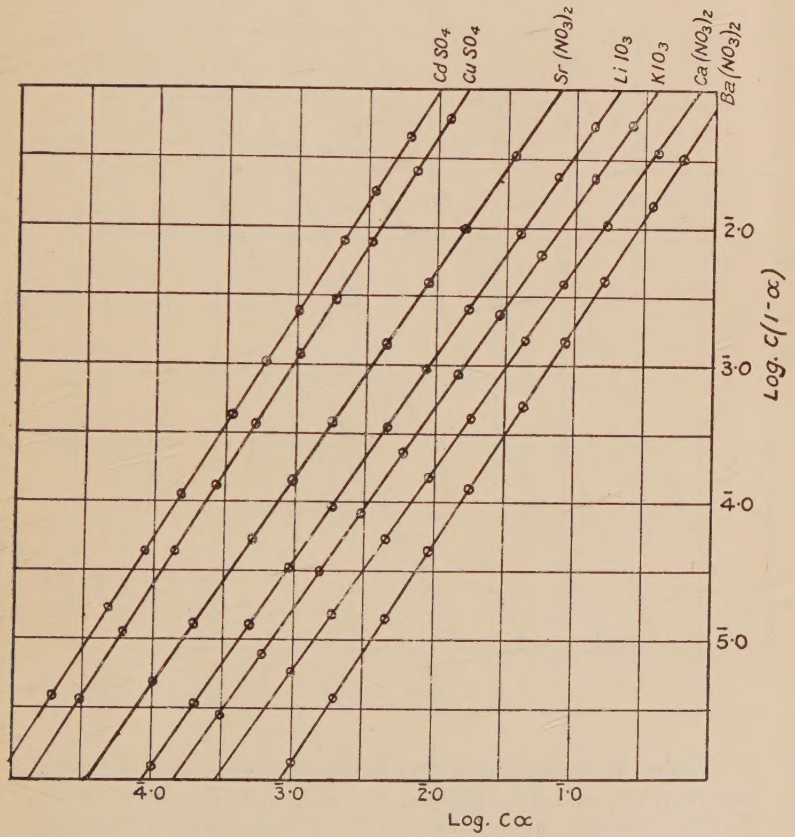

substances examined, and the closeness with which the solutions follow this law is measured by the rectilinearity of the line drawn through the observed points shown. Having

determined n from these lines, it is possible to calculate for each concentration a value for K, and any irregularities in the values so computed serve further to test the closeness with which, and the range over which, the law is followed.

Fig. 4.

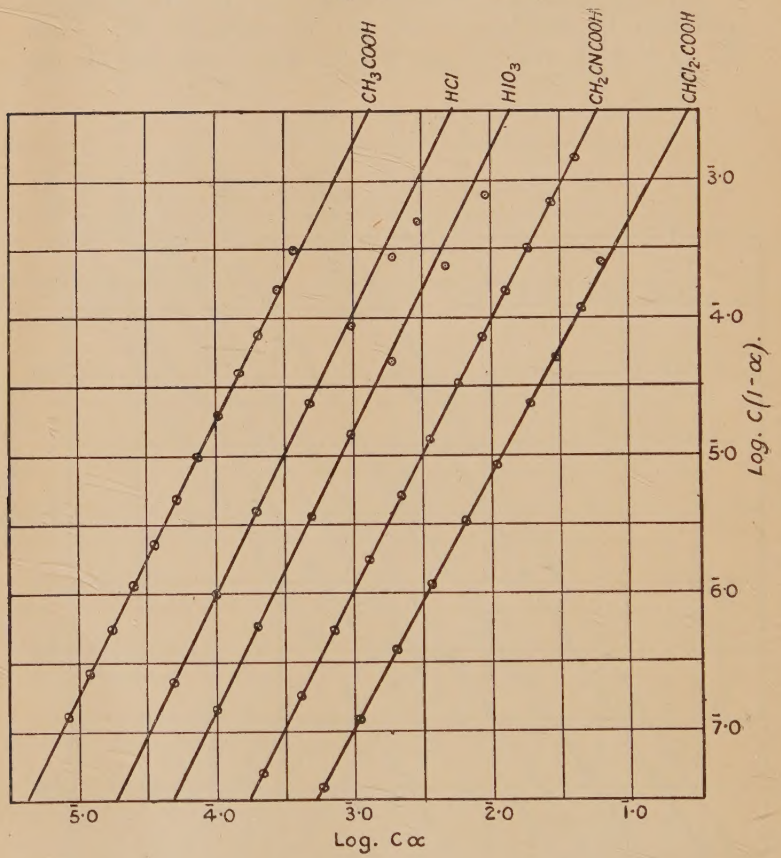

In Table IV. we exhibit a number of these values for typical electrolytes, and in Table V. we give a conspectus of the values of n, the mean values of K, and the range of validity of the equation for all the electrolytes studied.

Table IV.

"Strong" Electrolytes.

Concentration ..	$5{\cdot}0\times10^{-5}$	$1{\cdot}0\times10^{-4}$	$2{\cdot}0\times10^{-4}$	$5{\cdot}0\times10^{-4}$	$1{\cdot}0\times10^{-3}$	$2{\cdot}0\times10^{-3}$	$5{\cdot}0\times10^{-3}$	$1{\cdot}0\times10^{-2}$	$2{\cdot}0\times10^{-2}$	$5{\cdot}0\times10^{-2}$	$1{\cdot}0\times10^{-1}$	$2{\cdot}0\times10^{-1}$	$5{\cdot}0\times10^{-1}$	1
LiCl	-	1·50	1·57	1·54	1·56	1·55	1·55	1·54	1·55	1·57	1·57	1·57	1·55	1·44
$LiNO_3$		1·64	1·67	1·66	1·66	1·65	1·63	1·62	1·60	1·61	1·61	1·61	1·56	1 44
$Sr(NO_3)_2$	—	0·68	0·69	0 69	0·68	0·68	0·67	0·67	0·67	0·67	0·68	0·68	0·64	0·58
$Ba(NO_3)_2$	-	0·49	0·50	0·50	0·50	0·49	0·48	0 48	0·48	0·48	0·48	0·47	0·43	
$CuSO_4$		0·068	0·070	0·069	0·068	0·066	0·065	0 065	0·066	0·071	0·077	0·086	—	0·112
$CdSO_4$	—	0·056	0·058	0·059	0·059	0·058	0·058	0·058	0·059	0·063	0·068	0·075	0·087	0·093
HCl	0·096	0·094	0·093	0·092	0·102	0·129	0·158							
HIO_3	0 075	0·073	0 072	0·072	0·075	0·082	0·097	0·113	0·132	0·158	0 180	0·205		

"Intermediate" or "Transition" Electrolytes.

Concentration ...	$2{\cdot}322\times10^{-4}$	$4\,645\times10^{-4}$	$9{\cdot}290\times10^{-4}$	$1{\cdot}858\times10^{-3}$	$3{\cdot}716\times10^{-3}$	$7{\cdot}429\times10^{-3}$	$1{\cdot}486\times10^{-2}$	$2{\cdot}973\times10^{-2}$	$5{\cdot}945\times10^{-2}$	$1\,189\times10^{-1}$	$2{\cdot}378\times10^{-1}$	$4{\cdot}757\times10^{-1}$	
$CH_2.CN.COOH$	0·0041	0·0046	0·0047	0·0047	0·0046	0 0046	0·0046	0 0047	0·0047	0·0047	0·0046	0·0044	
Concentration ...	—	—	—	$1{\cdot}953\times10^{-3}$	$3{\cdot}906\times10^{-3}$	$7{\cdot}813\times10^{-3}$	$1{\cdot}563\times10^{-2}$	$3{\cdot}125\times10^{-2}$	$6{\cdot}250\times10^{-2}$	$1{\cdot}250\times10^{-1}$	$2{\cdot}500\times10^{-1}$	$5\,000\times10^{-1}$	1
$CHCl_2.COOH$ ...	-	—	—	0 079	0 088	0·091	0·091	0·091	0·089	0·089	0 088	0·082	0·069

"Weak" Electrolytes.

Concentration ...	– –	$4{\cdot}940\times10^{-4}$	$9{\cdot}879\times10^{-4}$	$1{\cdot}976\times10^{-3}$	$3{\cdot}952\times10^{-3}$	$7{\cdot}904\times10^{-3}$	$1{\cdot}581\times10^{-2}$	$3{\cdot}162\times10^{-2}$	$6{\cdot}323\times10^{-2}$	$1{\cdot}265\times10^{-1}$	$2{\cdot}529\times10^{-1}$	$5{\cdot}058\times10^{-1}$	1 011
$CH_3.COOH$	—	$1{\cdot}86\times10^{-6}$	$1{\cdot}85\times10^{-6}$	$1{\cdot}83\times10^{-6}$	$1{\cdot}85\times10^{-6}$	$1{\cdot}85\times10^{-6}$	$1{\cdot}85\times10^{-6}$	$1{\cdot}85\times10^{-6}$	$1{\cdot}85\times10^{-6}$	$1{\cdot}82\times10^{-6}$	$1{\cdot}77\times10^{-6}$	$1{\cdot}66\times10^{-6}$	$1{\cdot}44\times10^{-5}$

TABLE V.

Electrolyte.	n.	K.	Valid up to C=
NaCl	1·4763	1·54	$2{\cdot}0\times10^{-2}$
KCl.....	1·4867	1·62	$1{\cdot}0\times10^{-2}$
LiCl.....	1·4612	1·55	$5{\cdot}0\times10^{-1}$
$NaNO_3$	1·4484	1·75	$1{\cdot}0\times10^{-2}$
KNO_3	1·4916	1·52	$2{\cdot}0\times10^{-1}$
$LiNO_3$	1·4465	1·65	$2{\cdot}0\times10^{-1}$
$NaIO_3$.....	1·4877	1·07	$5{\cdot}0\times10^{-2}$
KIO_3	1·4566	1·63	$5{\cdot}0\times10^{-3}$
$LiIO_3$	1·4715	1·07	$2{\cdot}0\times10^{-2}$
$Ca(NO_3)_2$	1·4312	0·99	$5{\cdot}0\times10^{-1}$
$Sr(NO_3)_2$.....	1·4916	0·68	$2{\cdot}0\times10^{-1}$
$Ba(NO_3)_2$	1·5436	0·49	$1{\cdot}0\times10^{-1}$
$CuSO_4$.....	1·6429	0·068	$5{\cdot}0\times10^{-2}$
$CdSO_4$.....	1·6487	0·058	$5{\cdot}0\times10^{-2}$
$CHCl_2.COOH$ ...	1·8341	0·088	$2{\cdot}0\times10^{-1}$
$CH_2.CN.COOH$.	1·9574	0·0046	$5{\cdot}0\times10^{-1}$
HIO_3	2·0000	0·73	$1{\cdot}0\times10^{-3}$
HCl.....	2·0155	0·094	$1{\cdot}0\times10^{-3}$
$CH_3.COOH$	2·0000	0·00000185	$1{\cdot}0\times10^{-1}$

Some regularities are apparent in Table V. which may here be noted. For the chlorides, nitrates and iodates of sodium, potassium and lithium, and also for the nitrates of calcium, strontium and barium, the coefficient n increases with rise in atomic weight, the only exception being potassium iodate.

We may mention here that the experimental figures chosen were those of as high an order of accuracy as possible (Kohlrausch and Maltby, *Wiss. Abh. Techn. Reichs.* 1900, iii. p. 156 : *Ges. Abh.* 1911, ii. p. 826, for NaCl, KCl, LiCl, $NaNO_3$, KNO_3, and $LiNO_3$ at 18° ; Kohlrausch, *Berl. Ber.* 1900, p. 1002 : *Ges. Abh.* 1911, ii. p. 942, for $NaIO_3$, KIO_3, and $LiIO_3$ at 18° ; Kohlrausch and Grüneisen, *Berl. Ber.* 1904, p. 1215 : *Ges. Abh.* 1911, ii. p. 1078 : Grüneisen and Steinwehr, *Ges. Abh.* 1911, ii. p. 1223, for $Ca(NO_3)_2$, $Sr(NO_3)_2$, $Ba(NO_3)_2$, $CuSO_4$, and $CdSO_4$ at 18° ; Kraus and Parker, J. Amer. Chem. Soc. 1922, xliv. p. 2429, for iodic acid at 25° ; Parker, *ibid.* 1923, xlv. p. 2017, for hydrochloric acid at 25° ; Kendall, *Medd. K. Vetens. Nobelinstitut*, Bd. 2, no. 38 (1913), for cyanacetic acid, dichloracetic acid, and acetic acid at 25°). With these figures, and employing

large-scale graph paper, we found it quite feasible to determine our constants correct to four significant figures.

Now, if Weiland's figures (*loc. cit.*) as quoted, using Weiland's value for Λ_0, be plotted out in this way, it will be seen that, down to the lowest concentrations measured, Weiland's figures follow an accurate Storch equation, in which n is *not* equal to 2·000; and this we believe is the proper manner to test and to interpret his figures.

Turning now to the substances studied for which n is assumed equal to $a+bC$, we can test the equation and determine the constants by a graphical method of a reasonably high order of accuracy, which, however, necessitates rather laborious computations. Briefly, the method is as follows:—

Writing the Storch equation,

$$\left(C\frac{\Lambda}{\Lambda_0}\right)^n = K\left(C - C\frac{\Lambda}{\Lambda_0}\right),$$

and putting

$$C\frac{\Lambda}{\Lambda_0} = Y \quad \text{and} \quad C = X,$$

we have, taking logarithms, and assuming that $n = a + bC = a + bX$,

$$a \log Y + bX \log Y = \log (X - Y) + \log K. \quad . \quad . \quad (4)$$

Taking a convenient point X_0, Y_0 on this curve, we have

$$\log K = a \log Y_0 + bX_0 \log Y_0 - \log (X_0 - Y_0), \quad . \quad (5)$$

and eliminating K between (4) and (5), we arrive at

$$a + b\frac{X \log Y - X_0 \log Y_0}{\log Y - \log Y_0} = \frac{\log (X - Y) - \log (X_0 - Y_0)}{\log Y - \log Y_0},$$

yielding the linear plot

$$a + bx = y$$

if

$$x = \frac{X \log Y - X_0 \log Y_0}{\log Y - \log Y_0}$$

and

$$y = \frac{\log (X - Y) - \log (X_0 - Y_0)}{\log Y - \log Y_0}.$$

The method of tabulation is shown in Table VI. for sodium chloride at 18°, while in fig. 5 is shown the rectilinear plot from which the constants a and b have been computed.

TABLE VI.

Sodium Chloride, 18° C.

C.	A.	x.	y.	K.
$1{\cdot}0\times10^{-4}$	108·10	$-2{\cdot}6269\times10^{-3}$	1·4488	1·455
$2{\cdot}0\times10^{-4}$	107·82	$-3{\cdot}2721\times10^{-3}$	1·4747	1·546
$5{\cdot}0\times10^{-4}$	107·48	$-6{\cdot}2235\times10^{-3}$	1·4731	1·544
$1{\cdot}0\times10^{-3}$	106·49	—	—	1·544
$2{\cdot}0\times10^{-3}$	105·55	$-8{\cdot}1292\times10^{-3}$	1·4747	1·545
$5{\cdot}0\times10^{-3}$	103·78	$-1{\cdot}2507\times10^{-2}$	1·4760	1·546
$1{\cdot}0\times10^{-2}$	101·95	$-1{\cdot}17614\times10^{-2}$	1·4742	1·535
$2{\cdot}0\times10^{-2}$	99·62	$-2{\cdot}4961\times10^{-2}$	1·4709	1·536
$5{\cdot}0\times10^{-2}$	95·71	$-3{\cdot}9252\times10^{-2}$	1·4644	1·546
$1{\cdot}0\times10^{-1}$	92·02	$-5{\cdot}3885\times10^{-2}$	1·4600	1·546
$2{\cdot}0\times10^{-1}$	87·73	$-7{\cdot}0215\times10^{-2}$	1·4549	1·544
$5{\cdot}0\times10^{-1}$	80·94	$-8{\cdot}2245\times10^{-2}$	1·4514	1·546
1	74·35	$-5{\cdot}7390\times10^{-2}$	1·4546	1·590

$X_0=1{\cdot}00000\times10^{-3}$, $Y_0=9{\cdot}76793\times10^{-4}$.

$$\frac{(C\alpha)^{1{\cdot}4764+0{\cdot}3052C}}{C(1-\alpha)}=K.$$

Fig. 5

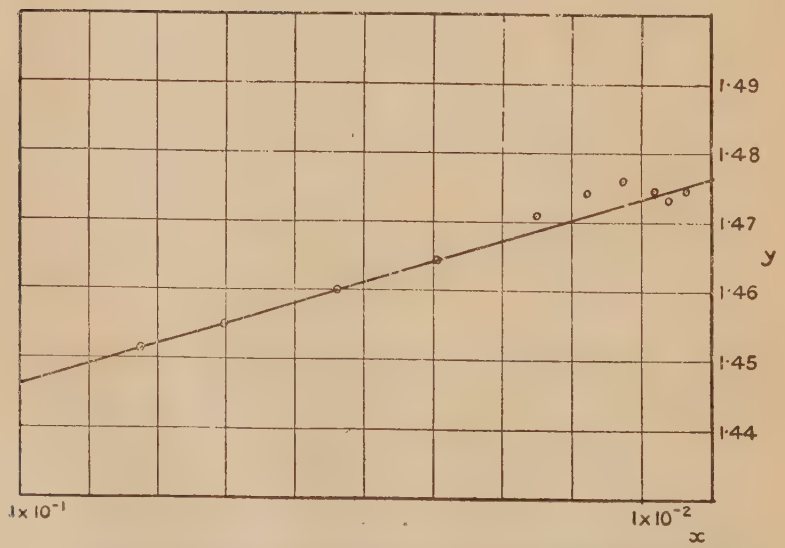

In this manner we have shown for various substances that n is a linear function of the concentration, and increases with rise in concentration. A summary of the results for

potassium chloride and lithium chloride (18°) is given in Table VII.*, while in Table VIII. is exhibited the variability

TABLE VII.

Concentration.	KCl.		LiCl.	
	Λ.	K.	Λ.	K.
$2{\cdot}0\times10^{-5}$	129·51	1·265		
$5{\cdot}0\times10^{-5}$	129·32	1·451		
$1{\cdot}0\times10^{-4}$	129·07	1·504	98·14	1·496
$2{\cdot}0\times10^{-4}$	128·77	1·602	97·85	1·564
$5{\cdot}0\times10^{-4}$	128·11	1·631	97·19	1·534
$1{\cdot}0\times10^{-3}$	127·34	1·616	96·52	1·552
$2{\cdot}0\times10^{-3}$	126·31	1·612	95·62	1·547
$5{\cdot}0\times10^{-3}$	124·41	1·620	93·92	1·540
$1{\cdot}0\times10^{-2}$	122·43	1·615	92·14	1·531
$2{\cdot}0\times10^{-2}$	119·96	1·623	89·91	1·536
$5{\cdot}0\times10^{-2}$	115·75	1·615	86·12	1·552
$1{\cdot}0\times10^{-1}$	112·03	1·616	82·42	1·552
$2{\cdot}0\times10^{-1}$	107·96	1·625	77·93	1·542
$5{\cdot}0\times10^{-1}$	102·41	1·752	70·71	1·512
1	98·27	2·259	63·36	1·413

$$\text{For KCl } \frac{(C\alpha)^{1\cdot4863+0\cdot6354\,C}}{C(1-\alpha)} = K.$$

$$\text{For LiCl } \frac{(C\alpha)^{1\cdot4616+0\cdot0484\,C}}{C(1-\alpha)} = K.$$

TABLE VIII.

Variation of the Exponent n with Concentration.

Concentration.	NaCl.	KCl.	LiCl.
	n.	n.	n.
$1{\cdot}0\times10^{-4}$	1·4764	1·4863	1·4616
$2{\cdot}0\times10^{-4}$	1·4764	1·4863	1·4616
$5{\cdot}0\times10^{-4}$	1·4766	1·4866	1·4616
$1{\cdot}0\times10^{-3}$	1·4769	1·4869	1·4616
$2{\cdot}0\times10^{-3}$	1·4770	1·4876	1·4617
$5{\cdot}0\times10^{-3}$	1·4779	1·4895	1·4618
$1{\cdot}0\times10^{-2}$	1·4795	1·4927	1·4621
$2{\cdot}0\times10^{-2}$	1·4825	1·4990	1·4626
$5{\cdot}0\times10^{-2}$	1·4917	1·5181	1·4640
$1{\cdot}0\times10^{-1}$	1·5069	1·5498	1·4664
$2{\cdot}0\times10^{-1}$	1·5374	1·6134	1·4713
$5{\cdot}0\times10^{-1}$	1·6290	1·8040	1·4858
1	1·7816	2·1217	1·5100

* Iodic acid (25°) does not appear to conform to this formula.

of the exponent n with concentration. It will be noticed that the value at low concentrations agrees reasonably well with the value deduced from the simple Storch equation.

These results are directly opposed to the conclusions of Noyes and his collaborators (*cf.* Noyes and Falk, J. Amer. Chem. Soc. 1912, xxxiv. p. 479), and especially of Bates (*ibid.* 1913, xxxv. p. 519), who states (*loc. cit.*): "It would appear that in general the value of n continues to increase as the concentration decreases, and that hence the assumption that n does not change appreciably below 0·01 normal is not justified."

The order of accuracy to be expected in comparing observed and calculated values of Λ over the range of validity of this dilution formula is shown in Table IX.*

TABLE IX.

Sodium Chloride, 18°.

$$\frac{(C\alpha)^{1\cdot4764+0\cdot3052\,C}}{C(1-\alpha)} = 1\cdot543.$$

Concentration.	Λ (observed).	Λ (calculated)
$1\cdot0\times10^{-4}$	108·10	108·15
$2\cdot0\times10^{-4}$	107·82	107·82
$5\cdot0\times10^{-4}$	107·18	107·18
$1\cdot0\times10^{-3}$	106·49	106·49
$2\cdot0\times10^{-3}$	105·55	105·56
$5\cdot0\times10^{-3}$	103·78	103·80
$1\cdot0\times10^{-2}$	101·95	101·99
$2\cdot0\times10^{-2}$	99·62	99·66
$5\cdot0\times10^{-2}$	95·71	95·72
$1\cdot0\times10^{-1}$	92·02	92·08
$2\cdot0\times10^{-1}$	87·73	87·67
$5\cdot0\times10^{-1}$	80·94	(80·60)
1	74·35	(73·62)

In brief, taking into account the number and diverse nature of the electrolytes examined (strong, intermediate or transition, weak, uni-uni-, uni-bi-, and bi-bivalent forms have been examined) and the range of concentration considered, our conclusions point to the Storch equation in its simple, or in a generalized, form as the equation which most satisfactorily represents the relation between $\alpha\ (=\Lambda/\Lambda_0)$

* The method employed for the computation of Λ is briefly described in a note at the end of this paper.

and C over a wide range of concentration. And this relation, which is undoubtedly followed accurately at low concentrations, serves to test Ostwald's law. We do not find that this law is followed as a general rule—of the substances which we have examined, only two out of a total of nineteen show reasonably good agreement with this formula.

NOTE.—Calculation of α from the equation $\frac{(C\alpha)^n}{C(1-\alpha)} = K$, where $n = a + bC$.

This equation may be written in the form

$$\alpha^n = \frac{K}{C^{n-1}}(1-\alpha) = -B\alpha + B, \quad \text{where} \quad B = \frac{K}{C^{n-1}},$$

$$\text{or} \qquad \alpha^n + B\alpha - B = 0.$$

The last equation may be readily solved for α, and therefore for Λ, by the method of iteration described in Whittaker and Robinson, 'The Calculus of Observations,' p. 81 (1926).

One of the authors (I. V.) wishes to acknowledge his indebtedness to the Trustees of the Dixon Fund for a grant with the aid of which part of the expenses of the research have been defrayed.

Imperial College of Science and
Technology, South Kensington.
East London College
(University of London).

II. *A Theoretical Investigation of the Phenomenon of Cavitation in Screw Propellers.* *By* JOHN TUTIN, *M.Sc.**

1. THE phenomenon of cavitation was first observed by Sir John Thornycroft, F.R.S., and S. W. Barnaby, on the trials of the destroyer 'Daring' in 1894 †. The propulsive efficiency was abnormally low, and the first five sets of propellers fitted to this vessel failed to propel her at the contract speed. The breakdown in thrust was accompanied by excessive slip and acute vibration. A cure was effected by fitting a sixth set of screws having about fifty per cent. greater blade area.

The phenomenon was attributed to the formation of cavities on the back of the blades. In subsequent experiments on a

* Communicated by the Author.

† Thornycroft and Barnaby, Inst. C.E. 1895.

model propeller in a special vacuum tank, the formation of such cavities was actually observed by Sir Charles Parsons, F.R.S.* In the course of some classical experiments carried out by D. W. Taylor in the Washington Tank, cavities were also observed on the blade face †. This latter phenomenon was both unexpected and surprising, because the slip and the nominal angle of incidence were positive. It was ascribed by Taylor to the water "cascading" from the back of the blade to the face, over the leading edge.

Since the "discovery" of the phenomenon in 1894, a large number of theories of cavitation ‡ have been formulated from time to time, but none of them can be regarded as giving an adequate and reliable explanation of the observed phenomena.

The formation of cavities on propeller blades is described in § 2, and the importance of face cavities is emphasized. The possibility that face cavitation may be due to excessive inflow leads to an investigation in § 3 of the momentum and energy equations of a simple form of propeller. Existing theory is here found to be incorrect, and a new set of equations are derived. In § 4 these results are applied to the blade elements of an actual propeller. A method for determining the real angle of incidence is given, and a simple extension gives the criterion for face cavitation in equation (19).

Finally, in § 5 the problem of eliminating cavitation is considered in the light of the present theory.

Formation of Cavities.

2. The thrust of a screw propeller is the resultant longitudinal component of the excess pressure on the face of the blades and the defect of pressure on the back. Both the pressure on the face and the suction on the back increase as the speed of advance and the revolutions are increased, but whereas an excess pressure may go on increasing indefinitely, the limit of suction at a given point is reached when the absolute pressure is reduced to zero, assuming for the moment an ideal fluid which does not evaporate, and

* Sir Charles Parsons, N.E.C. Inst. 1912–13.

† D. W. Taylor, 'Speed and Power of Ships,' pp. 118–158.

‡ Barnaby, Inst. Nav. Arch. 1897 and 1911. Normand, Inst. C.E. 1905. Wagner, *Jahrbuch S.G.* 1906. Taylor, *loc. cit.* Flamm, Inst. Nav. Arch. 1911. Gumbel, Inst. Nav. Arch. 1913. Mumford, Inst. C.E. 1921. Dyson, 'Screw Propellers,' Chapter on Cavitation. Bauer, *Schiffbautechnische Gesellschaft*, 1923. Horn, *Schiffbautechnische Gesellschaft*, 1926. Foetinger, *V. d. I.* 1926.

which contains no occluded gases. Any further increase in speed and revolutions will produce no further increase in thrust at this point, and will merely extend the boundaries of the region over which the pressure is zero.

In the case of a fluid which evaporates, the limit of pressure will be reached when the absolute pressure is equal to the vapour pressure. The cavity will then contain vapour at a pressure depending solely on the temperature. Further, as in the case of water, if the fluid contains air or other gases in solution, these will escape into the cavity, but it follows from the Law of Partial Pressures, that their presence will not alter the absolute pressure at which the cavity will form. This applies also to any air which may be drawn down from the surface.

Consider, therefore, a particular blade element of a screw propeller, at a given distance from the axis, and let the hydrostatic immersion be h feet. Let h_1 and h_2 denote the hydrostatic equivalents of the atmospheric and vapour pressures, respectively. When the propeller is revolving, the point of incipient cavitation will occur when the pressure drop at some point on the element reaches the value

$$p' = \rho g(h + h_1 - h_2). \quad . \quad . \quad . \quad . \quad . \quad (1)$$

For finite values of h, the formation of cavities on the back of a propeller blade at sufficiently high revolutions is clearly inevitable, and a method of calculating the critical speed of rotation at which back cavitation will be incipient can readily be developed from equation (1). [See equation (20).]

However, even extensive cavitation on the back of the blades could not, *per se*, account for the remarkable features of the phenomenon. Cavitation on the back of the blades would certainly result in a decrease in torque, and therefore in an increase in revolutions and slip for a given speed and thrust. Whilst this increase in slip will in most cases result in a moderate loss of propeller efficiency, this is not necessarily so, and, in fact, certain propellers have been known to run at higher efficiency due to the increased slip which accompanied back cavitation.

Normand * states that cavitation proper may result in the power required to attain a given speed being double that required when cavitation is absent. In another well-authenticated instance †, the estimated waste of power due to cavitation at 23 knots would alone have been sufficient to

* *Loc. cit.*

† The 'Drake' class of armoured cruisers.

propel the ship at a speed of 14 knots. D. W. Taylor found that at sufficiently high revolutions cavitation became so acute as to cause the thrust to vanish. Hence, some further explanation is required to account for losses of this magnitude.

A possible explanation of the phenomenon readily suggests itself, namely, that under certain conditions there may be excessive acceleration in the fluid ahead of the propeller and consequently abnormally high inflow. This might result in negative angles of incidence, which would account in a very simple manner for the cavities observed by Taylor and attributed by him to cascading at positive angles of incidence.

Momentum Theory.

3. In order to investigate this possibility, however, it is necessary to revert to the fundamental momentum and energy equations governing the action of a screw propeller. In the Froude-Rankine * theory and the Betz-Prandtl † vortex theory, the propeller itself is replaced by an "actuator," which is virtually a propeller consisting of an infinite number of blades, having no boss or hub, so that it becomes effectively a circular disk. It is assumed that the thrust is uniformly distributed over this disk, and the latter, therefore, exerts a discontinuity in pressure on the fluid passing through the disk.

Fig. 1.

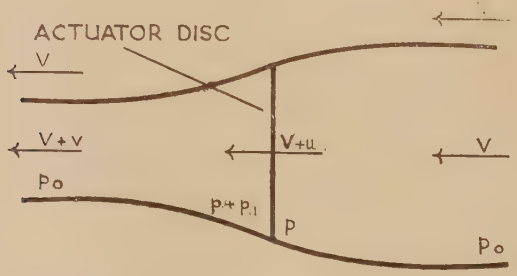

Referring to fig. 1, we see that on the hypothesis that it is legitimate to apply Bernoulli's law to the motion before

* Rankine, 'Scientific Papers,' p. 544. R. E. Froude, F.R.S., Inst. Nav. Arch. 1889 & 1911.

† Betz and Prandtl, *Nachr. v. d. Kyl. Gesellschaft des Wissenschaften*, 1919. Glauert, Aero. Research Comm. R. & M. 786 and 869.

and behind the screw disk separately, the Froude-Rankine theory gives

$$p_0+\tfrac{1}{2}\rho V^2=p+\tfrac{1}{2}\rho(V+u)^2, \quad . \quad . \quad . \quad (2)$$

$$p+p_1+\tfrac{1}{2}\rho(V+u)^2=p_0+\tfrac{1}{2}\rho(V+v)^2. \quad . \quad . \quad . \quad (3)$$

Also, equating the rate of increase of axial momentum to the forward thrust,

$$T=p_1A=A\rho(V+u)v. \quad . \quad . \quad . \quad . \quad . \quad (4)$$

From equations (2), (3), and (4) the well-known result is obtained

$$u=\tfrac{1}{2}v. \quad . \quad . \quad . \quad . \quad . \quad . \quad . \quad (5)$$

Thus, on the above assumptions, half the added velocity in the slip stream occurs in front of the screw disk and half behind it.

From equations (4) and (5) the inflow velocity u can be determined, and current air-screw research is largely based on the assumption that these equations are correct.

Let us consider, however, the dynamical equilibrium of the system. If it is proposed to apply Bernoulli's law to the inflow and outflow columns separately, it is legitimate to investigate, in the first instance, whether the suction $(p_0-p)A$, on the forward side of the screw disk, will produce and maintain an inflow velocity u. To satisfy this condition, we must have

$$(p_0-p)A=\rho A(V+u)u, \quad . \quad . \quad . \quad . \quad . \quad (6)$$

which is, however, quite incompatible with equation (2). An investigation of the outflow column reveals a similar inconsistency, since in lieu of equation (3) we obtain

$$[(p+p_1)-p_0]A=\rho A(V+u)(v-u). \quad . \quad . \quad . \quad (7)$$

It is, in fact, evident that the actuator is physically incapable of producing the slip-stream flow attributed to it.

Now, the force-momentum relationships expressed in equations (6) and (7) must necessarily hold good. Therefore there must be errors inherent in the energy equations (2) and (3).

In lieu of these, we have :

(a) *Inflow Column.*—Modifying equation (2) to satisfy equation (6) :—

$$p_0+\tfrac{1}{2}\rho V^2=p+\tfrac{1}{2}\rho(V+u)^2+\tfrac{1}{2}\rho u^2, \quad . \quad . \quad . \quad . \quad . \quad (8)$$

or

$$(p_0-p)A=\rho A(\underbrace{Vu}_{\text{useful work.}}+\underbrace{\tfrac{1}{2}u^2}_{\text{kinetic energy of inflow.}}+\underbrace{\tfrac{1}{2}u^2}_{\text{energy dissipated at screw disk.}}). \quad . \quad . \quad (9)$$

(b) *Outflow Column.*—Modifying equation (3) to satisfy equation (7) :—

$$p+p_1+\tfrac{1}{2}\rho(\mathrm{V}+u)^2+\tfrac{1}{2}\rho(v-u)^2=p_0+\tfrac{1}{2}\rho(\mathrm{V}+v)^2, \quad (10)$$

or

$$(p+p_1-p_0)\mathrm{A}=\mathrm{A}\rho[\underset{\text{useful work.}}{\mathrm{V}(v-u)}+\underset{\text{outflow quota of kinetic energy.}}{\tfrac{1}{2}(v^2-u^2)}-\underset{\text{energy dissipated at screw disk.}}{\tfrac{1}{2}(v-u)^2}].$$

. . . . . (11)

(c) *Combined Columns.*—Adding equations (9) and (11) should give the total thrust :

$$\mathrm{T}=p_1\mathrm{A}=\rho\mathrm{A}[\mathrm{V}v+\tfrac{1}{2}v^2+(uv-\tfrac{1}{2}v^2)] \quad . \quad . \quad (12)$$

$$=\rho\mathrm{A}(\mathrm{V}+u)v. \quad . \quad . \quad . \quad . \quad . \quad . \quad (13)$$

This result is identical with equation (4), as, of course, it should be. Denoting the inflow ratio $\frac{u}{v}$ by d, the inflow velocity becomes

$$u=\tfrac{1}{2}\sqrt{\mathrm{V}^2+\frac{4\mathrm{T}d}{\rho\mathrm{A}}}-\tfrac{1}{2}\mathrm{V}. \quad . \quad . \quad . \quad . \quad (14)$$

The total dissipation of energy at the screw disk is represented by

$$\tfrac{1}{2}u^2+\tfrac{1}{2}(v-u)^2, \quad . \quad . \quad . \quad . \quad . \quad (15)$$

and this term indicates an additional loss of energy of about the same order as the loss due to the axial kinetic energy of the slip stream. This additional loss is seen to be required by the dynamical equilibrium of the slip stream. The energy dissipated will, of course, reappear in the slip stream in the form of heat. There are a number of physical problems in which the conditions are analogous, as, for example, inelastic impact.

Efficiency.

$$\text{Actuator Efficiency}=\frac{\text{useful work}}{\text{useful work}+\text{kinetic energy}+\text{heat energy}}, \quad . \quad (16)$$

i. e.

$$\eta=\frac{\mathrm{V}v}{\mathrm{V}v+\tfrac{1}{2}v^2+\tfrac{1}{2}u^2+\tfrac{1}{2}(v-u)^2} \quad . \quad . \quad (17)$$

$$=\frac{\mathrm{V}v}{\mathrm{V}v+v^2-vu+u^2}. \quad . \quad . \quad . \quad . \quad (18)$$

Differentiating the above expression, the efficiency is a maximum for a given thrust T, when :

$$u = \tfrac{1}{6}(4V^2 + 8Vv + 13v^2)^{\frac{1}{2}} - \tfrac{1}{6}(2V - v).$$

If the ratio $\frac{v}{V}$ is small, this condition reduces to $u = \frac{1}{2}v$, and the maximum efficiency is then

$$\eta \max = \frac{V}{V + \frac{3}{4}v}.$$

The logical conclusion of this investigation is that an actuator cannot be made to deliver thrust by the assumption of a perfect "Bernoulli" flow and a discontinuity of pressure. It follows that the familiar Rankine-Froude theory and the corresponding vortex theory are incorrect. The inflow velocity and ideal efficiency deduced therefrom are misleading. This result is important, because these theories are extensively used in air-screw research in this country, France, Italy, Germany, and U.S.A.

The equations given above constitute a new theory, the main features of which may be summarized as follows :—

(1) There is an inevitable dissipation of energy at the screw disk, in addition to that due to the axial kinetic energy of the slip stream.

(2) The flow is elsewhere stream line and may be assumed to follow Bernoulli's law. Such conditions have been experimentally verified by Stanton * at the National Physical Laboratory, and by Fage † at the Royal Aircraft Establishment, Farnborough.

(3) Denoting the ratio of the inflow to the outflow by the term "inflow ratio," and the ratio of the suction to the total thrust by the term "suction ratio," it follows from equations (6) and (7) that the inflow ratio must be equal to the suction ratio. This may be regarded as a fundamental principle in propeller theory.

(4) In general, the inflow ratio may have any value, provided the above condition is satisfied.

(5) The maximum efficiency is $\frac{V}{V + \frac{3}{4}v}$, when the inflow ratio is $\frac{1}{2}$. This indicates a new line of research, since in order to improve the efficiency of present types of screw propeller we must compel the blade face to do more work ‡.

* Stanton and Marshall, Aero. Res. Comm. R. & M. 460.

† A. Fage, Aero. Res. Comm. R. & M. 699.

‡ The suction ratio of a normal screw propeller varies from about ·7 to 1·0, depending on the thickness and shape of the constituent aerofoils.

4. We are now in a position to consider the importance of inflow velocity in its relation to the blade elements of an actual propeller. Assuming in the first instance an isolated aerofoil at a distance r from the axis of rotation, it is evident from fig. 2 that if we know the outflow velocity EF we can

Fig. 2.

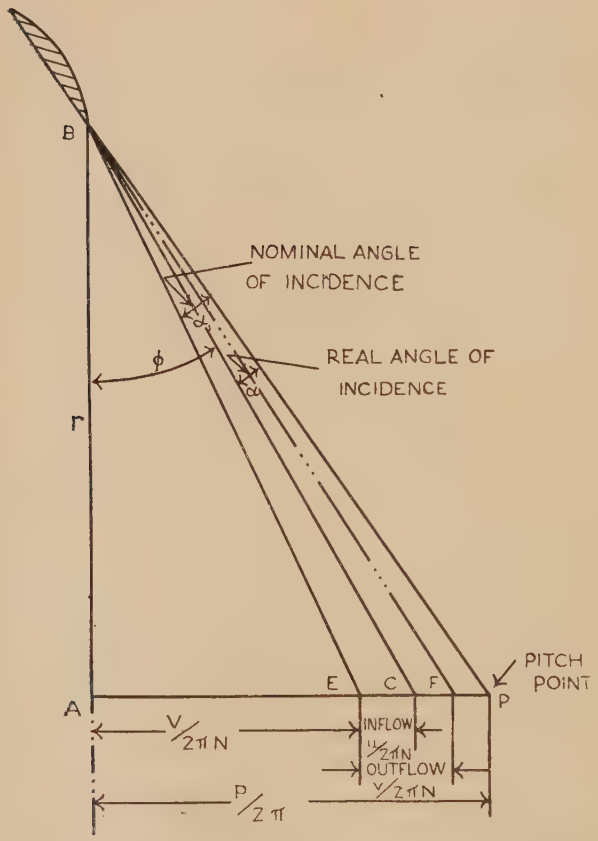

assume a sequence of values of the inflow ratio $\frac{EC}{EF}$, whence we can obtain a corresponding sequence of values of the angle of incidence α. We must then determine, in order to satisfy equations (6) and (7), the angle or angles for which the inflow ratio is equal to the suction ratio. Extensive

experiment data are already available from which the suction ratio of an aerofoil of given camber ratio over a range of angles of incidence can be derived.

Hence, if the sequence of values of the inflow ratio is plotted on a base of angle of incidence, together with the corresponding values of the suction ratio, as indicated in fig. 3, the solution is given by the points of intersection of the two curves. There are, in general, two solutions, one of which gives a positive and the other a negative angle of incidence. On investigation it is found, however, that in any given case only one solution will give the required thrust, and therefore the real angle of incidence.

Fig. 3.

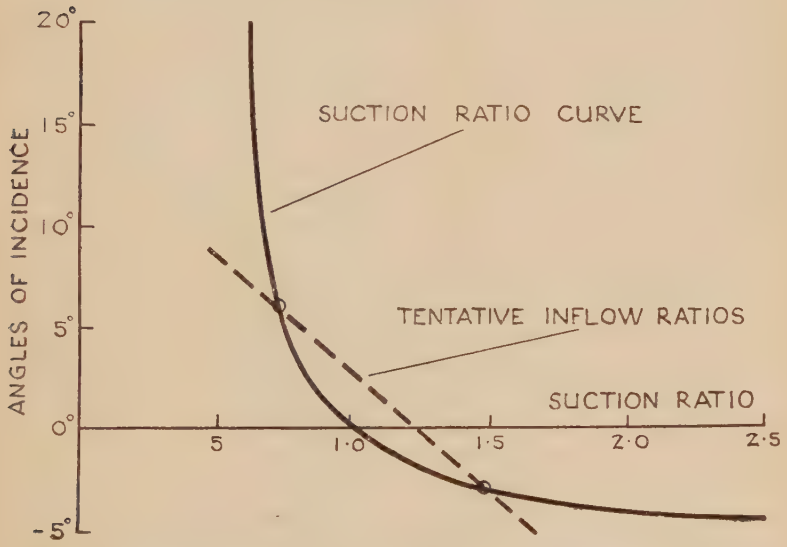

The inflow history of a normal screw propeller may now be described, assuming the revolutions to be indefinitely increased whilst the speed of advance is kept constant. Referring to fig. 2, at low revolutions the thrust is negative, and the propeller will act as a windmill and deliver torque. Inflow and outflow will both be negative. As revolutions are increased, however, the angle of incidence will eventually coincide with the angle of zero thrust. This point determines the "effective" or "experimental" pitch of the screw. According to the Froude-Rankine and vortex theories, there is no inflow at zero thrust, and therefore the effective pitch should invariably exceed the face pitch, owing to the finite

blade thickness. The present theory shows, however, that although there is necessarily no outflow, there will nevertheless be inflow, and this indicates the possibility of effective pitch being actually less than the face pitch in certain cases. This prediction is confirmed by experiments by Mumford at the Dumbarton Experiment Tank *.

In the vicinity of the point of zero thrust the angle of incidence becomes zero. Inflow and outflow are then necessarily equal and the inflow ratio unity. No additional momentum can be given to the fluid under these conditions after it has passed the screw disk, since the pressure on the blade face at zero angle of incidence is normal.

As the revolutions are further increased, the nominal slip increases and also the thrust. The inflow and outflow, being largely governed by thrust, will also increase. It will be seen that the variation in the angle of incidence will depend on whether the rate of increase of nominal slip is greater or less than the rate of increase of the inflow velocity.

In the light of the above theory, it is not difficult to see how and why an abnormal loss of thrust may arise. When the inflow increases to such an extent as to make the angle of incidence first of all zero and thereafter negative, a cavity may form on the *face* of the blade. When this occurs, it is obvious that the loss of thrust will become acute.

Since face cavitation is incipient when the angle of incidence has become zero, the critical speed at which it will occur can be determined as follows. Let u_0 be the inflow calculated on the assumption that the angle of incidence is zero at *all* thrusts. Then, from equation (14)

$$u_0 = \tfrac{1}{2}\sqrt{V^2 + \frac{4T}{\rho A}} - \tfrac{1}{2}V. \quad . \quad . \quad . \quad . \quad (19)$$

A curve of u_0 can then be plotted on the same base as nominal slip speed, and the point of intersection of the two curves will give the point of incipient face cavitation.

This criterion of cavitation throws some new light on the behaviour of the phenomenon. For example, in the case of H.M.S. 'Daring,' referred to above, Barnaby assumed that cavitation was incipient at a speed of 24 knots. The nominal slip of the 'Daring's' first pair of screws was, however, excessive over practically the whole range of speeds. For example, at 16 knots it was about 100 per cent. greater than the slip of the sixth pair of screws at 16 knots. Hence cavitation must have set in at a much lower speed than

* Baker and Schaffran, N.E.C. Inst. 1922–1924.

24 knots. The new theory shows that face cavitation was, in fact, incipient at about 13 knots.

In the case of Taylor's special cavitating propeller, on which well-defined cavities were actually observed by stroboscopic methods, investigation now shows that the real angle of incidence was negative over the entire range from 0 to 60 per cent. positive slip. Taylor's "cascading" hypothesis therefore becomes superfluous.

Methods of eliminating Cavitation.

5. It remains to consider, in the light of the above theory, by what means cavitation can be postponed. Equation (1) leads directly to the following criterion for back cavitation :

$$U = \sqrt{\frac{g\rho(h+h_1-h_2)}{ndk_L\left(\cos\alpha+\frac{1}{\delta}\sin\alpha\right)}}, \quad . \quad . \quad . \quad (20)$$

where U is the critical value of the relative velocity, α is the angle of incidence, k_L the lift coefficient of the aerofoil, δ the $\frac{\text{lift}}{\text{drag}}$ ratio of the aerofoil, n the ratio of the maximum suction intensity to the average suction intensity, and d the inflow ratio. Referring to fig. 2, the relative velocity under any given conditions may be determined from the relationship

$$U^2 = (4\pi^2N^2r^2) + (V+u)^2. \quad . \quad . \quad . \quad . \quad (21)$$

The value of U given by equation (20) is that at which cavitation sets in on the back of the blade element, and by applying the formula to sections of the blade at different distances r from the axis, it is possible to calculate whether cavitation will occur at any point on the back, and if so, to what extent.

If such cavitation is indicated at a particular section, and the revolutions, speed, diameter, and immersion are fixed, it is only possible to effect a cure by reducing either n, d, or k_L. Now n and d are both somewhat inflexible. On the other hand, the lift coefficient k_L is capable of relatively wide variation, by adjusting the camber ratio, and it is therefore possible to determine from equation (20), the maximum permissible camber ratio at any point. Having due regard to considerations of strength, the blade width and thickness can then be adjusted throughout such that back cavitation

may be prevented without unnecessarily large blade area and excessive frictional losses.

In order to postpone face cavitation, it is desirable not only to eliminate back cavitation, but also to reduce the inflow velocity, as indicated by the inflow-slip criterion of equation (19). This end can be achieved by reducing the suction ratio. Such a redistribution of load from the back of the blade to the face is evidently the only fundamental method of postponing face cavitation.

III. *Placing Plane Quadrilaterals in Perspective. Application to Photography.* *By* Thos. McHugh, *B.A.**

LEMMA 1.—RM, RN are two fixed str. lines and A is a fixed pt. through which is drawn a *variable* str. line meeting them in X, Y. Three str. lines *in the plane* PF, PG, PH, rigidly attached to one another in any order,

Fig. 1.

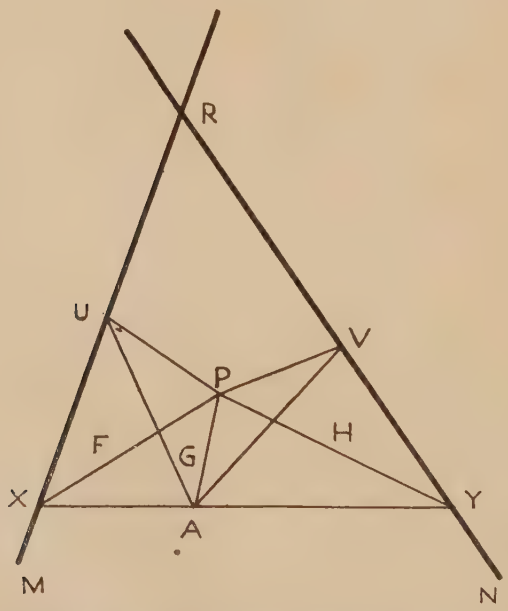

are placed so that they (produced through P when necessary) pass through X, A, Y *respectively*. The pt. P is then determined *uniquely*, and its locus is a circle (through R), fig. 1.

* Communicated by the Author.

Proof. Pts. U, V (fixed) being taken on RM, RN so

$$\widehat{AUM} = \widehat{GPF}, \quad \widehat{AVN} = \widehat{GPH} \quad \text{(fixed angles)},$$

APUX, APVY are each cyclic, and

$$\therefore \quad \widehat{PUR} = \widehat{PAX}, \quad \widehat{PVR} = \widehat{PAY}.$$

$$\therefore \quad \widehat{PUR} + \widehat{PVR} = \widehat{PAX} + \widehat{PAY} = 180°,$$

and hence P lies on the fixed ⊙ through R, U, V. Q.E.D.

Cor. 1. P is always real, and ∴ its locus is so.

Cor. 2. The same theorem holds when $\widehat{XAY}$ is any constant angle (=180°, above), but the ⊙ does not then pass through R.

Lemma 2.—ABCD, $A_1B_1C_1D_1$ are two given plane quads. Let $A_1B_1C_1D_1$ having definite aspect be placed (*in plano*) with respect to ABCD so that AA_1, BB_1, CC_1, DD_1 concur (at O, say), as in fig. 2. The problem of so placing them is

Fig. 2.

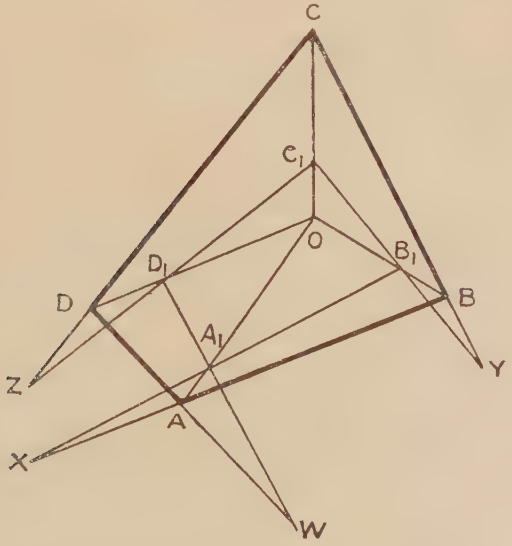

indeterminate, the locus of O being a certain curve on which we can get as many pts. as desired by ruler and compass. Let X, Y, Z, W be intersections of AB, A_1B_1; BC, B_1C_1; CD, C_1D_1; DA, D_1A_1.

Keeping O and ABCD fixed, and allowing vertices of $A_1B_1C_1D_1$ to move on OA, OB, OC, OD (including the parts produced through O) so that its sides retain their directions, it is clear that $A_1B_1C_1D_1$ retains its shape and aspect. Now shall XY, YZ, ZW, WX (but not XZ or WY) retain their directions.

Proof. Two sides, C_1Z, C_1Y, of the variable triangle C_1ZY, whose vertices move on the fixed concurrent lines CO, CD, CB, have fixed directions (hyp.); ∴ so has third side YZ etc. Q.E.D.

Lemma 3.—If for *any one* position of the varying quad. $A_1B_1C_1D_1$ of Lemma 2, X, Y, Z, W be *collinear*, they are so for *all* positions of $A_1B_1C_1D_1$, and the line of collinearity has a *fixed* direction. In particular, when A_1 falls on A the pts. Y, A, Z will be collinear, and like results hold when B_1 falls on B, C_1 falls on C, and D_1 falls on D.

Cor. 1. If when A_1 falls on A the pts. Y, A, Z be collinear, the pts. X, Y, Z, W will *always* be collinear, and in particular will Z, B, W be so when B_1 falls on B ; W, C, X be so when C_1 falls on C ; X, D, Y be so when D_1 falls on D ; and all the lines of collinearity will be parallel.

Lemma 4.—The problem referred to in Lemma 2 becomes *determinate* if in addition X, Y, Z, W are to be *collinear* ; and then there are as many pts. O as are yielded by the solution of the following problem (clear from results just established) :—

Problem.—ABCD, $A_1B_1C_1D_1$ are two given plane quadrilaterals (fig. 3) ; required to find in plane of ABCD a quadrilateral ALMN similar to and having same aspect as $A_1B_1C_1D_1$ such that BL, CM, DN concur (at O, say) and that at same time the str. line joining H (intersection of CB, ML) and K (intersection of CD, MN) passes through A.

Analysis. Because BCD, LMN are in perspective, BD, LN, HK concur (at S, say) and conversely. CB, CD are known lines, A a known pt., and the position relatively to each other of the lines MK, MA, MH is known (hyp.) ;

∴ by Lemma 1, M lies on a *known* ⊙ (through C), (1)

and hence, because ALM is of known species (hyp.),

L, too, lies on a known ⊙. . . . . (2)

BD, BH are known lines, A a known pt. and the position

relatively to each other, of the lines LS, LA, LH is known (hyp.);

$\therefore$ by Lemma 1, L lies on another known (through B);

. . . (3)

$\therefore$ L (and hence ALMN) can be found from (2) and (3). Q.E.F.

Fig. 3.

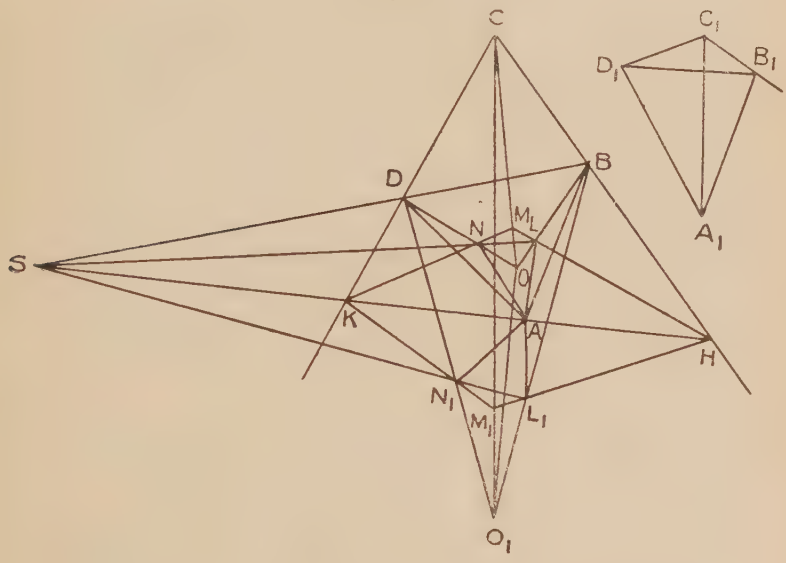

Cor. 1. There is *one* and only one real, non-degenerate solution—although apparently *two*—since the $\odot^s$ in (2) and (3) have one common pt., L_0, say, on CB, which is such that $\widehat{AL_0C} = \widehat{A_1B_1C_1}$. This degenerate case must be excluded. [There is another such degenerate case (not included) corresponding to a position of N on CD, N_0, say, which is such that $\widehat{AN_0C} = \widehat{A_1D_1C_1}$.] Thus O, ALMN, HAK are *uniquely* determined [*vide* Lemma 4].

[*Another method* consists in finding a figure similar to required one, etc., thus:—Take a str. line SA of any length to correspond to SA of fig. Then, because $\widehat{SDA}$, $\widehat{KDA}$ are known (hyp.), CD passes through a known pt. on the known $\odot$ SAD. Likewise MN, CB, ML pass though known pts. on the known $\odot^s$ SNA, SBA, SLA respectively. We have

now to construct the quadrilateral MHCK so that each of its sides shall pass through the corresponding one of said pts., so that the angles at M and C shall be equal to known ones, and so that, furthermore, the vertices at H and K shall lie on the basic line SA—which may be done readily by "double points" of involution etc.]

Cor. 2. The analogous problem for any one of the other vertices B, C, D yields the *same* pt. O.

Cor. 3. It is plain that $A_1B_1C_1D_1$ can be placed in similitude with ALMN, having O for centre, in *two* ways (conjointly forming a fig. having central symmetry w. r. to O), and that when it is so placed it (with aspect retained) is in perpective *in plano* with ABCD There being (Cor. 1) only *one* "*pt.* O", the problem in Lemma 4 is solved completely. *Two* solutions.

Cor. 4. All quads. *directly* similar to $A_1B_1C_1D_1$, when placed in perspective *in plano* with ABCD, have same centre of perspective, O, and their axes of perspective are lines ∥ HAK.

Theorem 1.—ALMN etc. being found as above, let it be tilted up unaltered through any angle about HAK for axis. BL, CM, DN still concur.

Proof.

DN (transversal of MKC) divides CM in ratio $-\frac{\overline{NK}}{\overline{MN}}\cdot\frac{\overline{DC}}{\overline{KD}}$

and

BL („ „ MHC) „ $\overline{CM}$ „ „ $-\frac{\overline{LH}}{\overline{ML}}\cdot\frac{\overline{BC}}{\overline{HB}}$,

but those ratios were *equal* before tilting, and they do not change clearly; ∴ BL, DN still divide $\overline{CM}$ (varying) in same ratio, *i. e.* cut it at *same* pt. Hence BL, CM, DN always concur. Q.E.D. [Otherwise since those lines are intersections of planes SDBLN, MKC, MHC.]

Cor. 1. CO : CM is constant.

Cor. 2. In particular when angle of tilt about axis HAK = 180°, we get on plane ABCD another quad. $A_1L_1M_1N_1$—reflexion of ALMN w. r. to HAK—satisfying conditions of Problem but for its *reversed* aspect.

Cor. 3—converse of Th. 1.—If ALMN be a quad. similar to $A_1B_1C_1D_1$ but in a plane different from that of ABCD and such that BL, CM, DN concur (at O, say), and if fig. ALMN be revolved unaltered about intersection of planes ABCD, ALMN—a str. line through A, of course—into the

position of *same* aspect as $A_1B_1C_1D_1$ on plane ABCD, *that* position is a solution of Problem.

Cor. 4. *All* the quads. satisfying requirements of Cor. 3 are found by revolving ALMN of Problem about the axis HAK [for if there were such a quad. not belonging to this assemblage, we could, (Cor. 3) by revolving it as in Cor. 3 into plane ABCD, get another solution of Problem, which is absurd (Cor. 1, Problem)].

Cor. 5. Since $MM_1 \perp HAK$ and $\overline{CO} : \overline{CM} :: \overline{CO_1} : CM_1$ (Cor. 1) $OO_1 \perp HAK$. O, O_1 depend only on *shape* of $A_1B_1C_1D_1$.

Cor. 6. In Cor. 3 the locus of O (intersection of BL, CM, DN) is a $\odot$ in space cutting plane ABCD at rt. $\angle^s$, for M describes such a $\odot$ by Cor. 4, C is fixed and $\overline{CO} : \overline{CM}$ is const. (Cor. 1). Q.E.D. Hence the theorem:—

Theorem 2.—A pyramid on a given quadrilateral base (ABCD) is such that plane sections of required shape ($A_1B_1C_1D_1$) * can be made on it (including part above apex). The locus of its apex (O, say) is a circle whose plane is perpendicular to plane of ABCD and whose centre lies on it. [It is the $\odot$ on OO_1 of above fig. before tilt, as diameter. HAK is $\perp$ plane of $\odot$.]

Note 1. (i.) Th. 1 etc. may be stated thus:—If one (BCD) of any two triangles (BCD, LMN) in perspective on a plane be kept fixed whilst the other (LMN) revolves about the axis of perspective (HKS), they are in perspective still in space and the centre of perspective (O) moves on a $\odot$ cutting plane of fixed one at rt. $\angle^s$.

(ii.) The same is true for *polygons* in *complete* perspective *in plano*. [This follows readily from (i.).]

(iii.) In particular (as in Cor. 2, Th. 1) when two figs. are in perspective in plano, so is either of them and the reflexion of the other w. r. to perspective axis.

(iv.) When two plane figs. are in perspective in space and one be kept fixed whilst the other is revolved about the intersection of their planes into a new position (*two* such, with different aspects) on plane of the fixed fig., they will be still in perspective (*in plano*).

Theorem 3.—If $A_1'B_1'C_1'D_1'$ be the quad. $A_1B_1C_1D_1$ placed in a position in perspective in space (fig. 4) with ABCD (fixed), the locus of O (centre of perspective) is $\odot$ cutting plane ABCD at O, O_1 orthogonally (Th. 2). Then shall the intersection of planes $A_1'B_1'C_1'D_1'$, ABCD

* See Note 4 below.

be a *fixed* line, which will be an *axis of pure rotation* for $A_1'B_1'C_1'D_1'$. [The section $\parallel A_1'B_1'C_1'D_1'$ through A, of O(ABCD) $\equiv$ ALMN, (Cor. 4, Th. 1) which is constant. Hence $\overline{AA_1'} : \overline{A_1'O}$ is constant; so, too, $B\overline{B_1'} : \overline{B_1'O}$ etc., and $\therefore$ (by transversals) the *constant* lines $\overline{AB}$, $\overline{A_1'B_1'}$ cut one other (produced if necessary) in *constant* segments; so, too, $\overline{B_1'C_1'}$, $\overline{BC}$, etc. But ABCD is fixed, $\therefore$ etc. Q.E.D.] Compare Note 1.

Fig. 4.

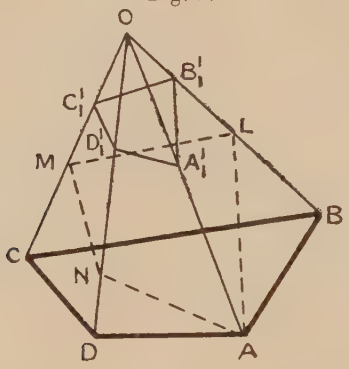

Note 2. (i.) $A_1B_1C_1D_1$ can (Cor. 3, Prob.) be placed with unchanged aspect in *plane* perspective with ABCD in *two* ways ($A_1'B_1'C_1'D_1'$, $A_1''B_1''C_1''D_1''$, say) having common centre of perspective O, but different axes H'K', H''K'', which are $\parallel$ HAK; and likewise for *changed* aspect in two *other* ways having common centre O_1, but the axes H'K', H''K'' are the same for *both* aspects since the reflexions of $A_1'B_1'C_1'D_1'$, $A_1''B_1''C_1''$, D_1'' w. r. to H'K', H''K'' respectively supply [by (iii.), Note 1] the solutions for reversed aspect. Now, revolving $A_1'B_1'C_1'D_1'$ about H'K', and $A_1''B_1''C_1''D_1''$ about H''K'', AA_1', BB_1', CC_1', DD_1' always concur, and so AA_1'', BB_1'', CC_1'', CD_1'' [by (ii.), Note 1] —the pts. of concurrency moving on the above circle cutting plane ABCD at rt. $\angle^s$ at OO_1. If the planes be kept *parallel* when moving, the pts. of concurrency coincide (at O, say), making (equal) sections *diametrically opposite to each other* w. r. to apex O on the *now common* pyramid O(ABCD).

We thus have a mode of generating *all* the "quads. $A_1'B_1'C_1'D_1'$" of Th. 3.

(ii.) All sections of O(ABCD) [fig. 4] parallel to $A_1'B_1'C_1'D_1'$ cut plane ABCD in $\parallel$ lines and are similar.

Revolving [as in (iv.), Note 1] each into position of same aspect on plane ABCD, we get again the theorem of Cor. 4 of Problem.

Application to Photography.

Theorem.—Theorem 2 has the practical application :—"The locus of the pt at which a camera-man must have the lens of his instrument so as to be able to take a photograph of required shape (quadrilateral) of a given quadrilateral lamina (the corresponding vertices of the quads. being assigned) is a circle in space cutting lamina at rt. angles."

Thus to take a photograph of ABCD similar to $A_1B_1C_1D_1$ of fig. 3, the lens must be on the ⊙ cutting plane of papers orthogonally at O, O_1. Let it be at O, in space. The corresponding pt. M is then determined from Cor. 1, Th. 1, and thence the plane MHK, to which the sensitive plate of camera must be parallel.

Note 3. If one quad. be transverse, or re-entrant, so must the other and in a *corresponding* way. *Photography* as such demands this, but *Geometry* does not. So that photography (as required) be possible for case just referred to, it is necessary that sections of required shape $A_1B_1C_1D_1$ can be taken of O(ABCD) without having recourse to part produced through O.

Note 4. It is assumed throughout that A corresponds to A_1, B to B_1, C to C_1 and D to D_1.

Note 5. A photo of required triangular shape, of a given triangle, may be taken from any pt. But from no pt. can one of given shape be taken of a plane pentagon. Quadrilaterals supply the interesting cases.

After deducing above theorems I learned that I had been virtually anticipated by Möbius (see Cremona's 'Elements of Projective Geometry,' English trans. by Leudesdorf (1893), p. 12, where the subject is presented in another light). For other methods of placing quadrilaterals in perspective, see that treatise, pp. 82–84.

Caltra, Claremorris,
Ireland.

IV. *On the Origin of Terms of the Spectrum of Cobalt.* *By* N. K. Sur, *Department of Physics, University of Allahabad* *.

THE recent work of Russell and Saunders †, Pauli ‡, Heisenberg §, and Hund ‖ on the origin of the fundamental spectral terms of elements of the periodic table marks a definite stage in the development of the theory of complex spectra. Very recently R. H. Fowler and Hartree ¶, Laporte **, McLennan, McLay, and H. G. Smith †† have applied these ideas to account for the nature of the spectral terms of several elements. These ideas have been further developed by Professor Saha ‡‡ to explain not only the nature of the fundamental but also of the other higher terms of the spectrum of Neon and alkaline earths. As pointed out by the writer himself, these ideas can be extended to all elements. The modifications introduced by Dr. Saha have also been fruitful in accounting for the anomalous terms of the alkaline earths. As the fundamental ideas have been discussed by these writers, it is unnecessary to repeat them here. Only a brief explanation of the symbols and the modifications introduced will be given here.

Ths chief modification introduced by Prof. Saha is in indicating the electron configuration of the atoms of different elements of the periodic table by a method slightly different from the Bohr-Stoner system. This is shown in Chart 1.

We now pass on to a brief discussion of the method of representation in the chart. The number below each level M denotes the total number of electrons required to fill up the level completely. As is evident, instead of splitting a level like L_2 or M_2 into two levels L_{21}, L_{22} or M_{21}, M_{22} containing two and four electrons respectively, we represent them as single levels for optical spectra with their complete quota of electrons. This merely suggests the idea that for optical spectra, as distinguished from

* Communicated by Prof. M. N. Saha, D.Sc., F.I.P.
Saunders and Russell, Astrophys. Journ. lxi. p. 38 (1925).
‡ Pauli, *Zs. f. Phys.* xxxi. p. 765 (1925).
§ Heisenberg, *Zs. f. Phys.* xxxii. p. 841 (1925).
‖ Hund, *Zs. f. Phys.* xxxiii. p. 345, and xxxiv. p. 296 (1925).
¶ R. H. Fowler and Hartree, Proc. Roy. Soc. cxi. p. 83 (1926).
** Laporte, Journ. Opt. Soc. Amer. xiii. p. 1 (1926).
†† McLennan, McLay, and Smith, Proc. Roy. Soc. lxxvi. p. 112 (1926).
‡‡ Saha, Phil. Mag., June 1927, p. 1265.

CHART 1, showing Structure of Atoms.

X-ray spectra, the probability of the occurrence of the electrons in either of the sub-levels M_{21}, M_{22} in which M_2 can be divided is the same. This simplification in the system of representing the levels is of great utility in

unravelling the origin of terms in any optical spectrum, complicated or simple, as will be shown later on.

The chart is self-explanatory as regards the formation of the atoms (3) Li to (10) Ne by successive filling up of L levels, and from (11) Na to (18) A by the closing up of M levels. The further successive addition of two fresh electrons leads us to the formation of K and Ca. Any fresh electron now introduced will pass on to the M_3 level. The formation of the atoms of the first transitional group of elements from (21) Sc to (28) Ni is thus accounted for by the simple process of successive introduction of new electrons in the M_3 level, while the N_1 level contains 2 electrons. The only exception is in the case of (24) Cr, which contains 1 electron in the N_1 level and has 5 electrons in the M_3 level. Similarly, we can pass on to other elements. It is also clear from the chart how the atoms of different transitional groups of elements are formed, and how the alkalies and alkaline earths persist throughout the whole system.

The above also explains the reason of assigning N_1 below M_2 in the same vertical column. As mentioned above for the formation of the atoms of K and Ca, we have to bring in two fresh electrons one after the other after the M_2 level has been filled up. These two electrons occupy the N_1 level, and not the M_3 level. Hence the negative energy value of the electron corresponding to N_1 is greater than M_3, at least for optical levels. For the electrons in the interior of the atom, *i.e.* for X-ray levels, this is, however, not true, and the negative energy in M_3 is larger than the negative energy in N_1. But for optical levels, the energy in N_1 is sometimes greater, sometimes less, and generally of the same order of magnitude as M_3. Transition also takes place from M_2 either to M_3 or to N_1. To indicate this fact, N_1 is put below M_2 and not after M_3 as is usually done. Thus

$$\begin{aligned} (K_1) \;>\; (L_1) \;&>\; (L_2),\ (M_1) \\ &>\; (M_2),\ (N_1) \\ &>\; (M)_3,\ (N_2),\ (O_1) \\ &\quad \text{etc.,} \end{aligned}$$

where (X) denotes the negative value of energy corresponding to the level. But though this is usually the rule, in certain cases, *e.g.* in Sc^+, the negative energy in the M_3 level is larger than the energy in the N_1 level.

To illustrate the utility of this chart to account for the terms of any optical spectrum, we start with a structure diagram for Potassium K (19):

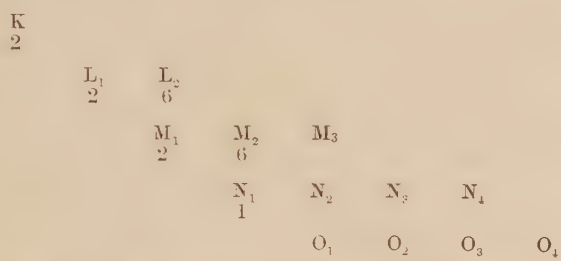

According to the fundamental assumption of Pauli, a single electron occupying any orbit by itself is to have a doublet character. Consequently the term which originates when the valence electron is occupying the N_1 level, which is the normal configuration of the electron in the atom, is $^2S_1$. We can write it as $1\,^2S_1$, which denotes that it is the first term of the S series. Transitions of the electron can take place either horizontally or vertically by one step; that is, it may pass on to N_2, and thence either to M_3, or to N_2 or to O_1. When the electron is at N_2, the terms $1\,^2P_{1,2}$ originate corresponding to the azimuthal quantum number $K=2$. At N_3 it gives rise to the terms $1\,^2D_{2,3}$, and at O_1 to $2\,^2S_1$, which forms the second Rydberg sequence to the S series. It should be noted that transitions cannot usually take place in a slanting direction, such as from N_1 to O_1, unless the selection principle is violated. Transitions of an electron by three steps such as from $N_1 \rightarrow N_2 \rightarrow O_1 \rightarrow O_2$ are also possible, for it corresponds to $1\,S-1\,P+1\,P-2\,S+2\,S-2\,P$, *i. e.* from $1\,S-2\,P$.

As mentioned above, the structure diagram also gives a rough indication of the values of successive terms. Thus

$$\begin{aligned} 1\,^2S_1 &> 1\,^2P_{1,2},\ 2\,^2S_1, \\ &> 1\,^2D_{2,3},\ 2\,^2P_{1,2},\ 3\,^2S_1, \\ &> 1\,^2F_{3,4},\ 2\,^2D_{2,3},\ 3\,^2P_{1,2},\ 4\,^2S_1, \end{aligned}$$

and so on. The terms in the same vertical column have also roughly the same order of values.

It is necessary at this stage to discuss in some detail the utility of this structure diagram of atoms in identifying without any ambiguity the terms forming a Rydberg

sequence. For this purpose we make use of the structure diagram of Ca :

K						
2						
	L_1	L_2				
	2	6				
		M_1	M_2	M_3		
		2	6			
			N_1	N_2	N_3	N_4
			2			
				O_1	O_2	O_3 .....
					P_1	P_2 .....
						Q_1 .....

If we fix one of the two valence electrons in the N_1 level and make the other run through successive higher levels in a diagonal direction, we obtain the following terms :—

N_1N_1	N_1O_1	N_1P_1	N_1Q_1	N_1R_1
$1\,^1S_0$	$2\,^1S_0$	$3\,^1S_0$	$4\,^1S_0$	$5\,^1S_0$
	$2\,^3S_1$	$3\,^3S_1$	$4\,^2S_1$	$5\,^3S_1$

Here the terms of the same multiplicity such as $1\,^1S_0$, $2\,^1S_0$, $3\,^1S_0$ or $2\,^3S_1$, $3\,^3S_1$, etc. form a Rydberg sequence. Similarly the p-sequence is formed from the combinations :

N_1N_2	N_1O_2	N_1P_2	N_1Q_2	N_1R_2
$2\,^1P_1$	$3\,^1P_1$	$4\,^1P_1$	5^1P_1	$6\,^1P_1$
$2\,^3P_{0,\,1,\,2}$	$3^3P_{0,\,1,\,2}$	$4^3P_{0,\,1,\,2}$	$5\,^3P_{0,\,1,\,2}$	$6\,^3P_{0,\,1,\,2}$

We have taken the total quantum number of the first p term $=2$, because the running electron starts from N_2 level having the total quantum number 2. For the d-sequence also the total quantum number will not be 3 but 2, because the starting level M_3 of the running electron has the total quantum number 2.

Thus

N_1M_3	N_1N_3	N_1O_3	N_1P_3
$2\,^1D_2$	$3\,^1D_2$	$4\,^1D_2$	
$2\,^3D_{1,\,2,\,3}$	$3\,^3D_{1,\,2,\,3}$	$4\,^3D_{1,\,2,\,3}$	

But in the case of Mg the first D term has the total quantum number 3, as a glance at the structure diagram of Mg will show.

It is to be emphasized here that we have assigned the total quantum number 1 to the N_1 level, where the shell is

completed in this case. This is not in accordance with Bohr; but this method of writing the structure diagram clears the point regarding the initial value of m in a Rydberg sequence more in accordance with the usual practice, though Bohr's method gives a uniform notation to both X-ray and optical spectra.

It should be mentioned that the terms like $3\,^1S_0$ and $3\,^3S_1$, or $4\,^1S_0$ and $4\,^3S_1$, which originate from the combination of electrons in the same level or levels, do not combine with each other: also two terms like $1\,^1S_0$ and $2\,^1S_0$ show some deviation from an exact Rydberg sequence owing to the presence of 2 electrons in the same level. This deviation is not well pronounced in the case of alkalies.

We have not explained here how to arrive at the terms which result either from the presence of more than one electron in the same level or from a combination of two or more electrons in two different levels; nor have we explained the case of simultaneous displacement of two electrons from their normal position. The nature of small positive or negative terms which result from simultaneous movements of two electrons has been fully discussed by Dr. Saha in a paper communicated to this journal. The other points will be illustrated with reference to Cobalt. But before we pass on to it, we have to explain briefly the symbols which are necessary for this purpose.

By a comparison of the various systems of symbols used by different writers, Laporte* considers Sommerfeld's system of notation to be more convenient than those of others. Hence, while retaining the usual symbol n^r_{kj} of Landé for each spectral term, we adopt Sommerfeld's notation with a slight change as has been done by Prof. Saha. Thus

I_r stands for Sommerfeld's j_s,

I_k stands for Sommerfeld's j_k,

and I_j denotes the effective quantum number.

In n^r_{kj}, r stands for the multiplicity of the term, k and j for the azimuthal and inner quantum numbers respectively, and n for the total quantum number.

Thus

$$I_r = j_s = \frac{r-1}{2} = 0,\ \tfrac{1}{2},\ \tfrac{2}{2},\ \tfrac{3}{2}, \ldots$$ for singlets, doublets, triplets, etc.,

$I_k = k-1 = 0, 1, 2, 3$ for $s, p, d, f \ldots$ terms etc.,

* Laporte, *loc. cit.*

and I_j = vector sum of I_r and I_k in the quantum sense, *i. e.* it has all successive whole or half-numbered values lying between $|I_r + I_k|$ and $|I_r - I_k|$.

We are now ready to discuss the origin of terms in the spectrum of CoI.

We start with the structure diagram of Cobalt (27).

K						
2						
	L_1	L_2				
	2	6				
		M_1	M_2	M_3		
		2	6	7		
			N_1	N_2	N_3	N_4
			2			
				O_1	O_2	O_3

According to Bohr and Stoner the most stable configuration of the electrons in the Cobalt atom is to have seven electrons in the M_3 and two in the N_1 level. But other configurations like eight electrons in the M_3 and one in the N_1 level or all the nine electrons in the M_3 level are also possible. To deduce the terms which arise from more than one electron in any level like 9 in M_3 or 8 in M_3, we have to make use of the principles formulated by Heisenberg, Pauli, and Hund. By introducing two magnetic quantum numbers m_1 and m_2 corresponding to weak or strong magnetic fields, and making use of the rule laid down by Pauli that for the orbits of two electrons characterized by the same values of the quantum numbers n and k, both the associated magnetic quantum numbers m_1 and m_2 cannot be the same, it is possible to calculate the terms which arise from the presence of more than one electron in any level. As this has been done by the previous writers, and specially by Laporte with lucidity, it is unnecessary to repeat the process here. The terms originating from different numbers of electrons in N_2 or N_3 orbits are given in two tables by Laporte*. Making use of his results, we find the terms resulting from the presence of nine electrons in the M_3 level to be ^2D. Next, to calculate the terms arising from 7 electrons in the M_3 level and 2 in the N_1, we note that the N_1 level has got its complete quota of electrons, for the total number N of electrons that can occupy an orbit characterized by the quantum numbers n and k is $N = 2(2k-1)$. The term resulting from the maximum number of electrons in any level such as 2 in the N_1, 6 in the N_2, or

* Laporte, *loc. cit.*

10 in the N_3 level is always $^1S_0$. If we combine this $^1S_0$ term with the terms which arise from the presence of 7 electrons in the M_3 level, the resulting effect is just the same as that due to 7 electrons in the M_3 shell. Thus from Laporte's table we have the following terms from this configuration :

$$^4F \quad ^4P \quad ^2H \quad ^2G \quad ^2F \quad ^2D \quad ^2D \quad ^2P.$$

Another possible metastable configuration of the electrons of the Cobalt atom is to have 8 electrons in the M_3 level and 1 in the N_1 level. We find from Laporte's above-mentioned table that the terms due to 8 electrons in the M_3 ring are

$$^3F \quad ^3P \quad ^1G \quad ^1D \quad ^1S.$$

To calculate the terms due to the combination of 8 electrons in the M_3 shell and 1 in the N_1 we proceed simply as follows, as Pauli's principle of exclusion does not hold in this case :—

	$I_r = \frac{r-1}{2}$.	$I_k = k-1$.	
^3F	$\frac{2}{2}$	3	$\therefore \ r = 4, 2; \ k = 4.$
			$\therefore$ the terms are ^4F, ^2F.
$1N_1$	$\frac{1}{2}$	$\frac{0}{3}$	
	$\frac{3}{2}, \frac{1}{2}$		
^3P	$\frac{2}{2}$	1	$\therefore \ r = 4, 2; \ k = 2.$
			$\therefore$ the terms are ^4P, ^2P.
$1N_1$	$\frac{1}{2}$	$\frac{0}{1}$	
	$\frac{3}{2}, \frac{1}{2}$		
^1G	0	4	$\therefore \ r = 2; \ k = 5.$
			$\therefore$ the term is ^2G.
$^1N_1$	$\frac{1}{2}$	$\frac{0}{4}$	
	$\frac{1}{2}$		

Similarly the terms from other combinations are ^2D and ^2S. Collecting all the terms from these three configurations we write thus:

(*a*) $9M_3$ $\quad ^2\overline{D}$,

(*b*) $7M_3$–$2N_1$ $\quad ^4F \ ^4P \ : \ ^2H \ ^2\overline{G} \ ^2F \ ^2\overline{D} \ ^2\overline{D} \ ^2P$,

(*c*) $8M_3$–$1N_1$ $\quad ^4F \ ^4P \ :$
$^2F \ ^2P \ : \quad ^2\overline{G} \ ^2\overline{D} \ ^2\overline{S}$

These three states (*a*) (*b*) (*c*) may be termed as equivalent states. It is not possible to pass from any one of these states to any other by a transition of one step either vertically or

horizontally. So the terms from any one state cannot combine with those from any other. This is exactly borne out by the classification of the spectrum of CoI by Catalan and Bechert *. Also the terms such as F, D, P, etc. from any one state, say (*b*), cannot enter into combination. To denote this possibility we have dashed the alternate set of terms as shown above. We could have dashed the remaining set of terms and kept ^{2}G, ^{2}D, ^{2}D from state (*b*) undashed. As the terms from these three states do not combine with each other, we have to dash the terms with the same designation from the other states also. It is therefore merely a matter of convention, the real significance being that S, P or P, D, or D, F terms arising from the same configuration of electrons in an atom possess identical combinatory powers as regards other levels and therefore they cannot combine with each other.

According to the principles developed by Pauli, Heisenberg, and Hund, we note that if in a group of terms resulting from a given electron configuration there are terms having the same value of k but with different multiplicities, the one with the highest multiplicity will be deepest ; also if there are terms of the same multiplicity but with different values of k, that with the highest k will be the deepest. Combining these two rules, we find that of the terms from (*b*) and (*c*) ^{4}F will be the deepest term in each case. We identify the ^{4}F term from the state $7M_3$–$2N_1$ with the deepest ^{4}F term as found by Catalan and Bechert, as, according to Bohr and Stoner, this is the most stable configuration of the electrons in the Cobalt atom. The terms next in order are ^{4}F and ^{2}F from $8M_3$ and $1N_1$. That this state is equally probable is shown by the fact that the terms ^{4}F and ^{2}F, both of which result from the combination $(^3F+1N_1)$, appear in the spectrum of Cobalt and their value is very little different from the fundamental ^{4}F. Neither the term $^2\overline{D}$ from state (*a*) nor the other terms from states (*b*) and (*c*) have been identified by Catalan and Bechert. We are not in a position to state whether the state (*a*) exists at all or not. The other terms from (*b*) and (*c*) also have not been identified by Catalan and Bechert. Probably they do not appear at all, but as yet we are unable to account for the preference of certain sets of terms over others.

The terms from the states (*b*) and (*c*) which correspond

* Catalan and Bechert, *Zs. f. Phys.* xxxii. p. 336 (1925).

to the terms discovered by Catalan and Bechert are shown in Table I.

Next we consider the two equivalent states

$$(d) \quad 7M_3\text{–}1N_1\text{–}1N_2$$

and

$$(e) \quad 8M_3\text{–}1N_2.$$

The electron configurations in (d) and (e) can result either from a single-step transition of an electron or from three-step transition from (a), (b), and (c). Thus from (a) an electron can pass in two steps to the N_1 level and another can pass on to the N_2 level in one step, resulting in the state (d) $7M_3\text{–}1N_1\text{–}1N_2$. Similarly the other transformations can be effected. To arrive at terms corresponding to (d) we first find the terms due to the combination of $1N_1$ and $1N_2$, remembering that each electron when occupying a level by itself has a doublet character. Thus:

	l.	l_k	
$1N_1$	$\frac{1}{2}$	0	$\therefore \; r = 3, 1; \quad k = 2.$
			$\therefore$ the terms are
$1N_2$	$\frac{1}{2}$	1	^3P and ^1P.
	$\frac{2}{2} \quad \frac{0}{2}$	1	

Of the terms from $7M_3$ we need only consider the ^4F term, as this is the deepest term, and combinations with this term would be more probable than with others. R. H. Fowler and Hartree* have shown that in the spectrum of O^+, where the orbit given by the running electron has to be combined with the orbits given by $2L_2$, all terms arising from $2L_2$ have to be considered. The most important term is $^3P_{0,1,2}$, and this gives the most important terms. The next combinations are $^1S_0$ and $^1D_2$, and terms arising from these levels are also present. Similarly, taking the ^3F term only out of the terms due to 8 electrons in the M_3 level, and, following the process detailed above, we arrive at the following sets of terms:—

(d) $7M_3\text{–}1N_1\text{–}1N_2$.

$$^4F + {}^3P = \begin{cases} {}^5G & {}^5F & {}^5D, \\ {}^4G & {}^4F & {}^4D, \\ {}^3G & {}^3F & {}^3D, \end{cases}$$

$$^1F + {}^1P = \quad {}^1G \quad {}^1F \quad {}^1D$$

(e) $8M_3\text{–}1N_2$.

$$^3F + {}^2P = \begin{cases} {}^4G & {}^4F & {}^4D, \\ {}^2G & {}^2F & {}^2D. \end{cases}$$

* R. H. Fowler and Hartree, Proc. Roy. Soc. cxi. (1926).

We have dashed the F terms to express the fact that these F terms combine with those from the states (*a*), (*b*), and (*c*). The other terms G and D combine with those from (*a*), (*b*), and (*c*) according to the usual rules of the selection principle. As (*d*) and (*e*) are equivalent states, the terms from (*d*) cannot combine with those from (*e*). Of the terms from (*d*), ^{6}G should be the deepest, but from the analysis of the spectrum of CoI we find that $^6\bar{\mathrm{F}}$ is the deepest of the group, and ^{6}D, ^{6}G terms are approximately of the same order.

An exception to the selection principle * $r+2$, r, $r--2$, governing the combination between terms of different multiplicity, has been noted by Catalan and Bechert. They have discovered a line due to the combination of a doublet $\bar{\mathrm{F}}$ term and a sextet $\bar{\mathrm{F}}$ term, *i. e.*, the line $\lambda=6143{\cdot}78$, $\mathrm{F}_3^1-\bar{\phi}_3^1$. Because the ^{6}F or $\bar{\phi}$ term from (*d*) can combine with the ^{2}F or F^1 term from (*c*), this apparent anomaly is explained.

As the ^{4}F from (*b*) is the deepest term, and the next deeper term with which ^{4}F can combine is $^6\bar{\mathrm{F}}$ from (*d*), resonance lines will also be due to the combination of these two sets of terms, as has been mentioned by Catalan and Bechert; but this will correspond to the line $1\mathrm{S}-2p_2$, $\nu=15210$ of Calcium, and not to 1S–2P, $\nu=23652$, which usually appears with great prominence in the absorption spectrum of the unexcited vapour of the metal.

All the terms from (*d*) and (*e*) have been identified by Catalan and Bechert, and are shown in Table I.

Finally, we come to the equivalent states :

(*f*) $7\mathrm{M}_3$—$1\mathrm{N}_1$—$1\mathrm{O}_1$,

(*g*) $7\mathrm{M}_3$—$1\mathrm{N}_1$—$1\mathrm{N}_3$,

(*h*) $8\mathrm{M}_3$—$1\mathrm{O}_1$,

(*i*) $8\mathrm{M}_3$—$1\mathrm{N}_3$.

* It may be emphasized that in the rule for transition given here—*i. e.* such transitions from a certain state to some other state are possible as are obtained by displacing an electron an odd number of times, the displacement being either vertically or horizontally (but never diagonally).—all apparent deviations from the selection principle are explained. Every one of the two sets of terms arising from such states will combine with the other, if the selection principle for the inner quantum number is satisfied, no matter whatever may be the multiplicity or the azimuthal quantum number of the two sets.

TABLE I.

State and term from structure diagram.	Term designation according to Catalan & Bechert.	Combining terms.
(*b*) ^{4}F	f_5^1—f_2^1	$^dD^1$ $^eD^2$ $^dF^1$ $^e\bar{F}^2$ $^dG^1$ $^eG^2$ $^df^1$ $^df^2$ $^ef^3$ $^d\bar{f}^1$ $^d\bar{f}^2$ $^e\bar{f}^3$ $^dg^1$ $^dg^2$ $^eg^3$ $^d\delta^1$ $^d\bar{\phi}^1$ $^d\gamma^1$
(*c*) ^{4}F	f_5^2—f_2	$^dD^1$ $^eD^2$ $^dF^1$ $^e\bar{F}^2$ $^dG^1$ $^dG^2$ $^df^1$ $^df^2$ $^ef^3$ $^d\bar{f}^1$ $^d\bar{f}^2$ $^e\bar{f}^3$ $^dg^1$ $^dg^2$ $^eg^3$ $^d\delta^1$ $^d\bar{\phi}^1$ $^d\gamma^1$
(*c*) ^{2}F	F_4^1—F_3^1	$^dD^1$ $^eD^2$ $^d\bar{F}^1$ $^e\bar{F}^2$ $^dG^1$ $^dG^2$ $^df^1$ $^df^2$ $^ef^3$ $^d\bar{f}^1$ $^d\bar{f}^2$ $^ef^3$ $^dg^1$ $^dg^2$ $^d\bar{\phi}^1$
(*b*) ^{4}P	p_3^1—p_1^1	$^eD^2$ $^d\bar{F}^1$ $^df^1$ $^df^2$ $^ef^3$ $^e\bar{f}^3$
(*c*) ^{4}P	p_3^2—p_1^2	$^dD^1$ $^eD^2$ $^d\bar{F}^1$ $^e\bar{F}^2$ $^df^1$ $^df^2$ $^ef^3$ $^d\bar{f}^1$ $^d\bar{f}^2$ $^e\bar{f}^3$
(*c*) ^{2}P	P_2^1 ?	$^dD^1$ $^eD^2$ $^d\bar{F}^1$ $^e\bar{F}^2$ $^df^1$ $^df^2$ $^ef^3$ $^d\bar{f}^1$ $^d\bar{f}^2$ $^e\bar{f}^3$
(*d*) ^{6}F	$\bar{\phi}_6^1$—$\bar{\phi}_2^1$	$^dF^1$ $^bf^1$ $^cf^2$ $f\phi^1$
(*d*) ^{6}D	$\bar{\delta}_5^1$—$\bar{c}_1^1$	$^bf^1$ $^cf^2$ $f\phi^1$
(*d*) ^{6}G	γ_7^1—γ_2^1	$^bf^1$ $^c\bar{f}^2$ $f\phi^1$
(*d*) $^4\bar{F}$ (From ^{4}F+^{3}P.)	$\bar{f}_5^1$—$\bar{f}_2^1$	$^dP^1$ $^cF^1$ $^bp^1$ $^cp^2$ $^bf^1$ $^cf^2$ ff^3
(*d*) ^{4}G (From ^{4}F+^{3}P.)	g_6^1—g_3^1	$^cF^1$ $^bf^1$ $^cf^2$ ff^3
(*d*) ^{4}D (From ^{4}F+^{3}P.)	d_4^1—d_1^1	$^cp^1$ $^cF^1$ $^bp^1$ $^cp^2$ $^bf^1$ $^cf^2$ ff^3
(*d*) ^{2}G	G_5^1—G_4^1	$^cF^1$ $^bf^1$ $^cf^2$ ff^3
(*d*) $^2\bar{F}$	$\bar{F}_4^1$—$\bar{F}_3^1$	$^cp^1$ $^cF^1$ $^bp^1$ $^cp^2$ $^bf^1$ $^cf^2$ ff^3 $^dd^1$ $^dd^2$ $^ed^3$
(*d*) ^{2}D	D_3^1—D_2^1	$^cp^1$ $^cF^1$ $^cp^2$ $^bf^1$ $^cf^2$
(*d*) ^{4}D (From ^{4}F+^{1}P.)	d_4^2—d_1^2	$^cP^1$ $^cF^1$ $^bp^1$ $^cp^1$ $^bf^1$ $^cf^2$ ff^3
(*d*) ^{4}G (From ^{4}F+^{1}P.)	g_6^2—g_3^2	$^cF^1$ $^bf^1$ $^cf^2$ ff^3
(*d*) ^{4}F (From ^{4}F+^{1}P.)	$\bar{f}_5^2$—$\bar{f}^2$	$^cp^1$ $^cF^1$ $^cp^2$ $^bf^1$ $^cf^2$ ff^3
(*e*) ^{2}G	G_5^2—G_4^2	$^cF^1$ $^bf^1$ $^cf^2$
(*e*) $^2\bar{F}$	$\bar{F}_4^2$—$\bar{F}_3^2$	$^cP^1$ $^cF^1$ $^cp^2$ $^bf^1$ $^cf^2$
(*e*) ^{2}D	D_3^2—D_2^2	$^cP^1$ $^cF^1$ $^bp^1$ $^cp^2$ $^bf^1$ $^cf^2$
(*e*) ^{4}D	d_4^3—d_1^3	$^cp^1$ $^cF^1$ $^bp^1$ $^bf^1$ $^cf^2$
(*e*) $^4\bar{F}$	$\bar{f}_5^3$—$\bar{f}_2^3$	$^cP^1$ $^cF^1$ $^bp^1$ $^cp^2$ $^bf^1$ $^cf^2$
(*e*) ^{4}G	g_6^3—g_3^3	$^bf^1$ $^cf^2$
(*f*) ^{6}F (From ^{4}F+^{3}S$_1$.)	ϕ_6^1—ϕ_1^1	$^d\delta^1$ $^d\bar{\phi}^1$ $^d\gamma^1$
(*f*) ^{4}F (From ^{4}F+^{3}S$_1$.)	f_5^3—f_2^3	$^dF^1$ $^dG^1$ $^eG^2$ $^dd^1$ $^dd^2$ $^df^1$ $^df^2$ $^dg^1$ $^dg^2$ $^d\delta^1$ $^d\phi^1$ $^d\gamma^1$

N.B.—In a term like $^dD^1$, *d* denotes the state from which the term originates, and D^1 is the term designation according to Catalan and Bechert.

The terms corresponding to these states may be easily found according to the method sketched before. Here we need only consider the terms from (f), as they are of special interest in tracing out the Rydberg sequence. The terms due to 1 electron in the N_1 level and 1 in the O_1 level are $^3S_1$ and $^1S_0$ respectively. Taking into account the ^4F term only from the $7M_3$ state, we get the following terms :

$$(f) \qquad {}^4F+{}^3S_1 = {}^6F, \quad {}^4F, \quad {}^2F,$$
$$\qquad\qquad {}^4F+{}^1S_0 = \qquad {}^4F.$$

These F terms will be undashed, as they combine with the F terms from (d) and (e). The terms ^6F and ^4F from $^4F+{}^3S$ have been identified as shown in Table I., but the remaining terms ^2F and ^4F have not been discovered. The state (b) $7M_3-2N_1$ is equivalent to $7M_3+{}^1S_0$, and hence $^4F+{}^1S_0$ from (f) will form a Rydberg sequence to the term $^4F+{}^1S_0$ from (e). This term has not yet been identified, but its value will roughly be of the same order as ^4F from (f).

Though the ionization potential of Cobalt cannot be correctly estimated until the term $^4F+{}^1S_0$ from (f) has been discovered, yet we can have a close estimate of it from the fact that the value of this term is approximately of the same order as $^4F+{}^3S_0$ from (f). We shall not be much in error if we take $^4F+{}^3S_0$ from the state (f) as the Rydberg sequence to $^4F+{}^1S_0$ from (b). The ionization potential is thus obtained as approximately 8·51 volts, which is only a lower limit, the actual value being slightly greater.

This work, therefore, points out that in the analysis of the arc spectrum of Cobalt as yet only a number of fundamental levels and some levels combining with these have been found. No Rydberg sequence has been discovered, but, as will be shown in a separate communication, better progress has been made in the case of Iron, where higher sequences have been correctly guessed by Laporte. Finally, it remains to be settled whether the $9M_3$ state is possible or not; for though according to Bohr and Stoner $7M_3-2N_1$ is the most stable configuration of the electrons in the Cobalt atom, the terms due to $8M_3-1N_1$ state occur prominently in the arc spectrum of Cobalt. Further work is being done in this direction.

In conclusion I wish to record my best thanks to Professor

Saha for suggesting this problem to me, and for the interest taken in the work.

Allahabad,
October 1926.

Addendum.—It may be mentioned here that some of the doublet terms arising out of the states (*b*) and (*c*) and terms of higher multiplicity from the states (*f*), (*g*), (*h*), etc., have been identified. Further analysis has also led to the identification of the Rydberg Sequence as mentioned before. These results will be published in a separate paper.

Allahabad,
May 1927.

V. *The Geissler Discharge in Argon.* *By* K. G. Emeléus, *M.A., Ph.D., Demonstrator in Physics, and* N. L. Harris, *B.Sc., King's College, University of London* *.

1. *Introduction.*

When an exploring electrode, or *collector*, is placed in the path of an electric discharge, its surface becomes covered with a layer often visibly different from the remainder of the ionized gas. The outer boundary of the sheath, which is a region of space-charge, marks the limit of the disturbing effect of the collector. It follows that a study of the current-potential characteristic of the latter will yield precise information about the potential of the surrounding space, and about the number and nature of the ions [1]. This method has been applied with considerable success to arcs in mercury vapour and other gases, to glow discharges from a hot filament, and to the scattering of electrons, and its validity and range of application have been dealt with theoretically in some detail [2]. It may also be used, as would be expected, to analyse the glow discharge from a cold cathode, and the present experiments are an extension of preliminary work in this field [3].

The number of variables in this type of discharge is large. We have confined our attention for the present to conditions

* Communicated by Prof. E. V. Appleton, D.Sc.

[1] Langmuir, Journ. Franklin Inst. 196, p. 751 (1923).

[2] Langmuir & Mott-Smith, Phys. Rev. xxviii. p. 727 (1926).

[3] Emeléus, Proc. Camb. Phil. Soc. xxiii. p. 531 (1927).

not very different from those corresponding to a normal cathode fall of potential, with a gas-pressure of the order of 1 mm. Hg, potentials of about 250 volts, and current densities of 0·1 milliampere per sq. cm. The cathode dark space is then less than a cm. across, and the region between the diffuse boundary of the negative glow and the anode is almost non-luminous. We have been concerned with the general features of the discharge rather than with their relation to the specific properties of the gas employed (argon).

2. *Experimental Arrangements.*

A discharge-tube was built to the design shown in fig. 1. It had two circular nickel electrodes (E), carried by a bent glass rod (G). One of them was connected by a nickel rod (R) to a piece of soft iron (F), so that the system could be

Fig. 1.

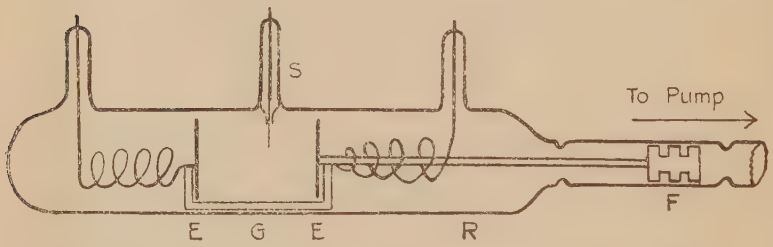

moved bodily by an external electromagnet. Electrical connexion was made with the electrodes by light nickel springs welded to copper strips, which were sealed through side tubes. A length of molybdenum wire (S), 0·2 mm. in diameter, served as collector : all but the last cm. was protected by a glass sheath, and the metal and glass were not in contact near the part exposed to the discharge. It was necessary to use a relatively large exploring electrode to obtain readily measurable currents. The main tube was 4 cm. in diameter, and the distance between the electrodes was 5 cm.

Argon, which had been purified by repeated passage over calcium, and stored over mercury, was admitted after exhausting the tube to a pressure of less than 10^{-4} mm. Hg by a small mercury-vapour pump. Between the reservoir and the discharge-tube it was passed over phosphorus pentoxide, and through a liquid-air trap. The spectroscopic impurities were hydrogen (H_α) and mercury, both of which

are enhanced by argon, but no bands associated with carbon or nitrogen could be detected. With liquid air on a trap between the tube and a McLeod gauge, the pressure did not vary by more than 5 per cent. with the discharge passing continuously for nine hours.

The electrical connexions are shown in fig. 2. The current from a battery of 300 lead accumulators was regulated by a thermionic diode (D) and measured on a multi-range microammeter (M). The collector (S) could be charged to a potential of ± 250 volts relative to the anode (A), and the current to it was measured on one of two galvanometers (G), provided with a variety of shunts, with a range

Fig. 2.

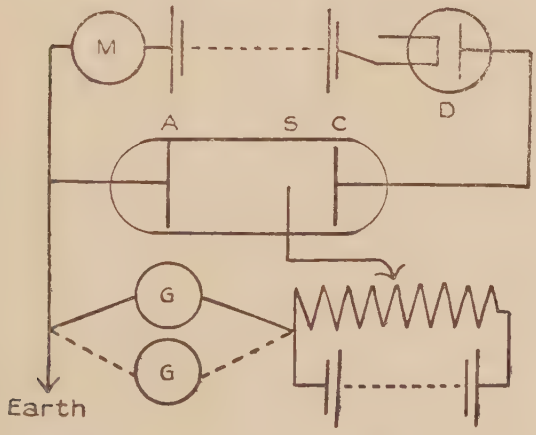

between 10^{-10} amp. and 10^{-3} amp. The apparatus between S and A was carefully insulated, to avoid stray currents.

At the low current densities employed, there is a marked tendency for the cathode dark space to be thicker close to the glass walls of the tube than at the axis. A gap of 2 mm. was therefore left between the rim of the cathode and the glass, which had the effect of making the edge of the dark space flat in the neighbourhood of the collector. This prevented the use of high current densities, when the discharge became intermittent, and passed to the back of the electrode, but was essential in order to obtain uniform conditions over the length of the exploring electrode.

When the discharge was passing, there was a blue negative glow, which was moderately sharply bounded towards the cathode, and faded diffusely into a Faraday dark space

which extended to the anode. An anode glow was sometimes present (§ 4), and the mercury spectrum, if present, was particularly prominent in this part of the tube.

It has been shown by a variety of methods that the discharge was not oscillatory or intermittent.

3. *Method of Analysis.*

Simultaneous readings were taken of the current through the tube (i_t), and of the current to the collector (i_c), as the potential (V) of the latter was varied. To allow for slight variations in the main discharge, the ratio i_c/i_t was used in the subsequent analysis ; this will not be described in detail, since it has been elaborated in previous papers[4].

The formulæ used to find the concentrations and temperatures of the slow electrons when they were collected in a retarding field were :—

$$\frac{d \log \mathrm{I}}{d\mathrm{V}} = \frac{e}{k\mathrm{T}}. \quad . \quad . \quad . \quad . \quad . \quad . \quad (1)$$

and

$$\mathrm{I}_0 = \mathrm{N}e(k\mathrm{T}/2\pi m)^{\frac{1}{2}}, \quad . \quad . \quad . \quad . \quad . \quad . \quad (2)$$

where I is the electron current to the collector at potential V, corrected for positive ions, and I_0 is the electron current to it per unit area at the space potential. N, T, and e/m are the concentration, temperature, and specific charge of the electrons, and k is the gas-constant per molecule. The space potential was taken to be that potential of the exploring electrode beyond which the linear relation (1) ceased to hold, and the effective area of the collector was assumed to be that of its cylindrical surface. In some cases when the relation between log I and V was not linear, the current could be analysed into two components, each of which satisfied equation (1). This has been interpreted as showing the presence of two groups of electrons, each with a definite temperature[5]. No use has been made of that part of the characteristic of the collector which corresponds to reception of electrons in an accelerating field, since the main discharge was then markedly affected by their removal.

The information to be derived by collecting positive ions in an accelerating field is less definite. Dauvillier has shown that there is frequently present in the negative glow radiation which requires for its excitation electrons of energy corresponding to almost the full cathode fall of potential[6].

[4] Langmuir and Mott-Smith, General Electric Review, 1924.
[5] Langmuir, Phys. Rev. xxvi. p. 585 (1925).
[6] Dauvillier, *Journ. de Phys.* vii. p. 369 (1926).

Absorption of soft X-rays, with emission of photo-electrons from the molybdenum, would cause an apparent increase in the positive ion current, but the direct effect of such electrons on the characteristic cannot be predicted with certainty, as they may give rise to secondary electrons on impact on the metal. When the square of the positive ion current was plotted against the potential across the positive ion sheath, almost linear curves were obtained, which often showed two distinct portions. An example of one of these is shown in fig. 3. The break seems to indicate that at the lower potentials "primary"[5] electrons were penetrating the positive ion sheath. The data available are insufficient to correlate the position of the breaks with other conditions in the discharge.

Fig. 3.

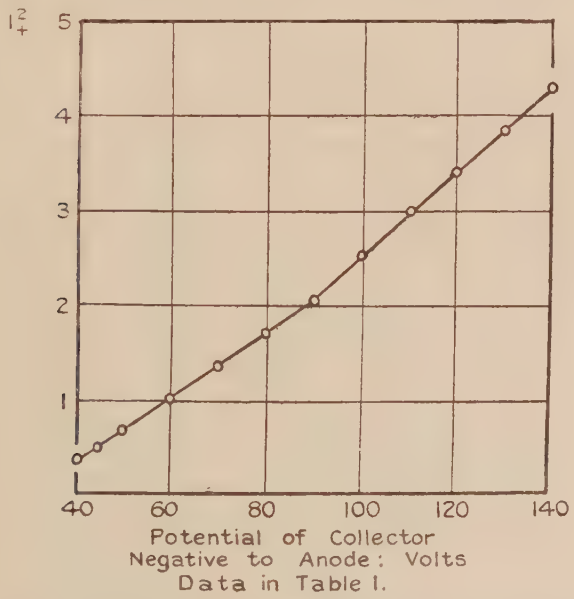

A further difficulty arises if we attempt to allow for the effect of collisions made by the positive ions in traversing the sheath, since they were too infrequent to give the ions a drift velocity proportional to the local field. We have therefore employed the cylindrical solution of Poisson's equation in which the effect of collisions is neglected, to obtain an approximate value for the random positive ion current in the discharge[7]. Table I. contains a typical set

[7] Langmuir and Blodgett, Phys. Rev. xxii. p. 347 (1923).

TABLE I.

	Potential between Collector and Space.	121	111	101	91	81	71	61	51	41	31	volts.
I.	Sheath radius.....	*0·91	0·86	0·81	0·80	0·70	0·65	0·60	0·53	0·47	0·40	cm.
	Random positive ion current.	1·24	1·25	1·24	1·24	1·24	1·22	1·20	1·21	1·20	1·16	$\times 10^{-6}$ amp. per cm.^{2}
II.	Sheath radius.....	0·103	0·100	0·094	0·089	0·083	0·080	0·076	0·073	—	—	cm.
	Random positive ion current.	1·04	1·07	1·06	1·05	1·05	0·99	0·95	0·89	—	—	$\times 10^{-5}$ amp. per cm.^{2}

Collector just to Anode side of the brightest part of the Negative Glow.

Tube pressure 0·61 mm.; Tube volts 210; Tube current 0·3 milliamp.; Space potential, −19 volts relative to Anode.

I. Values calculated assuming no collisions within the sheath.

II. Values calculated from mobility motion.

* At this potential the visible sheath radius was about 3 mm.

of results obtained for various collecting voltages: a break occurred in the i^2–V curve at 90 volts. Since there is, in addition, uncertainty as to the temperature of the positive ions, we have not calculated their concentration by equation (2).

In spite of these sources of error, the ratio of the random positive ion and electron currents is about the same as has been found previously, and the results may be relied upon to show in a general way how the positive ion concentration varies along the path of the discharge. Less consistent results are obtained when the characteristics are analysed on the assumption that the positive ions have a mobility motion [8], but the distribution curve for their concentration is of the same form. A set of results obtained by this method has been included in Table I.

4. *Experimental Data and Results.*

Experimental data, which have been chosen to illustrate the changes observed as the pressure was varied, are contained in Tables II.–V. and figs. 4–7. It will be seen that in all cases the total electron density (n_e) and random positive ion current (i_+), reach a maximum near the middle of the negative glow, and that the electric field is reversed between the point of maximum concentration and the edge of the cathode dark space. The electron peak does not in general coincide with the positive ion peak, probably because the electron concentrations were obtained from the current at the space potential, when the sheath vanishes, and the data for the positive ions with a sheath the outer radius of which was of the order of a mm. Beyond the edge of the cathode dark space, the characteristic curves changed markedly in form, and have not yet been satisfactorily analysed. The collector throws a shadow towards both anode and cathode, and it may be questioned if reliable information can be obtained about this region by any method in which a probe has to be introduced.

The electric field between the negative glow and the anode changes with pressure. At the three highest pressures there was a positive anode fall of potential of the order of 20 volts, with which was associated an anode glow; the potential was almost constant in the Faraday dark space. At 0·9 mm. there was also a direct field of 8 volts per cm. in the positive side of the negative glow. At 0·19 mm. the field was completely reversed between the anode and the cathode dark space, and there was no anode glow.

[8] McCurdy, Phys. Rev. xxvii. p. 157 (1926).

TABLE II.

Part of Discharge.	Distance from Anode.	Space Potential relative to Anode.	Random Electron Current.	Random Positive Ion Current.	Fast Group of Electrons.		Slow Group of Electrons.	
					Temperature.	Concentration.	Temperature.	Concentration.
	cms.	volts.	amps./cm.^{2}	amps./cm.^{2}	volts.	No./c.c.	volts.	No./c.c.
Faraday Dark Space.	0·52	−24·5	$1·18\times10^{-5}$	$1·89\times10^{-6}$	—	—	4·45	$2·59\times10^{6}$
	2·38	−23·0	$2·24\times10^{-5}$	$1·72\times10^{-6}$	—	—	4·87	$4·59\times10^{6}$
	3·88	−23·4	$3·24\times10^{-5}$	$2·18\times10^{-6}$	—	—	4·93	$6·70\times10^{6}$
Negative Glow.	4·28	−27·0	$2·66\times10^{-5}$	$2·75\times10^{-6}$	—	—	3·83	$6·21\times10^{6}$
	4·46	−28·3	$4·07\times10^{-5}$	$3·64\times10^{-6}$	—	—	3·33	$1·03\times10^{7}$
	4·54	−28·2	$7·36\times10^{-5}$	$1·34\times10^{-5}$	—	—	3·11	$1·92\times10^{7}$
	4·65	−24·7	$2·52\times10^{-4}$	$1·05\times10^{-5}$	—	—	2·74	$6·95\times10^{7}$
	4·71	−25·9	$1·77\times10^{-3}$	$6·09\times10^{-6}$	4·51	$1·47\times10^{7}$	1·75	$3·93\times10^{7}$
	4·75	−16·1	$6·20\times10^{-3}$	$3·08\times10^{-6}$	5·42	$2·90\times10^{7}$	2·32	$1·42\times10^{8}$
	4·81	−13·0	$1·65\times10^{-3}$	$1·34\times10^{-6}$	7·67	$1·33\times10^{7}$	2·43	$2·70\times10^{7}$

Tube pressure 0·9 mm.; Tube volts 325; Tube current, 1·5 milliamp.
Cathode dark space 0·19 cm. thick.

TABLE III.

Part of Discharge.	Distance from Anode.	Space Potential relative to Anode.	Random Electron Current.	Random Positive Ion Current.	Fast Group of Electrons.		Slow Group of Electrons.	
					Temperature.	Concentration.	Temperature.	Concentration.
	cms.	volts.	amps./cm.^{2}	amps./cm.^{2}	volts.	No./c.c.	volts.	No./c.c.
Faraday Dark Space.	0·66	−17·5	$4·97\times10^{-5}$	$1·47\times10^{-6}$	—	—	3·46	$1·22\times10^{7}$
	1·49	−19·5	$3·82\times10^{-5}$	$1·52\times10^{-6}$	—	—	2·11	$1·21\times10^{7}$
	2·48	−18·8	$1·09\times10^{-4}$	$2·14\times10^{-6}$	—	—	2·19	$3·37\times10^{7}$
	3·05	−18·25	$4·05\times10^{-4}$	$2·60\times10^{-6}$	—	—	2·05	$1·30\times10^{8}$
	3·33	−17 8	$1·13\times10^{-3}$	$3·34\times10^{-6}$	—	—	1·37	$4·67\times10^{8}$
	3·67	− 18·0	$1·72\times10^{-3}$	$4·82\times10^{-6}$	—	—	1·24	$7·12\times10^{8}$
	3·85	−17·9	$1·98\times10^{-3}$	$5·00\times10^{-6}$	—	—	1·33	$7·83\times10^{8}$
	4·08	−18·4	$1·52\times10^{-3}$	$7·51\times10^{-6}$	..	—	1·06	$6·77\times10^{8}$
	4·14	−18·2	$1·88\times10^{-3}$	$9·42\times10^{-6}$	3·47	$1·02\times10^{9}$	0·72	$6·89\times10^{8}$
Negative Glow.	4·28	−18·3	$1·43\times10^{-3}$	$7·98\times10^{-6}$	2·26	$1·30\times10^{8}$	0·70	$6·95\times10^{8}$
	4·33	−17·9	$1·59\times10^{-3}$	$7·71\times10^{-6}$	—	—	1·36	$6·25\times10^{8}$
	4·45	−16·25	$1·32\times10^{-3}$	$4·13\times10^{-6}$	2·88	$2·48\times10^{9}$	1·78	$4·22\times10^{8}$
	4·54	−10·5	$1·29\times10^{-3}$	$3·30\times10^{-6}$	3·97	$2·98\times10^{8}$	—	—
	4·65	− 0·1	$1·10\times10^{-3}$	$1·54\times10^{-6}$	5·02	$2·27\times10^{8}$	—	—

Tube pressure 0·52 mm.; Tube volts 220; Tube current 0·3 milliamp.
Cathode dark space, 0·35 cm. thick.

TABLE IV.

Part of Discharge.	Distance from Anode.	Space Potential relative to Anode.	Random Electron Current.	Random Positive Ion Current.	Single Group of Electrons.	
					Temperature.	Concentration.
	cms.	volts.	amps./cm.^{2}	amps./cm.^{2}	volts.	No./c.c.
Faraday Dark Space.	3·17	−18·3	$1·78\times10^{-4}$	$5·51\times10^{-6}$	3·10	$4·01\times10^{7}$
	3·56	−17·5	$3·78\times10^{-4}$	$8·60\times10^{-6}$	3·92	$7·72\times10^{7}$
Negative Glow.	3·79	−16·8	$4·10\times10^{-4}$	$9·60\times10^{-6}$	3·44	$8·97\times10^{7}$
	3·98	−16·6	$3·07\times10^{-4}$	$6·65\times10^{-6}$	3·71	$6·97\times10^{7}$
	4·06	−16·1	$3·51\times10^{-4}$	$4·83\times10^{-6}$	3·92	$7·72\times10^{7}$
	4·17	−15·7	$2·62\times10^{-4}$	$2·13\times10^{-6}$	4·46	$5·42\times10^{7}$
	4·28	−15·6	$1·38\times10^{-4}$	$9·35\times10^{-7}$	7·55	$2·18\times10^{7}$

Tube pressure 0·29 mm.; Tube volts 275; Tube current 0·4 milliamp.
Cathode dark space 0·72 cm. thick.

TABLE V.

Part of Discharge.	Distance from Anode.	Space Potential relative to Anode.	Random Electron Current.	Random Positive Ion Current.	Single Group of Electrons.	
					Temperature.	Concentration.
	cms.	volts.	amps./cm.^{2}	amps./cm.^{2}	volts.	No./c.c.
Faraday Dark Space.	0·35	0·0	$8·85\times10^{-5}$	$9·40\times10^{-7}$	4·48	$1·58\times10^{6}$
	1·95	+ 5·5	$7·11\times10^{-5}$	$9·70\times10^{-7}$	4·52	$7·10\times10^{6}$
Negative Glow.	3·05	+ 8·8	$1·59\times10^{-4}$	$1·70\times10^{-6}$	5·10	$2·97\times10^{7}$
	3·50	+11·7	$1·72\times10^{-4}$	$1·56\times10^{-6}$	4·47	$4·42\times10^{7}$
	3·62	+12·6	$1·86\times10^{-4}$	$1·44\times10^{-6}$	4·84	$5·14\times10^{7}$
	3·74	+16·1	$1·87\times10^{-4}$	$1·14\times10^{-6}$	6·52	$3·66\times10^{7}$
	3·93	+21·5	$5·92\times10^{-5}$	$1·86\times10^{-7}$	9·73	$4·86\times10^{6}$

Tube pressure 0·19 mm.; Tube volts 420; Tube current 0·25 milliamp.
Cathode dark space 1·07 cm. thick.

Fig. 4.—Data in Table II. Pressure 0·9 mm.

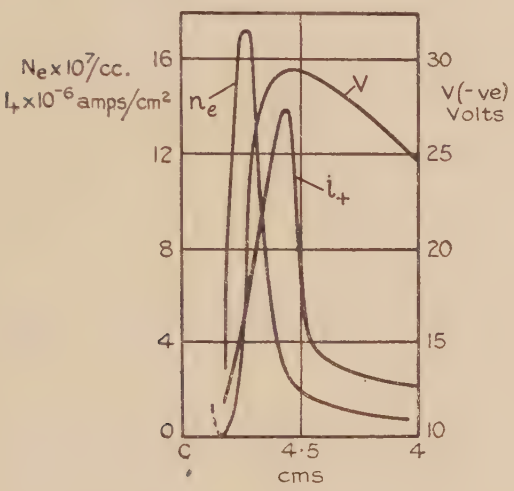

Fig. 5.—Data in Table III. Pressure 0·52 mm.

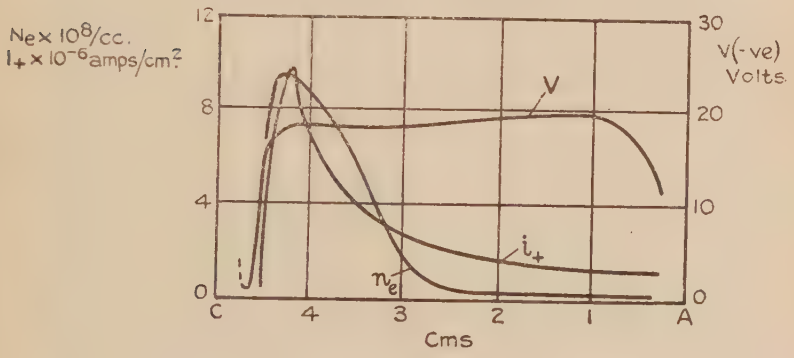

Fig. 6.—Data in Table IV. Pressure 0·29 mm.

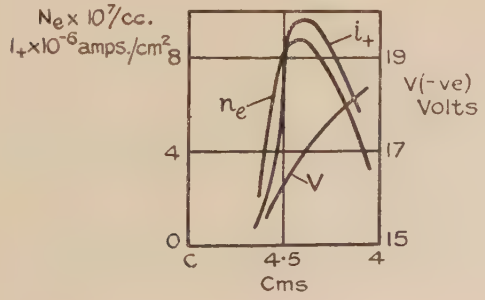

Fig. 7.

Data in Table V. Pressure 0·19 mm.

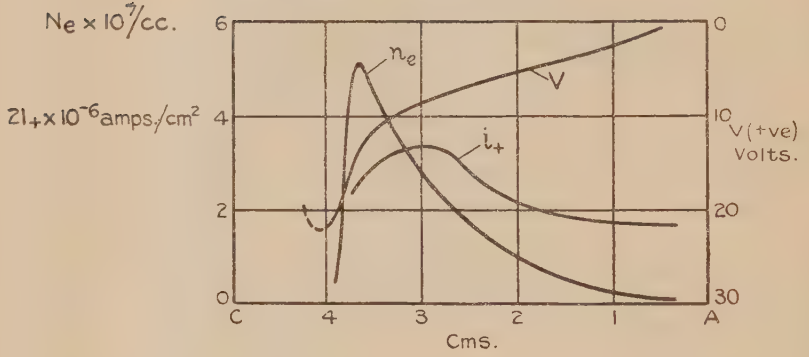

In Figs. 4–7, V is the space-potential relative to the anode. The abscissæ represent distances from the anode A towards the cathode C. The cathode dark space extended from C° to the left-hand limit of the full curves.

The electron temperatures show little change along the Faraday dark space. There is a tendency to increase near the anode, which may be due to superposition of a considerable velocity or drift on the random motion. At 0·52 mm. there was a single fast group of electrons at the edge of the cathode dark space, and an additional slower group in the middle of the negative glow. The single fast group was not recorded at the highest pressure, probably because of the contraction of the negative end of the discharge. At the lowest pressures, only one group was present, as was the case at all pressures in the Faraday dark space.

We shall not give a detailed comparison between our results and those obtained with the older method of using a cold exploring electrode, because of the uncertainty attached to the latter. Reversal of the electric field has, however, been known to occur in the Faraday dark space under conditions similar to those which we have employed [9], and it has been shown more recently by the present method that it is readily produced in low-voltage arcs in argon [10]. The differences between our results and those obtained by similar methods in recent work on glow discharges is to be attributed, in general, to our use of a cold cathode and very small current densities.

[9] J. J. Thomson, Phil. Mag. xviii. p. 441 (1909).
[10] K. T. Compton and Eckart, Phys. Rev. xxv. p. 139 (1925).

5. *Discussion of Results.*

The main features of the present work are the presence or absence of an anode fall of potential, the mechanism of conduction along the Faraday dark space, the origin of the intense ionization in the negative glow, and the nature of the current in the reversed field between the middle of the negative glow and the cathode dark space. We shall consider these individually on the lines proposed by K. T. Compton and others [11].

(a) *Anode Glow.*

In these experiments, the presence of an anode glow has always been associated with a direct local fall of potential rather greater than the ionization potential of argon (15·3 volts), and absence of the glow with a smaller reversed field, whatever the pressure. In the former case, the change from the small electric field in the Faraday dark space to the large direct field at the anode glow must take place in a region of negative space-charge, to satisfy Poisson's relation, but mechanical difficulties have prevented the collector from being brought sufficiently near to the anode to verify this. An anode glow often increases the effective area of the electrode [12], and it probably serves in any event as a source of positive ions for neighbouring parts of the Faraday dark space.

(b) *Faraday Dark Space.*

Tables II.–V. show that this is almost an equipotential region, except at the lower pressures, and that the concentration of electrons and positive ions increases largely towards the maximum in the negative glow. If the mobility of a positive ion is neglected in comparison with that of an electron, the concentration-gradient is equivalent to an electromotive force whose magnitude is given approximately by

$$E = kT/e \log N_2/N_1, \quad . \quad . \quad . \quad . \quad . \quad (3)$$

where T is the electron temperature, and N_1, N_2 the electron concentrations at the points between which E is to be evaluated. When this relation is used to find E between the region of maximum concentration in the negative glow, and the point nearest the anode in the discharges analysed in

[11] McCurdy, Phil. Mag. xlviii. p. 898 (1924); K. T. Compton, Turner, and McCurdy, Phys. Rev. xxiv. p. 597 (1924).

[12] Langmuir and Mott-Smith, Gen. Elect. Rev. xxvii. p. 767 (1924).

Tables II.–V., we find for its value about 11, 6, 1½, and 11 volts. The second figure is certainly too large, since the luminosity on the anode was confined to the side remote from the collector, leading to too low an estimate of the concentration of electrons. The last two numbers are almost equal and opposite to the potential differences in the reversed fields. The resultant force on the electrons due to the combined effect of the electric and diffusion fields was therefore little different from zero at the lowest pressures, definitely positive at the highest pressure, and probably positive at 0·52 mm.

An independent estimate of the effective field may be obtained if it is assumed that the electrons have acquired a terminal random velocity; the field to which this is due may then be calculated from a knowledge of the mobility of an electron in argon [13]. This method gives 0·74, 0·18, 0·14, 0·15 volts per cm. respectively for the fields corresponding to figs. 4–7, which are of the order of magnitude indicated by the method of the preceding paragraph. Moreover, the random current of electrons near the anode is sufficient to carry the observed current through the tube, and the number of fast electrons from the cathode dark space which reach the anode must be negligibly small, since the mean free path of a 100 volt electron in argon at a pressure of 1 bar at 74° C. is 69 cm., and 70 per cent. of the collisions result in complete loss of energy [14]. Our results therefore afford strong evidence that in this type of discharge the current between the negative glow and the anode is mainly carried by slow electrons moving in combined electric and diffusion fields.

(c) *Negative Glow and Cathode Dark Space.*

The visual edge of the cathode dark space was coincident with the point beyond which characteristics of the usual type were no longer obtained with the collector. Existence of a sharp boundary, although partly a physiological effect [15], is intimately connected with the fact that the dark space is a region of positive space-charge. The maximum of ionization in the negative glow is presumably related to the mean free path of the radiation quanta [16] and fast electrons produced in the cathode dark space.

The reversed field in this part of the tube can be correlated with the local distribution of space-charge. The

[13] K. T. Compton, Phys. Rev. xxii. p. 432 (1923).
[14] Langmuir and Jones, Science, lix. p. 761 (1924).
[15] Seeliger and Lindow, *Phys. Zeit.* xxvi. p. 393 (1925).
[16] J. J. Thomson, Phil. Mag. xlviii. p. 1 (1924).

curvature of the potential curves in figs. 4, 5, and 7, shows that there is an excess of negative electricity in the middle of the negative glow, which, together with the positive ions in the cathode dark space, will give a component potential gradient opposite in sign to that arising from the surface charges on the electrodes. This will hinder the diffusion of positive ions from the middle of the negative glow towards the cathode, and the magnitude of the resultant electric field does in fact run parallel with that of the concentration gradient, as will be seen by comparison of fig. 4 with fig. 6. On the other hand, both concentration gradient and electric field will exert forces tending to move the slow electrons towards the cathode, and their disappearance must be brought about by recombination, and, probably to a less extent, by diffusion to the walls. This may account for the fact that the brightest part of the glow was observed to be to the cathode side of the region of maximum concentration, and that with very small currents, when the discharge was on the point of extinction and unstable, the negative glow was annular.

The two groups of electrons are comparable with the "secondary" and "ultimate" groups present in discharges from a hot filament at very low pressures [17]. The temperature of the group of greater energy increases towards the cathode dark space, but both groups have an average energy well below that required for ionization of the argon by a single impact. The information bearing on their production is meagre. Nevertheless, when taken in conjunction with some measurements which have been made in the discharge from a hot filament in hydrogen [18], our results, though not conclusive, suggest that the current is carried from the cathode dark space to the negative glow by primary electrons, and that the positive ions in the cathode dark space are produced *in situ* [19], and do not have their origin in the negative glow.

6. *Summary.*

The Geissler discharge between cold electrodes in argon has been studied by means of a cold exploring electrode. The main results, which are probably of general validity for

[17] Langmuir, Phys. Rev. xxvi. p. 585 (1925).
[18] Bramley, Phys. Rev. xxvi. p. 794 (1925).
[19] As, for example, in the theory of J. J. Thomson, Phil. Mag. xlviii. p. 1 (1924).

similar discharges in wide tubes at low potentials and with small current densities, are :—

(i.) The electron concentration and random positive ion current attain a maximum in the middle of the negative glow.

(ii.) The current is carried from the negative glow through the Faraday dark space by slow electrons moving in combined electric and diffusion fields. The average energy of the electrons is very approximately constant in this part of the discharge.

(iii.) The electric field is reversed between the cathode dark space and the middle of the negative glow, and primary electrons are probably present.

The greatest sources of uncertainty are :—

(iv.) The estimation of the concentration of positive ions.

(v.) The detection of primary electrons, which depends on the analysis of the positive ion currents.

It is anticipated that further experiments will make it possible to find the velocity distribution of the primary electrons.

We are indebted to Prof. E. V. Appleton both for very generous provision of apparatus and for valuable criticism and advice.

Wheatstone Laboratory,
King's College, W.C. 2,
6th May, 1927.

VI. *Comparison of Discharges produced by Two and Three Electrode Systems in Hydrogen.* *By* Miss B. Trevelyan, *B.A.**

IN a previous investigation † of low-voltage glows in hydrogen, the discharge was produced by a stream of electrons from a hot filament, accelerated towards a widely spaced grid placed about two millimetres in front of the filament. The main glow extended through the grid and some way up the tube away from the electrodes.

This discharge is definitely of a different type from that of a three-electrode tube or one containing two electrodes at a distance apart considerably greater than the distance between the walls. The method of employing an auxiliary

* Communicated by Prof. E. V. Appleton, D.Sc.

† G. Stead and B. Trevelyan, Phil. Mag. xlviii. pp. 978–1006 (1924).

collecting electrode has been used as a means of investigating the distribution of potential, and of determining the concentration and temperature of the electrons in the glow. Some similar measurements have been made with a three-electrode tube. Although the discharge is complicated, it is possible to obtain definite information in both cases, provided that the collecting electrode does not take more than a small fraction of the main current.

Apparatus.

The form of tube used is shown in fig. 1. It was of diameter 3·5 cm., and contained a tungsten filament F capable of carrying up to 3 amperes and a widely spaced grid G made of nickel wire 0·8 mm. in diameter and bent so that there were six parallel wires about 5 mm. apart. The grid was about 2 mm. in front of the filament. The exploring electrode E was a nickel wire 0·17 mm. in diameter and 1·14 mm. long, which was placed about 10 cm. from the grid, and could be moved transversely to the main tube (fig. 1).

Fig. 1.

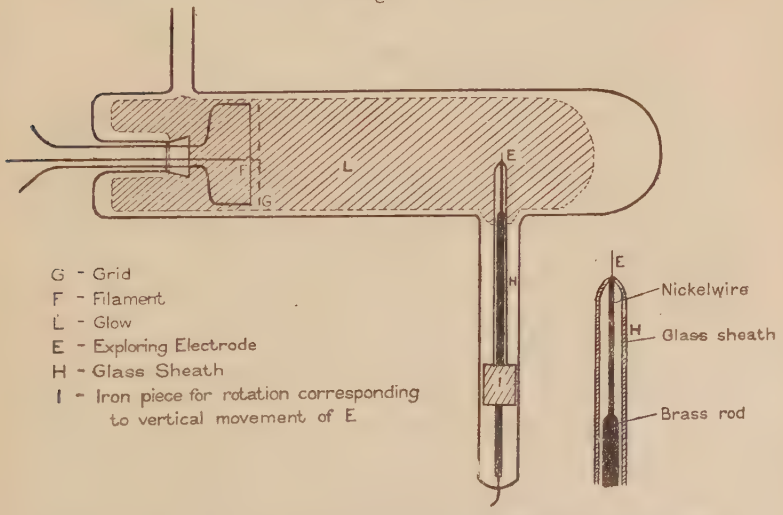

The three-electrode tube, of the same diameter, had a similar grid and filament, and in addition a nickel ball anode 6·1 mm. in diameter placed about 7 cm. from the grid. The exploring electrode was in this case a circular disk of nickel, 0·85 cm. in diameter, placed parallel to the main discharge, with a guard ring to prevent distortion

of the sheath as far as possible. The disk was at about the same distance from the grid as the anode, and could be moved transversely to the main tube, but in these experiments it was kept fixed about 3 mm. in front of the walls.

Before use, the tube employed was exhausted to a pressure of the order of 10^{-4} mm. Hg. Hydrogen was admitted by means of a palladium tube and mercury vapour excluded as far as possible. This was done for the two-electrode tube by means of liquid air traps, and for the three-electrode tube by means of sodium potassium alloy. The latter method was found to be the more reliable. There were undoubted traces of mercury vapour in the two-electrode tube, but mercury was not detected spectroscopically in the three-electrode tube.

The procedure was as follows :—

The characteristic curves for the respective exploring electrodes were plotted under various conditions, and the space potential, electron concentration, and electron temperature determined by a direct application of Langmuir's analysis *. The space potential was referred in the case of the two-electrode tube to the grid, and in the three-electrode tube to the anode.

Results.

A. *Two-Electrode Tube.*

Within a certain range of pressures, and with the grid 40–80 volts positive with respect to the filament, a bright purple glow projected beyond the grid; it was convex towards the end of the tube, and also extended behind the filament. The general appearance is shown in fig. 1. The spectrum of the glow showed the Balmer series, and hydrogen secondary spectrum. Mercury lines were also visible.

The length of the glow was very sensitive to changes of pressure, grid potential, and filament current, but in these experiments the last two were kept constant and the length made to vary by change of pressure. The position of the exploring electrode relative to the glow was varied in this way, and the space potential inside and outside the glow could be determined. The range of pressure was from about 0·07 mm. to 0·01 mm., but above 0·05 mm. the glow was diffuse and the boundary indeterminate.

Typical results are given in Tables I. and II., and the general type of characteristic curve in fig. 2. To obtain

* Langmuir, Journ. Frankl. Inst. 196. p. 751 (1923).

TABLE I.

Exploring Electrode level with the walls.

Pressure. mms. of Hg.	Grid Potential relative to filament. volts.	Filament Current. amperes.	Grid Current. milliamps.	Position of glow.	Space Potential relative to grid. volts.	Electron Concentration per c.c.	*Electron Temperature in volts.
·072	84·7	2·67	1·8	Electrode in glow. Glow was diffuse and filled whole tube.	+15	$4·0\times10^{8}$	12·5
·050	84·7	2·69	1·9	As above.	0	$3·4\times10^{8}$	12·8
·033	84·7	2·68	2·4	As above.	−8	$4·6\times10^{8}$	12·0
·032	84·7	2·68	2·4	As above.	−9	$6·1\times10^{8}$	13·7
·029	84·7	2·67	2·8	Glow did not reach end of tube. Electrode was at edge of glow.	−4	$10·8\times10^{8}$	14·9

* (Average Energy of Electrons, $Ve=\frac{3}{2}kT$.)

TABLE II.

Exploring Electrode in centre of main tube.

Pressure. mms. Hg.	Grid Potential relative to filament. volts.	Filament Current. amperes.	Grid Current. milliamps.	Position of glow.	Space Potential relative to grid volts.	Electron Concentration per c.c.	Electron Temperature in volts.
·029	85·2	2·60	1·9	End of glow beyond tip of exploring electrode. Tip in glow.	−3	$2{\cdot}5\times10^{7}$	14·5
·021	85·2	2·60	2·0	Tip at edge of glow.	−10	$1{\cdot}4\times10^{7}$	16·5
·016	85·2	2 59	2·1	Glow less than 2 cm. behind tip. Tip in dark space beyond glow.	−40	$\cdot76\times10^{7}$	15·3
·009	85·2	2·59	2·4	Glow contracted, end close to grid. Most of tube, and tip in dark space.	−61	$\cdot85\times10^{7}$	8·6

the electron current at a given voltage, the value on the extrapolated part of the curve (BC) was subtracted from that on the part BD, since ABC is taken to represent the positive ion current to the electrode, which is practically linear for a few volts below the space potential.

Fig. 2.

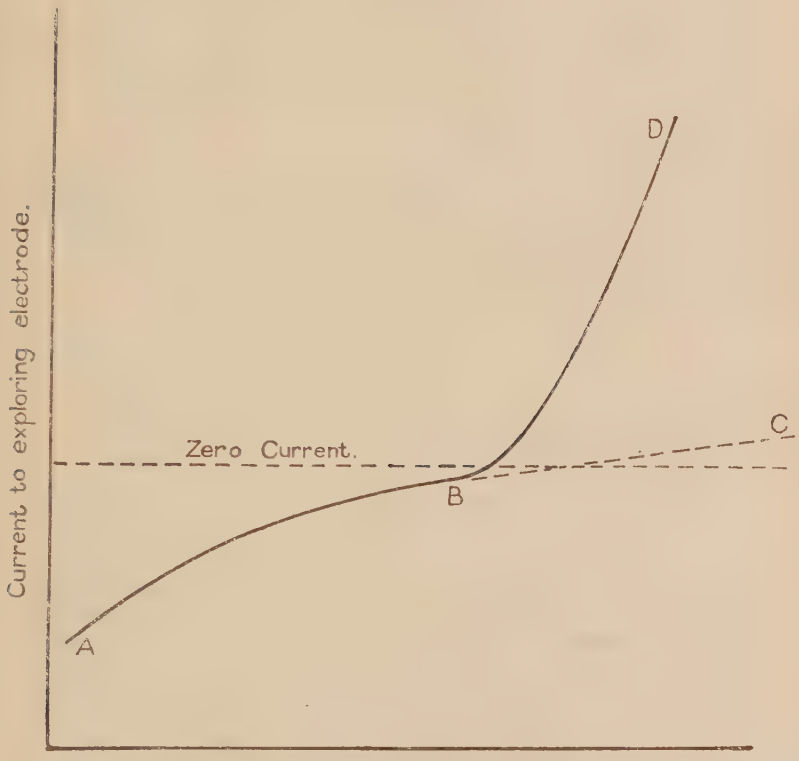

The space potential can be located in two ways *:—

(*a*) By the break in the straight line obtained by plotting values of $\log i$ against V for collection of electrons in a retarding field, where i is the current to the electrode and V the potential of the electrode relative to the grid.

(*b*) † By the intersection of the straight line obtained by plotting i^2 against V with the V axis when electrons are

* Langmuir and Mott-Smith, General Electric Review, xxvii. p. 451 (1924).

† Langmuir and Mott-Smith, *loc. cit.* p. 455.

being collected in an accelerating field. This gives a value T/11,600 volts negative to the space potential, where T is the temperature of the electrons as determined by the slope of the $(\log i)/V$ line. The space potentials were measured relative to the grid.

Results obtained by the first method were generally used in estimating the space potential. The second method gave values slightly higher than those determined from the $\log i$ against V line.

The concentration of the electrons could also be measured in two ways :—

(i.) From the formula,

$$I = \tfrac{1}{4} n e \bar{v}, \quad . \quad . \quad . \quad . \quad . \quad . \quad . \quad (1)$$

where I is the current per unit area of the electrode at the space potential, $\bar{v}$ the average velocity of the electrons, n the number of electrons per c.c.

The formula may also be written as

$$I = ne\sqrt{\frac{e\bar{V}}{3\pi m}}, \quad . \quad . \quad . \quad . \quad . \quad . \quad (2)$$

where $e\bar{V}$ is the average energy of the electrons (as determined from the temperature).

(ii.)* By means of the relation

$$n = \frac{\pi}{\sqrt{2e/m}} \cdot \frac{\sqrt{S}}{Ae}, \quad . \quad . \quad . \quad . \quad . \quad . \quad (3)$$

where S is the slope of the i^2 against V line in accelerating fields, A is the surface area of the electrode, e and m are the charge and mass of the electron.

The two methods gave almost the same values, but the first was more reliable, and values for the concentration under different conditions were obtained from it.

The results may be summarized as follows :—

(*a*) When the exploring electrode is in the glow, the space potential is approximately that of the grid ; but, in some cases, at the higher pressures it is more positive, which suggests that something analogous to striations may occur in this form of discharge, although they are not visible.

(*b*) When the electrode is out of the glow, and in the dark space between it and the walls, the space potential becomes rapidly negative to the grid, and probably approaches the potential of the filament at the walls; when the glow is close to the grid, the floating potential of the electrode

* Langmuir and Mott-Smith, *loc. cit.* p. 455.

in the dark space farther up the tube is practically that of the filament.

(*c*) Further evidence of the presence of the striations is furnished by the curves of fig. 3. These show the change in length of the glow when the grid potential increased, the

Fig. 3.

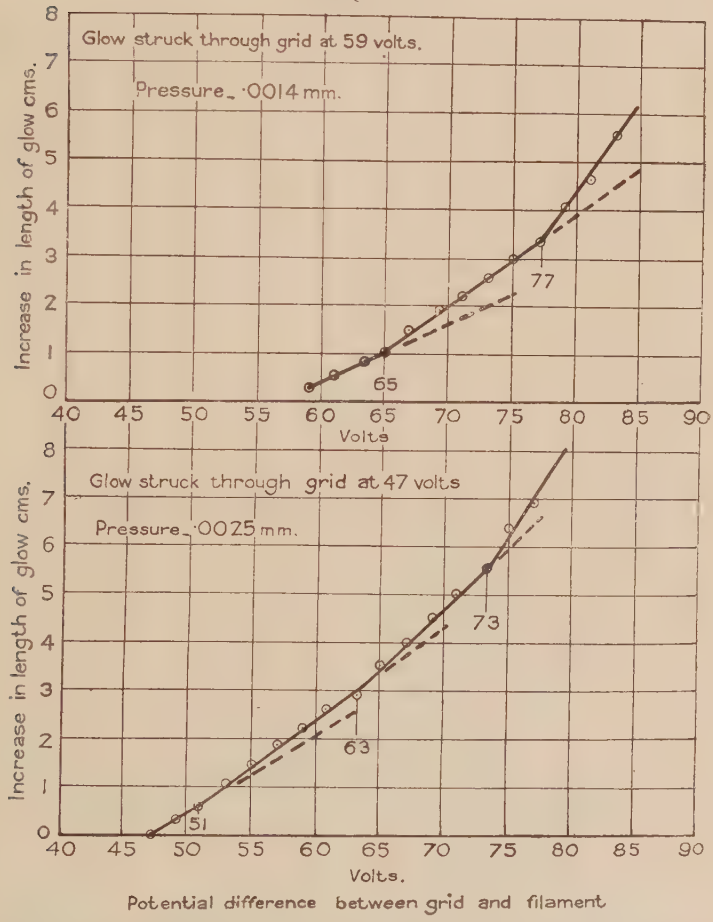

pressure being kept constant as far as possible. In order to obtain a well defined end to the glow, the experiments were performed at very low pressure, hence mercury vapour may have been present in large proportion compared with the gas. It is seen that there are changes in the slope of the length/grid voltage line which occur at intervals of

about 11 to 15 volts (fig. 3). Grotrian * has found low-voltage striations in mercury vapour, the number depending on the potential difference between filament and anode, an additional 4·9 volts being necessary to bring out a new striation.

(*d*) Increase of filament current increased the length of the glow. If the pressure was diminished while the discharge was running, the glow contracted and became intrinsically brighter; but if the discharge was first put on at low pressure, the glow ran along to the end of the tube, then immediately recoiled and came to a steady position.

(*e*) There appears to be one main group of electrons, and these have acquired a Maxwellian distribution. The temperature of the group is high, and on comparing the values in the tables on pages 67 and 68 it may be seen that although the pressure and position of the glow are both changing at the same time, their individual effects on the system may be to a certain extent distinguished from one another. While the electrode is in the glow, in general the temperature tends to increase with diminution of pressure, but as it moves out of the glow, the temperature decreases. At a given pressure, if the filament current increases, the temperature decreases.

(*f*) As would be expected, the electron concentration increases with increase in emission from the filament. The change of concentration with pressure is somewhat masked by the change of relative position of the glow and electrode. Low pressures and high concentrations are shown in Table II. As the pressure decreases, the main current to the grid increases; hence the concentration of electrons in the glow beyond the grid is likely to increase. At higher pressures, as in Table I., the effect is masked by the fact that there is a large electron concentration in the parts of the glow which have a space potential positive with respect to the grid. Table II. shows that the concentration of electrons falls off rapidly outside the glow, with a simultaneous decrease in electron temperature.

B. *Three-Electrode Tube.*

The discharge obtained in this tube may be considered similar to that of A, but with the field between grid and anode helping the diffusion along the tube. Sufficient data have not yet been acquired to explain completely the appearance and action of the discharge; however, the results

* W. Grotrian, *Zeit. f. Phys.* v. p. 148 (1921).

obtained so far are interesting when compared with those of section A. Further experiments are now in progress in order to elucidate the mechanism of the three-electrode system.

Since, in this tube, the collecting plate was parallel to the direction of the main discharge, it is reasonable to suppose that few of the direct beam of electrons (if these are present) reach it, and that the majority of the electrons collected are those referred to by Langmuir as the secondary and ultimate groups.

Current-voltage curves for the disk were taken under a variety of conditions, when it was about 3 mm. in front of the wall. The electron temperature was obtained as before from the slope of the $\log i$ against V line, and the concentrations by the formula (2).

The results may be summarized as follows :—

Space Potential, Electron Temperature and Concentration.

Gas pressure of the order of 0·02 mm.

A single group of low-temperature electrons (about 10,000° K.) appears near the walls, when the field between filament and grid and that between grid and anode are of the same order. When the latter is the greater the single group is again present, but when the former is the greater the $(\log i)/V$ line consists of two straight lines of different slopes, showing that a second group of high-temperature electrons is also present near the walls (20,000°–80,000° K.). Both groups have an approximately Maxwellian distribution ; the concentration of the high temperature group is small, and this group is present alone at low pressures. The concentration of the low-temperature group is a linear function of the potential between grid and anode, when the potential between filament and grid is kept constant (fig. 4).

At the higher pressures, concentric glows appear round the anode, these seem to be of the nature of striations ; the number of glows increases with the potential between grid and anode.

When the latter is small, and the potential between grid and filament also small, of the order of 40 volts, the space potential near the walls is approximately that of the grid ; as both potentials are increased the space potential becomes more nearly that of the anode. An abrupt change occurs corresponding to the formation of a new glow round the anode. A similar abrupt change in the wall charges can

be shown by means of a sounding ball attached to an electroscope, placed near the outside of the tube.

With a large emission from the filament, the grid current is negative (grid collecting positive ions in excess of electrons); the effect is most marked with a large field between grid and anode. A dark space is visible in front of the grid on the opposite side to the filament and extends into the main glow. For smaller filament currents the grid

Fig. 4.

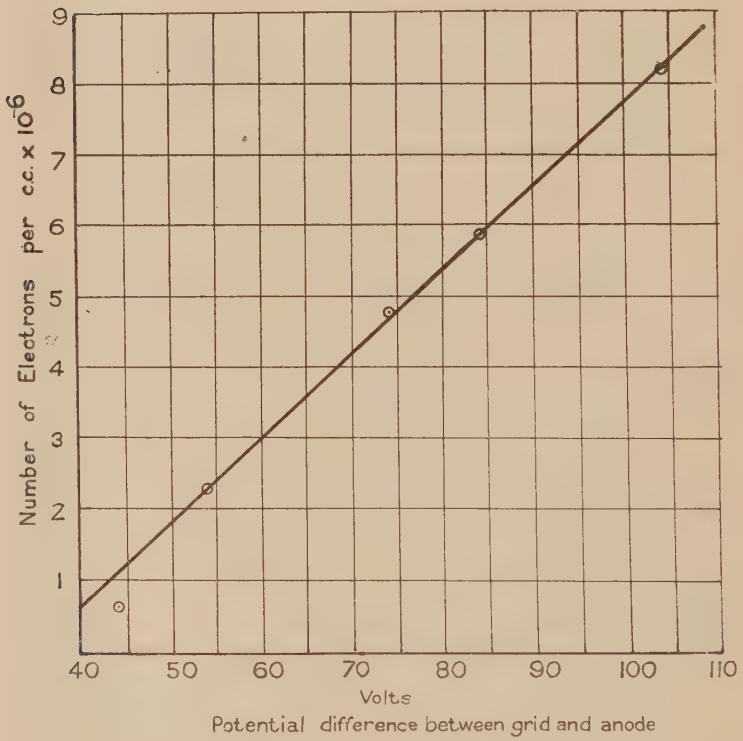

current is positive (excess of electrons). Under these conditions there is therefore a definite value of the filament current corresponding to zero current to the grid, since the latter collects both electrons from the filament and positive ions from the discharge between grid and anode.

Positive Ions.

The nature of the positive ions was roughly determined by approximate measurements of the sheath thickness over

the disk electrode when it was charged so as to collect positive ions. The relation used was *

$$I = 2{\cdot}33 \times 10^{-6} \sqrt{\frac{m}{M}} \cdot \frac{V^{3/2}\left(1 + 0{\cdot}0247\sqrt{\frac{I}{V}}\right)}{x^2}, \quad . \quad . \quad (4)$$

where x was the sheath thickness, m and M the mass of the electron and positive ion respectively, V the difference in potential (expressed in volts) between the two boundaries of the sheath (the disk and glow), I the current per unit area of the electrode (expressed in amps. cm.$^{-2}$), T the temperature of the positive ions in ° K. A value of 8000° was taken as roughly representing this temperature.

The values of $\frac{M}{m}$ varied between 1000 and 5000, and were of the right order for hydrogen, but were not sufficiently precise to determine the nature of the carrier (H^+, H_2^+, or H_3^+).

General Conclusions.

The current which passes in a discharge is governed by two factors, the applied electric field and the unequal rate of diffusion of the ions, and variation in the conditions of the discharge causes one or other to be predominant. Under conditions which give rise to large concentration of electrons and small potential gradient due to applied field, the current may be carried chiefly by diffusion.

In the two-electrode tube large fields are absent, the main fall of potential occurs between the filament and grid, and the potential of all the luminous region beyond is not far different from that of the grid. There will therefore be practically no resultant field along the glow except that due to local concentration and diffusion effects. When there are no striations, the system may be regarded as consisting roughly of two equipotential surfaces, the walls and filament forming one, and the grid and the glow the other, practically the whole fall of potential occurring in the dark space between them.

By inserting an anode as third electrode, and superposing a field between anode and grid, the system is altered. If the field between grid and filament is not too large, the grid and walls now form an approximately equipotential surface. The former acts as cathode in the main discharge between grid and anode, but here the cathode and anode are far apart

* Langmuir and Mott-Smith, *loc. cit.* p. 452.

and the main luminous region is between them, while in the two-electrode tube the distance between cathode and anode was small compared with the diameter of the tube, and the luminous region was beyond the grid. In one case there is a field along the glow, and in the other the applied field has practically no effect in the luminous part. In the presence of the field, diffusion along the tube is helped, but diffusion towards the walls is hindered.

The greatest difference between the two and three electrode systems lies in the energy of the electrons. In the former, the electron temperatures in the glow are high, and of the order of the ionization potential of hydrogen; in the latter, the temperatures are much lower. This suggests that in the two-electrode system the luminosity was produced by fast electrons able to ionize the gas directly, but in the three-electrode system by less direct means.

It has been shown * that the effect of superposing a drift current on a random current is apparently to increase the temperature of the electrons as measured by an exploring electrode. This may partly account for the high random energies recorded in the two-electrode tube. With the cathode and anode far apart and the glow between them, the temperatures measured near the walls are much lower and of the same order as those observed by Bramley † in the hydrogen discharge. In this case diffusion to the walls is hindered and the observed currents are due to electrons produced near them by primary or secondary processes of ionization.

These experiments have also a bearing on the use of charged plates as "ion-traps," to act as a shield for one part of a tube from the effects of a discharge produced in another part of the same tube. The current to the plates must be governed chiefly by the ionic sheath formed over them, and the influence of potential applied to them will extend only to the outer edge of the sheath. For a flat plate, the relation between the current density I, sheath thickness x, and the potential difference between the plate and the ionized gas is

$$Ix^2 = kV^{3/2}, \quad . \quad . \quad . \quad . \quad . \quad . \quad (5)$$

where k is a constant depending on the charge and mass of the ions. If I is small, x is large, and vice versa. It follows that if x is to be of the order of the dimensions of the tube,

* Langmuir and Mott-Smith, Phys. Rev. xxviii. p. 741 (1926).
† Bramley, Phys. Rev. xxvi. pp. 794–799 (1925).

in order that the path of the main discharge may be so confined that the latter ceases to pass, a very large potential must be applied to the plates when the current density is large.

In the present experiments the current to the grid must have been largely determined by similar considerations, the discharge beyond the grid being chiefly due to those electrons which succeeded in passing through or between the sheaths formed over the grid wires. The form of these sheaths could not be determined since the discharge was of a different nature on the two sides of the grid.

In Lord Rayleigh's* experiments on the persistence of luminosity in mercury vapour, he subjected the glow to an electric field supplied by two successive charged cylinders. He assumed that the first cylinder had acted as an efficient ion trap, since no current reached the second. This is in agreement with the equation (5) given above, since the current to the first cylinder was small, and the potential difference between it and the anode large. It is interesting to note that, under these conditions, the line spectrum, apart from λ 2537, died out first, the bright glow tapering to a point. This can be ascribed to the line spectrum having its origin in the positive ions which went to form a sheath on the first charged cylinder, the thickness of the sheath increasing as the concentration diminished in accordance with the equation

$$Ix^2 = kV^{3/2}.$$

Another origin has been ascribed to the line λ 2537 and to the continuous spectrum. Both these radiations persist after the line spectrum has died out.

The writer wishes to thank Professor O. W. Richardson for his permission to carry out this work at King's College, London; and Dr. K. G. Emeléus for much valuable help and advice.

* Lord Rayleigh, Proc Roy. Soc. A, cviii. pp. 262–279 (1925).

VII. *On the Constants of Receiving and Transmitting Antennæ.* *By* Raymond M. Wilmotte, *B.A., of the National Physical Laboratory* *.

Abstract.

The distribution of current and voltage in a circuit depends on the distribution of the applied E.M.F. in that circuit, and it would be reasonable to suppose that the effective impedance measured at any given point of the circuit would depend on the distribution of the E.M.F.

In the case of an antenna, it is proved theoretically that, if we can assume that the distribution of capacity, inductance, and resistance is the same for transmission as for reception, the effective capacity, inductance, and resistance, as well as the effective height measured at the base, is identical for transmission and reception.

The fundamental assumption is shown not to be strictly correct, particularly as regards the radiation resistance, which is shown to be dependent on the distribution of the applied E.M.F. An experimental study shows that the approximations produce undetectable errors, except in the case of the resistance, in which small differences appear to be detectable.

1. General Considerations.

In a paper on "Induced Currents in a Wireless Telegraph Receiving Antenna" †, E. B. Moullin compared the effective heights of receiving and transmitting antennæ and proved them to be equal. He mentioned that it does not appear that this theorem can be proved from general considerations of energy. Moullin's proof is not general, as it applies only to the special case of antennæ with uniformly distributed capacity, inductance, and resistance.

F. M. Colebrook, in a paper which is in the course of publication, has shown that the effective impedance of an antenna is the same for transmission as for reception, but he has also limited the case to that of uniformly distributed constants and applied E.M.F.

We have no reason to assume that the constants are

* Communicated by Sir J. E. Petavel, K.B.E., F.R.S. Communicated by permission of the Radio Research Board.

† E. B. Moullin, "Induced Currents in a Wireless Telegraph Receiving Antenna." Proc. Camb. Phil. Soc. vol. xxii. p. 567 (1925).

uniformly distributed, and, in fact, we know that, owing to end-effects and the positions of the various parts relative to earth, the constants of an ordinary antenna are not so distributed.

The following analysis is intended to generalize the results of Moullin and Colebrook by making no assumptions on the law according to which the constants of the antenna are distributed along its length. A fundamental assumption remains, however, that the law of distribution of the constants is the same for transmission as for reception. The validity of this assumption is discussed below in section 3.

2. Proof.

Consider an element of length δr of an antenna. Let its direction cosines be l, m, n. Suppose the components of the electric intensity of an approaching wave have instantaneous values E_x, E_y, E_z, and that an E.M.F. of instantaneous value V be applied at the foot of the antenna, the frequency of the E.M.F.'s being the same.

We shall write R, L, C for the resistance, self-inductance, and capacity per unit length of the element δr of the antenna.

If v and i are the potentials and current respectively at any point r of the antenna, then the differential equations for the electric conditions at any point are

$$-\frac{dv}{dr}=(\mathrm{R}+j\mathrm{L}w)i-(l\mathrm{E}_x+m\mathrm{E}_y+n\mathrm{E}_z) \quad . \quad . \quad (1)$$

and

$$-\frac{di}{dr}=j\mathrm{C}wv, \quad . \quad . \quad . \quad . \quad . \quad . \quad (2)$$

where $j=\sqrt{-1}$ and $w=2\pi$ (frequency).

It should be noticed that in these two equations R, L, C, E_x, E_y, E_z are any functions of r.

Eliminating v from (1) and (2), we have

$$\frac{d^2i}{dr^2}-\frac{1}{\mathrm{C}}\frac{d\mathrm{C}}{dr}\frac{di}{dr}-(\mathrm{R}+j\mathrm{L}w)j\mathrm{C}wi=-j\mathrm{C}w(l\mathrm{E}_x+m\mathrm{E}_y+n\mathrm{E}_z). \quad . \quad . \quad . \quad (3)$$

To solve this, suppose s is a solution of the equation

$$\frac{d^2i}{dr^2}-\frac{1}{\mathrm{C}}\frac{d\mathrm{C}}{dr}\frac{di}{dr}-(\mathrm{R}+j\mathrm{L}w)j\mathrm{C}wi=0 \quad . \quad . \quad . \quad (4)$$

Putting $i=us$, we obtain

$$\frac{d^2u}{dr^2}+\frac{du}{dr}\left(\frac{2}{s}\frac{ds}{dr}-\frac{1}{\mathrm{C}}\frac{d\mathrm{C}}{dr}\right)=-\frac{j\mathrm{C}w}{s}(l\mathrm{E}_x+m\mathrm{E}_y+n\mathrm{E}_z).$$

This is a linear equation in du/dr, and the solution is

$$u=\int\frac{C}{s^2}\int(lE_x+mE_y+nE_z)sjw\,dr\,dr+A\int\frac{C}{s^2}dr+B,$$

where A and B are constants of integration.

Let $$Q=\int\frac{C}{s^2}\int(lE_x+mE_y+nE_z)sjw\,dr\,dr. \quad . \quad . \quad (5)$$

and $$P=\int\frac{C}{s^2}dr, \quad \text{so that} \quad \frac{dP}{dr}=\frac{C}{s^2}. \quad . \quad . \quad . \quad (6)$$

Hence we can write

$$i=(Q+AP+B)s. \quad . \quad . \quad . \quad . \quad . \quad (7)$$

We shall also find the following formula useful:

$$\begin{aligned}Q&=\int\frac{dP}{dr}\int E_r sjw\,dr\,dr\\&=\left[P\int E_r s\,dr-\int PE_r s\,dr\right]jw, \quad . \quad . \quad . \quad (8)\end{aligned}$$

where $$E_r=lE_x+mE_y+nE_z.$$

In these equations it should be noticed that the variables P and s are functions of the antenna constants only, while Q is a function of both the antenna constants and of the approaching field.

There now remains to insert the boundary conditions. Let the impedance of the apparatus between the foot of the antenna and earth be Z, and let i_0 be the value of the current at the foot of the antenna, then

$$\text{when } r=0,\ v=V-Zi_0$$
$$i=i_0,$$

and, if h is the length of the antenna,

$$\text{when } r=h,\ i=0.$$

On substituting these boundary conditions, we obtain

$$i_0\left\{Z-\frac{1}{s_0C_0jw}\frac{ds_0}{dr}-\frac{1}{(P_0-P_h)s_0^2jw}\right\}=V-\frac{(Q_0-Q_h)}{s_0(P_0-P_h)jw}+\frac{s_0}{jC_0w}\frac{dQ_0}{dr}, \quad . \quad . \quad (9)$$

where s_0, C_0, P_0, Q_0 are the values of s, C, P, Q when $r=0$, and P_h, Q_h are the values of P, Q when $r=h$.

Effective Impedance.

Let us examine equation (9). It will be seen that the right-hand side is a function of applied electric intensities, and the units are those of an E.M.F. Also the coefficient of i_0 is independent of the applied electric intensities, and its units are those of an impedance.

Now, comparing equation (9) with the equation

$$i_0(Z+Z_0)=V+E_0, \quad . \quad . \quad . \quad . \quad . \quad (10)$$

where Z_0 is the effective impedance of the antenna and E_0 is the equivalent E.M.F. at the base which produces the same current i_0 as the approaching wave, we obtain at once

$$Z_0=-\frac{1}{s_0 C_0 jw}\frac{ds_0}{dr}-\frac{1}{(P_0-P_h)s_0^2 jw}. \quad . \quad . \quad (11)$$

and

$$E_0=\frac{s_0}{jC_0 w}\frac{dQ_0}{dr}-\frac{Q_0-Q_h}{s_0 jw(P_0-P_h)}. \quad . \quad . \quad . \quad (12)$$

Equation (11) shows that Z_0 is independent of Z and of the applied E.M.F.'s, while E_0 is a function of both the applied E.M.F.'s and the constants of the antenna. This proves the following proposition :—

> *If the distribution of the constants along an antenna is unaffected by the applied E.M.F.'s, the effective impedance measured at any point is also unaffected by the applied E.M.F.'s, and is therefore the same for transmission as for reception.*

Incidentally, this proposition applies equally well to any form of transmission line.

Effective Height.

In defining the effective height of an antenna we should consider only those parts, or resolved parts of the antenna, which are effective in radiating energy, in the case of a transmitting antenna, or absorbing energy from the approaching wave, in the case of a receiving antenna.

In the case of transmission over a perfectly conducting earth, it is only the resolved parts of the antenna along the vertical axis that are effective in producing an electromagnetic field at a distance, unless the wave-length is comparable to the height of the horizontal portions. If OZ is the vertical axis, the effective height T_z of a transmitting

antenna can therefore be generally defined by

$$T_z = \frac{1}{I_0}\int_0^h nI\,dr, \quad \ldots\ldots \quad (13)$$

where I, I_0 are the maximum values of i, i_0.

Substituting equation (7), we have

$$T_z = \frac{\int_0^h n(P-P_h)s\,dr}{s_0(P_0-P_h)} \quad \ldots\ldots \quad (14)$$

In the general case, when the horizontal components have some effect in producing an electromagnetic field, the "effective heights" in the horizontal directions can be defined by

$$T_x = \frac{1}{I_0}\int_0^h lI\,dr \quad \text{and} \quad T_y = \frac{1}{I_0}\int_0^h mI\,dr,$$

which will give the results similar to equation (14).

In the case of a receiving antenna, suppose the current produced at the foot by a vertical approaching field E_z is i_0, and that the same current is produced by an E.M.F. V of the same frequency applied at the foot of the antenna, then the effective height R_z can be defined by

$$R_z = V/E_z. \quad \ldots\ldots \quad (15)$$

We have similar definitions for R_x and R_y.

In this case the approaching field must be uniform, otherwise the effective height will depend on the distribution of this field, and thus become meaningless.

From equation (9) we can find i_0 in the two cases by first putting $V=0$ and then $E_r=0$. On substituting in equation (15), we have

$$R_z = \frac{\int_0^h n(P-P_h)s\,dr}{s_0(P_h-P_0)}, \quad \ldots\ldots \quad (16)$$

and similarly for R_x and R_y.

It will be seen that equations (14) and (16) are identical, and we thus obtain the following proposition :—

If the distribution of the constants along an antenna is unaffected by the applied E.M.F.'s, the effective height is the same for transmission as for reception.

3. Validity of Assumptions.

The whole of the analysis in the previous section depends on the assumption that the distribution of resistance, capacity, and self-inductance is independent of the applied E.M.F.'s. Now, we know that the current distribution must be slightly affected by the distribution of the E.M.F.'s, and the reaction of one part of the antenna on another, whether electric or magnetic, must depend on the distribution of the current.

Suppose the antenna is split up into sections of length l, sufficiently small that the current can be assumed constant in each section. We shall consider the magnetic induction of one section on the next one, assumed to be in the same straight line. From Rosa's * formulæ for straight conductors we obtain for the mutual inductances of two consecutive sections

$$M = 2l \log 2,$$

and for the self-inductance of each section

$$L = 2l\left[\log\left(\frac{2l}{r}\right) - 1\right],$$

where r, the radius of the conductor, is small compared with the length.

It is seen that L is very much larger than M so long as the wave-length is very large compared with the radius, for this permits conditions to be assumed involving large values of l/r.

These formulæ are not, in the author's opinion, rigorously correct, but, when l is large compared with r, they no doubt give a fair representation of the actual state of affairs.

The electric reaction will give similar results since the integrals involved are similar.

It is therefore not to be expected that small changes in the distribution of current will produce any appreciable difference in the distribution of the effective values of the self-inductance and capacity per unit length of the antenna. This is confirmed by the experimental results described below.

There is, however, a part of the effective impedance, namely the radiation resistance, which may be slightly different when the antenna is used for transmission and when used for reception.

The radiation resistance of an antenna depends on the distribution of current along it and on the field produced by that current, and therefore on the dielectric characteristics

* E. B. Rosa, "Self and Mutual Inductances of Linear Conductors Bull. Bureau of Standards, vol. iv. p. 301 (1907).

of the surrounding objects. As a general rule, however, the radiation will depend mainly on the three integrals:

$$\frac{1}{I_0}\int_0^h lI\,dr, \quad \frac{1}{I_0}\int_0^h mI\,dr, \quad \frac{1}{I_0}\int_0^h nI\,dr.$$

The greater the value of these integrals, the greater the radiation resistance. Over a perfect earth, for wave-lengths long compared with the height, the last integral will be the most important.

For transmission these integrals, by the definition of effective height (equation 13), are

$$T_x, \quad T_y, \quad T_z. \quad . \quad . \quad . \quad . \quad . \quad . \quad . \quad (17)$$

For reception, however, the first of these integrals using equation (16) will be found to be

$$\frac{1}{I_0}\int_0^h ls(Q-Q)\,dr - \frac{s_0}{I_0}(Q_0-Q_h)R_x + R_x. \quad . \quad (18)$$

There will be similar expressions for the other two integrals.

It will be seen that, in general, the radiation resistance is different for transmission and reception.

4. Application of Formulæ.

In making use of the above formulæ, suppose a value is found for s which is a solution of equation (4). The value of P can be found from the integral (6), while the value of Q is best obtained from equation (8).

The effective resistance is obtained by finding the real part of equation (11), while the imaginary part will give the effective reactance. The effective heights are given by equation (14).

In connexion with the effective impedance, it is usual to represent an antenna by a resistance R_0, a capacity C_0, and a self-inductance L_0, all in series, so that

$$Z_0 = R_0 + L_0 jw + \frac{1}{C_0 jw}.$$

If Lw is the effective reactance equivalent to the reactance of this representation, we have

$$L = -\frac{(1-L_0C_0w^2)}{C_0w^2};$$

therefore

$$C_0 = \frac{2}{w^3}\Big/\frac{dL}{dw} \quad . \quad . \quad . \quad . \quad . \quad . \quad (19)$$

and

$$L_0 = L + \frac{w}{2}\frac{dL}{dw}. \quad . \quad . \quad . \quad . \quad . \quad (20)$$

When the frequency is low, it is more usual to measure the effective capacity C of the whole, so that

$$C = \frac{C_0}{1 - L_0 C_0 w^2};$$

therefore

$$L_0 = \frac{1}{2C^2 w} \frac{dC}{dw} \quad . \quad . \quad . \quad . \quad . \quad . \quad (21)$$

and

$$C_0 = \frac{2C^2}{2C + w \frac{dC}{dw}} \quad . \quad . \quad . \quad . \quad . \quad . \quad . \quad (22)$$

Hence, by plotting X or C against w and finding the differential or the gradient, we can find the effective inductance and capacity at any given point. It should be noticed that equations (21) and (22) break down when the antenna acts as a pure resistance ; this occurs at the natural frequency and near odd multiples of the natural frequency of the antenna.

Near even multiples of the natural frequency, dL/dw becomes small ; the effective impedance of the antenna then resembles more that of a parallel tuned circuit, for which the usual representation is very unsatisfactory. Near these points it is therefore inadvisable to try to split up the effective reactance into a capacity and a self-inductance. In any case such representations are essentially fictitious and of very doubtful value unless the constants of the representative circuit remain unaltered over a considerable range of frequency.

We shall now apply the formulæ obtained above to the well-known case of an antenna having uniformly-distributed resistance, capacity, and self-inductance. In these conditions an obvious solution of equation (4) is

$$s = e^{Kr},$$

where

$$K^2 = (R + jLw)jCw.$$

Therefore

$$P = -\frac{Ce^{-2Kr}}{2K}$$

and

$$Q = -\frac{jCwe^{-Kr}}{K^2} E_r.$$

Substituting in equation (11), we have

$$Z_0 = \frac{K}{jCw} \coth (Kh),$$

which is the well-known formula for a uniform transmission line.

Expanding, this becomes

$$Z_0 = R\frac{h}{3} + \frac{1}{hjCw} + \frac{hjLw}{3} + \ldots\ldots$$

From equation (12) we readily find the effective height to be

$$T_z = \frac{1}{K}\tanh\left(\frac{Kh}{2}\right)$$
$$= \frac{h}{2}\left(1 + \frac{h^2 LCw^2}{12} + \ldots\ldots\right),$$

as obtained by Moullin *.

To compare the radiation resistance in the two cases of transmission and reception, we have to evaluate $\frac{1}{I_0}\int_0^h I\,dr$. For transmission, this integral is (equation 17)

$$\frac{I}{K}\tanh\left(\frac{Kh}{2}\right).$$

For reception, the integral—assuming E_r to be uniformly distributed along the antenna—is

$$\frac{1}{K}\tanh\left(\frac{Kh}{2}\right) + \frac{jCw}{K^2}\frac{E_r}{I_0}\left[\frac{2}{K}\tanh\left(\frac{Kh}{2}\right) - h\right];$$

that is,

$$\frac{1}{K}\tanh\left(\frac{Kh}{2}\right) - \frac{jCw}{K\tanh\left(\frac{Kh}{2}\right)}\left[\frac{2}{K}\tanh\left(\frac{Kh}{2}\right) - h\right](Z + Z_0).$$

We would therefore expect the radiation resistance to be slightly different in the two cases. If $(Z + Z_0)$ is a pure resistance, the resistance will generally be greater for reception than for transmission.

It is interesting to note that the difference is dependent on the value of the impedance Z of the apparatus between the antenna and earth. In fact, when Z is infinite the difference in the radiation resistance is also infinite. The physical interpretation of this is easily found. If Z is infinite the current I_0 at the foot of the antenna will be zero. Thus in

* *Loc. cit.*

the case of transmission there would be no current whatever in the antenna, while, owing to capacity and inductance effects, some currents will flow on reception: this current will produce a re-radiated field. Thus, on reception, some power is re-radiated, although the current at the base may be zero, giving rise to an infinite effective radiation resistance.

Other cases where the constants of the antenna are not uniformly distributed can be treated in a similar way.

5. Experimental Verification.

In order to ensure that the antenna under measurement had not uniformly distributed constants, loops of wire were added to it until its shape was as shown in fig. 1. A counterpoise earth was used.

Fig. 1.

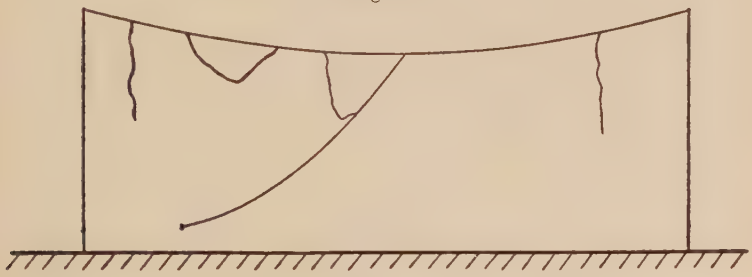

Fig. 2.

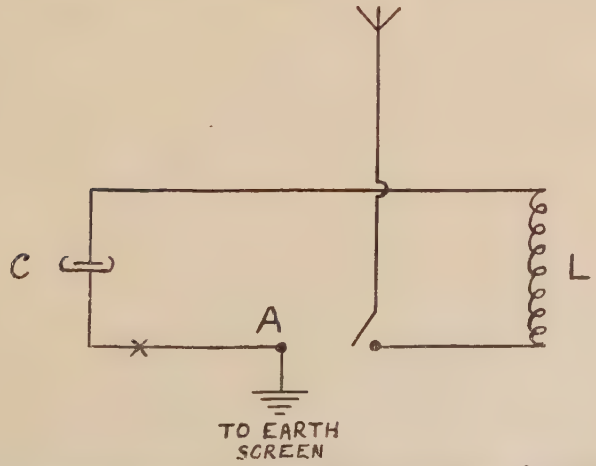

The measurements were made by inserting the antenna in series in a circuit (fig. 2) which was measured with and

without the aerial, the counterpoise remaining connected to the point A during all the measurements.

The resistance was measured by the variation of reactance method by varying a very small accurately calibrated condenser in parallel with condenser C.

The measurements were carried out for transmission by inducing from a small power set into the coil L, and for reception by inducing into the antenna from another antenna excited by a larger set about 50 yards distant. A large army hut running within a few feet of the receiving antenna for the whole of its length and situated in between the two antennæ, ensured that the field at the receiving antenna was not uniform. It was ascertained that the direct induction into the coils was small. The two power sets were adjusted to the same frequency by means of the same wavemeter without alteration of setting, so as to eliminate small errors due to frequency adjustments.

Since differences are only to be expected at high frequencies, the wave-lengths used were all under 210 metres. Table I. gives the results of the measurements. The figures for reactance and resistance refer to the antenna alone without the rest of the circuit.

Table I.

Wave-length in metres.	Reception.			Transmission.		
	Setting of Condenser C.	Reactance in ohms.	Resistance in ohms.	Setting of Condenser C.	Reactance in ohms.	Resistance in ohms.
208·5	119·8	−297	4·2	120	−297	4·2
140·0	283	− 74	5·0	283	− 74	4·9
127·0	186	− 7·8	7·2	186	− 7·8	7·0
114·0	215	+ 89	64	215	+ 89	70

The last results at a wave-length of 114 metres are interesting, for they represent the antenna beginning to act as a rejector circuit. Owing to its shape, the downcoming lead is for a long portion of its length quite close to the earth screen, thus acting as a large capacity. The rest of the antenna acts as a positive impedance at that frequency, o that a rejector circuit is formed. That is the reason for

the sudden rise in the value of the resistance. This condition could be altered by changing the shape of the downcoming lead. This was done and, though no very accurate measurements were taken, the effective resistance decreased to the order of 15 ohms.

From the table we see that the natural wave-length of the antenna is slightly below 127 metres. This, incidentally, is a very accurate way of finding the natural frequency of an antenna without having instruments in series liable to alter the value searched for. The process consists in exciting the circuit by inducing into the coil L and varying the frequency until resonance is obtained with and without the antenna in circuit for the same reading of condenser C. The earth should remain permanently connected to the point A, and it is advisable to disconnect the antenna when it is not in series in the circuit. In practice the exact point

Fig. 3.

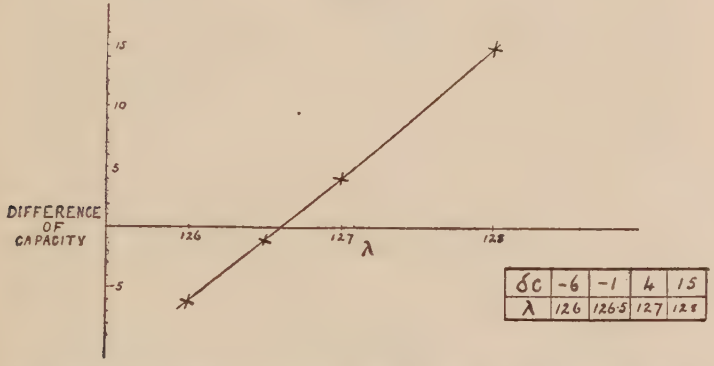

is a little troublesome to find, and it is best to plot the differences in the readings of condenser C, with and without the antenna in series, against the frequency for a number of points near the natural frequency, which is then found by interpolation. A typical diagram of results is shown in fig. 3. Readings at higher frequencies were not taken owing to the difficulties of measurement, particularly because of the very high effective resistance which the antenna attained, rendering the deflexion of the ammeter too small to be useful for resistance measurements, which, in any case, are very uncertain at these frequencies and therefore of very doubtful value.

The values obtained are seen from the table to confirm the theoretical deductions. No differences in the condenser settings were detectable, while the resistance appears to be

slightly greater for reception than for transmission, which difference increases with increasing frequency. At 114 metres the resistance was very difficult to measure, but the resistance for transmission appeared to be greater than for reception. This is probably due to the action of the antenna as a rejector circuit, for in that case the greater the resistance within the circuit the smaller the effective resistance.

Too great reliance, however, should not be placed on the small differences of resistance given in the table, as they are within the limits of experimental error. The fact that the errors of measurement due to the arrangement of the circuit are similar for transmission and reception gives, however, greater weight to the reality of the small differences observed.

To test this further, measurements were made near the natural frequency of the antenna ($\lambda = 1.27$ m.) using thermo-ammeters having different resistances Since the radiation resistance for reception depends on the value of Z, we should expect the difference to increase with increasing resistance of the ammeters. These differences for different values of thermo-ammeter resistance are given in Table II.

It was found that, owing to the effect of the observer on the large capacity *viâ* the earth between the screen of the condenser and the counterpoise, and also to the capacity of the coil to earth, the measurements became increasingly difficult as the resistance of the thermo-ammeter was increased.

Table II.

Resistance of Thermo-ammeter.	(Resistance for reception) — (resistance for transmission).
1 ohm.	0·2 ohm.
5 ohms.	0·3 ohm.
30 ohms.	0·7 ohm.

The resistance of the rest of the circuit was of the order of 8 ohms.

The differences are small and within the limits of experimental error for absolute values, but probably not for the differences themselves. It should be further noticed that any error caused by reaction back on to the source would

produce an increase in the apparent resistance on the transmission measurements, whereas the resistance on reception was found to be always slightly greater than on transmission.

6. Conclusion.

To summarize: we have found theoretically that, if the distribution of the constants of an antenna is the same for transmission as for reception, the effective resistance, reactance, and the effective height are also the same in the two cases. The radiation resistance, however, is slightly different.

Experimental evidence down to about 100 metres wavelength showed that the difference in the reactance in the two cases was undetectable, while there was strong evidence that there was a small difference in the resistance, that for reception being slightly greater than that for transmission.

This investigation was carried out for the Radio Research Board established under the Department of Scientific and Industrial Research, and the author is indebted to the Board for permission to publish this paper.

VIII. *The Three-Point Spark Gap.*

By J. D. Morgan, *D.Sc.**

It is well known that the sparking voltage of a gap is greater—sometimes much greater—when the voltage is applied impulsively, than when it is applied gradually or is sustained. The ratio of the two voltages is commonly termed the impulse ratio. It is also well known that the impulse ratio of a gap can be reduced or irregular sparking made regular by the use of a third point. In its ordinary form the three-point gap comprises a pair of main electrodes forming the main gap, and an insulated third electrode forming between it and one of the main electrodes a small auxiliary gap situated adjacent to the main gap. The efficacy of the small spark across the auxiliary gap depends upon the quantity of electricity passing through it and also upon its position relatively to the main gap. When one of the main electrodes is earthed the auxiliary gap must be arranged near the other electrode. The faint and tiny spark which passes across the auxiliary gap is necessary to the performance of the ordinary three-point gap. A common

* Communicated by Prof. E. Taylor Jones, D.Sc.

form of the three-point gap is shown in fig. 1, where *a* and *b* are the main electrodes carried by metal pillars *c*, *d* on an insulating base *e*, and *f* is the third point forming with *a* the small auxiliary gap. The third point is also carried on the insulating base, but has no connexion with either of the metal pillars. Sometimes the adjacent ends of the main electrodes are made of spherical form.

The problem of the action of the auxiliary spark has received much attention from those whose work involves the use of spark gaps. Until about a year ago no satisfactory explanation of the action of the auxiliary spark appears to have been given. To assert, as was done, that the action is due to ionization was merely to guess at a probability. The most satisfactory solution of the problem yet offered appears

Fig. 1.

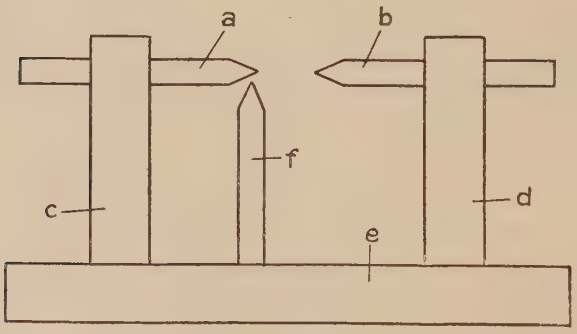

to be that due to Mr. Wynn-Williams*. According to Wynn-Williams the action is due to ionization of the gas in the main gap by radiation from the auxiliary spark. In addition to this contribution to the problem, Wynn-Williams also discovered a novel third-point effect. He found that a sharp needle-point held at some distance from, but electrically connected to, one of the electrodes was apparently more effective than the usual auxiliary spark. The same result can be obtained by holding an insulated needle across and in contact with one of the electrodes so that the point is "in view" of the gap. A sharp point like that of a needle is essential to the effect observed by Wynn-Williams. A blunt electrode raised to the same potential has no effect.

The work of Wynn-Williams merits close examination

* "An Investigation into the Theory of the Three-Point Gap." C. E. Wynn-Williams, M.Sc., Phil. Mag. vol. i. Feb. 1926.

and, if possible, further development, and as the validity of at least one of Wynn-Williams's experiments appears to be not beyond doubt, the problem of the three-point gap has been subjected to a further attack on rather different lines from those which he followed.

As already stated, Wynn-Williams found that a sharp needle-point electrically connected to one of the electrodes produced an effect equivalent to that of the auxiliary spark of the ordinary three-point gap, and, presumably because of its greater convenience, he used a needle so connected throughout his major experiments. These undoubtedly support the deduction made from them, but the equivalence of such a needle and an auxiliary spark does not appear to have been established fully. He finds, for example, that the needle-point when activated by a Wimshurst machine has the same effect as when connected to the main gap. It is possible to show, however, that under suitable conditions a needle-point connected to a Wimshurst machine has no effect whatever on the main gap. Further, he seems to suggest that an auxiliary spark produced by a Wimshurst machine or other continuously acting source of electricity has no effect on the main gap, whereas under suitable conditions the contrary can be proved. These facts are sufficient, if any justification were required, to warrant a re-examination of the problem of the three-point gap, in the light of the notable contribution made by Wynn-Williams.

Prof. E. Taylor Jones has for a long time used a gap one of the electrodes of which contains a small quantity of radium placed in a tiny hole on the axis of the gap. The sparking voltage of this gap is remarkably regular, and appears to be in no way improved by any external "third-point" action. This gap demonstrates that direct ionization of the gas in the gap is an effective means of obtaining regular action. It also suggests a line of approach to the problem of the three-point gap.

In the first series of experiments now to be described it was decided to employ a gap of about 2 mm. formed between hemispherical ends of a pair of brass rods of 5 mm. diameter. The electrodes were connected to the opposite terminals of an induction coil actuated by an ordinary vibratory interrupter. It is important to note that one of the electrodes was earthed. Apparently Wynn-Williams did not include this condition in his experiments. Otherwise he would have noticed some of the effects described below. The primary current was adjusted until it was barely sufficient to cause a spark to pass. With the coil in action, but no spark passing at the

gap, a sharp needle connected to one of the poles of a Wimshurst machine was brought to a position about 6 cm. from the gap, and the following effects were observed.

When the high-tension (h.t.) electrode of the gap was of negative sign, and the needle was excited by the positive terminal of the Wimshurst, the gap sparked with perfect regularity. Still keeping the h.t. electrode negative, the needle was transferred to the negative pole of the Wimshurst. Then no sparking occurred at the gap. On reversing the polarity of the h.t. electrode, sparking occurred at the gap when the needle was negatively electrified, but none when the needle was positive. These experiments show that when the needle is excited by a Wimshurst machine, the needle only affects the gap when its polarity is opposite to that of the h.t. electrode of the main gap. The results are only apparent when one of the main gap electrodes is earthed. Without the earth connexion, the effect of polarity on the action of the needle is masked, because the appropriate polarity then always exists at one or the other of the gap electrodes.

In the second series of experiments the needle was connected to the h.t. electrode of the gap. Two facts became evident. It was noticed that when the needle-point was placed near the h.t. electrode, no effect was produced in the gap, and no sparks passed; but when it was placed near the earthed electrode, a spark occurred, so long as the Wynn-Williams condition was satisfied that a straight line could be drawn from the needle-point to any part of the spark path between the main electrodes. Clearly, before the Wynn-Williams effect can be obtained, it is necessary for the needle-point to be subjected to a sufficient potential gradient. Further, it was noticed that the effect of the needle-point on the gap was independent of the polarity of the h.t. electrode. As a check the needle was fixed in the last position, nearer the earthed than the h.t. electrode, and the experiment with the Wimshurst machine was repeated. When connected to the Wimshurst the needle was only operative when of opposite polarity to the h.t. electrode.

Seeing that the action of the needle-point on the gap was, in the first series of experiments, dependent on the polarity of the needle, and, in the second series, independent of polarity, it must be concluded that the action associated with the needle-point was different in the two experiments.

The effect of the discharge from the needle on an electroscope was then examined. It was found that when the needle was connected to either pole of the Wimshurst machine, the electroscope became strongly charged, even

when the needle was held at considerable distance (as much as 25 cm. or more) away from the electroscope. When the needle was connected to the h.t. electrode of the gap, or induction coil, there was but little, if any, charging effect on an uncharged electroscope, but there was a strong discharging effect when the electroscope was charged either positively or negatively. This suggests that in the first series of experiments the effect was due to direct ionization of the gap, whilst in the second the effect was that found and explained by Wynn-Williams. Reference to confirmatory experiments will be deferred while brief consideration is given to the question as to why the Wynn-Williams effect was not obtained in both experiments.

It is surprising and not a little perplexing that the needle-point should behave in a certain manner when connected to the h.t. electrode, and in a different manner when connected to the Wimshurst machine. Assuming that in both experiments the needle-point was subjected to the same potential gradient, the only difference that existed in the conditions of the experiments was that of the manner in which the potential was applied. In the first experiment the voltage, or potential, was applied steadily, whilst in the second it was applied impulsively. Possibly an impulsive action at the needle-point is essential to the Wynn-Williams effect. If so, it ought to be capable of demonstration. To test the matter, the needle-point was first disconnected from the Wimshurst, and the latter was operated until the poles were raised to a sufficiently high potential. With the h.t. electrode negative, a wire attached to the needle was then suddenly brought into contact with the negative pole of the Wimshurst, and momentary sparking occurred at the gap. With the h.t. electrode positive, sudden connexion of the needle with the positive pole of the Wimshurst was also followed by momentary sparking at the gap. Continued connexion of the needle with the Wimshurst in both tests gave the same results as has already been mentioned, namely, no sparking at the gap. It follows that to obtain indirect ionization of the gap by radiation issuing from the needle-point, the latter must be subjected to an impulsive action. In other words, the Wynn-Williams effect is a transitory one, and is not obtained when the needle-point is maintained at a high potential. Under the latter condition the discharge is of the nature of an ionized stream which is only operative on a gap (in which one electrode is earthed) when the stream is of appropriate sign.

Reflection on the results of the experiments led to the

construction of a new form of gap the essential features of which are shown in fig. 2. The use of this gap throws an interesting side light on the question under examination and affords confirmation of the conclusions already reached.

The h.t. electrode *a* is a metal disk of about two inches diameter. This is attached at its edge to the upper end of a vertical insulating pillar. The earthed electrode *b* consists of a metal rod having a hemispherical end adjacent to the disk. This electrode is also carried on an insulating pillar. At the centre of the electrode *a* is formed a tiny hole.

Fig. 2.

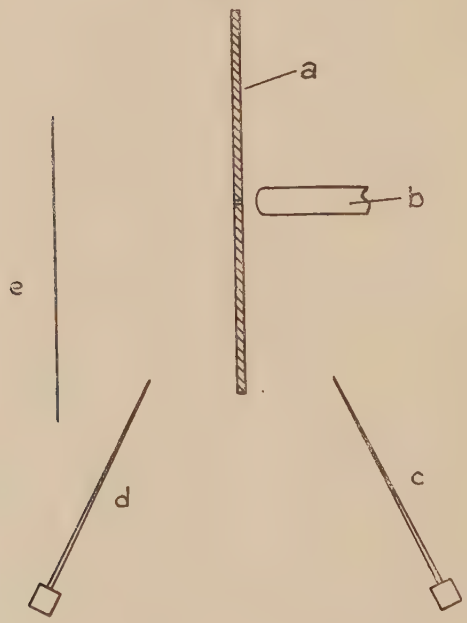

Viewing the gap in plan, a needle was placed in or about the position indicated at *c*.

After adjusting the current in the primary winding of the inductance coil so that a spark just failed to occur at the gap between *a* and *b*, the needle was connected by a wire to the electrode *a*. Sparking then occurred at the gap. With the h.t. electrode negative, sparking also occurred when the needle was connected to the positive terminal of a Wimshurst machine. When the needle was connected to the negative terminal of the Wimshurst, the sparking at the gap became

very irregular, and it was found that on closing the back of the hole in the electrode *a* this sparking ceased.

On transferring the needle to the position *d*, and connecting the needle to the electrode *a*, sparking did not occur at the gap, but on bringing an earthed plate into the neighbourhood of the needle and so increasing the potential gradient to the needle-point, some sparking occurred; it was not, however, so regular as when the needle was at *c*. Sparking became quite regular when the needle-point was advanced to a position on or near the axis of the hole in *a*, an earthed plate being held in the neighbourhood of the point as above mentioned. With the needle still at *d* and the h.t. electrode negative, connecting of the needle to the negative terminal of the Wimshurst machine resulted in regular sparking at the gap. Closing of the hole in the electrode *a* caused the sparking to cease. Sparking also ceased when the needle was connected to the positive terminal.

A curious effect was observed when the needle, whilst at *d*, was connected to the negative terminal of the Wimshurst machine, the electrode *a* being connected as already mentioned to the negative terminal of the induction coil. On placing a sheet of mica or an insulated metal plate in the position *e*, or above or below the needle with its plane parallel to the axis of the gap, the sparking at the gap ceased, the needle-point being always "in view" of the hole in *a*, and therefore not obstructed. The plate had no effect when the needle was connected to the electrode *a*.

It is remarkable that when an ionized stream is caused to issue from the needle-point for the purpose of facilitating the passage of sparks in the main gap, the needle must be of opposite polarity to the electrode *a* when placed at the front, or gap side, of that electrode, and of the same polarity when placed at the rear of the electrode. This fact requires further investigation.

The experiments with the gap shown in fig. 2 confirm what was found in the experiments first described, namely, that the action of the needle-point on the main gap when the needle is excited impulsively is different from the action when the needle is excited from a steady source such as a Wimshurst machine.

It is now convenient to consider the main question, and inquire in what manner the auxiliary spark in the three-point gap performs its function when the gap is subjected to the action of an induction coil. The gap shown in fig. 2 enables a decisive answer to be obtained.

Instead of producing the auxiliary spark across a small

or auxiliary gap adjacent to the h.t. electrode as in fig. 1, it was more convenient to employ a separate small gap between needle or other suitable electrodes mounted on a handle so that the small gap could easily be presented to different parts of the main gap, one of the electrodes of the small gap being connected to the h.t. electrode of the main gap, or one of the terminals of a Wimshurst machine, and the other to a very small leak, or very high resistance connexion to earth, to insure the requisite discharge of electricity across the small gap.

In the first place it was found that when the small spark was produced by a connexion to either terminal of a Wimshurst machine, and was therefore of the nature of a small but continuous discharge, the spark produced a charging effect on an uncharged electroscope, but the effect was not nearly so strong as that obtained from a needle-point. When the small spark was produced by the induction coil to which the main gap was connected, and was therefore of an intermittent or impulsive character, there was no charging effect on an electroscope. On the contrary, the electroscope, when charged either positively or negatively, was discharged, though the discharging action was not so strong as that obtained when the needle was connected to the coil.

With the small gap connected to the same terminal of the induction coil as the electrode *a* and placed in about the same position as the point of the needle at *c* (fig. 2), perfectly regular sparking occurred at the main gap. The same result was obtained when the small spark occupied a position at the back of *a* on or about the axis of the hole. On moving the small gap to the position *d*, sparking at the main gap ceased. It follows that the action of the small spark was similar to that of the needle-point when the latter was electrified by connexion to the electrode *a*.

The small gap was then connected to each in turn of the terminals of a Wimshurst machine. Unfortunately the results were not very definite. With the electrode *a* negative, and the small gap placed at *c* (fig. 2) and connected to the positive terminal of the machine, rather erratic sparking occurred at the main gap, and none when the small gap was connected to the negative terminal of the machine. On transferring the small gap to the position *d*, the reverse results were obtained. But the erratic or occasional character of the sparking at the main gap when the small sparks were produced by the Wimshurst machine makes it impossible to say that the results were convincing. It was,

therefore, decided to use for the production of the continuous small spark a condenser charged negatively from the induction coil through a thermionic valve. The small spark thus obained had a fairly strong charging effect on an electroscope. When placed at *d*, the electrode *a* being negative, perfectly regular sparking occurred at the main gap, and the sparking at the main gap ceased when a mica plate was placed at *e*, proving that with the small spark in this position its effect was due to a stream of negative ionization. When placed at *c*, occasional sparking occurred at the main gap, and it was not possible to decide whether this result was due to intermittency in the small gap, producing the same effect as a spark derived directly from the induction coil, or to ultra-violet radiation, it being unlikely that a stream of positive ionization was responsible. If the effect was due to ultra-violet radiation, the experiment showed, as Wynn-Williams appears to have found, that such radiation is not nearly so active as the Entladungstrahlen to which he attributes the properties of the needle-point and auxiliary spark. The Wimshurst machine experiments above described also support the conclusion that ultra-violet radiation is relatively weaker in its action, otherwise the Wimshurst sparks would have given different results.

Notwithstanding the partial success of the experiments with sparks produced by the Wimshurst machine, the evidence obtained from all the experiments adequately supports the conclusion that small sparks obtained from a continuously acting source are different in effect from those obtained intermittently from an induction coil, as in the usual three-point gap, and that the action of the auxiliary sparks in such a gap depends upon a highly active form of radiation due to the impulsive character of the spark. This action is not, however, so strong as that obtained from a needle-point.

Finally, it may be mentioned, though merely as a matter of interest, that a lighted match held in the neighbourhood of the front of the electrode *a* (fig. 2) caused regular sparking at the gap, but had no effect at the back of that electrode, excepting when placed near and opposite the hole, and then it had a slight effect in that an occasional spark passed at the gap.

Summary.

The experiments described confirm the conclusion previously established by Wynn-Williams that the action of the auxiliary spark in a three-point gap is due to ionization

of the gas in the main gap by radiation given off from the auxiliary spark. They also go further, and show that the Wynn-Williams effect is due to an impulsive or transient condition. Moreover, they show that when a needle-point or an auxiliary spark-gap is connected to a steady source of potential, such as a Wimshurst machine, the action of the needle-point or the auxiliary spark on the main gap is then due not to radiation but to an ionized stream.

IX. *Refraction of X-Rays by Method of Total Reflexion.*

By Richard L. Doan, *Ph.D., Ryerson Physical Laboratory, University of Chicago, U.S.A.* *

[Plate I.]

THE classical Drude-Lorentz theory of dispersion leads to an expression for the index of refraction of a substance which may be written in the following manner :

$$1-\mu=\delta=2{\cdot}714(10)^{-6}\frac{D}{W}\lambda^2\sum\frac{n_r\lambda_r^2}{\lambda_r^2-\lambda^2},$$

where μ = index of refraction for monochromatic radiation of wave-length λ,

D = density of refracting substance,

W = atomic weight,

n_r = number of electrons per atom of natural frequency $c\lambda_r$.

This theory is based upon the assumption of elastically and isotropically bound electrons which are set into forced vibration by the action of the electromagnetic field of any radiation which is allowed to traverse the substance. The resultant absorption of energy is accompanied by an emission of scattered radiation. If the frequency of the radiation is much higher than the natural frequencies of the electrons, then the latter will scatter as if free and will absorb a minimum amount of energy. But when the natural frequency of a particular group of electrons is approached, the electronic vibrations will increase in amplitude and there will be a greater absorption of energy. The classical theory attempts to account for the dispersion of a substance near an absorption edge simply by an application of the idea of resonance.

* Communicated by the Author.

A quantum theory of X-ray dispersion has recently been developed by R. de L. Kronig *. This theory is of a more empirical nature, in that it introduces known facts concerning atomic absorption coefficients, and an attempt is made to bring the phenomenon of dispersion into close correlation with that of absorption. The picture of elastic and isotropic binding of electrons is rejected as being too specialized and not in accord with available experimental information. It is replaced by the results of a theoretical investigation of Kramers concerning the behaviour of a multiply periodic system under the action of an alternating electric field, and it is from this source that a value for the scattering moment per atom is obtained. The general expression which is deduced for the index of refraction can, after some manipulation, be put into the form

$$1-\mu=\delta=\frac{NZe^2}{2\pi m\nu^2}+\frac{Nc^4CZ^4}{8\pi^2\nu^4}\ln\left(\frac{\nu_r^2-\nu^2}{\nu_r^2}\right)^2,$$

in which N and Z are respectively the number of atoms per unit volume and the atomic number of the refracting material, and C is the constant which enters into the expression for the fluorescent absorption coefficient. Its value † is about 0·023 for radiations on the short wave-length side of the K-limit and from one fifth to one eighth of this on the long wave-length side.

For light refracting materials in which no resonance effect is involved the second term on the right, above, becomes negligible and the equation reduces to the ordinary Lorentz form. Differences between the two expressions are therefore to be expected only in the presence of resonance effects.

Experimental Tests of Dispersion Formulas.

Most of the experimental work along this line has been carried out with light substances, and the results obtained are in satisfactory agreement with the theoretical expression :

$$\delta=2\cdot714(10)^{-6}D\lambda^2Z/W.$$

The accuracy secured in the measurements has varied from one to five per cent., depending upon the method of experimentation used. Probably the most accurate measurements have been made by Larsson, Siegbahn, and Waller ‡ on glass, but other measurements have been made on various

* Journ. Optical Soc. of America, xii. p. 547 (1926).
† See F. K. Richtmeyer, Phys. Rev. xviii. p. 13 (1921).
‡ *Die Naturwissenschaften*, December, 1924.

materials and for several different X-ray wave-lengths by Bergen Davis and his students *. Some measurements made on iron pyrites should be mentioned as showing the kind of information one may hope to get by studying indices of refraction. In calculating a value for the index of refraction in a case in which resonance occurs, one needs to assume some value for the number of electrons per atom which are situated in the particular frequency-level concerned. If, for instance, the incident radiation has a frequency near that of the K-electrons of the refracting substance, then we need to know the number of K-electrons per atom in order to make use of the theoretical formula. Von Nardroff † carried out this calculation for iron pyrites assuming successive values of one, two, and three for the number of electrons in this level. For copper Kα and Kβ radiation the experimentally determined value of the index of refraction agreed best with the theoretical value when the number of K-electrons was taken as two. This result is interesting in that it shows the possibility of getting independent checks on other methods which have been used to study the distribution of electrons among the various atomic levels.

The experiments described in the present paper were undertaken for the purpose of extending the measurements of indices of refraction to other substances, particularly to those substances in which rather definite resonance effects are to be expected. By comparing the experimental and theoretical values in such cases, one may expect to test further the validity of the theory in the neighbourhood of an absorption edge and also to get an idea of the relative values of the two theories that have already been discussed.

The Experimental Method.

All measurements were made by the method of total reflexion ‡. If θ is the glancing angle of incidence of a beam of X-rays on a plane surface and μ is the index of refraction with reference to air, then the critical angle of total reflexion is determined by

$$\cos\theta = \mu ;$$

then
$$1-\cos\theta_c = 1-\mu = \delta,$$

or,
$$2\sin^2\theta/2 = \delta.$$

* Proc. National Academy of Science, x. p. 60 (1924); Phys. Rev. xxvii. p. 18 (1926).

† Robert von Nardroff, Phys. Rev. xxiv. p. 143 (1924).

‡ *Cf.* A. H. Compton, Phil. Mag. xlv. p. 1121 (1923).

For the small angles concerned, the angle may be set equal to the sine, and we get the simple expression which was used in making the calculations,

$$\theta^2 = 2\delta.$$

Most of the surfaces that were used were prepared by depositing various metals on optical glass surfaces by sputtering *in vacuo* from a cathode of the pure metal. Relatively thick films of considerable brilliance and great uniformity were obtained in this way. As a general rule the sputtering was continued for a length of time varying from six to ten times the period required to produce an opaque film. The reflecting power of these surfaces was high and was increased by burnishing before use. The metallic surfaces so prepared were used in connexion with the K-radiation from molybdenum and copper water-cooled Coolidge tubes. Measurements were also made upon the

Fig. 1.

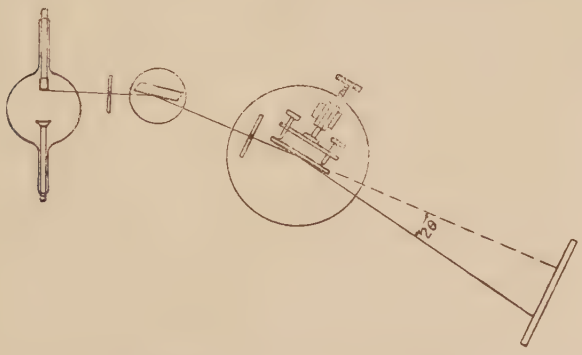

glass surface itself before sputtering and upon a surface of speculum metal polished to optical planeness.

In making the critical angle measurements a surface was mounted on a spectrometer table in such a way that a collimated beam of X-rays, made monochromatic by reflexion from a calcite crystal, fell upon it at a very small glancing angle (fig. 1). Under these conditions a reflected beam was obtained which was in most cases just as sharply defined as the primary beam. Preliminary photographs were first taken to locate the critical angle approximately, after which a photographic plate was mounted at a given distance (about 165 cm. for most of the experiments) from the mirror, and the latter given an effective slow motion of rotation past the critical angle during a continuous exposure.

In the first experiments this effective slow motion took the form of a series of individual exposures at angular intervals of a few seconds of arc, the turning being accomplished by hand, but later this method was replaced by a mechanical device for giving the desired rotation. This consisted of an electromagnet connected through a relay system to a large clock in such a way that the circuit was closed once every two seconds. Each time the circuit was closed a small arm to which was attached a pawl operating in connexion with a ratchet-wheel was drawn over to the core of the magnet, giving rise to an angular motion of the mirror of a fraction of a second of arc. The motion of rotation was thus made uniform and was reduced to such an extent that an angular range of five minutes of arc was covered in about an hour and a half, a period of time adequate to give a good photograph. Some of the photographs obtained are shown in fig. 2 (Pl. I.). It will be observed that the critical angles are quite sharply defined, thus enabling one to make an accurate setting on the extreme position. The sharpness of the critical angle varied in the different cases studied, and the effect of this upon the accuracy of the measurements is discussed below.

Method of Measurement and Considerations of Accuracy.

In more than half of the experiments angular measurements were made directly on the scale of a large spectrometer which was equipped with microscopes and which could be read to seconds of arc. The mounting for the photographic plate was fixed rigidly at the desired distance from the mirror, and this distance remained unchanged during a given experiment. After mounting the plate in position, the mirror was drawn back out of the path of the beam of X-rays and a short exposure was made to give a reference line from which to measure the critical angle. The finished plate was placed upon the table of a comparator and the critical angle measured simply as the distance between the reference line and the point where the reflexion stopped. In order to determine the angle to which this distance corresponded, an "angle plate" exposure was made which consisted in taking two exposures of the reflected beam by turning the mirror through a definite angle, the value of which could be read directly on the spectrometer scale. The distance between these two lines, as measured on the comparator, served as a scale by which the critical angle was determined. In later experiments essentially the same method was used, the only

difference being the substitution of a mirror and illuminated scale for the spectrometer in the initial angular measurements. An interferometer mirror was mounted rigidly on the revolving table by means of a one-inch steel support in such a way that the plane of its surface intersected the plane of the surface upon which experiments were being made in a line which formed the axis of the table. The scale was located at a distance of about ten feet from the mirror, and the telescope was mounted firmly on a stone block. This arrangement was used to calibrate a graduated dial attached through a system of two worm gears to the revolving table. One turn of this dial corresponded to a rotation of 36″ of arc and its circumference was divided into two hundred parts. In making subsequent angular measurements the lamp and scale method was used only to check the readings of the dial.

The accuracy of measurements such as those described here is affected by three factors. (1) The angular measurement itself is an indirect one, consisting of a spectrometer reading and a comparator reading. Both of these can be made with considerable accuracy, and probably contribute very little to the possible error of the experiments. (2) Width of line. Since measurements were made to the edge of the continuous band at which reflexion ceased, it will be seen that a half-line too much has been included. In most of the experiments the lines had an angular width of from 10 to 14 seconds of arc, and in two or three cases where the sharpness of the critical angle justified the procedure a half of this value was subtracted from the measurement as made to the edge of the band. (3) Sharpness of the critical angle. This factor introduces what is perhaps the largest single source of uncertainty in the measurements. In most of the cases in which the critical angle was small the limiting position was very sharply defined, but this was not always true, particularly for the large angles encountered in the use of the characteristic copper radiation. Since the sharpness of definition varied in the different photographs, the probable accuracy of the measurements is more or less a matter of judgment and is therefore indicated separately for each case. (4) Length of the mirror. In the case of small glancing angles it becomes necessary to consider the length of the mirror as affecting the value of the measured angle. In most of the experiments a mirror 78 mm. in length was used. Let us suppose that in an extreme case the reflexion occurred entirely on one half of the mirror during an angle-plate exposure and that during the critical angle exposure the

mirror was pushed forward so that reflexion occurred entirely on the other half. Obviously any measurements made under these conditions would be in error because the distance from the mirror to the photographic plate is not the same in the two cases. This possible source of error was avoided by making a series of exposures to test the correct position of the mirror. The mounting upon which the latter was fixed was provided with a slow-motion screw having a pitch of 1/100 inch, and this was equipped with a graduated wheel whose circumference was divided into fifty parts. With this arrangement a given setting of the mirror could be repeated to about 5/1000 of an inch. The procedure in determining the correct position of the mirror consisted in making a series of short exposures, starting with the mirror back out of the path of the X-ray beam and pushing it forward at intervals of ten divisions of the wheel, the photographic film being shifted a short distance for each exposure. The finished film showed the position at which reflexion just began on one edge of the mirror and also the position at which it ended on the other edge after the mirror had been pushed entirely across the beam. The distance between these two extremes was usually about fifty divisions of the wheel, or about one turn, and in this interval the reflected beam first increased in intensity, reached a maximum, and then decreased. The correct position of the mirror was taken as the mid-point between the two extremes.

Discussion of Results.

Results of the measurements on various surfaces are shown in Table I. Theoretical values of the index of refraction given there were calculated from the Drude-Lorentz dispersion formula, making use of critical absorption limits listed in the fourth edition of Sommerfeld *.

It is possible to check the results obtained by the total reflexion method against those obtained by other methods by making some comparisons in a few cases. The index of refraction of glass for the two wave-lengths listed above has been determined by Larsson, Siegbahn, and Waller, who measured the refraction in an ordinary prism. The agreement between their values and those given in the above table is within experimental error. The refraction of $MoK\alpha_1$ in silver has been studied by Slack, using a double X-ray spectrometer method in which the primary X-ray beam was

* Arnold Sommerfeld, *Atombau und Spektrallinien*, pp. 295–6.

allowed to enter one surface of a silver prism at normal incidence, refraction taking place upon emergence at the other surface. The agreement between the results arrived at by the two methods is again quite satisfactory, being well within the probable error of measurement by either method.

TABLE I.

Data on Refraction of X-rays by the Total Reflexion Method.

Line.	λ(A.U.).	Surface.	θ_c.	$\delta(10)^6$ (expt.).	δ (theory).
$MoK\alpha_1$	0·7078	glass	6′ 18″	1·67 ± ·03	1·73
,,	,,	steel	9 35	3·41 ± ·15	4·98
,,	,,	nickel	10 15	4·42 ± ·15	5·78
,,	,,	silver	11 42	5·76 ± ·10	5·77
,,	,,	speculum	10 52	4·96 ± ·10	5·1
$CuK\alpha_1$	1·537	glass	13 36	7·8 ± ·2	8·14
,,	,,	copper	20 34	17·74 ± ·3	17·5
,,	,,	silver	26 42	30·0 ± 1·5	29·88
,,	,,	nickel	24 40	25·5 ± ·8	.....
,,	,,	gold	31 24	41·6 ± 1·6	40·3
,,	,,	speculum	23 8	22·4 ± ·4	18·84
$CuK\beta$	1·389	copper	19 36	16·25 ± ·4	.....
,,	,,	nickel	16 9	10·98 ± ·5	32·6

An examination of Table I. shows that for radiation frequencies not too close to an absorption edge the Lorentz dispersion formula represents the facts in a fairly satisfactory manner, although there are some exceptions. Perhaps the most striking example of agreement is in the case of the line $CuK\alpha_1$ reflected from copper. Here the frequency of radiation is very near to the natural frequency of the K-electrons, and since the absorption edge lies on the short wavelength side of the radiation, the magnitude of the critical angle is considerably diminished. One may calculate values for the index of refraction for this case, assuming successively one, two, and three K-electrons, and the results thus obtained differ from one another by as much as fifteen or twenty per cent. It is interesting to note that the experimental value agrees very closely with the calculation based on two electrons. This agreement is shown below.

Refraction of $CuK\alpha_1$ in Copper.

Number of K-electrons...	0	1	2	3
$\delta(10)^6$ (theory)	26·1	21·9	17·5	13·2
$\delta(10)^6$ (experiment)			17·74 ± ·3	

The same kind of calculations may be made for silver in connexion with the line MoKα_1, and although the differences are not so large one obtains, on the basis of the measurements here presented, the same kind of information as in the case of copper, and this is also in favour of a two-electron distribution in the K-level.

In the case of refraction of the copper Kα_1 line in gold, the binding of the L-electrons must be taken into consideration. Since there are presumably eight electrons distributed among the three L-levels, it is desirable to have some information concerning the method of this distribution in order to make the necessary calculations. In the absence of more definite information in this connexion the calculations have been made following Stoner's suggested distribution of 2 L_1-, 2 L_2-, and 4 L_3-electrons. The value of the index of refraction thus calculated differs from that obtained on the assumption of no resonance by about twenty per cent., but agrees with the experimental measurement.

The expected failure of theory when an absorption edge is approached too closely is demonstrated in the case of CuKβ reflected from copper. Here the wave-length of the radiation exceeds that of the absorption limit by only 0·011 Ångström unit, and as a result a calculation made from the theoretical formula gives an index of refraction greater than unity and thus predicts that there should be no reflexion at all. But of course there is some reflexion, and it is possible to find an experimental δ in the usual way. This departure from theory is shown in fig. 3, which is a graphical representation of the dispersion in the vicinity of an absorption edge. The curve is plotted for copper as the refracting substance. Three experimental determinations are indicated on this graph, one of which (for $\lambda = \cdot 708$ Å.U.) has been taken from some measurements made by Slack *. It will be noticed that for two of the cases the experimental points lie on the theoretical curve.

A convenient and interesting method of displaying the results of all measurements made with one particular wave-length is illustrated in fig. 4. As indicated previously, the Lorentz dispersion formula may be written as follows :

$$\frac{\delta}{2{\cdot}714(10)^{-6}\frac{D}{W}\lambda^2} = \sum \frac{n_r \lambda_r^2}{\lambda_r^2 - \lambda^2}.$$

* C. M. Slack, Phys. Rev. xxvii. p. 691 (1926).

Now suppose we inquire as to the behaviour of the quantity on the right as we pass from element to element along the scale of increasing atomic numbers. For the lighter elements, if X-rays of ordinary hardness are used, the value of this summation will be identical with that of the atomic number since λ is negligible compared with λ_r. But with increasing atomic numbers the binding of the K-electrons comes into consideration and a discontinuity is registered at

Fig. 3.

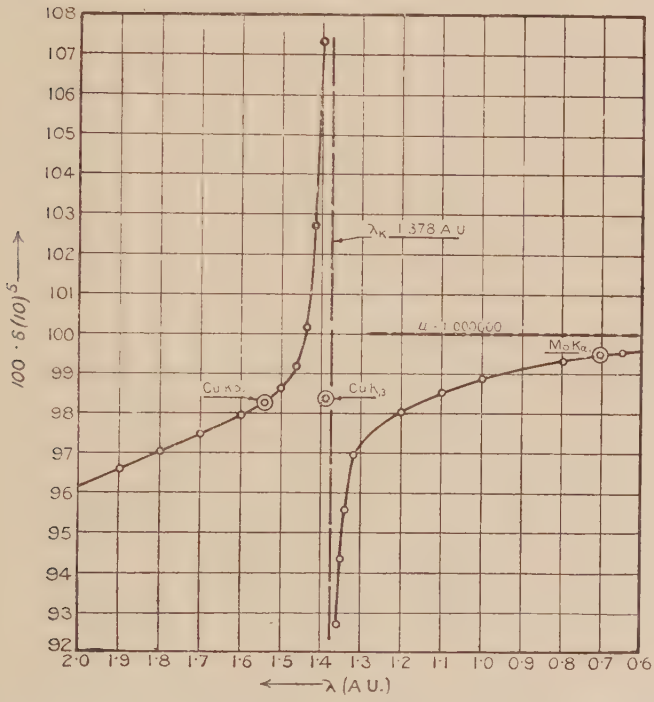

the point where the K critical absorption wave-length of the element lies nearest the wave-length of the radiation. Passing to still higher atomic numbers a similar discontinuity is introduced by the L-electrons. The theoretical curve obtained by plotting the summation against the atomic number is shown in fig. 4 for copper $K\alpha_1$ radiation ($\lambda = 1{\cdot}538$). The experimental values given on this curve were obtained by carrying out the calculation indicated on the left side of the above equation, using experimentally determined δ's. The value for aluminium was taken from

the results of Davis and Slack *. All of the points lie on the curve (or very near it) except that for nickel, whose K-absorption wave-length is 1·489 ångströms.

The low experimental value found for nickel and steel when used with MoKα radiation is somewhat difficult to understand and no ready explanation seems available.

Fig. 4.

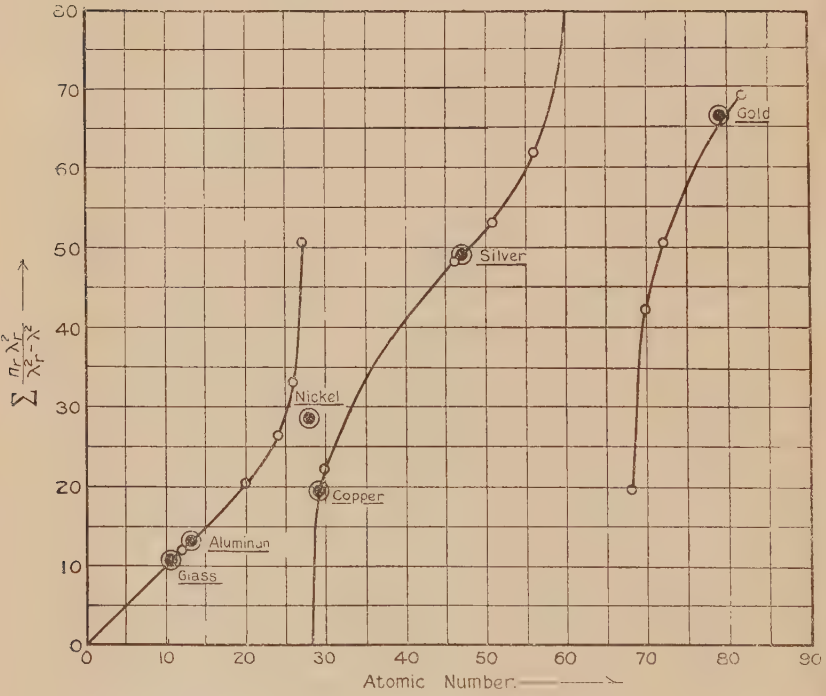

In both of these cases the critical angle was as sharply defined as usual, and it is certain that no reflexion at all occurred at angles of a magnitude as great as that predicted by the theory. Before drawing any conclusions as to the meaning of this discrepancy, it is perhaps desirable that the results given here be checked by one of the other methods described above. Of course, so far as the steel is concerned, it always contains a small amount of combined carbon, and the effect of this would be to decrease the value of δ, but such an effect

* Proc. National Academy of Science, x. p. 60 (1924); Phys. Rev. xxvii. p. 18 (1926).

would be far smaller than the observed difference, since the amount of carbon usually does not exceed two per cent. At any rate, the same argument would not apply to the difference found in the case of nickel, for this surface was prepared by sputtering from a pure nickel plate.

Only one of the cases studied is suitable to test the validity of the theory developed by Kronig as against the classical theory of Lorentz. As indicated previously, the two expressions for the index of refraction become identical when no resonance is involved, differing only when an absorption edge is approached. Furthermore, a better test of the quantum expression can be made for radiations of a wave-length less than one ångström because in the derivation of the formula an empirical relation was used for the fluorescent absorption coefficient which applies better to wave-lengths less than an ångström than to those farther up the scale. Therefore, the refraction of $MoK\alpha_1$ in silver seems to offer the only possibility of testing the formula, and in this case the test is not favourable. The value of δ calculated on the assumption of no resonance comes out to be $6{\cdot}33(10)^{-6}$, taking into consideration the resonance of the K-electrons, the Lorentz expression gives a value of 5·77 while that of Kronig gives 6·30. (In making this calculation the value of C was taken as ·023/8 because the radiation used lies on the low frequency side of the K-limit of silver.*) The experimental δ is 5·76. Therefore in this one case the classical theory seems to have preference. However, it would seem that the method of attack used by Kronig is to be preferred from the standpoint of experimentally known facts. The Lorentz formula does not give the kind of variation of the index of refraction near an absorption band that one might expect from absorption data. This is made evident in the fact that the difference between the calculated index in the immediate vicinity of an absorption limit and the index for no resonance is greater on the long wave-length side of the limit than on the short wave-length side. Kronig's formula is not open to this criticism.

Conclusions.

Additional cases have been presented in which the Drude-Lorentz theory of dispersion represents the facts, not only in regions remote from an absorption edge, but also in some instances in which the frequency of the radiation approaches the natural frequency of certain groups of electrons. The

* F. K. Richtmeyer, Phys. Rev. January, 1926.

interesting possibility of studying the distribution of electrons among the lower atomic levels has received additional support. The information obtained here is very definite so far as the K-electrons are concerned, but the distribution among the various L-levels is a much more complex problem. However, the determination made for gold shows that it is not impossible to have some measure of success even here. Of course, it will be necessary to increase the accuracy of the measurements by a considerable amount before one can hope to be in a position to decide between various groupings, but there is no reason to believe that this will not be done if the method of attack proves fruitful.

The experiments described in this paper were carried out under the supervision of Professor A. H. Compton, to whom the writer wishes to express his sincere thanks for many valuable suggestions.

Ryerson Physical Laboratory,
The University of Chicago,
September 22, 1926.

X. *On the Fine Structure of the Spectrum Lines of Cadmium in the Ultra-Violet.* *By* Wali Mohammad, *M.A.* (*Punjab*), *B.A.* (*Cantab.*), *Ph.D.* (*Göttingen*), *Professor of Physics, Lucknow University, and* S. B. L. Mathur, *M.Sc.**

I. *Introduction.*

An accurate knowledge of the fine structure of the spectrum lines of elements is of the greatest importance in the determination of their atomic structure.

The observation of the fine structures discloses th mechanism of the intra-atomic motions as far as the perihelion of the elliptic orbits. It also throws light on the varying orientations of the nucleus. Merton [1], Nagaoka, Sugiura and Mishima [2], Brunetti [3], and others have, by a knowledge of the structure of the spectrum lines, been able to determine the isotopes to which some of the satellites are due. But the contribution of the knowledge of the fine structure of spectrum lines does not end here. Spectroscopy is now in a position to lend support to and to receive support from the theory of relativity, and to furnish facts for discussing the question of the variability

* Communicated by the Authors.

of mass of the electron. Recently Ruark, Mohler and Chenault [4], Ruark and Chenault [5], and Joos [6] have attempted to deduce the energy levels of certain elements from the fine structure of their spectrum lines.

II. *Previous Work.*

Michelson, Janicki, Gehrcke, von Baeyer, Wali Mohammad, Nagaoka, and a host of other workers have, naturally, been attracted to this important branch of spectroscopy; and instrument after instrument of the highest precision has been constructed and most refined methods devised for the investigation of the fine structure.

Almost all the above-named workers have confined their attention to the visible part of the spectrum. This is obviously due to the difficulties experienced in working in the other regions of the spectrum.

Owing to the ease with which a mercury arc can be set up and controlled, all the attempts of investigating the ultra-violet region have been confined to mercury, and the fine structure of some of the mercury lines in the ultra-violet region has been determined by Takamine [7], Galli and Forsterling [8], Lucy Wilson [9], Nagaoka, Sugiura and Mishima [10], and Wood [11].

Realizing the need of full information regarding the fine structure of the spectrum lines in the invisible region, the authors have undertaken a systematic investigation of the ultra-violet region, and some of the results obtained by them are reported here.

III. *Present Work.*

Any method adopted for investigation should provide for the following essentials:

(i.) A suitable source of illumination.

(ii.) A suitable instrument of high resolving power.

Regarding (i.), a most suitable source of illumination is offered by an oxy-cathode arc described by Wali Mohammad and successfully used by him and a number of other workers for the investigation of the fine structure. This source possesses the peculiar advantages of yielding lines which are both *sharp* and *bright* and the intensity of which can be controlled with ease.

Regarding (ii.), the instruments available were a Quartz Lummer Plate and a Quartz Fabry and Perot Etalon.

In spite of what has been said about the defects of the Lummer Plate by van Cittert[12] and G. Hansen[13], it is perhaps the most convenient instrument for use.

IV. *Experimental Arrangement.*

(a) *Source of illumination.*

The source of light was a Wali Mohammad lamp[13], which was fixed up vertically. Briefly stated, the arrangement consisted of a Wehnelt oxy-cathode of platinum and an anode of the substance under investigation, both placed in a water-cooled tube which was exhausted by means of a rotary pump. The oxy-cathode was heated to incandescence, and by applying a steady potential of 220 volts a suitable anode current was allowed to pass between the cathode and the anode, thus melting and evaporating at any desired rate the metal which formed the anode. The current employed for heating the oxy-cathode was usually about 15 amperes; while a thermionic current varying from a fraction of an ampere to several amperes was available.

(b) *Production of the Interference Fringes.*

The upper end of the lamp was closed with a quartz plate or a quartz lens of suitable focal length, which rendered the beam of light emerging from the lamp parallel. This beam was rendered horizontal by means of a specially made tungsten mirror held at 45° to the vertical. The parallel beam thus rendered horizontal fell on a Hilger quartz Lummer-Gehrcke plate of the dimensions:

Length	13 cm.
Thickness	0·46 „

and the interference fringes from the upper face of the Lummer plate were focussed upon the slit of a Hilger E quartz spectrograph by means of a quartz fluorite achromat of 40 cm. focal length. A double-image prism was placed in front of the Lummer plate, in order to transmit the beam polarized with the electric vector parallel to the parallel surfaces of the Lummer plate. The fringes were photographed in the usual way in the spectrograph, and Ilford Special Rapid plates were used throughout for the purpose. The time of exposure varied from 3 to 5 minutes only, during which conditions could be kept constant. This arrangement has the advantage that all the lines of the spectrum, in the visible as well

as in the ultra-violet regions, could be photographed simultaneously.

(c) *Calculation of Wave-lengths.*

As the mount supplied by Hilger for the Lummer plate did not allow the interference fringes due to the lower face to be photographed, the elegant method described by McLennan and McLeod [15] for measuring the distance of satellites could not be adopted. Measurements were consequently taken upon the fringe system from the upper face of the Lummer plate, and the fringes of the lowest orders were measured and the mean of several observations taken. In this way the distances between two main line fringes and between a main line fringe and the satellites were determined. Lummer [16], Lummer and Gehrcke [17], von Baeyer [18], Koláček [19], McLennan and McLeod [20], Takamine [21], and more recently Galli and Forsterling [22], Worsnop and Flint [23], and P. Kunze [24] have each developed a formula of their own, which are all modifications of the original formula given by Lummer. The method adopted by the authors was the calculation of the distance in A.U. between the order of the fringe system of a spectrum line from the dimensions and the optical constants of the quartz Lummer plate. The formula due to von Baeyer; and used also by Nagaoka [25] and Simeon [26], gives

$$\Delta\lambda = \frac{n\lambda^2}{n^2\lambda - 4t^2\mu\, d\mu/d\lambda},$$

where

λ = the refractive index of quartz with respect to the ray under investigation,

n = order of the fringe given by

$$n\lambda = 2t\sqrt{\mu^2 - 1},$$

λ = wave-length of the ray,

t = thickness of the Lummer plate,

and $d\mu/d\lambda$ is the dispersion of quartz about λ.

A curve was drawn with the refractive indices of quartz for the extraordinary ray as abscissa and the corresponding wave-lengths in A.U. as ordinates. The data for this were gathered from Landolt and Börnstein's latest tables. Thus not only the refractive index for any wave-length, but also the dispersion of the quartz about that wave-length, could be determined easily from the curve.

The position of a satellite was fixed in the following way :—

Let a = the distance between two main line fringes,
b = the distance between the satellite and the lower order fringe.

Then if b was $< a/2$, the satellite was positive ;
but if b was $> a/2$, the satellite was negative ;

and then the distance between the satellite and the higher order fringe was taken.

In either case the wave-length of the satellite was given by

$$\Delta\lambda \cdot \frac{b}{a}.$$

This obviously is an arbitrary method, and the conclusions arrived at are liable to error which can be removed only by some other means ; for example, the use of greater resolving power or the employment of the method of crossed spectra.

V. *Preliminary Test.*

As a test of the performance of the given Lummer plate as regards its theoretical and actual resolving power, the Cadmium line 4800 was examined and its structure found to be as follows :

$$+0{\cdot}057\ \text{Å} ;\quad 0{\cdot}000 ;\quad -0{\cdot}037\ \text{Å} ;\quad -0{\cdot}085\ \text{Å}.$$

The results of other workers as well as ours on this line are given below :

+0·058(¼),	0·000(1),	−0·034(¼),	−0·081(½)	Janicki.
+0·058(6),	0·000(10),	−0·034(3),	−0·081(6)	Wali Mohammad.
+0·059(3),	0·000(10),	−0·033(1),	−0·080(2)	Takamine.
+0·058(6),	0·000(10),	−0·034(3),	−0·081(3)	MacNair [27].
+0·057(6),	0·000(10),	−0·037(3),	−0·085(2)	Authors.

The agreement is fairly close, and it was safe to conclude that the Lummer plate available gave satisfactory results.

VI. *Measurements on Cadmium Lines in the Ultra-Violet Region.*

When the results obtained by the authors were nearly ready for publication, a highly interesting and valuable paper giving the results of fine structure of the Cadmium

lines in the ultra-violet region was published by W. A. MacNair in the Philosophical Magazine (Sept. 1926). His values are given side by side with those of the authors for sake of comparison.

The wave-lengths are taken from Exner and Haschek, and the figures in brackets indicate the intensity as visually estimated by the authors.

(1), (2) Lines 3614·62, 3613·11, and 3610·72.

According to Exner and Haschek, there are three lines in this region, with wave-lengths of

3614·62(10),
3613·11(50),
3610·72(500).

The line 3614·62 is faintly visible in only one of the many photographs taken and cannot be seen in any other. MacNair has measured satellites belonging to 3614·62 and 3610·72, and says that line 3613 appears also on one plate, but he gives no structure for the same.

Assuming that satellites are due to lines 3614·62 and 3610·72, the structure of these lines is as follows :

Line 3614·62. $2p_1$–$3d_3$.

+0·034(4), 0·000(10), −0·020(2)	Authors.
+0·037(2), 0·000(10), −0·023(4)	MacNair

Line 3610·5. $2p_1$–$3d_3$.

0·000(10), −0·032(2)	Authors.
0·000(10), −0·035 0·000(10), −0·037 } (3)	MacNair.

The agreement of the authors' values with those of MacNair is very close indeed. The authors, however, think that the satellites are due to the lines 3613·11 and 3610·72, and not to the line 3614·62, which is too faint to be photographed. They find the structure to be as follows :

Line 3613·11.

0·000(10), −0·052(4), −0·020(1).

Line 3610·72.

0·000(10), −0·035(2).

(3) Line 3500·2. $2p_2$–$3d$.

This line appears to have only one satellite, while MacNair has found two.

	0·000(10),	−0·039(7)	Authors.
+0·017(2),	0·000(10),	−0·010(4)	MacNair.

(4) & (5) Line 3467·81. $2p_2$–$3d_5$.
and Line 3466·37. $2p_2$–$3d_3$.

According to Exner and Haschek there are two lines very close to each other of wave-length

3467·81(50) and 3466·37(100).

The closeness of the lines makes the assignment of the satellites very difficult, and the conclusions drawn are not without some doubt.

Line 3467·81.

This line appears to be single, and MacNair also finds it single.

Line 3466·37 has the following structure :

+0·033(4),	0·000(10),	−0·021(5)	Authors.
+0·031(3),	0·000(10),	−0·015(5)	MacNair.

(6) Line 3403·86. $2p_3$–$3d_3$.

The authors find two satellites, while MacNair finds only one.

+0·024(9),	0·000(10),	−0·023(1)	Authors.
+0·017(5),	0·000(10)		MacNair.

(7) Line 3261·23. $1{\cdot}5s$–$2p_2$.

The satellites of this line are not well separated, and two of them are unusually faint.

The structure is as follows :

+0·033(2), +0·015(2), 0·000(10), −0·016(9), −0·036(8) Authors.

This line has been investigated by R. W. Wood, who has found only one satellite −0·019.

(8) Line 3252·86. $2p_1$–$2{\cdot}5s$.

The structure is as follows :

+0·036(8),	0·000(10)		Authors.
+0·031(2),	0·000(10),	−0·010(3)	MacNair.

The authors believe that, since the satellite appears ill-defined, their results may not be final.

(9) Line 3133·47. $2p_2$–$2{\cdot}5s$.

This line gives the following structure :

+0·033(6), 0·000(10), −0·028(1)	Authors.
+0·024(1), 0·000(10), −0·033(1), −0·012(1)	MacNair.

The satellites of this line are somewhat diffused and ill-defined.

(10) Line 3081 00. $2p_3$–$2{\cdot}5s$.

+0·015(2), 0·000(10), −0·023(3)	Authors.
+0·013(3), 0·000(10), −0·023(2)	MacNair.

The values of MacNair and those of the authors seem to be in very good agreement.

(11) Line 2980·80. $2p_1$–$4d_2$.

This line appears to be simple. MacNair, too, does not give any satellite.

(12) Line 2980·65. $2p_1$–$4d_1$.

This line appears simple. MacNair gets a satellite at −0·025(1).

(13) Line 2881·35. $2p_2$–$4d_3$.

This line appears single. MacNair gets two satellites at −0·021(1) and −0·010(5) respectively.

Exner and Haschek give two lines, as follows :

2881·35 and 2880·89.

The difference in the wave-length of these two lines is so small that in our photographs the fringes produced by these two lines cannot be separated. The authors think that perhaps MacNair might have taken the main line fringe of 2880·78 to be the satellite of 2881·24.

(14) Line 2880·89. $2p_2$–$4d_2$.

This line shows no satellites.

(15) Line 2837·05. $2p_3$–$4d_3$.

There is one satellite as follows :

0·000(10), −0·030(5)	Authors.
0·000(10), −0·011(4)	MacNair.

(16) Line 2775·20. $2p_2$–$3{\cdot}5s$.

This line has a satellite at −0·027 Å. MacNair has not investigated this line.

VII. *Summary.*

The authors have made an attempt to investigate the structure of the most prominent of Cadmium lines between 4800 and 2775. They find that their results generally are in fair agreement with those of MacNair, who happens to be the only other worker in the field which the authors have investigated. Further results will be communicated in another paper.

References.

1. Merton. Roy. Soc. Proc. A, xci. p. 198 (1915).
   Merton. Roy. Soc. Proc. xcvi. p. 388 (Jan. 2, 1920).
2. Nagaoka, Sugiura, and Mishima. 'Nature,' cxiii. p. 459 (March 29, 1924).
3. Brunetti. *N. Cimento*, July, Aug., Sept. 1924.
4. Ruark, Mohler, and Chenault. 'Nature,' cxiv. p. 575 (1924).
5. Ruark and Chenault. Phil. Mag. i. p. 937 (1925).
6. Joos. *Phys. Zeits.* xxvi. No. 10 (1925).
7. Takamine. Math.-Phys. Soc. Tokyo, Nov. 1915.
8. Galli and Forsterling. *Phys. Zeits.* xviii. p. 155 (April 15, 1917).
9. Lucy Wilson. Astro.-Phys. Journ. p. 340 (Dec. 1917).
10. Nagaoka, Sugiura, and Mishima. 'Japanese Journal of Physics,' ii. p. 121 (1924).
11. Wood. Phil. Mag. p. 761 (October 1925).
12. van Cittert. *Ann. d. Phys.* lxxvii. p. 372 (1925); also *ibid.* xxix. p. 94 (1926).
13. G. Hansen. *Ann. d. Phys.* lxxviii. p. 552 (1925).
14. Wali Mohammad. Astro.-Phys. Journ. xxxix. no. 3 (1914).
15. McLennan and McLeod. Roy. Soc. Proc. A, xc. p. 243 (May 28, 1914).
16. Lummer. *Verh. Deutsch. Phys. Ges.* iii. (1901).
17. Lummer and Gehrcke. *Ann. d. Phys.* x. p. 457 (1903).
18. von Baeyer. *Phys. Zeit.* ix. p. 831 (1908).
19. Kolâček. *Ann. d. Phys.* xxxix. p. 1431 (1912).
20. McLennan and McLeod. Proc. Roy. Soc. A, xc. p. 243 (1914).
21. Takamine. Proc. Math.-Phys. Tokyo, ix. p. 296 (1915).
22. Galli and Forsterling. *Phys. Zeit.* xviii. p. 155 (1917).
23. Worsnop and Flint. 'Advanced Practical Physics,' p. 358.
24. P. Kunze. *Ann. d. Phys.* lxxix. p. 294.
25. Nagaoka. Proc. Tokyo Math.-Phys. Soc. viii. (ser. 2) p. 296.
26. F. Simeon. Journ. Scientific Instruments, i. No. 10 (July 1924).
27. W. A. MacNair. Phil. Mag. No. 9, p. 613 (Sept. 1926).

XI. *The Lag in Electrical Discharges.* *By* WILLIAM CLARKSON, *M.Sc., A.Inst.P., The Physical Laboratory of the University, Utrecht* *.

ABSTRACT.

THE variation of the "peak" voltage in the intermittent discharge in discharge-tubes of scrupulous cleanliness are considered, and possible causes, both in the gas and in the electrodes, are sought for and applied in explanation. Experimental results would agree with a "corona" lag, a theory of which is developed, if a slow "build up" is assumed. This assumption is shown to be justified from results obtained by a method, here described, for measuring the time of duration of a "flash," or condenser discharge. The small preliminary discharges often preceding a "flash" are explained on the same assumption, due to the form of the "corona characteristic." Possible causes of this slow "build up" are discussed, and it is tentatively associated with the apparently inevitable modification of the cathode surface by the filling gas.

1. PEAK POTENTIAL VARIATIONS.

THE characteristic and systematic variation of the "peak" voltage with respect to the statical sparking potential in the intermittent—"flashing"—discharge has been the subject of many references in recent years, by Mauz and Seeliger [1], Taylor and Sayce [2], and Penning [3], for example; but a thorough investigation had not been made, and as a certain degree of confusion had resulted, the need of a solution was apparent if a definite sparking potential as a characteristic property of all discharge tubes was to retain any significance in work on intermittency.

It was the aim, then, of the writer to investigate these variations; but as they could conceivably be due to some irregularities in the tube, such as gas or electrode impurities, or to wall effects, and not inherent properties, it was essential that the work should be carried out in tubes as free as possible from such influences. Fortunately a suitable technique was at the writer's disposal [4].

Tubes.

A typical tube consisted of a spherical glass bulb, some 10 cm. in diameter, in which were mounted convex nickel electrodes 5 cm. in diameter and about 1 cm. apart, with

* Communicated by Prof. L. S. Ornstein.

their sealed-in leads sheathed with glass up to the back of the electrodes in order to minimize any chance of leakage round the walls of the bulb (and for overrunning).

After having been carefully washed with acid, water and alcohol, and dried, they were exhausted to black vacuum and baked for half an hour or more, and then filled through a liquid-air trap with Neon or Argon to a pressure of some millimetres, the gas having previously stood for several hours in contact with heated calcium, and sealed-off. Finally, by introducing metallic sodium electrolytically through a side-tube, any remaining impurities first were removed and then a bright film of pure metallic sodium deposited on the electrodes.

Properties of the Tubes.

Even in tubes so carefully prepared it was found that the sparking potential only attained constancy after some hours, and also that "polarization" always occurred during use, though only to the extent of a volt or two at the most, this maximum effect not necessarily being attained until after several "flashes." Both of these observations, together with the fact that "polarization" often may be removed simply by passing a "flash" in the reverse direction, indicate electrode changes which at present may be assumed to be an inevitable phenomenon in discharge-tubes, since they have been found to be present despite the most thorough precautions [4].

Though in the light, as was to be expected, such tubes gave a most marked photoelectric current, this in some cases being of the order of a microampere even at some volts below the sparking potential (fig. 3), in the dark no current could be detected, this proving the nature of the effect and the absence of electrical leakage in the discharge-tube. In general the sparking potential was a volt or two higher in the dark than in the light (fig. 3, A and B).

Measuring Apparatus.

The method employed was similar to that used on previous occasions [2, 3], and was retained after due consideration and thorough testing, as capable of giving results most accurately and quickly with a minimum disturbance of the discharge.

The negative side of the circuit was most carefully insulated on paraffin-wax blocks, and the positive side was earthed in several places. The potential was obtained from an M–L anode-converter, this giving any desired voltage up to

600 volts D.C. with remarkable constancy, and the circuit current was regulated by a diode (with variable filament-current) placed in the negative side, and being measured by a shunted micro-ammeter on the earthed side of the circuit, capable of detecting currents down to 0·03 μA.

Though with high sparking potentials and large filament currents the micro-ammeter did not give a reading corresponding to the actual current at the moment of discharge, this value could easily be found if required.

The electrostatic voltmeter, reading to 400 volts, was quick-acting, coming completely to rest in about ten seconds. As it was most sensitive in the region of 300 volts, dry batteries were placed between it and the accompanying diode in order that this part of the scale could be employed whatever the actual voltages were.

With a small condenser in parallel with the voltmeter (giving a system with a capacity of 0·0016 μF.), and with careful insulation, the voltmeter leakage could be reduced to 0·2 volt in the time required for a reading. The only time a correction had to be considered was in the case of very slow or "single" flashes.

Results.

The following symbols will be used in this paper:— v_c is the (statical) sparking potential, and would appear to be essentially a constant in any tube. Its connexion with the "corona characteristic" is given later. V_C is the "peak" potential (alternatively, the apparent upper critical voltage or the dynamic sparking potential)* and is the voltage recorded by the measuring apparatus, and ΔV_C is the difference between v and V_C.

Where V_B is the minimum potential recorded, the time of flash (T) is given quite closely by

$$T = \frac{C(V_C - V_B)}{i}, \quad . \quad . \quad . \quad . \quad . \quad . \quad (1)$$

where C is the capacity and i the current in the circuit. It may be stated, however, that as V_B was rarely measured the apparatus was generally modified to measure V_C only, the insulation being improved by this simplification. The time of flash or frequency n is measured directly in this case.

In addition to those described all other available tubes were examined and the variation of V_C observed under the

* This title can more aptly be applied to v, the voltage at which build-up" occurs when space-charge is present.

usual conditions, but as the results differed merely in degree and repeatability and not in kind no details are given.

Typical results are given in fig. 1, which shows the relation between ΔV_C and (*a*) the current, the capacity constant, and (*b*) the capacity, the current being constant, whether in the light or in darkness.

As fig. 1 (*a*), however, may also represent the variation of ΔV_C with the frequency ($n \propto i$) or the rate of increase of voltage of the condenser ($V_C - V_B/T \propto i$), and fig. 1 (*b*) the variation with the reciprocal of these, it was of interest to combine on one graph (for convenience showing the T, ΔV_C relation) all the readings taken in the two cases. In general, these points fell on one smooth curve similar in form to fig. 1 (*b*) as prolonged.

Fig. 1.

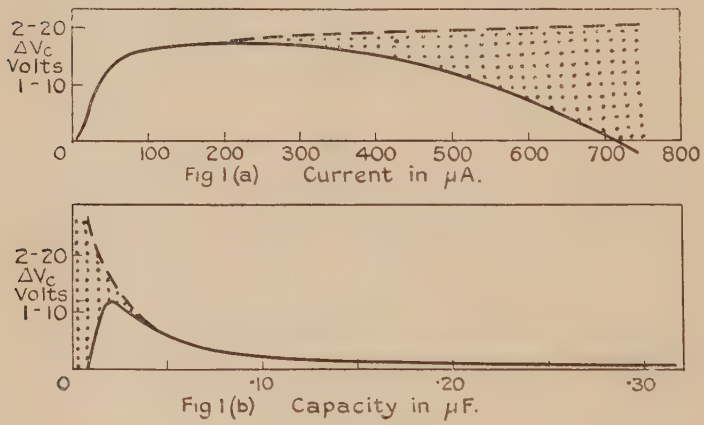

This last curve did not regularly show the diminution of V_C at the higher frequencies, and this lent additional support to the belief that this phenomenon could be assigned to a separate cause.

It has been shown that corresponding to any small current i in a discharge-tube there is a certain (minimum) voltage v at which a "flash" can occur, this in essence being the sparking-potential for this current. Actually this voltage is the same as that given by the "corona characteristic," and, as fig. 3 will show, though v is almost constant for the smallest currents, in fact being v_c, there is a more or less rapid fall in value as i increases.

As in "flashing" there is a residual current (decreasing with time) after each "flash," due to the "clear-up" of the "space-charge," it is conceivable that with rapid rates of increase of voltage, that is to say at higher frequencies, a current may still be flowing in the tube when the corresponding v, as given by (v, i) the "corona characteristic" or the analogous current and sparking-potential relation existing under the conditions, is reached. The effect of this would be that v, and consequently V_c, would increase as the frequency of the flashes increased, the dotted line (fig. 1) showing a gradual increase with frequency, giving the probable variation of ΔV_c in the absence of this "overlapping" of the discharge.

2. Consideration of Results.

Though in practice several influences may be acting at once, on analysis the occurrence of a V_c always higher than v_c may be attributed to two main causes: either (1) the discharge does not immediately start when v_c is reached, or (2) the discharge does commence but some appreciable time is required for the current to attain a high value, *i.e.* to "build-up." In both of these cases, since the voltage across the tube is increasing so long as the circuit current is greater than the current in the discharge-tube (if any), the final voltage V_c is greater than v_c.

Since these causes may be referred to properties either of (*a*) the filling gas or (*b*) the electrodes, the following explanations are possible:—

(1 *a*). Apart from a change in the properties of the gas, this would imply a lack of ionization in a suitable place in the tube at the moment v_c was reached, and V would rise till such ionization did occur, the probability increasing both with time and with voltage. The existence of such a state of affairs in practice has been inferred by many workers, Zuber [5] for instance, and though not conclusively proven its possibility cannot be disregarded.

(2 *a*). This would correspond to a "corona lag," and it is obvious that some time, however small, must be taken to establish the discharge. It has been advanced for the case of magneto sparks by Peek [6] and has been discussed by Campbell [6].

(1 *b*) and (2 *b*). Here the modification of the electrodes, more particularly the cathode, by layers of gas by sorption or sputtering seems the probable cause, and the effect, in the absence of definite data, may be imagined as the

prevention or inhibition of the passage or multiplication of electrons. In 1 *b* the film would have the effect of preventing altogether the production of electrons until higher voltages were reached, and in 2 *b* it would merely act by retarding their passage or liberation in the discharge, perhaps merely acting as a simple resistance. In either case we can imagine the film either as being an inherent or permanent property of an electrode or of being only temporarily established by a discharge and of being removable or, an assumption returned to later, of decaying with time. Cathodic films have been postulated by Zelany[7] to explain results obtained for spark discharges and for the α-particle counter, and are considered also by Campbell, and on a previous occasion the writer was compelled to postulate them to explain changes in the critical voltage variations in discharge-tubes. Recently they have been submitted to direct examination by Taylor[4], and though much remains to be done their existence and the fact that they play a role in the discharge cannot be doubted.

Fortunately here causes 1 *a* and 1 *b* can both be rejected at the outset. A positive ΔV_c was observed in circumstances where there certainly was no lack of electrons, as in cases where a photoelectric current was passing (fig. 3), and also, if our explanation is correct, where "overlapping" occurred, in which case of course ΔV_c should have vanished to zero. It is true that 1 *b* could account for the form of the T, ΔV_c graphs, though "polarizations" of 20 volts were highly improbable, but it was soon discredited as rapid "flashes," previously associated with a high V_c, could be obtained with a voltage of v_c providing the circuit current was large enough, the high V_c presumably being due to the particular properties of the usual circuit.

Neglecting "wall-effects" as at the least a very improbable cause, there remained then a "lag" attributable to a slow "build-up," and the following theory was developed which was applicable to either 2 *a* or 2 *b*.

Theory of corona lag.

Let the circuit-current be i,
and let the initial ($t=0$) current in the tube be i_0
and at the time t be i_t.

Consider the capacity C.
Charging current at time t is $i-i_t$.
Therefore increment of voltage in time t is

$$\Delta V = \frac{1}{C}\left[\int_0^t i\,dt - \int_0^t i_t\,dt\right] \quad . \quad . \quad . \quad . \quad (2)$$

As the variation of i_t with t is not known direct calculations cannot be made, but sufficiently justifiable assumptions of a general nature can be made for the variation of ΔV_c to be deduced with fair certainty. We may assume that the discharge current will be a function both of the time and of the voltage, increasing rapidly with time, the rate of increase depending on the voltage. We may express i_t then by $\phi(i_0, t, V)$, in which case the voltage (V) at any instant will be given by

$$V = v_c + \Delta V = v_c + \frac{1}{C}\left[it - \int_0^t \phi(i_0, t, V)\,dt\right]. \quad . \quad (3)$$

Two times emerge from a consideration of this relation: first, i_t will equal i at a time τ, when the voltage of course will be V_c; and second, i_t will be increasing so rapidly at a time θ, that beyond this even a very great increase of i_t will not imply a significant increase in the duration of the discharge which for practical purposes may be said to last a time θ.

The following properties of ΔV_c, τ, and θ can be inferred for the case of a constant C and increasing i. θ will be a maximum for small currents and will decrease as i increases. The ratio, however, of τ/θ will increase rapidly until τ approximates in value to θ. The actual effect on τ will be that it increases rapidly at first, attains a maximum, and thereafter varies as θ.

Furthermore, if i_t varies in the manner assumed here we can simplify equation (2) to read:

$$\Delta V_c = \frac{i\tau}{C}, \quad . \quad . \quad . \quad . \quad . \quad . \quad . \quad . \quad (4)$$

which would give values of τ which were relatively accurate though a little lower than the actual values. With $\Delta V_c \propto i\tau$, C constant, we may follow the variation of ΔV_c with i, and we find that ΔV_c should increase at first quickly and then slowly as in fig. 1, and that "overlapping" should reduce its value progressively as the initial current is greater. Actual values of τ are calculable since the values of ΔV_c, C, and i are known. To this end a thorough investigation was made of the variation of ΔV_c for small values of i, as it was here that the variation of τ should be most pronounced. A closer study of previous curves (fig. 1) showed that they gave the variation in that region quite well, so they were utilized in the calculations. The form of the ΔV_c curve for small currents together with a curve showing the variation of τ as calculated from such a curve is given in fig. 2.

As will be seen, the form of the curve was that expected from theory, but the actual values of τ were found to be much too large for a "lag" based solely on the known properties of the gas. Values of the order of 0·001–0·01 second were obtained quite frequently, whereas calculations based on the gas constants gave as a maximum value 10^{-4} sec., with values of the order of 10^{-6} sec. as more probable ones.

Short of other experiments confirming the time values and a slow "build-up" proof of a "corona" lag was lacking, though the forms of the curves obtained were in essential agreement with that hypothesis.

3. Duration of a Condenser Discharge.

So far it had not been proved whether the lag was an inherent property of discharges or merely due to their succession in "flashing." By effecting slight changes in the measuring apparatus, it was found possible to measure the time of duration of a "single flash" and also to gain some insight into the variation of the voltage with time in such a discharge.

A well-insulated key was inserted in the circuit so that the condenser could be charged from the voltage supply to a known potential E and then applied to the tube, the voltmeter being placed directly across the tube with a high resistance (R) of many megohms preceding the divide valve.

In such a circuit, if during the flash the condenser voltage falls instantaneously to V_B, then, unless the initial reading of the voltmeter (V_0) is less than this, no charging-up should be observed. If it takes an appreciable time however, the voltmeter (capacity C) will be charged to an extent depending on the time required to reach the voltage (V_H) finally recorded. Long "lags" or the absence of a flash at all will permit complete mixing of the charges and, if the condenser capacity is large, V_H will approximate to E.

The time taken for the condenser to become discharger to a voltage V_H equals the time (t) for the voltmeter (C) to charge from V_0 to V_H, this being given by

$$t = CR \log_e \left(\frac{E - V_0}{E - V_H} \right), \quad . \quad . \quad . \quad . \quad . \quad . \quad (5)$$

neglecting at this stage the correction for the valve, which in practice may well be done.

Without going into details, it may be said that the results were highly satisfactory. It was found that the time of

duration of the discharge was always appreciable, no instantaneous flashes being observed, and that, though the "lag" varied, it was in a systematic not random fashion. Observations supported the suggestion that the voltage fell at first very slowly and then very rapidly. The curve showing the variation of θ with $E = V_c$ for the same capacity as for τ is given in fig. 2, and it will be seen that despite the inevitable inaccuracies of the results the curves are essentially in agreement.

Fig. 2.

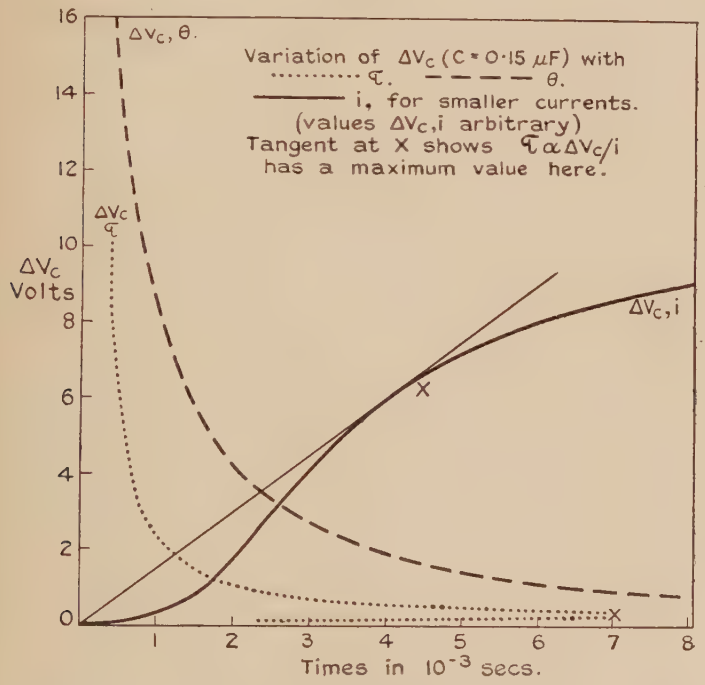

Furthermore, visual evidence of the operation of a factor influencing the "build-up" in the manner postulated was obtained several times when using one tube selected on account of the large "lags" it displayed, as often only a low current ("corona") discharge of appreciable duration occurred instead of the usual brief, intense flash. This was proved to be due to factors in the tube itself and unattributable to leakage or to bad contacts in the circuit. That the retardation could vary was in accordance with many previous observations.

The presence of an excess potential ΔV_c in the intermittent discharge in discharge-tubes could now with confidence be attributed to a "corona" lag of the form postulated.

4. Voltage Fluctuations preceding Discharges.

These preceding results re-directed the attention of the writer to another, and not unfamiliar phenomenon, exhibited markedly by this tube, namely, that of showing voltage fluctuations, also indicating "corona" discharges, preliminary to "flashes" when "flashing" slowly, that is to say, with small currents.

The tube was examined in the dark, so that even faint discharges could be seen, though the fluctuations had first been observed in daylight; and when necessary the voltmeter was connected to the tube without the insertion of the diode so that the voltage variations could be followed, the microammeter being connected to read either the current through the tube or in the condenser lead.

The following results, taken with the capacity (C) constant, are typical of those obtained.

A discharge occurred as soon as v_c was reached, but even with very small currents this was fluctuating. The intensity of the discharge increased with i with corresponding increases in the voltage fluctuations and in the discharge-tube currents, and with i greater than 0·3 μA. "flashing" occurred, each 'flash" being preceded by a series of "corona" discharges, which, at first drawn-out and faint and merging into one another, became brief and intense with a definite dark "interval" as the "flash" drew near.

The frequency of these discharges depended on C or i, and the number was reduced as these were increased, so that at $i=1{\cdot}0\,\mu$A. they ceased to be observed.

Fig. 3 (A and B) shows the V_c and "corona characteristic" curves in this case, but the slight increase of V_c at smaller currents is schematic, the observations not being very conclusive. "Corona" discharges were observed along the first part of the graph, the probability of a normal "flash" finally occurring increasing with C and i, until at the point where the corona and V_c graphs diverge normal "flashing" supervened, though the slow "build-up" doubtlessly still existed. Fig. 3 C gives the corresponding curves for a small tube distinguished for its small "lags," and it will be seen that their forms are precisely the same,

though the phenomena here were on a reduced scale, preliminary discharges being observed only for very small currents ($<0{\cdot}1$ μA.) and small capacities ($<0{\cdot}002$ μF.).

Considering what has already been said on the "corona characteristic," it will be seen to be readily conceivable that if the capacity is but small enough, or if the "build-up" is prolonged, the depreciation of the voltage of the condenser may be such that, before the current is very large, the v corresponding to the existing i in the tube is reached and the

Fig. 3.

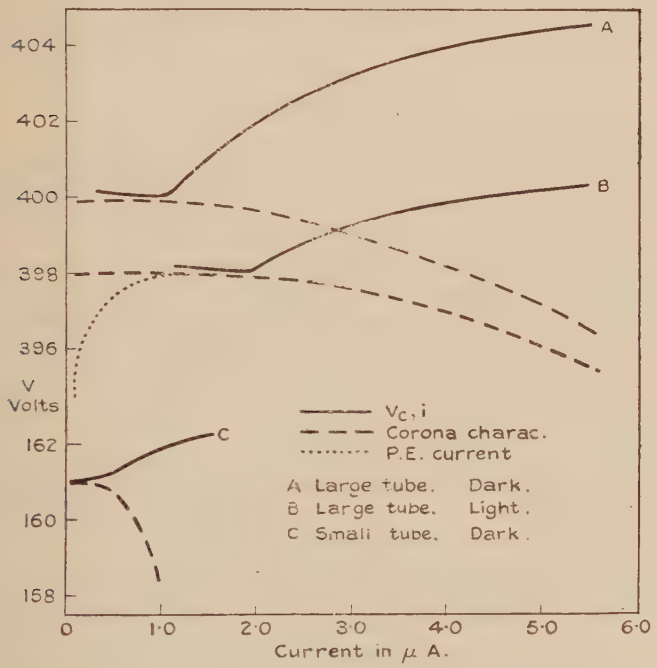

discharge ceases. The shorter the initial (constant v) portion of the characteristic, the more rapidly v increases with i in the succeeding part, and the greater C or i, the less should be the chance of this occurring.

The observations are in agreement with these predictions.

Reference already has been made to variations in the "lag" with time, for "single flashes" the lag being possibly twice as great at one time as at another, a variation of the same order being produced by light; and further evidence

was obtained in this work, the number of "corona" discharges preliminary to a flash varying from time to time, though in a systematic not random fashion, generally being constant for several flashes in succession. For example, in one case, with $C=0{\cdot}15\ \mu F.$ and $i=0{\cdot}7\ \mu A.$, the number was ten (at intervals of two seconds) for five flashes, then two for six flashes, and then five for a further set.

In addition to changes with time or use, changes in the retarding agent by the preliminary discharges, perhaps manifested by accompanying changes in the "corona characteristic," must be postulated to account for all the phenomena associated with such discharges, though the precise significance of the results has not yet been definitely decided.

5. Conclusion.

Though scarcely falling within the scope of this present paper, reference may be made to the speculations made on the cause of the slow "build-up" and to the conclusions arrived at, though only the briefest outline is attempted and the considerations applied are frankly tentative.

Such an effect must be attributed to a mechanism which limits the rate of increase of the number of electrons at any time, either by resisting the passage of a current, or by reducing the rate of production of electrons in the discharge, the current in practice increasing at less than one-hundredth of the rate anticipated from theory.

Since for calculations of discharge durations, to give results in agreement with observations very improbable values would have to be assumed for the velocity of the ions or for their rate of diffusion, possible causes of the retardation were sought for in the electrodes.

For several reasons it was concluded that the cause could not lie in a permanent modification of the electrode surfaces, by the filling gas (or chance impurities) merely introducing a resistance into the circuit, the idea that thick surface films might be responsible being discredited at the same time.

The retardation could, however, be attributed to (probably temporary) modification of the cathode surface by the filling gas or to variable ("polarization") layers, whose screening action on all or part of the cathode with a consequent stoppage or selective effect on bombarding ions (or emitted electrons ?) would explain the reduced emissivity.

There appears to be good support for this hypothesis in evidence from experiments on kindred problems, and

it is quite compatible with the additional phenomena included in this paper.

In conclusion the writer would like to record with gratitude his obligation to Professor Ornstein, whose generous support alone enabled this work to be carried out, to the members of his Staff, and to Dr. J. Taylor for his friendly assistance on all possible occasions.

20th January, 1927.

References.

1. Mauz and Seeliger, *Phys. Zeit.* xxvi. p. 47 (1925).
2. Taylor and Sayce, Phil. Mag. li. p. 918 (1925).
3. Penning, *Phys. Zeit.* xxvii. p. 187 (1926).
4. Taylor, Phil. Mag. iii. Suppl. p. 753 (1927).
5. Züber, *Ann. d. Phys.* lxxvi. p. 231 (1925).
6. Peek, 'Dielectric Phenomena' (1915). Campbell, Phil. Mag. xxxviii. p. 214 (1919).
7. Zeleny, Phys. Rev. xxiv. p. 255 (1924).
8. Clarkson, Proc. Phys. Soc. xxviii. p. 19 (1925).

XII. *The Atomic Structure of AuSn.* *By* G. D. Preston, *B.A., and* E. A. Owen, *M.A., D.Sc., The National Physical Laboratory* *.

[Plate II.]

THIS paper gives the results obtained in an investigation of the structure of the compound AuSn and is a continuation of previous work carried out by the authors on intermetallic compounds †.

The material was examined in the first instance by the powder method and the results were confirmed by the rotating crystal method. The latter part of the paper deals with the Laue method, which yielded further information regarding the structure of the material.

(a) *Results obtained by the Powder Method.*

In Table I. are given the intensities and the values of $\sin\theta$ for the lines obtained by the powder method. The photographs were taken with a Müller camera, the radiation employed being that emitted by a tube ‡ furnished with a copper anticathode and operated at 8 m.a. and 30,000 volts.

* Communicated by the Authors.
† See Phil. Mag. ii. p. 1266 (1926).
‡ See Journ. Sci. Instr. iv. Pt. 1, p. 1 (1926).

TABLE I.

Intensity.	Sin θ.	Indices.	λ.	(c=1·275). a.
7	0·2048	$10\bar{1}0$	α	4·334 Å
18	0·2244	$10\bar{1}1$	β	4·320
6	0·2490	$10\bar{1}1$	α	4·309
14	0·3123	$10\bar{1}2$	β	4·332
15	0·3226	$11\bar{2}0$	β	4·305
1	0·3469	$10\bar{1}2$	α	4·316
2	0·3570	$11\bar{2}0$	α	4·305
22	0·4134	$20\bar{2}0$	α	4·293
22	0·4363	$20\bar{2}1$	α	4·296
22	0·4503	$11\bar{2}2$	α	4·338
		$20\bar{2}2$	β	4·306
22	0·4672	$10\bar{1}3$	α	4·313
5	0·4978	$20\bar{2}2$	α	4·310
16	0·5613	$21\bar{3}1$	α	4·319
		0004	α	4·295
17	0·5992	$10\bar{1}4$	α	4·288
		$11\bar{2}4$	β	4·314
3	0·6150	$30\bar{3}0$	α	4·329
		$21\bar{3}2$	α	4·291
4	0·6643	$11\bar{2}4$	α	4·305
18	0·7169	$22\bar{4}0$	α	4·288
19	0·7556	$31\bar{4}1$	α	4·310
		$40\bar{4}1$	β	4·307
19	0·7820	$21\bar{3}4$	α	4·304
9	0·7949	$31\bar{4}2$	α	4·302
8	0·8354	$40\bar{4}1$	α	4·311
10	0·8632	$10\bar{1}6$	α	4·315
10	0·8705	$40\bar{4}2$	α	4·307
10	0·9079	$32\bar{5}1$	α	4·313
		$22\bar{4}4$	α	4·303
22	0·9340	$31\bar{4}4$	α	4·290
		$20\bar{2}6$	α	4·315
10	0·9422	$32\bar{5}2$	α	4·300

Mean ..... a=4·309 ± 0·01 Å.

The exposures occupied about three hours. The figures given in the Table are typical of those obtained on several films, a specimen of which is shown in Pl. II. fig. 1. In calculating the spacings, the values of K_α and K_β wavelengths have been taken as λ_α=1·537 Å and λ_β=1·389 Å. It will be seen from the Table that the twenty-six observed

lines can all be accounted for by assuming the structure to be a hexagonal lattice of side $a=4{\cdot}309\pm0{\cdot}01$ Å and axial ratio $c=1{\cdot}275$.

The maximum error in the value of a calculated from the observed value of $\sin\theta$ is less than 0·25 per cent. The volume of the unit hexagonal prism is

$$V=\frac{\sqrt{3}}{2}a^2c=88{\cdot}28\ \text{A}^3,$$

the observed density is $\rho=11{\cdot}6$ grammes per c.c., and the molecular weight of AuSn is $M=315{\cdot}9$ (O=16).

If n be the number of molecules associated with the unit cell, then

$$V=\frac{1{\cdot}65nM}{\rho},$$

whence we find $n=1{\cdot}97$, so that within the limits of the error of observation there are two molecules of AuSn associated with the unit hexagonal prism.

The last line in the powder photograph corresponds to indices 3252, and within this region a simple hexagonal structure, the parameters of which are $a=4{\cdot}309$ and $c=1{\cdot}275$, should give 56 reflexions. The order in which they would occur is given in column I. of Table II. In column II. are the calculated values of

$$d=a\Big/\sqrt{\frac{4}{3}(h^2+hk+k^2)+\frac{l^2}{c^2}},$$

and in column III. the values of $d=\lambda/2\sin\theta$ are given for comparison. Column IV. gives the observed values of the intensities of the lines arranged in descending order, 1 being the most intense and 22 the weakest line in the photograph.

In placing the atoms within the unit we are helped to some extent by consideration of space. The nearest distance between atoms in pure tin is 2·80 Å, and in pure gold 2·88 A. If in the hexagonal prism an atom be placed at the point (000) and another at $(\frac{1}{3}\,\frac{2}{3}\,\frac{1}{4})$, the distance between them is

$$a\sqrt{\frac{1}{3}+\frac{c^2}{16}}=2{\cdot}842\ \text{Å},$$

which is almost exactly the mean diameter of a gold and a tin atom.

TABLE II.

	I.	II.	III	IV.	V.		VI.		
	Indices.	d Calcd.	d Obsd.	I Obsd.	I_1 Calcd.	Δ_1.	I_2 Calcd.	Δ_2.	
1	0001	5·49	—	—	0		0		
2	$10\bar{1}0$	3·73	3·75	7	—	18	4	3	
3	$10\bar{1}1$	3·09	3·09	6	1	5	6		
4	0002	2·74		—	—		—		
5	$10\bar{1}2$	2·21	2·22	1	2	1	1		
6	$11\bar{2}0$	2·15	2·15	2	3	1	2		
7	$11\bar{2}1$	2·00		—	0		0		
8	$20\bar{2}0$	1·87	1·86	22	—	3	19	3	
9	0003	1·83		—	0		0		
10	$20\bar{2}1$	1·77	1·76	22	8	14	17	5	
11	$11\bar{2}2$	1·70	1·71	22	—		—		? $\beta 20\bar{2}2$
12	$10\bar{1}3$	1·64	1·64	22	9	13	21	1	
13	$20\bar{2}2$	1·54	1·54	5	6	1	5		
14	$21\bar{3}0$	1·41		—	—		19	6	
15	$11\bar{2}3$	1·39		—	0		0		
16	0004	1·37	1·37	16	7	9	16		
17	$21\bar{3}1$	1·37							
18	$20\bar{2}3$	1·31		—	18	7	—		
19	$10\bar{1}4$	1·29	1·28	17	—		23		? $\beta 11\bar{2}4$
20	$21\bar{3}2$	1·26	1·25	3	4	1	3		
21	$30\bar{3}0$	1·24			11		9		
22	$30\bar{3}1$	1·21		—	0		0		
23	$11\bar{2}4$	1·16	1·16	4	5	1	7	3	
24	$30\bar{3}2$	1·13		—	—		—		
25	$21\bar{3}3$	1·12		—	14	11	24	1	
26	$20\bar{2}4$	1·10		—	—		—		
27	0005	1·10		—	0		0		
28	$22\bar{4}0$	1·08	1·07	18	16	2	13	5	
29	$22\bar{4}1$	1·06		—	0		0		
30	$10\bar{1}5$	1·05		—	24	1	—		
31	$31\bar{4}0$	1·04		—	—		—		
32	$30\bar{3}3$	1·03		—	0		0		
33	$31\bar{4}1$	1·02	1·02	19	17	2	25	6	? $\beta 40\bar{4}1$
34	$22\bar{4}3$	1·00		—	—		—		
35	$21\bar{3}4$	·984	·983	19	—	6	22	3	
36	$11\bar{2}5$	·978		—	0		0		
37	$31\bar{4}2$	·969	·967	9	10	1	8	1	
38	$20\bar{2}5$	·947		—	—		—		
39	$40\bar{4}0$	·934		—	—		—		
40	$22\bar{4}3$	·928		—	0		0		
41	$30\bar{3}4$	·922	·920	8	12	4	10	2	
42	$40\bar{4}1$	·920							
43	0006	·916		—	—		—		

TABLE II. (*continued*).

	I.	II.	III.	IV.	V.		VI.	
	Indices.	d Calcd.	d Obsd.	I Obsd.	I_1 Calcd.	Δ_1.	I_2 Calcd.	Δ_2.
44	$31\bar{4}3$	·901		—	19	6	—	
45	$10\bar{1}6$	·889	·891	10	22	12	14	4
46	$40\bar{4}2$	·883	·883	10	22	12	14	4
47	$21\bar{3}5$	·867		—	21	4	—	
48	$32\bar{5}0$	·853		—	—		—	
49	$22\bar{4}4$	·847	·847	10	15	5	11	1
50	$32\bar{5}1$	·846			20	5	—	
51	$11\bar{2}6$	·843		—	—		—	
52	$40\bar{4}3$	·831		—	—		—	
53	$31\bar{4}4$	827		—	—		—	
54	$30\bar{3}5$	·824		—	0		0	
55	$20\bar{2}6$	·822	·823	22	25	3	18	4
56	$32\bar{5}2$	·817	·816	10	13	3	12	2
						151		54

In calculating the intensities to be expected, atoms of atomic number N_1 have been placed at (000) and $(00\frac{1}{2})$, and atoms N_2 at $(\frac{1}{3}\,\frac{2}{3}\,\frac{1}{4})$ and $(\frac{2}{3}\,\frac{1}{3}\,\frac{3}{4})$.

The intensity I is given by

$$I \propto d_{hkl}^{2\cdot35}\, J\,.\,(A^2+B^2),$$

where J is the number of co-operating planes, d_{hkl} is the spacing, and

$$A = \Sigma N_s \cos 2\pi(hx_s+ky_s+lz_s),$$

$$B = \Sigma N_s \sin 2\pi(hx_s+ky_s+lz_s).$$

In the present case, substituting the values of $(x_s\,y_s\,z_s)$ given above, the factor B vanishes and we are left with

$$I \propto d_{hkl}^{2\cdot35}\,.\,J\Big\{N_1(1+\cos\pi l) + 2N_2\cos\pi(h+k)\cos\pi\left(\frac{h-k}{3}-\frac{l}{2}\right)\Big\}^2.$$

The quantity within the brackets vanishes if l is odd and $(h-k)$ is a multiple of 3. The lines $000l$, $11\bar{2}l$, $30\bar{3}l$, and $22\bar{4}l$, should not appear when l is odd. This is confirmed by experiment, none of these lines being observed in the photographs. In columns V. and VI. (Table II.), in which are entered the calculated intensities, these lines are indicated by a 0.

If l is odd and $(h-k)$ is not a multiple of 3, the factor within the brackets becomes $\sqrt{3}\,N_2$. When l is even, it has one of the following values:

$2N_1+2N_2$ when $(h-k)=3p$, $l=4q$;

$2N_1-2N_2$ when $(h-k)=3p$, $l=2q$ (q odd);

$2N_1+N_2$;

or $2N_1-N_2$.

For tin, $N=50$ and for gold, $N=79$, so the values of I have been computed for the two cases:

(1) $N_1=50$, $N_2=79$,

and (2) $N_1=79$, $N_2=50$.

Numbers ranging from 1 to 25 have been assigned in order to the twenty-five most intense lines in each case. The resulting figures appear in columns V. and VI. of Table II. It will be seen that the figures in column V. under I_1 are not so near the observed values as those in column VI. under I_2. For instance, there is a marked discrepancy in the first two observed lines $10\bar{1}0$, and $10\bar{1}1$. In order to compare the observed and calculated intensities the figures for I_1 and I_2 have been subtracted from those for I giving Δ_1 and Δ_2. The spaces occupied by a dash have for this purpose been considered to contain the number 25. The sum of the resulting differences is 151 units in the first case when $N_1=50$, whereas in the second case when $N_1=79$ it is only 54 units, which leaves little doubt but that the gold atoms are at the points (000) and $(00\frac{1}{2})$ while the tin atoms are at $(\frac{1}{3}\,\frac{2}{3}\,\frac{1}{4})$ and $(\frac{2}{3}\,\frac{1}{3}\,\frac{3}{4})$. The errors hardly exceed the accuracy with which the lines in the photograph can be placed in order of intensity. A unit cell of the lattice is shown in fig. 2.

(b) *Results obtained by the Rotating Crystal method.*

The specimen used to obtain the photograph shown in fig. 3 (Pl. II.), was a small chip of material about 1 mm. in cross-section, and 3 mm. long. It was mounted on a spindle situated at the centre of a cylindrical film-holder of radius 3·19 cm., and was rotated during an exposure of two hours in a fine pencil of radiation from a copper anticathode. The photograph thus obtained should be symmetrical about a vertical and a horizontal line drawn through the image of the undeflected spot. Owing, however, to the great opacity

of the material to the soft copper radiation and to the irregular nature of the surfaces of the specimen, some planes are in positions which favour reflexion and others are not, with the result that the symmetry of the photograph is spoiled. For the same reason the relative intensities of the spots are liable to be misleading. The information which can be obtained from the photograph is (1) the value of the glancing angle θ for each spot, and (2) the value of the angle ψ between the axis of rotation and the normal to the reflecting plane.

Fig. 2.

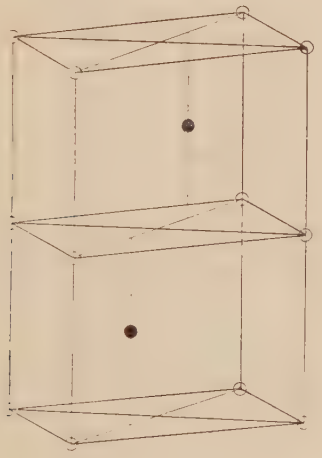

○ Gold

● Tin

If x and y are the co-ordinates of a spot on the photograph referred to rectangular axes OX, OY drawn through the central spot and with OY parallel to the axis of rotation, then θ and ψ are given by the following relations where r is the radius of the camera—

$$\cos 2\theta = \frac{r \cos x/r}{\sqrt{y^2 + r^2}}, \quad \ldots \ldots \quad (1)$$

$$\sin \theta \,.\, \cos \psi = \frac{y}{2\sqrt{y^2 + r^2}}. \quad \ldots \ldots \quad (2)$$

TABLE III.

Sin θ.	Sin θ . cos ψ.	*hkil*.	$0{\cdot}1964\,h + 0{\cdot}1464\,k + 0{\cdot}024\,l$
·8701	·2004	$4\bar{4}02$	·2048
·8704	−·2030	$\bar{4}40\bar{2}$	−·2048
·8638	·2100	$10\bar{1}6$	·2108
·8652	·1825	$\bar{1}0\bar{1}6$	·1820
·8638	·1613	$01\bar{1}6$	·1608
·8646	·1315	$0\bar{1}\bar{1}6$	·1320
·8626	·0622	$1\bar{1}06$	·0644
·8646	·0330	$1\bar{1}0\bar{6}$	·0356
·8626	−·0355	$\bar{1}106$	−·0356
·8640	−·0657	$\bar{1}10\bar{6}$	−·0644
·8620	−·1327	$0\bar{1}16$	−·1320
·8631	−·1629	$0\bar{1}1\bar{6}$	−·1608
·8620	−·1835	$\bar{1}016$	−·1835
·8629	−·2108	$\bar{1}01\bar{6}$	−·2108
·8322	·1455	$33\bar{0}4$	−·1404
·8331	−·1569	$\bar{3}30\bar{4}$	−·1596
·7955	·3972	$\bar{1}432$	·3940
·7941	·0008	$\bar{3}412$	·0012
·7938	−·3452	$\bar{4}312$	−·3412
·7578	·0008	$3\bar{4}1\bar{1}$	·0012
·7447	·0008	$3\bar{4}10$	·0036
·7060	·1941	$\bar{2}42\bar{0}$	·1928
·7124	−·1976	$24\bar{2}0$	−·1928
·6654	·3360	$11\bar{2}4$	·3332
·6624	·2566	$2\bar{1}\bar{1}4$	·2560
·6659	·2380	$2\bar{1}1\bar{4}$	·2368
·6652	·0848	$\bar{1}2\bar{1}4$	·0868
·6617	−·0927	$1\bar{2}14$	−·0868
·6646	−·1092	$1\bar{2}1\bar{4}$	−·1060
·6637	−·2590	$\bar{2}11\bar{4}$	−·2560
·6617	−·3360	$\bar{1}\bar{1}24$	−·3332
·6633	−·3560	$\bar{1}1\bar{2}4$	−·3524
·6170	·1515	$33\bar{0}0$	·1500
·6192	−·1535	$\bar{3}300$	−·1500

TABLE III. (*continued*).

Sin θ.	Sin θ . cos ψ.	*hkil.*	$0{\cdot}1964\,h + 0{\cdot}1464\,k + 0{\cdot}0024\,l$
·6120	·3030	$3\bar{2}12$	·3012
·6134	·2474	$\bar{1}322$	·2476
·6129	·0479	$\bar{2}312$	·0512
·6115	−·0452	$2\bar{3}12$	−·0416
·6106	−·2444	$1\bar{3}2\bar{2}$	−·2476
·6122	−·2970	$\bar{3}21\bar{2}$	−·3012
·5595	·0084	0004	·0096
·5595	−·0113	$000\bar{4}$	−·0096
·3540	·2450	$2\bar{1}\bar{1}0$	·2464
·3587	·0976	$\bar{1}2\bar{1}0$	·0964
·3592	−·1071	$1\bar{2}10$	−·0964
·3464	·2032	1012	·2012
·3472	−·2033	$101\bar{2}$	−·2012

The measurement of the positions of all the points on the photograph would be an exceedingly laborious work and would not be justified on account of the imperfection of the photograph referred to above. We have accordingly made measurements of fifty spots and propose to show that they are situated on the photograph in the places to be expected from the structure deduced from the powder photograph.

In Table III. columns 1 and 2 are set down the values of $\sin\theta$ and $\sin\theta\,.\cos\psi$ computed from the measurements of fifty of the most intense spots. The values of $\sin\theta$ have been put down for comparison with the results obtained by the powder method given in Table I.

Let us suppose that the information derived from the powder photograph is correct, and that the structure is hexagonal of side a and axial ratio c.

Then

$$\sin\theta_{hkl} = \frac{\lambda}{2a}\sqrt{\frac{4}{3}(h^2+hk+k^2)+\frac{l^2}{c^2}},$$

and ψ the angle between the normals to the planes (hkl) and $(h_1k_1l_1)$ is given by :

$$\cos\psi_{hkl} = \frac{\frac{4}{3}\left[hh_1+kk_1+\frac{1}{2}(hk_1+h_1k)\right]+\frac{ll_1}{c^2}}{\left[\frac{4}{3}(h^2+hk+k^2)+\frac{l^2}{c^2}\right]^{1/2}\left[\frac{4}{3}(h_1^2+h_1k_1+k_1^2)+\frac{l_1^2}{c^2}\right]^{1/2}}$$

So, if $(h_1k_1l_1)$ is the line in the crystal about which rotation takes place, then

$$\sin\theta\,.\,\cos\psi = \frac{\lambda\left[\frac{4}{3}\{hh_1+kk_1+\frac{1}{2}(hk_1+h_1k)\}+\frac{ll_1}{c^2}\right]}{2a\left\{\frac{4}{3}(h_1^2+h_1k_1+k_1^2)+\frac{l_1^2}{c^2}\right\}^{1/2}}$$

$$\equiv Ah+Bk+Cl, \quad \ldots\ldots\ldots \quad (3)$$

where

$$A=\frac{4}{3}\left(h_1+\frac{k_1}{2}\right).\frac{\lambda}{2a\sqrt{\frac{4}{3}(h_1^2+h_1k_1+k_1^2)+\frac{l_1^2}{c^2}}},$$

$$B=\frac{4}{3}\left(k_1+\frac{h_1}{2}\right).\frac{\lambda}{2a\sqrt{\frac{4}{3}(h_1^2+h_1k_1+k_1^2)+\frac{l_1^2}{c^2}}},$$

$$C=\frac{l_1}{c^2}.\frac{\lambda}{2a\sqrt{\frac{4}{3}(h_1^2+h_1k_1+k_1^2)+\frac{l_1^2}{c^2}}},$$

and

$$A^2-AB+B^2+c^2C^2\equiv\lambda^2/4a^2. \quad \ldots \quad (4)$$

In the present case the values of $\sin\theta\cos\psi$ can all be accounted for by putting

$$\sin\theta\cos\psi = 0{\cdot}1964\,h+0{\cdot}1464\,k+0{\cdot}0024\,l, \quad . \quad (5)$$

as is shown by the last column of Table III., the appropriate values of hkl being given in column 3.

In Table IV. the mean values of $\sin\theta$ for the 13 different sets of planes to which indices have been assigned in Table III. are collected. The value of c is calculated from the values of $\sin\theta$ for (0004) and (11$\bar{2}$0) and the values of "a" are then computed for each plane. The resulting mean $4{\cdot}305\pm0{\cdot}007$ Å is in good agreement with figure $4{\cdot}309\pm0{\cdot}01$ Å obtained from the powder photograph. The values of c are 1·278 and 1·275 respectively. The expression (4) above gives $a=4{\cdot}35$ Å, showing that the assumed values of A, B, and C in expression (5) are consistent with a hexagonal structure.

The results obtained by the measurement of the rotating crystal photograph are thus in agreement with those obtained from the powder photograph. This brief analysis of part of the rotating crystal photograph cannot determine the unit of the structure, but it does afford very substantial confirmation of the results arrived at by the powder method.

TABLE IV.

Mean from Table III. Sin θ.	*hkil.*	(c=1·278) a
·8702	$40\bar{4}2$	4·307 Å
·8634	$10\bar{1}6$	4·303
·8327	$30\bar{3}4$	4·308
·7945	$31\bar{4}2$	4·302
·7587	$31\bar{4}1$	4·291
·7447	$31\bar{4}0$	4·296
·7092	$22\bar{4}0$	4·335
·6638	$11\bar{2}4$	4·300
·6181	$30\bar{3}0$	4·307
·6121	$21\bar{3}2$	4·309
·5595	0004	4·299
·3573	$11\bar{2}0$	4·301
·3468	$10\bar{1}2$	4·309

Mean ..... $a = 4{\cdot}305 \pm 0007$ Å.

(c) *Results obtained by the Laue Method.*

A small chip of the material was chosen and mounted on the crystal holder of the Müller spectrograph. After a preliminary exposure the necessary adjustment to the crystal was made and the photograph shown in fig. 4 (Pl. II.) was obtained—the incident beam being nearly parallel to the hexagonal axis. An exposure of four hours at 3 to 4 m.a. and 60,000 volts was required to obtain the picture. The symmetry of the arrangement of diffraction spots is more clearly seen in the stereographic projection, fig. 5, and is that of point group D_{6h}. This corresponds to a crystal having the symmetry of groups D_{3h}, C_{6v}, D_6, or D_{6h}*. The indices of the spots are most easily determined from the gnomonic projection (fig. 6) from which they can be read off at once. The result is analysed in fig. 7 †, where the ordinates are $y=h^2+hk+k^2$ and the abscissæ $x=l$. For a hexagonal structure with the incident beam parallel to [0001]

$$\lambda = \frac{2lac}{\frac{4}{3}(h^2+hk+k^2)c^2+l^2} = \frac{x}{\frac{4}{3}c^2y+x^2} \cdot 2\,ac,$$

or substituting the values of a and c found from the powder method,

$$\lambda = \frac{10{\cdot}99\,x}{2{\cdot}171\,y+x^2}.$$

* Wyckoff, 'The Structure of Crystals,' p. 118.
† Bragg, 'X-Rays and Crystal Structure,' p. 284.

Fig. 5.

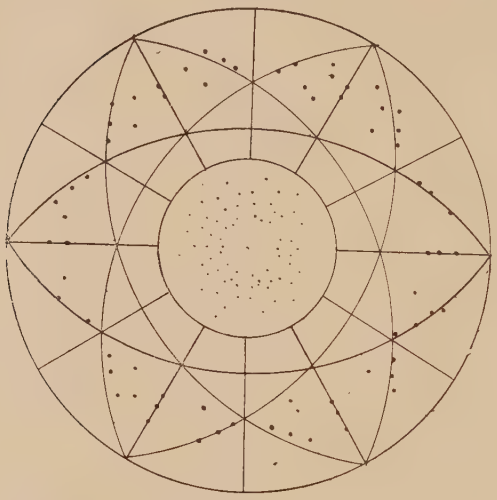

Fig. 6.

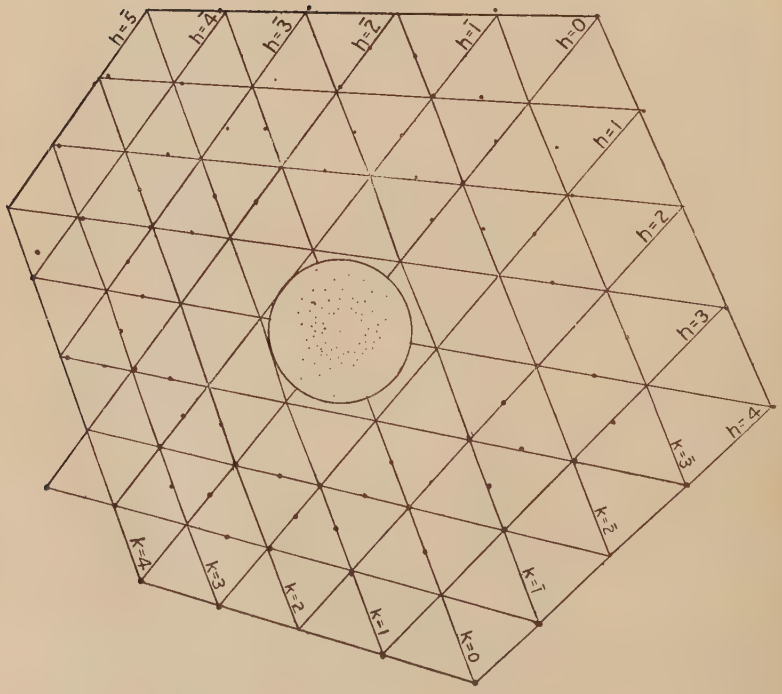

The limiting value of λ for a peak voltage of 60,000 volts is 0·206 Å. This line is shown in fig. 7 and all the observed spots should fall to the right of it. The other limit is set by the size of the photographic plate and is given by

$$\sin\theta = \frac{x/c}{\sqrt{\frac{4}{3}y + x^2/c^2}}.$$

In the case under consideration $\theta_{max.} = 24°$.

The spots which appear on the photograph are shown by a

Fig. 7.

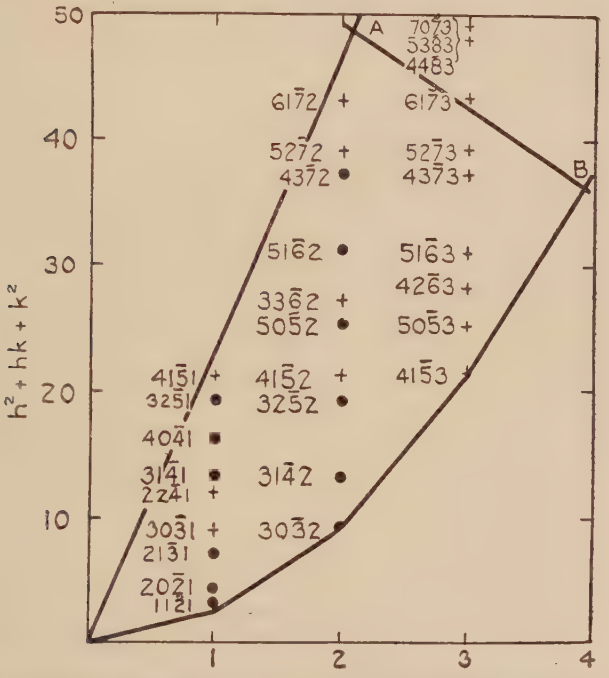

circle on the diagram, those which are absent by a cross. It has been pointed out above in connexion with the intensities of the reflexions from the powdered material, that when l is odd and $(h-k)=3p$ the intensity factor vanishes if the atoms are in the positions assumed. The first order reflexions from $11\bar{2}1$, $30\bar{3}1$, $22\bar{4}1$, and $41\bar{5}1$ should therefore be absent. Of these planes only the first is observed in the Laue photograph, and in this case its presence may be accounted for by 2nd and 4th order reflexions since the indices are small. Further, considering the case when $l=2$, the intensity factor (see above) is small when $(h-k)=3p$ and the planes $30\bar{3}2$,

$41\bar{5}2$, $33\bar{6}2$, and $52\bar{7}2$ might not appear on the Laue photograph. Of these $30\bar{3}2$ only is observed, and its second order reflexion ($l=4$) will be very intense. The plane $61\bar{7}2$ falls near the wave-length limit and is not observed for that reason. When $l=3$ the intensity factor again vanishes if $(h-k)=3p$, and is small when $(h-k)$ has other values. No spots for which $l=3$ are observed. If we assume that the intensity of points lying beyond the line AB in fig. 7 is too small to be observed, the points on the photograph are satisfactorily accounted for when the atoms are situated in the positions given above. The mean length of the side of the hexagonal net in fig. 6 gives an axial ratio of 1·30 approximately, which is in agreement with the results obtained by the other methods.

As stated above, the space group is fixed by the symmetry of the Laue photograph to be either D_{3h}, C_{6v}, D_6, or D_{6h}. Referring to the tables of Astbury and Yardley*, some of these groups may be eliminated. For instance, the presence of the first order reflexions from the planes $10\bar{1}1$, $20\bar{2}1$, and $40\bar{4}1$ † eliminates D_{3h}^2, C_{6v}^2, C_{6v}^3, D_{6v}^2, and D_{6h}^3; the presence of 0004 eliminates D_6^2, D_6^3, D_6^4, and D_6^5. If we may assume that the X-ray spectra of this material are characterized by the absence when l is odd of first order reflexions from planes $(hh\,2\bar{h}l)$ none of which have been observed, then the space group must be D_{3h}^4, C_{6v}^4, or D_{6h}^4. The possible positions of atoms within the unit in these groups are ‡ :—

D_{3h}^4, D_{6h}^4	(a) 000, $00\frac{1}{2}$.	(c) $\frac{1}{3}\,\frac{2}{3}\,\frac{1}{4}$, $\frac{2}{3}\,\frac{1}{3}\,\frac{3}{4}$.
	(b) $00\frac{1}{4}$, $00\frac{3}{4}$.	(d) $\frac{1}{3}\,\frac{2}{3}\,\frac{3}{4}$, $\frac{2}{3}\,\frac{1}{3}\,\frac{1}{4}$.
C_{6v}^4	(a) $00u$, $00u+\frac{1}{2}$.	(b) $\frac{1}{3}\,\frac{2}{3}\,u$, $\frac{2}{3}\,\frac{1}{3}\,u+\frac{1}{2}$.

It has been shown above that the intensities of the powder photograph are in good agreement with theory if gold atoms are placed at the points (000) and $(00\frac{1}{2})$ and tin atoms at $(\frac{1}{3}\,\frac{2}{3}\,\frac{1}{4})$ and $(\frac{2}{3}\,\frac{1}{3}\,\frac{3}{4})$, a result in agreement with the possible positions found from symmetry considerations, and the assumption that the planes $(hh\,2hl)$ are absent if l is odd.

Summary.

The atomic structure of the intermetallic compound AuSn has been examined by the powder and the Laue methods, the result of the powder method being confirmed by the rotating crystal method. The analysis shows that AuSn crystallizes

* Phil. Trans. Roy. Soc. A, vol. ccxxiv. pp. 250–252.

† In another film, $10\bar{1}3$, $10\bar{1}5$ were also observed.

‡ Wyckoff, 'The Analytical Expression of the Results of the Theory of Space Groups,' pp. 159–169.

on a hexagonal lattice of side 4·307 Å and axial ratio 1·276, the density requiring two molecules of AuSn to be associated with this unit. The space group is found to be D_{3h}^4, C_{6v}^4, or D_{6h}^4, and the intensities of the reflexions agree with a structure in which gold atoms are situated at the points (000) and $(00\frac{1}{2})$ and tin atoms at the points $(\frac{1}{3}\ \frac{2}{3}\ \frac{1}{4})$ and $(\frac{2}{3}\ \frac{1}{3}\ \frac{3}{4})$.

March 1927.

XIII. *Transmission of Electric Waves through the Ionized Medium.* *By* T. L. Eckersley, *M.A.**

IN a recent paper in the Phil. Mag. the writer showed that the state of ionization had a profound influence on the spreading-out of the electromagnetic waves originating in a localized pulse. The loading of the æther with free ions gives it a dispersive character, with the result that the various frequency components of the pulse are all separated out after a sufficient time; the higher frequencies arrive at any distant point first, the lower frequencies following at progressively later times, giving a disturbance of constantly lowering pitch. A casual examination of the problem might lead one to expect a gradual lowering of the frequency, going on continuously to zero frequency, since all frequencies are represented in the pulse; but contrary to this expectation, it was found that a certain limiting frequency n_0 was reached, this depending on the state of the medium, the value of n_0 being given by the relation:

$$n_0^2 = \frac{Ne^2}{\pi m}. \quad . \quad . \quad . \quad . \quad . \quad . \quad . \quad (1,1)$$

It is with the object of inquiring more closely into this characteristic frequency of the medium that the following investigation was undertaken.

At the outset it is better to limit to the consideration of one frequency n say, and to follow the method due to Sommerfeld. We are concerned at the moment with the transmission of waves in the medium, and not with the manner in which the waves get into it, so that we can leave the problems of the reflexion at the surface till a later stage and consider the subsequent history in space and time of a periodic disturbance, just within the boundary of the medium lasting from $t=0$ to $t=\infty$.

The disturbance spreads out into the body of the medium; and it is shown that this disturbance consists of two parts, which may be calculated from certain contour integrals.

* Communicated by the Author.

In the first place consider :

$$\frac{\mathrm{R}}{2\pi}\int_{-\infty}^{+\infty}\frac{e^{-ipt}dp}{p-p_1}, \quad . \quad . \quad . \quad . \quad . \quad . \quad (2,1)$$

where $p_1 = 2\pi n_1$, n_1 being the frequency of the disturbance, and where the letter R indicates that the real part is to be taken.

The contour is one which passes from $-\infty$ to $+\infty$ along the real axis except at the point p_1, which is encircled by an infinitesimal semicircle lying in the first quadrant, as in fig. 1.

Fig. 1.

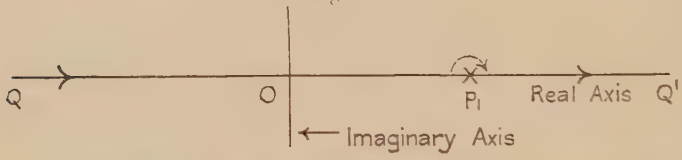

If t is negative and the imaginary p tends to ∞, i.e. p tends to $+i\infty$ above the line QOQ′, then

$$e^{-ipt} = e^{-i(\mathrm{R})(-\tau)} = e^{-\mathrm{R}\tau}, \quad . \quad . \quad . \quad . \quad (3,1)$$

and the integrand tends to zero exponentially. Now the contour can be transferred to a line parallel to QQ′ at $i\infty$ without crossing over any pole of the integrand, and $f(t)$ is therefore zero if $t<0$; on the other hand, if $t>0$ the integrand only vanishes when $p=a-i\infty$, the contour cannot be transformed without passing over p_1 and leaving a circle enclosing it. The integral in this case is equal to

$$\frac{\mathrm{R}}{2\pi}\int_{0}^{\infty}\frac{e^{-ipt}dp}{p-p_1} = \mathrm{R}\,e^{ip_1t}. \quad . \quad . \quad . \quad . \quad (4,1)$$

This integral therefore represents the initial disturbance at $x=0$ say, which is zero for all negative values of t, and equal to $\mathrm{R}e^{-ip_1t}$ for all positive values of t.

Each frequency component of which this integral is composed will travel in the medium with its appropriate phase velocity v_p say, so that at a distance x the integral

$$\mathrm{R}\frac{1}{2\pi}\int_{-\infty}^{+\infty}\frac{e^{-ip\left(t-\frac{x}{v_p}\right)}dp}{p-p_1} \quad . \quad . \quad . \quad . \quad (5,1)$$

will represent the complete disturbance due to a given infinite train of waves.

The value of v_p can be determined from the differential equation of transmission.

Thus, if there are N ions per c.c. of charge e and mass m,

and if f is a frictional force per unit velocity, so that under a steady force the ions move with a mean velocity $\frac{eX}{f}$, then the differential equation for the medium is

$$\frac{\partial^2 z}{\partial t^2} = -\left\{\frac{p^2}{c^2}\left(1-\frac{p_0^2}{p^2}\frac{1}{1+\frac{f^2}{m^2p^2}}\right)+i4\pi\frac{pfNe^2}{m^2p^2+f^2}\right\}z, \quad (6,1)$$

if n' is the mean frequency of the collisions,

$$\frac{f}{mp} = \frac{n'}{\pi n_1}, \quad . \quad . \quad . \quad . \quad . \quad . \quad (7,1)$$

$$p_0^2 = \frac{4\pi Ne^2c^2}{m}, \text{ and is } (2\pi n_0)^2 \quad . \quad . \quad . \quad (8,1)$$

where n_0 is the critical frequency already described ;

$$\frac{\partial^2 z}{\partial t^2} = -\left\{\frac{p^2}{c^2}\left(1-\frac{p_0'^2}{p^2}\right)+\frac{i\sigma_0 p4\pi}{c\left(1+\left(\frac{\pi n_1}{n'}\right)^2\right)}\right\}z, \quad (9,1)$$

so that

$$\left(\frac{c}{v_p}\right)^2 = (p^2-p_0'^2)+\frac{i\sigma_0 p4\pi c}{1+\left(\frac{\pi n_1}{n'}\right)^2},$$

$$\frac{c}{v_p} = \{(p^2-p_0'^2)+i\sigma_1 p\}^{1/2}, \quad . \quad . \quad . \quad (10,1)$$

where σ_0 is the conductivity, *i.e.*, $\frac{Ne^2}{f}$,

where

$$p_0' = \frac{p_0}{1+\left(\frac{n'}{\pi n_1}\right)^2} \quad \text{and} \quad \sigma_1 = \frac{4\pi c\sigma_0}{1+\left(\frac{\pi n_1}{n'}\right)^2}, \quad (11,1)$$

so that the integral representing the disturbance is

$$\frac{R}{2\pi_i}\int_{-\infty}^{+\infty} \frac{e^{-ipt+\frac{i}{c}\left\{(p^2-p_0'^2)+i\sigma_1 p\right\}^{1/2}x}}{p-p_1}\,dp.$$

The integrand has branch points at the roots of

$$p^2-p_0'^2+i\sigma_1 p = 0,$$

$$\text{i. e.} \qquad p = \frac{i\sigma_1}{2} \pm \sqrt{\frac{4p_0'^2-\sigma_1^2}{4}}. \quad . \quad . \quad . \quad (12,1)$$

Fig. 2.

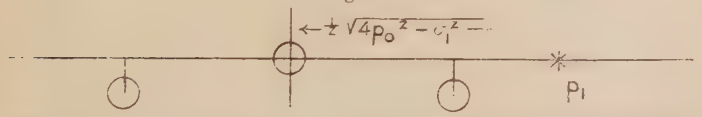

These are shown in fig. 2 ; the roots lie symmetrically in the 3rd and 4th quadrants.

Let us suppose that σ_1 is vanishingly small; then two cases arise according as p_1 is less than or greater than p_0, *i. e.* according as the frequency of the impressed wave is greater or less than the critical frequency.

In either case the integral is zero if $x > ct$, for, as before, we can transform the contour in this case to the locus

$$p = y + i\mathrm{R},$$

where R is a very large quantity, since all the singularities are in the lower half of the plane, in which case the exponential in the integral tends to $e^{+(\mathrm{R}+iy)(t-x/c)}$, which when $x > ct$ can be made as small as we please by increasing R. It therefore follows that c is the limiting velocity of the disturbances, *i. e.* nothing is received at a distant point x until after a time $t = \frac{x}{c}$.

If, however, $x < ct$, we must transform the contour to one at $-i\infty$.

If $p_1 > p_0$, let us join $\pm p_0$ with a cut; then the integrand is regular in the whole plane, and we may transform the contour from

Fig. 3.

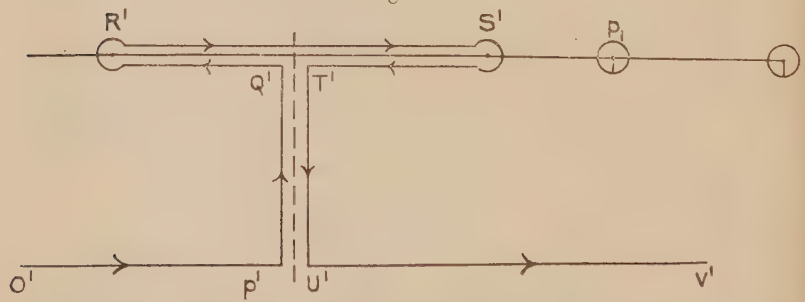

together with the circle round p_1, *i. e.* the original integral is equal to the integral round p_1 and that round the cut joining $\pm p_0$.

Fig. 4.

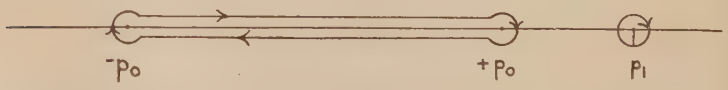

The former is the residue at p_1, i. e.

$$\mathrm{R}e^{-ip_1t+\frac{i}{c}\left\{(p_1'^2-p_0^2)+i\right\}^{1/2}x} \quad ; \quad . \quad . \quad . \quad (13, 1)$$

so that

$$\begin{aligned} Y &= \mathrm{R}e^{-ip_1t+\frac{i}{c}\left\{(p_1^2-p_0^2)+i\right\}^{1/2}x} \\ &\quad +2\mathrm{R}\int_{-p_0}^{+p_0} e^{-ipt-\frac{i}{c}\left\{p^2-p_0^2+i\right\}^{1/2}x}\,\frac{dp}{p-p_1} \\ &= 2\mathrm{R}\int_{-p_0}^{+p_0} \frac{e^{ipt}\sinh\,(p_0^2-p^2)^{1/2}\,x/c\,dp}{p-p_1} \\ &\quad +\mathrm{R}e^{-ip_1t+i(p_1^2-p_0^2)^{1/2}x/c}, \quad . \quad . \quad . \quad . \quad . \quad (14,1) \end{aligned}$$

where σ_1 is sufficiently small.

The integrated part consists of a wave of phase-velocity

$$\frac{c}{\left(1-\left(\frac{p_0}{p_1}\right)^2\right)^{1/2}}. \quad . \quad . \quad . \quad . \quad . \quad (15,1)$$

Similarly, if $p_0>p_1$, we can join p_0 with $+\infty$ and $-p_0$ with $-\infty$ and obtain the contour in fig. 5.

Fig. 5.

The integral round p_1 gives rise, as before, to the expression

$$\mathrm{R}e^{-ip_1t-x/c\sqrt{p_0^2-p_1^2}}; \quad . \quad . \quad . \quad . \quad (16,1)$$

but in this case the phase-velocity is imaginary and gives rise to a large damping coefficient, i. e. $e^{-x/c\,(p_0^2-p^2)^{1/2}}$, so that at large distances from the surface of the medium the disturbance has died right out.

The other part of the integral is

$$\begin{aligned} &\frac{\mathrm{R}}{2\pi}\int_{\infty}^{p_0}\frac{e^{-ipt+i\sqrt{p^2-p_0^2}\,x/c}}{p-p_1}\,dp+\frac{\mathrm{R}}{2\pi}\int_{p_0}^{\infty}\frac{e^{-ipt-i\sqrt{p^2-p_0^2}\,x/c}}{p-p_1}\,dp \quad (17,1) \\ &+\frac{\mathrm{R}}{2\pi}\int_{-p_0}^{-\infty}\frac{e^{-ipt-i\sqrt{p^2-p_0^2}\,x/c}\,dp}{p-p_1}+\frac{\mathrm{R}}{2\pi}\int_{-\infty}^{-p_0}\frac{e^{-ipt-i\sqrt{p^2-p_0^2}\,x/c}\,dp}{p-p_1} \\ &=\frac{\mathrm{R}}{2\pi}\int_{\infty}^{p_0}2i\sin\sqrt{p^2-p_0^2}\,x/c\left(\frac{e^{-ipt}}{p-p_1}+\frac{e^{+ipt}}{p+p_1}\right)dp. \quad (18,1) \end{aligned}$$

It will be observed that after a considerable time has elapsed from the beginning of the disturbances, *i. e.* when t is big compared with x/c, both the integrals,

$$\frac{\mathrm{R}}{2\pi}\int_{-p_0}^{+p_0}\frac{e^{-ipt}}{p-p_1}\sinh\sqrt{p_0^2-p^2}\,x/c\,dp, \quad . \quad . \quad . \quad . \quad (19,1)$$

$$\frac{\mathrm{R}}{2\pi}\int_{\infty}^{p_0}2i\sin\sqrt{p_1^2-p_0^2}\,x/c\left(\frac{e^{-ipt}}{p-p_1}+\frac{e^{+ipt}}{p+p_1}\right)dp, \quad (20,1)$$

tend to zero very rapidly as t is increased, so that

$$\mathrm{R}e^{-ip_1t-x/c\sqrt{p_1^2-p_0^2}}$$

represents the steady state in both cases. The other parts, 1 and 2, represent a disturbance which is only appreciable near the head of the wave, *i. e.* in the neighbourhood of $x=ct$.

Thus, for example, when p_1 is large compared with p_0, the integral (1) is approximately

$$\mathrm{Z}=-\frac{\mathrm{R}}{2\pi p_1}\int_{-p_0}^{+p_0}e^{-ipt\pm i\sqrt{p_0^2-p^2}\,x/c}\,dp \quad . \quad (21,1)$$

and

$$p_1\int\mathrm{Z}\,dx=-\frac{\mathrm{R}}{2\pi}\int_{-p_0}^{+p_0}\frac{ce^{-ipt+i\sqrt{p_0^2-p^2}\,x/c}}{\sqrt{p_0^2-p^2}}\,dp. \quad . \quad (22,1)$$

Let $y=p/p_0$; range of y is from -1 to $+1$,

$$-p_1\int\mathrm{Z}\,dx=\frac{\mathrm{R}}{2\pi}\int_{-1}^{+1}\frac{ce^{-ip_0t+ip_0\sqrt{1-y^2}\,x/c}}{\sqrt{1-y^2}}dy$$

$$=\frac{1}{2\pi}c\mathrm{J}_0(p_0\sqrt{t^2-x^2/c^2}),$$

so that

$$\mathrm{Z}=-\frac{\mathrm{R}}{2\pi p_1}\frac{\partial}{\partial x}c\sqrt{\frac{\pi}{p_0\sqrt{(t^2-x^2/c^2)}}}\cdot e^{ip_0\sqrt{t^2-x^2/c^2}} \quad (23,1)$$

approx. when $p_0\sqrt{t^2-x^2/c^2}$ is large.

In dealing with the final steady state ($t>>x/c$) the disturbance represented by integrals 1 and 2 can be safely neglected. We can now state that "the critical frequency is the frequency at which the nature of the transmission changes from an unattenuated progressive wave to a highly attenuated pulsation or standing wave." The reason for the existence of this limiting frequency, in the case of the pulse already investigated, is now clear. Frequencies lower than n_0 are not

represented because those which were originally present in the pulse are not transmitted by the medium.

§ 2. Physically this failure to transmit the wave must be pictured as caused by a mechanical reaction against the electrons.

For at the critical frequency the magnetic force

$$\frac{1}{ip}\frac{\partial E}{\partial x} \quad . \quad . \quad . \quad . \quad . \quad . \quad (1, 2)$$

in the medium is zero by (14, 1), and no ætherial momentum $\left(i.e.\ \frac{EH}{4\pi}\right)$ can be transferred across any plane in the medium perpendicular to the direction of the ray. But the momentum arriving at the surface is $\frac{E^2}{4\pi}$, so that in order to preserve the conservation of momentum at least $\frac{E^2}{4\pi}$ units of momentum per unit time must be given up to the electrons. This quantity may be more, depending as it does on the amount of momentum reversed on reflexion.

According to the solution given, there is a deficit of momentum of amount

$$\geq \frac{E^2}{4\pi} \text{ per unit time. } . \quad . \quad . \quad . \quad (2, 2)$$

Since this is a purely electrical problem, it should at least be self-consistent as regards the conservation of momentum and energy. The solution (9, 1) of the equations of propagation must be inaccurate to a certain extent.

According to this solution the ions are only moved in a periodic manner in the Z direction with a velocity amplitude $\frac{eE}{mp}$, and there is no material momentum produced in the X direction.

The inaccuracy in the derivation of the previous wave equation is due to the neglect of the action of the magnetic field in the wave front on the moving electrons. It is not difficult to see, even without the aid of mathematics, that this field must produce an average momentum in the X direction. For the electric force Z produces an ionic velocity in the Z direction ; this, in conjunction with the magnetic force H, produces a force on the ion in the X direction, which, although zero when averaged over a long period and

incapable of producing any average acceleration of the ion, nevertheless produces an ionic drift in this direction.

The precise details of this drift have been worked out by Sir J. J. Thomson, who has shown that if v_x is the average velocity of drift in the x direction, then, neglecting the relativity variation of mass,

$$c^2-(c-v_x)^2=\frac{e^2c^2\mathrm{H}^2}{m^2p^2}. \quad . \quad . \quad . \quad . \quad . \quad (7,2)$$

The value of v_x may be connected up with the critical frequency as follows:—

When v_x is small we can replace $c^2-(c-v_x)^2$ by $2cv_x$, and we get

$$v_x=\frac{e^2c\mathrm{H}^2}{2m^2p^2}, \quad . \quad . \quad . \quad . \quad . \quad . \quad . \quad (8,2)$$

and if N is the number of ions per c.c. each of mass m, the average ionic momentum produced is

$$\mathrm{N}mv_x=\frac{\mathrm{N}e^2\mathrm{H}^2}{2mp^2}. \quad . \quad . \quad . \quad . \quad . \quad . \quad (9,2)$$

Now
$$\frac{\mathrm{N}e^2c^2}{m}=\frac{p_0^2}{4\pi}.$$

$$\therefore \quad \mathrm{N}mv_x=\frac{p_0^2}{2p^2}\cdot\frac{1}{4\pi}\frac{\mathrm{H}^2}{c}=\frac{p_0^2}{2p^2}\times(\text{ætherial momentum}).$$

$$. \quad . \quad . \quad (10,2)$$

Thus in the neighbourhood of the critical frequency the momentum of the wave is used up in producing ionic momentum, and in this we have the physical explanation of the reason why waves of lesser frequency are not transmitted by the medium, *i. e.* the demand for momentum by the ions is greater than can be supplied by the wave.

The formula (7, 2) was derived by Sir J. J. Thomson on the assumption that the wave propagation was unmodified by the effect of ionic motions, so that H = E in the wave front. But we have seen that this is certainly incorrect in the neighbourhood of the critical frequency where the relation between E and H is

$$\mathrm{H}=\mathrm{E}\sqrt{1-\frac{p_0^2}{p^2}} \quad . \quad . \quad . \quad . \quad (11,2)$$

or
$$\mathrm{H}=\beta\mathrm{E}.$$

It will therefore be well to verify at this stage that the equations on which this result is based are correct when

the motion of the ions in the magnetic field of the wave is taken account of. To do this we must remove the restriction that $H=E$ in the wave front, and assume $H=\beta_1 E$ where $\beta_1=\beta$ if the relations are unmodified, $\beta_1 c$ being the group-velocity. The motion of the ions may then be computed by a similar method to that used by Sir J. J. Thomson, and the conclusion arrived at is that the velocity of drift may be calculated from the formula:

$$\left(1-\left(\frac{c_1-v_x}{c_1}\right)^2\right) = \sin^2\left(\frac{eH}{mp}\cos pt\right), \quad . \quad (12, 2)$$

where $c_1=\frac{c}{\beta_1}$ and is the phase-velocity. If $\frac{eH}{mp}$ is small enough, this gives approximately:

$$\frac{dv_x}{dt}=\frac{eHE}{m^2p^2}\sin pt\cos pt; \quad . \quad . \quad . \quad (13, 2)$$

and since

$$v_z=\frac{m}{eH\sin pt}\frac{dv_x}{dt},$$

$$v_z=\frac{E_0 e}{mp}.\cos pt, \quad . \quad . \quad . \quad . \quad . \quad (14, 2)$$

which is exactly the value in the previous approximate theory, so that to the first order of $\frac{EH_0}{mp}$ the simpler theory is correct. Also, if we assume as a simplification that the positive and negative ions are equal in number and in mass, the total current in the X direction is still zero and the original equations are still valid.

These equations, which were linear, are no longer so when the effect of the magnetic field is taken into account, but they only diverge from linearity when $\frac{EH}{mp}$ is large.

The relation between momentum of the ions and the momentum of the field still holds, for it may easily be shown that

$$Nmv_x=\frac{p_0^2}{2p^2}.\frac{EH}{4\pi}, \quad . \quad . \quad . \quad . \quad (15, 2)$$

as before in eq. (10, 2).

The discrepancy as regards the conservation of momentum in the beginning of § 2 may now be cleared up.

For simplicity, consider the case where p/p_0 is small, and

where the electric and magnetic forces in the wave are so small that the deviations from linearity of the equations can be neglected. We have to determine the deficit in ætherial energy in this case.

It has been shown by L. Brillouin * that all but an entirely insignificant part of the energy and momentum in the wave (in the loaded medium) is contained in the region between the surface of the medium and another surface which travels forward with the *group-velocity*:

$$\frac{\partial \mathrm{KV}}{\partial \mathrm{K}} = \mathrm{U},$$

where $\mathrm{K} = \frac{1}{\lambda}$, and V is the phase-velocity.

Now

$$\frac{\partial \mathrm{KV}}{\partial \mathrm{K}} = \beta c = \sqrt{1 - \frac{p_0^2}{p^2}}\, c. \quad . \quad . \quad (16, 2)$$

This is equivalent to saying that the head of the wave in the medium travels with the *group-velocity*, not the phase-velocity, or that the energy and momentum in the head of the wave, *i. e.* between the region

$$x = ct \quad \text{and} \quad x' = \mathrm{U}t,$$

can be neglected. Under these conditions we can calculate the deficit of ætherial energy as follows :—

The electric force in the medium is

$$\mathrm{E} = \mathrm{E} \sin\left(pt - p\frac{\beta x}{c}\right) \quad \text{and} \quad \mathrm{H} = -\beta \mathrm{E},$$

so that the rate of supply of momentum over any surface inside the medium is $\frac{\mathrm{E}^2\beta}{4\pi}$.

Now the rate of increase of momentum at the head-end of the wave is $\frac{\mathrm{EHU}}{4\pi c}$.

Since $\frac{\mathrm{EH}}{4\pi e}$ is the momentum per unit volume, and the increase of volume (per sq. cm. of area) per unit time is U, this quantity is

$$\frac{\mathrm{EH}\beta c}{4\pi c} = \frac{\mathrm{E}^2\beta^2}{4\pi}.$$

* *Annalen der Physik*, No. 10, p. 203 (1914).

There is therefore a deficit of ætherial momentum of amount $\frac{E^2\beta(1-\beta)}{4\pi}$ or $\frac{EH(1-\beta)}{4\pi}$.

When $\frac{p^2}{p_0^2}$ is small, $\beta \doteq 1$ and $1-\beta \doteq \frac{p_0^2}{2p^2}$, and the apparent loss of momentum is

$$\frac{EH}{4\pi}\frac{1}{2}\frac{p_0^2}{p^2}, \quad . \quad . \quad . \quad . \quad . \quad (17, 2)$$

and the rate of gain of ionic momentum is

$$Nmv_x\beta c = \frac{1}{2}\frac{p_0^2}{p^2}\cdot\frac{EH\beta}{4\pi}, \quad . \quad . \quad . \quad (18, 2)$$

which to the first approximation balances the apparent loss by momentum.

The conservation of energy also holds to the first approximation, for the rate of supply of energy across SS′ is

$$\frac{EHc}{4\pi} = \frac{\beta E^2 c}{4\pi}, \quad . \quad . \quad . \quad . \quad . \quad . \quad (19, 2)$$

the rate of gain of energy at the front of the wave

$$\frac{E^2+H^2}{8\pi}c\beta = \frac{E^2c\beta}{8\pi}(1+\beta^2), \quad . \quad . \quad (20, 2)$$

and the apparent loss of energy is

$$\frac{E^2c\beta}{8\pi}(2-(1+\beta^2)) = \frac{E^2c\beta}{8\pi}(1+\beta)(1-\beta)$$

assuming $1+\beta = 2$ $$= \frac{E^2c\beta}{4\pi}(1-\beta) \text{ approx.}$$

$$= \frac{EHc}{4\pi}(1-\beta). \quad . \quad . \quad (21, 2)$$

Now from (12, 2)

$$\dot{v}_x = \frac{1}{4}\frac{e^2HE}{m^2p^2} \quad . \quad . \quad . \quad . \quad . \quad (22, 2)$$

and

$$\bar{v}_z^2 = \frac{E^2e^2}{m^2p^2}\overline{\sin^2 pt} = \frac{E^2e^2}{2m^2p^2},$$

$$Nm\bar{v}_x c = Nm\beta\frac{E^2e^2}{m^2p^2}\frac{1}{4} = \frac{1}{2}Nmv_z^2.$$

Now

$$\mathrm{N}mv_x c = (1-\beta)\frac{\mathrm{EH}}{4\pi}c.$$

$$\therefore \quad \tfrac{1}{2}\mathrm{N}m\bar{v}_z^{\,2} = (1-\beta)\frac{\mathrm{EH}}{4\pi}c, \quad . \quad . \quad . \quad (23, 2)$$

and just balances the apparent deficit of energy.

The v_x energy is of the second order in $(1-\beta)$, and can be neglected in comparison with $\frac{1}{2}\mathrm{N}mv_z^2$.

These solutions are not quite exact, for we have neglected the momentum and energy carried off in the head of the wave (represented by expression (20, 1)), and also neglected the divergence of the solution from true linearity.

For this reason the case where $p \gg p_0$, and v_x/c small, was chosen to illustrate the conservation of energy and momentum, for under these conditions the momentum and energy in the head of the wave are small, and the divergence from true linearity can also be neglected.

But there seems little doubt that the solutions would be exact if we took these minor adjustments into account.

It is clear anyhow that the critical frequency occurs in virtue of the fact that the ions rob the energy and momentum of the main wave, so that it can no longer travel through the medium.

The velocity of drift is in general small compared with the velocity of light unless enormous wave energies are involved, for we have approximately :

$$\frac{v_x}{c} = \frac{1}{2}\frac{p_0^2}{p^2}\frac{\mathrm{HE}c^2}{\mathrm{N}m\,.\,4\pi} \quad . \quad . \quad . \quad . \quad (24, 2)$$

$$= \frac{1}{2}\frac{p_0^2}{p^2}\frac{\mathrm{M}}{\mathrm{N}m}, \quad . \quad . \quad . \quad . \quad . \quad (25, 2)$$

where M is the electromagnetic mass per unit volume.

So that $v_x \to c$ in the neighbourhood of the critical frequency only when the electromagnetic mass per unit volume approaches the ionic mass per unit volume ; a simple calculation shows that this requires enormous energy densities in the wave if N has any value comparable with the number of molecules per c.c. in a gas at normal temperature and pressure.

The result is only approximate as the neglect of the velocity variation of mass is serious when velocities approaching that of light are considered.

An exact computation of these effects has been made, but

the mathematical complexity rather obscures the underlying physical relations.

It is significant to compare this relation with that obtained by Compton* and myself† in the case of an individual quantum acting on a single electron which is considered by the former from a purely quantum point of view and the latter from a more or less classical point of view, which show that the velocity of recoil of an electron gets comparable with that of light when the mass $\left(\frac{h\nu}{2c^2} \text{ of the quantum}\right)$ approaches that of the electron it acts upon. The relation (25, 2) is obviously the same as ((5, 6) (p. 280, Phil. Mag. July 1926) when generalized so as to apply to an aggregate of electrons instead of an individual one.

§ 3. This critical frequency has another interpretation connected with the quantum theory of the Compton effect.

We have shown that the critical frequency is given by the relation:

$$\frac{Ne^2}{\pi m\nu^2} = 1, \quad \ldots\ldots \quad (1, 3)$$

and it is shown (Compton, "Scattering and Structure of Radiation," Phil. Mag. July 1926) that in order to satisfy the quantum conditions we must have the relation:

$$\frac{h\nu}{H^2/4\pi} = \frac{e^2}{\pi m\nu^2}, \quad \ldots\ldots \quad (2, 3)$$

where $h\nu$ is the energy of a quantum engaged in an encounter with an electron, and H is the magnetic force in the wave reckoned in the usual classical manner; $\frac{H^2}{4\pi}$ therefore representing the radiant energy per unit volume. The ratio $\frac{4\pi\, h\nu}{H^2}$ must therefore be of the dimension of a volume, which, for want of a better expression, was termed "the volume of a quantum," V_q, say.

The relation giving the critical frequency can therefore be put in the simple form:

$$V_q N = 1, \quad \ldots\ldots \quad (3, 3)$$

and since $\frac{1}{N}$ is the average volume occupied by each

* Phys. Rev. † Phil. Mag.

electron, we may say that the critical frequency is such that the volume occupied by the quantum at the frequency is equal to the average volume occupied by an electron, or, as we may put it crudely, the quanta and electrons are paired off.

Perhaps the idea of the volume of a quantum is too materialistic a conception to be accepted readily, and it is therefore preferable to use the conception of probability, which is more conformable to the ideas of quantum mechanics. From the quantum point of view, long wave phenomena, such as envisaged here, are undoubtedly cases of statistical mechanics.

We can think of the wave as a well-ordered swarm of quanta encountering a swarm of electrons.

To introduce the idea of probability, consider the quantity :

$$\frac{4\pi N h\nu}{H^2} \quad . \quad . \quad . \quad . \quad . \quad . \quad . \quad (4, 3)$$

It is of zero dimensions and is unity when all the quanta per unit volume are paired off with the electrons per unit volume, which suggests that it may be considered as the probability of a direct hit of a quantum in unit volume with one of the electrons in unit volume, or more precisely as the fraction of the number of quanta per unit volume in direct collision with the electrons per unit volume. This conception derives some weight from the following considerations : In each encounter some of the momentum of the quantum is given up to the electron, the amount being expressed by the relation :

$$M_x = \frac{h\nu}{c}(1-\cos\theta), \quad . \quad . \quad . \quad . \quad (5, 3)$$

where M_x is the gain in electron momentum, and θ is the angle of scattering of the individual quanta. On the average the momentum gained by the electrons will be the product of the probability that each quantum will find an objective in an electron and the average momentum given to the electron in an encounter, *i. e.*

$$\frac{P h\nu}{c}\overline{(1-\cos\theta)f(\theta\phi)}, \quad . \quad . \quad . \quad . \quad (6, 3)$$

where $f(\theta\phi)$ is the distribution of the scattered quanta as a function of θ and ϕ, and P is the probability of a direct hit, which we have tentatively suggested is $\frac{n_0^2}{n^2}$. The average

value of $(1-\cos\theta)f(\theta\phi)$ is not known exactly, but by the correspondence principle it should agree with the scattered radiation from an electron calculated in the ordinary way. Taking the classical value, this comes out at 1/3, so that following up this suggestion, electron momentum $= \frac{1}{3}\frac{n_0^2}{n^2}$ M æther on the average say. More generally, Momentum of electrons $= k\frac{n_0^2}{n^2}$ M æther. Actually to make this agree with (15, 2) we must have $k=\frac{1}{2}$.

In view of the uncertainty of this distribution factor, the agreement, except for the numerical factor, suggests that the interpretation of $\frac{n_0^2}{n^2}$ as the probability factor is correct.

Speaking approximately, the critical frequency occurs when the probability of a direct hit between the quanta in the incoming wave and the electrons is unity, in which case the momentum in each quantum is on the average handed over to one of the electrons, and the momentum of the wave is used up and it can travel no farther.

This interpretation of the quantity

$$\frac{4\pi \mathrm{N}\, h\nu}{\mathrm{H}^2} = \frac{n_0^2}{n^2}$$

can also be used to calculate the scattering of X-rays. From the quantum point of view, an encounter between a quantum and an electron raises the latter to an energy level $h\nu$, and after an average time τ, which represents the average life in this excited state, this quantum is scattered.

Now $\frac{\mathrm{N}_1}{\tau} = \mathrm{A}_{12}\mathrm{N}_1$ is Einstein's probability coefficient representing the number of emissions of a scattered quantum per unit time per unit volume where there are N_1 electrons in the excited state. Now N_1 can be computed from the expression (1), the fraction of the total number of quanta in collision for

$$\frac{\mathrm{N}_1}{\bar{\mathrm{N}}} = \frac{4\pi\, h\nu\, \mathrm{N}}{\mathrm{H}^2} = \frac{n_0^2}{n^2},$$

where $\bar{\mathrm{N}}$ = total number of quanta per unit volume, so that the energy scattered per unit time per unit volume is

$$\frac{n_0^2}{n^2}\mathrm{A}_{12}\bar{\mathrm{N}}\, h\nu. \quad . \quad . \quad . \quad . \quad . \quad (7, 3)$$

The rate of supply of energy is $\bar{N}\,h\nu\,c$, so the absorption-coefficient is

$$\frac{n_0^2}{n^2} A_{12} \frac{\bar{N}\,h\nu}{\bar{N}\,h\nu\,c} = \frac{n_0^2}{n^2} A_{12}.$$

A_{12} is shown to be

$$\frac{e^2 4\pi^2 n^2}{3m_0 c^3}, \quad . \quad . \quad . \quad . \quad . \quad . \quad . \quad (8,3)$$

so that the absorption-coefficient

$$\frac{n_0^2}{n^2 c} \frac{2e^2 4\pi^2 n^2}{3m_0 c^2} = \frac{8\pi^2}{3} \frac{n_0^2 e^2}{c m_0 c^3}, \quad . \quad . \quad . \quad (9,3)$$

and since

$$n_0^2 = \frac{N e^2 c^2}{\pi m_0},$$

$$\alpha = \frac{N e^2 c^2}{\pi m_0 c} \frac{8\pi^2}{3} \cdot \frac{e^2}{m_0 c^3} = \frac{8\pi N e^4}{m_0^2 c^2}. \quad . \quad . \quad (10,3)$$

in agreement with the ordinary values.

§ 4. *Frequency Change.*

On account of the average velocity produced in the electrons, the frequency of the scattered waves is changed according to the Doppler principle by an amount $\frac{\delta n}{v} = v_{x/c}$.

In the case where the medium is finely structured compared with the wave-length, it is the reflected wave which is altered in frequency. This change is small except when the ætherial mass (per unit volume) approaches the mass of the electrons per unit volume—a very exceptional case requiring enormous wave energies.

This effect will therefore not be of importance in the investigation of the momentum relations if we confine ourselves to small wave energies where v/c is everywhere small.

Non-Reversible Transmission.

Transmission through this type of medium affords an example of the irreversible effects which have been observed in radio transmission (Proc. I.E.E. vol. lxiii. no. 346, Oct. 1925), where it is shown that there is an apparent difference between East and West transmission and West to East transmission. An example can be constructed as follows:—

Suppose A and B are two sources of electromagnetic

waves. A slab of ionized gas is supposed to be situated between A and B, the ionization being maintained by some external agency—X-ray for example.

Let the critical frequency of this medium be n_0.

Fig. 6.

If the frequency n of waves emitted by A and B is greater than n_0, then the medium will be transparent and A can send energy to B, and *vice versâ*. If, however, $n < n_0$, the waves will be absorbed in the medium.

If, now, the ionized slab be considered to be moving from left to right with a velocity v, then, referred to axes moving with the slab, the frequency of the waves from A is $n(1-v/c)$, and from B is $n(1+v/c)$ (the frequency referred to A and B axes being n).

We will again suppose the critical frequency of the medium (referred to the moving axes) is n_0, which we are quite at liberty to do. If, now,

$$n(1+v_{x/c}) > n_0 > (n)(1-v/c), \quad . \quad . \quad . \quad (1,4)$$

the medium will be transparent to waves from B, but opaque to those from A, and the system is irreversible. This argument refers to the steady state. In considering the conveyance of an intelligible message from A to B, and *vice versâ*, such as we are concerned with in radio telegraphy, for instance, it is insufficient to have only a single steady wave of constant frequency, for this has no character to convey the intelligible message. In general, the message must be considered to be conveyed by a band of frequencies between $n+\delta n$ and $n-\delta n$, say. The above argument, however, applies if the band is so narrow that all the frequencies from A (referred to axes moving with the slab) are less than the critical frequency, and all those from B are greater than this.

Thus

$$(n+\delta n)(1-v/c) > n_0, \quad . \quad . \quad . \quad . \quad (2,4)$$

$$(n-\delta n)(1+v/c) < n_0\ ; \quad . \quad . \quad . \quad . \quad (3,4)$$

$$\text{i. e.} \qquad \delta n/n > v/c. \quad . \quad . \quad . \quad . \quad . \quad . \quad . \quad . \quad (4,4)$$

The possibility of such irreversible effects seems to be inconsistent with the usually-accepted notions as regards the reversibility of optical phenomena, which appears to be based on a theorem of the following type.

Consider a group of fixed conductors and a series of forces of the types $E_r e^{ipt}$, and a series of corresponding velocity coordinates

$$I_1 e^{ipt}, \ldots I_r e^{ipt}. \quad . \quad . \quad . \quad . \quad . \quad (5, 4)$$

Then, if the energy T can be expressed as a homogeneous quadratic function of the I's, there is a dissipation function of the same type and a normal potential function W, the motion is expressed by the Lagrangian equations of the type :

$$\frac{\partial}{\delta t}\left(\frac{\partial (T-W)}{\partial I_r}\right) + \frac{\partial (T-W)}{\partial q_r} + \frac{\partial \phi}{\partial I_r} = E_r, \quad . \quad . \quad (6, 4)$$

etc.,

and it follows that

$$\frac{\partial E_r}{\partial I_s} = \frac{\partial E_s}{\partial I_r} \quad . \quad . \quad . \quad . \quad . \quad . \quad (7, 4)$$

and the E.M.F. induced in r by unit current in S is equal to the E.M.F. induced in δ by unit current in r, and the effects are reversible in this sense.

This specification implies that the connexions of the system are such that the forces of this specified type $E_r e^{ipt}$ should produce currents only of this specified type, as will be seen on expressing equation (6, 4) explicitly in terms of the velocity coordinates etc. For if we calculate the EM energy from the usual formulæ :

$$\left.\begin{aligned} T &= \tfrac{1}{2}\iiint (F u_0 + G v_0 + H w_0)\, dv \\ \text{and} \qquad W^2 &= \tfrac{1}{2}\iiint (X^2 + Y^2 + Z^2)\, dv, \end{aligned}\right\} \quad . \quad . \quad (8, 4)$$

where F G H is the vector potential, and $u_0\, v_0\, w_0$ the total convection current at any point ; and assume that only currents of this type are present, we get expressions for the kinetic and dissipation energies which are homogeneous quadratic functions of the currents as before *.

Thus it is sufficient for a reciprocal relation to have a linear relation between the E.M.F. and currents.

In the example cited of the transmission through a moving dispersive medium, the currents and movements produced in

* Sommerfeld, *Jahrbuch der drahtlosen Telegraphie und Telephonie*, vol. xxvi. book 4, pp. 93-98 (1925).

the medium are not linear, and the fact that the reciprocal relation does not hold good in this case does not violate the above theorem.

§ 5. Summarizing, it is shown that in a medium containing free electrons there is a certain critical frequency characterized by the fact that waves of lower frequency than this cannot travel through the medium.

The physical reason for the existence of such a critical frequency is shown to be connected with the fact that the electrons in the medium rob the wave of its momentum, and at the critical frequency also rob this momentum completely so that the wave can travel no further.

This fact is shown to be connected with the theory of Compton scattering, in which an individual quantum gives up its momentum in collision with an electron. The wave is brought to a standstill when all the quanta (per unit volume) are brought into collision with the electrons, which event occurs when the critical frequency is approached.

XIV. *A Method of Measuring the Mean Free Path of Electrons in Ionized Mercury Vapour* *. *By* KATHARINE B. BLODGETT, *Ph.D., General Electric Co., Schenectady, New York* †.

Introduction.

IT has been shown by Stead and Stoner ‡ that in gases at very low pressures glow-discharges of considerable length can be produced in a tube which has electrodes at one end only. The anode is an open grid which is placed immediately in front of the hot cathode so that electrons are accelerated past the grid and ionize the gas in their path along the tube. Stead has used a tube which extended about 35 cm. from the grid, and under suitable conditions the glow could easily be made to reach to the end of it.

If a low accelerating potential is applied to the grid, of the order of 25 volts or less, the glow will not extend to the end of a long tube, but will come to a limit at a distance which is principally determined by the grid

* The experiments described in this paper were made in the Cavendish Laboratory when the writer was a Research Student of Newnham College, Cambridge.

† Communicated by Sir E. Rutherford, O.M., D.Sc., F.R.S.

‡ Stead and Stoner, Proc. Camb. Phil. Soc. xxi. p. 66 (1922).

voltage. This limit is dome-shaped, and, in mercury vapour which is free from contamination by other gases, is very sharply defined. The effect in a darkened room is striking, for the glow can be contracted or extended to great lengths simply by varying the grid voltage, and the space in the tube beyond the sharp limit of the glow appears to be completely dark, as if all sources of luminosity were halted and could not pass beyond that point. The variation of length with voltage is continuous and shows no lag.

Stead and Stoner pointed out the need for a theory of the glow that would explain the sharp tip, and they put forward a theory based on speculative considerations. More recently, the method devised by Langmuir * for investigating the properties of gaseous discharges has made it possible to revise the theory in the light of experimental data. Langmuir's method consists in measuring the current which is taken up at different voltages by an auxiliary electrode in a discharge, called a collector, and interpreting the data thus obtained with the aid of a theory which he has developed. This paper will describe some results of applying the method of collectors to long glows, which show that these glows supply a means of measuring the mean free path of electrons in an ionized gas.

Apparatus.

The apparatus, which was built with the assistance of Mr. Stead, is drawn to scale in fig. 1. The grid was made of molybdenum wire, 0·2 mm. in diameter, bent into a flat, open zigzag with a spacing of about 3 mm. between consecutive turns, so that the wire presented very little target area to the electrons. It was at the upper end of the tube when the tube stood in a vertical position, with the hot cathode immediately above it in the form of a straight filament of 0·2 mm. tungsten wire stretched across the diameter of the tube about 3 mm. above the grid. The potential drop along the filament was 2·7 to 3·0 volts with heating currents of 3·5 to 4·0 amperes. The area of the grid filled the greater part of the cross-section of the tube which was 3·4 cm. in diameter, and the tube had this diameter for a length of 78 cm. from the grid.

* Langmuir, Journ. Frankl. Inst. cxcvi. p. 751 (1923). Langmuir, Gen. Elec. Rev. xxvi. p. 731 (1923). Langmuir and Mott-Smith, Gen. Elec. Rev. xxvii. pp. 449, 538, 616, 762, 810 (1924).

The collector was operated on a glass float which rested on mercury and could be raised or lowered over a range of 60 cm. by lifting a mercury reservoir to which it was connected through a barometric column. This column of mercury also served to make electrical contact from the float to the external circuit and to supply mercury vapour for the discharge. The collector was supported on a length of stout nickel wire, 1·0 mm. in diameter and 78 cm. long, insulated throughout its length by fine glass tubing. The glass float was drawn out into a capillary at the top which was just large enough to receive the nickel wire and hold it firmly in a vertical position; the end of the wire rested on the bottom of the float to support the weight of the nickel, and there, with the aid of a drop of mercury, it made electrical contact with a short lead sealed through the bottom of the float and submerged in the mercury on the other side. With a float of this simple design it was possible to change collectors, using the same float; to facilitate this change the tube was made with a ground-glass joint at the lower end through which the float could be withdrawn.

Fig. 1.
Discharge-tube.

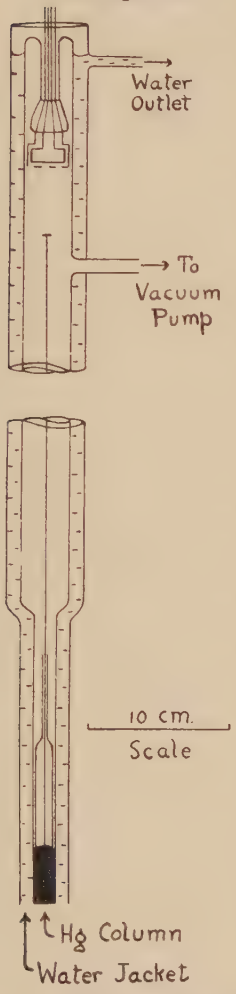

The middle section omitted from this drawing is 50 cm. in length.

It became evident in the course of the experiments that it was important that the collector should be set accurately on the axis of the tube. To accomplish this, it was convenient to make use of the slight flexibility of the long nickel wire. With the lower end held rigidly in the float, the upper end could easily be displaced a small amount to one side or the other by inclining the tube through a very small angle from the vertical. For this purpose the whole apparatus was given freedom to be tipped slightly in any direction, by mounting the long vertical tube and the mercury condensation pump

which was connected to it both on the same stand so that they moved together.

Control of the mercury vapour pressure was secured by means of a glass water-jacket which enclosed the discharge-tube throughout its entire length, with the jacket extending 50 cm. down the lower tube in which the float operated. In addition, the connecting tube leading to the pump was jacketed for 45 cm. of its length. Only circulating water was used, and a thermometer suspended inside the large jacket measured the temperature, which could be held constant to 0·2 degree during a run. The condensation pump was kept running throughout every experiment to keep the mercury vapour pure.

With the water-jacket in place it was no longer possible to exhaust the tube by baking it in the standard manner, and therefore another method had to be employed to rid the surface of the walls of water vapour and other gases. For, in addition to the need for safeguarding the tungsten filament in these experiments, the mercury glow itself called for the cleanest possible conditions inside the tube, since the glow presents a sharp tip only when the mercury vapour is free from contaminating gases. With traces of water vapour present, the glow is faint, and the tip diffuse and indistinct. The appearance of the glow is the surest indication of conditions inside the tube, and a little familiarity with the behaviour of glows in clean and contaminated tubes enables one to tell the condition of the tube at a glance. The method of exhaust employed in these experiments consisted in putting to use the fact that in a glow discharge the walls of the tube become negatively charged, so that positive ions are continually bombarding the walls and thereby dislodging gas molecules from the surface. In other words, a glow will clean its own tube, if given the opportunity to do so by the aid of fast pumping. Campbell * has pointed out that a mercury glow will evolve large quantities of hydrogen from the walls of a tube which has previously been baked just below the softening-point of the glass, indicating that the mechanism of the glow is more effective in this respect than heat treatment. In his experiment the filament wasted rapidly, and broke after 48 hours of running the glow, though the gas was being pumped away all the time. But in the present experiments it was found that if the gas is pumped away sufficiently rapidly as it is evolved, the filament suffers no harmful effects and the walls of the tube are very effectively cleaned. The tube

* Research Staff of the General Electric Company, London (Work conducted by N. R. Campbell), Phil. Mag. xli. p. 685 (1921)

may safely be opened to the atmosphere and left open for several days, and then evacuated and cleaned again by this method.

The practice in cleaning the tube after it had been opened to the atmosphere was to run the glow for a few seconds at about 70 volts grid potential, and then shut it off long enough to allow the pump to remove all the gas that had been evolved. At first the glow would be so faint as to be hardly perceptible, partly because of the lowered emission of electrons from the filament in the presence of oxygen, though with the filament raised to such a high temperature that it gave the usual 20 milliamperes emission even in the presence of oxygen, the glow was very faint. As the process of cleaning progressed, by alternately running the glow and pumping out the gas, the glow became brighter and longer, and the tip grew more distinct. For example, at a certain stage of the process the glow would extend for 40 cm. down the tube for a given grid voltage; if, then, the glow was shut off for a minute, it would extend for 45 cm. when it was next turned on. In this way the cleaning process was carried to completion. It was never found practicable in the early stages of the process to keep the glow running and expect the gas to be pumped off as fast as it was evolved, though some care had been taken to make the distance to the pump short, with large enough connecting tubing to ensure fast pumping; perhaps with more ideal conditions the glow could be run in this way. It may be added that at one time, when a trap made of a spiral of small-sized glass tubing was inserted between the discharge-tube and the pump, it was found quite impossible to clean the tube in the ordinary manner with this hindrance in the way, and the trap had to be removed. This is pointed out merely to emphasize the fact that really fast pumping is essential for the success of the process, or the filament will waste and break in the presence of the water vapour, as it did in Campbell's experiments.

Factors that determine Length of Glow.

Fig. 2 shows the lengths to which a glow in saturated mercury vapour at ordinary temperatures will extend in a tube 3·4 cm. in diameter. These data were taken with the collector removed from the glow. The curves illustrate the low range of grid voltage that is required to produce a glow 65 cm. long, the tip moving 3 or 4 cm. along the tube for every increase in potential of one volt. The current flowing to the grid and the mercury-vapour pressure are

also seen to be factors determining the length ; these will be discussed in a later section of this paper. The trend of the curves leaves no doubt that in a longer tube, at low pressures, glows more than a metre in length could be obtained at moderate voltages.

The circle on each curve marks the striking voltage. At this voltage the current jumps discontinuously to a value ten or more times its value immediately before the arc strikes, and at the same time the glow appears to dart out

Fig. 2.

Plots of Length of Hg Glow against Grid Voltage.
Circle on each curve marks striking voltage.

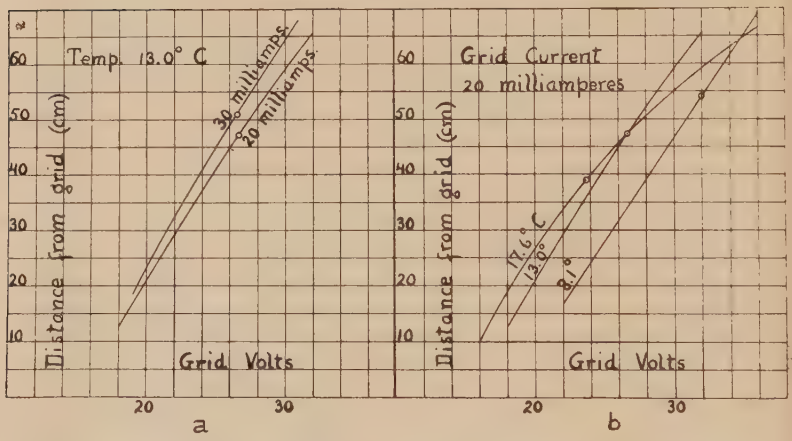

from the filament to the distance which corresponds to this voltage under the conditions of the experiment. It may then be contracted to a third or a quarter of the striking length, but by decreasing the voltage farther the glow is extinguished when it has shrunk to about 10 cm.

General Nature of Data obtained with Plane Collector.

The collector that was used to take most of the data in this investigation was a plane disk of nickel 0·70 cm. in diameter, mounted in a horizontal position on the upper end of the long vertical lead wire that has been described. The metal face of the disk was toward the cathode, and the back was insulated with mica. A plate of this size could be projected far into the heart of the glow, but could not be used to explore inside the glow anywhere near the tip ; for if the plate were withdrawn to a position near the tip

the glow promptly shrank till it no longer passed the plate but appeared to rest on its surface. The plate was always well inside the glow whenever data were taken, except where the contrary is stated. Usually the glow extended the full

Fig. 3.

Typical Current-Voltage Curve drawn to Three Scales of Current. Data taken with Disk Collector 0·7 cm. in diameter.

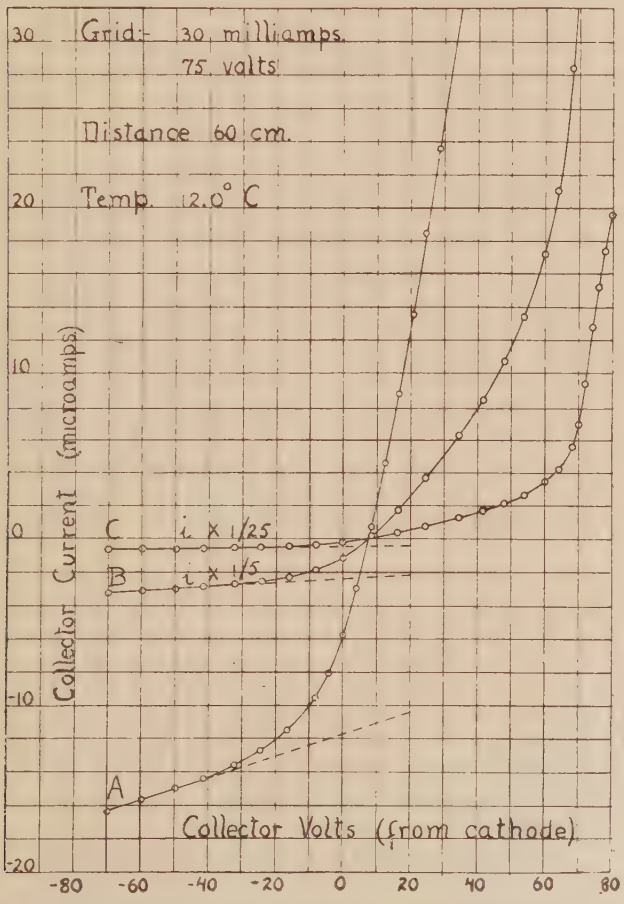

length of the large tube in spite of the presence of the collector support down the axis.

The general form which the data take is illustrated in fig. 3. This is a typical plot of the current flowing to a collector with potential differences applied between the collector and the cathode; the potentials were measurep

from the negative end of the cathode. The smaller currents were measured with a Nalder Bros. & Co.'s galvanometer, used with light and scale, which gave a deflexion of 2 cm. for 1 microampere.

Fig. 3 shows a current-voltage curve drawn to three different scales of current, so as to give the complete range of the data. The currents in Curve B are plotted on a scale reduced to 1/5, and in Curve C to 1/25 of the scale marked on the graph. In plotting the data the convention with regard to sign which Langmuir adopts has been used, *i. e.* "that the sign of a current is positive when positive current flows from the electrode into the space." Currents plotted below the zero line are therefore the positive ion currents which flow to a collector when it is at a negative potential with respect to the space surrounding it. Langmuir has shown that with negative potentials sufficient to repel all electrons the positive ions form a sheath about the collector, and the whole drop in potential becomes concentrated within the sheath. The current is then limited by the positive ion space-charge within the sheath, and is related in magnitude to the sheath thickness by the ordinary space-charge equations. For example, in the case of the present experiments, if the plane collector at a potential 100 volts negative with respect to the mercury glow which surrounds it takes up a positive ion current of 20 microamperes per cm.^{2}, the sheath thickness becomes 0·44 cm. Whenever such a sheath covers the collector it is always plainly visible as a dark space, since it is a region of no ionization.

Curve C, which gives the complete range of the data plotted in fig. 3, shows how the current rises gradually from a small positive ion current at negative voltages to a much larger electron current at positive voltages, and does not begin to rise rapidly until it approaches the potential of the grid, which in this case was 75 volts. The potential of the glow is approximately that of the grid, since large numbers of electrons begin to reach a collector as soon as it approaches the potential of the space surrounding it. From 75 volts upwards the curve does not reach a current saturation value, such as Langmuir finds for similar curves in a mercury arc, but continues upward indefinitely, and a brightly luminous sheath over the collector indicates that ionization by collision is occurring close to the surface. Meanwhile the current to the grid decreases, as the collector is now acting as a second anode, robbing the grid of some of the anode current.

The intermediate range of the data is best studied in Curve A. This shows how the positive ion current decreases slowly with decreasing negative voltage, according to an approximately linear relationship. The continuation of this part of the curve in a dotted straight line marks the current that would be received if only positive ions were present; but with decreasing negative voltage, electrons begin to reach the collector, and the curve takes an upward trend. Since the space filled by the glow is at the potential of the grid, the electrons which reach the collector in this range must move against a retarding field, and can reach it only according to the energies they possess. It will be seen from the sloping nature of the curve in this range that electrons of all energies are present, and are not readily classified into groups. Some of these electrons are found to have energies higher than that corresponding to the grid potential by which they have been accelerated, as indicated in this instance by the fact that the curve starts upward at a potential about 40 volts lower than that of the cathode. In other words, some few electrons in being accelerated by 75 volts have somehow gained an energy corresponding to 115 volts. This phenomenon of the scattering of electrons has been observed and described by Langmuir *, but has not yet been explained.

The curves in fig. 3 are perfectly typical of all the data that were taken, though the actual magnitudes of the currents varied widely according to the conditions of each experiment. With changes in grid potential the sharp rise in the upper end of the curve was always close to the grid voltage, and the rest of the curve was shifted a corresponding amount to the left or to the right. With increase in grid current there was more intense ionization of the entire glow, and both positive ion and electron currents were increased.

The data in fig. 3 were all taken with the collector at a fixed distance of 60 cm.; all distances were measured from the grid. Fig. 4 shows how the curves varied with the distance of the collector from the grid. The glow conditions were identical in each of the five cases represented in the figure, and only the position of the collector along the axis of the tube was altered. It is clear that the trend of the curves was the same at each distance, and only the magnitude of the currents was different. Though it is impossible to station the collector in the glow close to the tip, there is no reason to doubt that the nature of the data

* Langmuir, Phys. Rev. xxvi. p. 585 (1925).

would be exactly the same if they could be obtained practically all the way to the end. In other words, the interior of the glow throughout its length is at approximately the potential of the grid, and one section differs from the next only in the densities of electron and positive ion currents.

Fig. 4.

Current-Voltage Curves for Collector stationed at Different Distances along the same Glow.

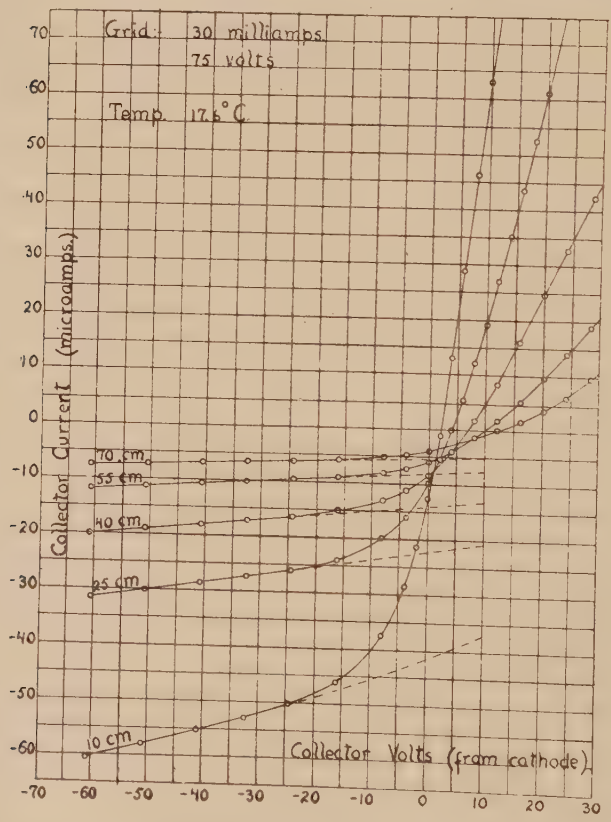

Theory of the Glow.

Length of Glow.—An explanation of how such a glow can extend to great lengths and how it can end in a sharp tip is furnished by the theory of positive ion sheaths which cover a negatively-charged surface in the path of a discharge. It is known that the wall of a glass tube enclosing a uniform glow is charged to a negative potential which is nearly as

high as the energy of those electrons which strike it with the highest velocities normal to its surface; the line of reasoning which leads to this knowledge is given in Langmuir's paper. In the case of these experiments, some knowledge of the value of this potential is obtained from curves such as those in fig. 4, for the potential at which the collector receives zero current is that which an *insulated* surface would have that stood normal to the path of the electrons streaming down the tube. Under the conditions of the experiment of fig. 4 this potential is seen to be in the range from +2·1 volts (with respect to the cathode) at 10 cm. to +12·5 volts at 70 cm.; in an experiment at lower vapour-pressure, made at 7·9° C., the range was from −4·8 volts at 10 cm. to −1·3 volts at 70 cm. Since the surface of the wall which actually encloses the glow is not normal but parallel to the electron stream from the cathode, its potentials must be somewhat less negative with respect to the glow than these, for experiments to be described later show that when the collector is turned so that it no longer faces the electron stream coming from the cathode, the electron current is decreased, whereas the positive ion current remains practically unchanged, so that zero current would not be reached on the current-voltage curve until the curve had arrived at higher positive potentials

Consider, now, what happens with a glow at the anode potential and a wall at only a little more than the cathode potential, so that the wall is negative with respect to the glow and therefore repels electrons from its neighbourhood but gathers positive ions. Throughout the length of the glow the wall thus becomes covered by a sheath of positive ions, and the whole drop in potential between the ionized gas and the wall becomes concentrated within this sheath. It has been pointed out that the thickness of the sheath is determined by the positive ion current density; with the current densities that prevail throughout the greater part of the length of a glow the sheath is not more than 2 or 3 mm. thick, and is often less than this, so that the field of the wall does not extend beyond a distance which is small compared with the tube diameter. Under these circumstances the entire core of the tube is a region of no electrostatic field. This is the region which the observer sees filled with luminous glow, and he also sees that it is separated from the walls by a dark space which is the sheath, unless it happens that the sheath is too thin to be visible.

An electron which is shot through the grid, and enters this core along a path that runs parallel to the axis, will travel

the entire length of the glow with unchanged velocity unless deflected from its path by a collision with a gas molecule or by a magnetic field. On the other hand, an electron which follows a path that makes an angle with the axis will be repelled by the wall as soon as it enters the positive ion sheath, and will be reflected back into the glow unless it possesses a radial velocity sufficient to enable it to penetrate against the retarding field and reach the wall. Thus, as long as electrons remain in the glow, the presence of the positive ion sheath screens them from the field of the wall and affords them a field-free region along which to travel, and when they attempt to leave the glow the field of the wall tends to drive them back into it again. Since both factors act to herd the electrons along the tube, the longitudinal velocities which they receive when they leave the cathode will carry them for long distances.

This state of affairs, however, cannot be maintained for more than a certain distance. For although the glow appears to the eye to be of uniform intensity throughout its length (except at the grid end of the tube, where the light from the filament is too bright to allow the intensity to be estimated), curves such as those in fig. 4 make it clear that there is a marked falling-off in the positive ion current density with increasing distance from the grid. With decreasing positive ion concentration the field of the wall extends farther into the tube, so that the core within which the field is neutralized becomes confined to a narrower region. In other words, the dark sheath becomes thicker, and the glow appears to the observer to have drawn away from the wall. In the limit, at a distance such that the positive ion concentration has fallen to such a low value that it no longer screens the electrons adequately from the field of the wall, this field brings the glow to an end ; for the wall beyond this distance then acts as a negatively-charged Faraday cylinder which prevents the electron stream from passing farther down the tube.

Shape of Tip.—On this theory, for a tube of a given diameter the end of the glow is fixed by the distance at which the positive ion concentration has fallen to a certain minimum value. The requirement that the concentration shall not be less than a certain value will also explain why the tip is a blunt-shaped surface and not a long, narrow point. With the glow in a steady state the rate at which ions arrive in any section of its length is equal to the rate at which they are removed. Ions arrive by the formation of new ions as a result of electron collisions and of radiation, and by

diffusion from a neighbouring section; they are removed by recombination with electrons, and by diffusion to the wall or to another section. The observed falling-off in ion concentration along the tube makes it clear that at the grid end of the tube the rate of formation of new ions and the rate of removal by diffusion are both high, whereas far from the grid these rates are both low. If in any region the rate of arrival of ions were to fall so low that it fell below the rate of removal, the glow could not maintain a steady concentration in that region. This is precisely what would happen in the case of a narrow pointed tip, for the formation of new ions takes place only in the path of the electron stream, and this path has been shown to be confined to the luminous core of the tube. Since the rate at which ions could diffuse outward through the surface of a long, narrow point is greater than the rate at which they could be formed within its volume, this shape is impossible for a steady state; a tip which assumed such a state momentarily must promptly "shut up" and take a shape that would meet the requirements of this state. Thus only a blunt-shaped surface is possible.

Experiment that Illustrates.—A picture of how the field in a tube is altered by the striking of a long glow was obtained accidentally with a tube that had a lime-coated Pt strip as a cathode. With a tube of this type the glow makes its appearance in two distinct stages: at voltages below the striking potential of the long glow there appears a luminous blue casing covering the wire of the grid and the grid supports. At low voltages the casing is less than 1 mm. thick, and can be clearly seen outlining the zigzag of the grid and following the nickel supports all the way to the point where they are sealed into the glass; at higher voltages it thickens and projects forward from the grid to a distance of 1 or 2 cm. It is imperceptible when it makes its first appearance at a voltage a little above the ionizing potential, and the accompanying current increase shows no discontinuity. But if, with the glow extending about 2 cm. in front of the grid, the voltage is raised still farther, the glow suddenly "breaks" and fills the entire tube with luminosity of the familiar type.

This short glow illustrates how the electron stream is confined to a short path unless it is able to produce enough ions to screen its path from the field of the wall. As long as the positive ion concentration remains insufficient to neutralize the electron space-charge at the cathode, only a comparatively small stream of electrons is emitted at low

voltages, and the charge on the walls prevents their escape down the tube. At potentials a little above 10·4 volts they acquire enough energy to ionize just before they reach any part of the grid or its supports, and so produce the luminous casing. But as soon as increased emission from the cathode can supply enough electrons to increase the ion concentration to an amount at which this can begin to neutralize the field of the wall, electrons are free to begin passing along the tube, and the higher electron current thus drawn from the cathode will in turn produce more positive ions so that an unstable state of affairs prevails : in other words, the glow breaks. This picture is borne out by observations on the different lengths to which the short glow can be extended before it breaks. The length increases with voltage since more electrons are emitted from the filament and they can produce more ions. But with the cathode as hot as is used in ordinary practice, the glow breaks before it reaches a length of 1 cm. To obtain the longest glows, about 4 cm. in length, the Pt strip must be at the lowest temperature at which it will function as a hot cathode ; the emission of electrons is then not sufficient to allow the glow to break until the voltage reaches a high value. This type of glow was never observed with a tungsten filament; and although the vastly greater brightness of this type of cathode makes it much less easy to observe a discharge in its immediate neighbourhood, it is felt with certainty that the glow does not appear, but that the long glow strikes at once with no intermediate stage. It would appear that the difference between the two cases lies in the shape of the cathode, since under the limiting action of space-charge more electrons could pass from a flat strip 1 mm. wide than from a 0·2 mm. filament, so that there would be enough electrons to excite this glow even before the space-charge was wholly neutralized.

Dependence on Current, Voltage, Pressure, and Tube Diameter.—An explanation of how the length of the glow varies with changing conditions, as illustrated in fig. 2, follows at once from the hypothesis that the glow requires more than a minimum concentration of positive ions to maintain itself, and that the tip marks the distance at which the concentration has fallen to this minimum, which will be called the "critical" concentration. With increasing emission from the cathode the number of electrons that are shot through the grid and escape down the tube will be greater, thereby increasing the positive ion concentration at every point, which in turn will allow the glow to extend farther before the concentration falls to the critical value. Raising

the grid voltage increases the velocity with which electrons leave the positive ion sheath at the cathode in all radial directions, and thus adds to the energy available for ionization, so that the result is again a longer glow. The dependence of length on mercury-vapour pressure exhibits the two balancing effects that one would expect—*i. e.*, the current density of electrons that can penetrate a distance through a gas at a given pressure, and the concentration of molecules available for ionization by these electrons. At high pressure the concentration of positive ions is high near the grid, but falls off rapidly with distance along the glow, due to the rapid falling-off in concentration of the electrons which produce the ions ; at low pressure, and with the same grid current and voltage, the ion concentration near the grid is lower, but decreases less rapidly with distance. This shows why the curves in fig. 2 (*b*) cross over, since at low pressure more voltage is required to maintain the critical positive ion concentration at a given *short* distance than is required at high pressure, whereas it is maintained at a given *long* distance more readily at low pressure. It is seen that the curve marked 13·0° C. has a slight curvature at the upper end, while the curve marked 8·1° C. is perfectly straight in this range ; apparently the third curve would cross the second at a little distance farther up, just as both have already crossed the first.

The actual magnitudes of the quantities plotted in fig. 2 are for a tube 3·4 cm. in diameter. In a larger tube the glow would extend farther in each case, for the volume of the glow per unit length would then be greater in proportion to the surface through which ions would be lost out of this volume by diffusion to the wall. It is noticeable that the glow will not readily enter constricted tubing, and was never observed to pass the point at which the lower tube 1·6 cm. in diameter joined the discharge-tube, although this was in a direct line with the discharge.

Positive Ion Current Data.—One would like to measure the critical positive ion current density that the glow requires. It may prove to be possible to determine this quantity by measuring the current densities with a collector somewhere near the tip, and extrapolating from these data. The currents received by the collector measure the number of positive ions that reach the surface of the sheath by virtue of their random motions in the discharge. Therefore the surface area of the sheath and the distribution of random motion of the ions must be known before the current density can be calculated. The area of the collector was 0·385 cm.^{2} in

these experiments, but the surface of the sheath was often two or three times that area.

Table I. gives positive ion current data taken from two widely different sets of experiments. They illustrate the effect of the balancing of electron current density against concentration of Hg molecules, for in the second set of data, at lower pressure than the first set, the positive ion currents are decreased near the grid and increased far away from it. All voltages given in the table are measured from the cathode.

Effect of a Magnetic Field.—In explaining that the tip of a glow cannot be a narrow point because positive ions could not be produced at a sufficiently rapid rate in an electron stream that is very narrow, it was assumed that electron impact is essential for this ionization, and that radiation alone is not sufficient. This assumption was the result of a demonstration by Mr. Stead of the effect of arbitrarily halting the electrons earlier in their course by means of an ordinary bar magnet. Sir J. J. Thomson * has tried the effect of stopping the stream of electrons into the side-arm of a cold cathode discharge-tube by means of a powerful electromagnet placed outside the tube, and finds that the glow extends along a side-arm 50 cm. long with a brightness which does not seem much affected by the magnetic field, although it is extinguished locally in a short layer opposite the magnet. But although this shows that in the intense high-voltage discharges of a cold cathode tube there is sufficient energy of radiation to maintain the glow in a region from which the electron stream has been debarred, there was every indication that this was not the case in the low voltage glows under discussion ; for it always happened that when an ordinary bar magnet was brought close to the tube, the glow contracted and could not be excited beyond the point opposite which the magnet was held.

If, however, a much weaker magnetic field is applied to the tube, such that the curved path along which the electrons are made to travel approaches the positive ion sheath which constitutes the boundary of the glow at an angle which is too small to enable the electrons to penetrate to the wall against the retarding field which they meet when they reach this boundary, Langmuir's theory shows that they will be specularly reflected back into the glow. In this case the magnetic field does not succeed in halting the passage of electrons down the tube, but only curves the path into a

* Thomson, Phil. Mag. xlviii. p. 1 (1924).

TABLE I.—Currents with Collector at Negative Potentials in Mercury Glows.

Disk Collector 0·70 cm. in diameter.

Temp. °C.	Grid Volts.	Grid Current (milliamps.).	Collector Volts.	Collector Current (microamps.).				
				10 cm.	25 cm.	40 cm.	55 cm.	70 cm.
17·6	60	30	−71·0	−63·0	−33·2	−21·0	−12·5	− 7·8
			−60·7	−60·5	−31·7	−20·0	−11·9	− 7·5
			−50·8	−58·0	−30·2	−19·0	−11·3	− 7·1
			−40 8	−55·2	−28·7	−18·0	−10·7	− 6·8
			−32·4	−53·0	−27·5	−17·2	−10·2	− 6·5
			−24·4	−50·2	−26·2	−16·3	− 9 7	− 6 1
			−16·2	−46·2	−24·0	−15·2	− 9·1	− 5·8
			− 8·0	−37·5	−20 0	−13·2	− 8·0	− 5·2
			− 4·0	−28·5	−16·0	−11·3	− 7·2	− 4·7
			0	−21·5	− 9 7	− 8·4	− 5·8	− 4·1
7·9	60	20	−71·0	−37·0	−27·1	−22·2	−17·3	−14·5
			−60·9	−35·3	−26·0	−21·2	−16·5	−13·8
			−50·8	−33·5	−24·7	−20·2	−15·7	−13·2
			−40·7	−30·9	−23·5	−19·1	−14·9	−12·5
			−32·4	−27·9	−22·1	−18·0	−14·1	−11·9
			−24·3	−23·5	−20 0	−16·7	−13·0	−11·0
			−16·2	−17·0	−16·2	−14·2	−11·0	− 9·5
			−12·0	−12·7	−12·7			
			− 8·0	− 7·2	− 7·7	− 8·5	− 6·2	− 6·1
			− 4·0	+ 2·0	0	− 2·7	− 2·1	− 3·0
			0	+17·0	+11·5	+ 6·2	+ 4·0	+ 1·7

series of arcs of a circle, the outline of the path traced out being that of a series of scallops with their cusps pointing toward the wall. The earth's magnetic field is an important instance of this effect. Calculation shows that the horizontal component of this field, of intensity approximately 0·185 gauss, is sufficient to bend the path of 60-volt electrons moving in a vertical direction into a path with radius of curvature 141 cm. This is by no means negligible in comparison with the dimensions of the tube. An electron that is shot into a glow 3 cm. in diameter, with a path that originally follows the axis, and is deflected at once along an arc of this radius of curvature, will meet the boundary of the glow at a distance of 20·5 cm., and, on the theory of specular reflexion at the boundary, will meet it again 41 cm. farther along the tube (distances being measured from the cathode and parallel to the axis). At each reflexion the path will make an angle of 8° 22′ with the boundary. The length of the path will be increased 0·3 per cent. over what it would have been if the electron had followed the axis.

Experiments were made which bear out the reasoning that the wall field causes electrons to continue streaming along the glow even in the presence of the earth's magnetic field, and that if their mean path is increased by being curved it is increased only very slightly. A tube 80 cm. long, which was evacuated by a charcoal tube with liquid air so that it could be moved about, was set in the direction of the earth's magnetic field, and was then set perpendicular to this direction, while the length of the glow was measured for different voltages. No difference could be detected between the two positions by this means. No attempt was made in taking any of the data in this paper to employ means to counteract the earth's field.

Experiments beyond the Glow.

The data plotted in fig. 3 and fig. 4 yield values for electron currents as the algebraic difference of total current and estimated positive ion current. But electron currents can be measured by themselves if the collector is stationed in the dark region beyond the glow. Current-voltage plots obtained with the collector 4 or 5 cm. beyond the tip show that with the collector at negative potentials the current was practically zero ; the values actually measured were of the order of 0·2 microamp., and may have been photoelectric currents. With decreasing negative potentials the current curve started upward from zero at precisely the same voltage at which curves taken with the collector *inside* a similar glow

had started to rise, but rose to not nearly such high values. The current varied exactly with the three-halves power of the voltage, if the voltage was measured from the potential at which the curve first began to rise. This current-voltage relationship was measured in one instance up to + 140 volts from the cathode. The glow, which in this instance was operating at 18 volts, appeared entirely unaffected by the presence of an electrode at 122 volts higher potential only 5·5 cm. away, which at this voltage was drawing 27·5 micro-amperes of electron current across the intervening space.

In these experiments the tip of the glow acts, in effect, as a nearly plane thermionic emitter, at a potential which is that of the grid, and at a very high temperature, since the electrons have suffered so wide a scattering of energy as they passed through the glow. However, when the ordinary space-charge equation for thermionic current between parallel planes is corrected for the initial velocities of electrons at a high temperature *, it gives a value for the current which is no longer exactly proportional to $V^{3/2}$. The relationship established by these data awaits further mathematical analysis.

Method of measuring Mean Free Paths.

A common method of measuring the mean free path of particles in a gas is to project the particles with equal velocity into the gas and determine the number of them which arrive per unit time at measured intervals along the path. Then, if N_0 is the initial number projected and N the number arriving at any distance d, the mean free path λ is given by

$$N = N_0 e^{-d/\lambda}.$$

The picture that has been given of the action taking place suggests that some of the electrons travel long distances down the tube without making a collision. It should therefore be possible, by making suitable assumptions with regard to the singling-out of electrons of the same velocity, to use data similar to those shown in fig. 4 to arrive at a value for the mean free path of electrons through ionized mercury vapour.

Experiments with Back Collector.—Before this could be done it was necessary to prove that the electrons to be dealt with actually came directly from the cathode, and were not simply drawn out of the concentration of electrons of random motion in the general glow. Langmuir describes

* Langmuir, Phys. Rev. xxi. p. 419 (1923).

an experiment using a disk-shaped collector mounted in a plane *parallel* to the direction of his electron beam, in which he finds that with the collector in this position the group of electrons of highest energy are absent from his current-curves, although other groups are present in exactly the same quantities as with the collector mounted in the usual plane, i. e. *vertical* to the path of the beam. He calls this group of electrons of highest energy "primary electrons," and defines them as being "those which reach the collector with a large part of the momentum which they acquired in passing through the positive ion sheath" around the cathode. They are the group which undergo scattering of energy. He concludes from his experiment that the primaries move mainly in one direction, while the other groups, which contain the vast majority of the electrons in the discharge, move mainly in all directions.

An adaptation of this idea was employed for the purposes of the present experiments, to find out whether the same distinction between primaries and other electrons holds at 60 cm. from the grid that Langmuir found at 3 or 4 cm. A collector was made from a nickel disk of the same diameter (0·7 cm.) as the one previously used, but completely reversed. with the insulated back toward the cathode ; a narrow tongue extending from the edge of the disk was bent back and fastened to the support wire, and then encased in glass. This collector will be called the "back collector," and the one used in all other experiments the "front collector."

The first data obtained with the back collector are illustrated by Curve A in fig. 5 (*a*). These were taken with the back collector used in exactly the same way that the front collector had been used. It was found that the primary current received at +10 volts was reduced to 28 per cent. and at +20 volts to 29 per cent. of what it had been with the front collector under exactly the same glow conditions, whereas the currents of electrons of low energy received near the glow potential, and the positive ion currents, were very nearly the same as before. Though this made it appear certain that the primary electrons were moving mainly in one direction, away from the cathode, the fact that 29 per cent. of the primaries still reached the collector was not wholly satisfactory to the argument. It seemed likely that, since the collector was only 18 cm. from the end of the tube, these might be electrons which had shot straight past the collector on their path *down* the tube, but were then turned back at the end of the tube since

there was no other electrode there to receive them, and returned to the collector.

Fig. 5.

Current-Voltage Plots for Different Collectors in the same Glow.

i_c is collector current.
Area of each collector 0·385 cm.²
Distance of each collector 60 cm.
Grid current 30 milliamperes.
Grid potential 75 volts.
Temp. 12·0° C.

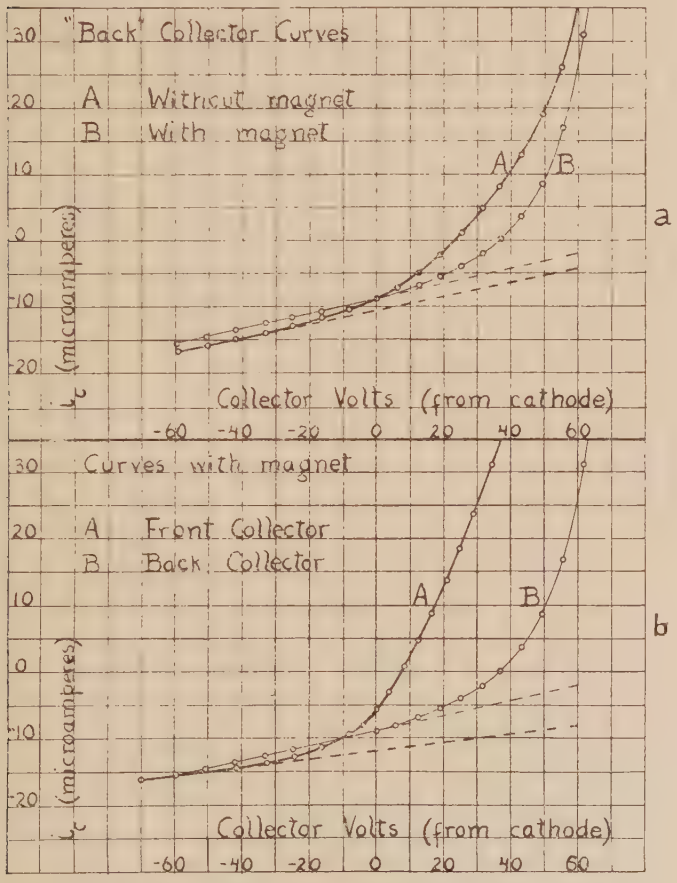

In order to test this theory an experiment was tried to see if it was possible to prevent their return by driving them into the walls with a small bar magnet outside the tube, held at a position 10 cm. *below* the collector. In this position it would not affect them until they had passed the collector ; and if their velocities were not in one direction,

it should affect them no more than it did the electrons of low energy which were known to have random velocities. Curve B in fig. 5 (*a*) shows the result of the experiment. The magnet was placed by trial in the position near the tube which gave the greatest current reduction ; the current is measured in each case by the difference between the solid and the dotted line. It is seen that the positive ion currents are not very different in the two cases, and above +50 volts the lower curve mounts rapidly toward the upper curve (they meet at +69 volts), showing that the currents of random electrons are the same; but the primary current has been reduced to one-fifth its previous value.

Curve B is plotted again in fig. 5 (*b*) for comparison with the curve of fig. 3, which was taken with the front collector under identical glow conditions. For the sake of comparison this second curve was taken with a magnet also, fixed in the same position ; as one would expect, a magnet lower than the collector had no effect upon the currents in this case. The curves show that the current is now reduced to 3·7 per cent. at +10 volts and 6 per cent. at +20 volts. A percentage increase above +10 volts does not necessarily mean that more *primary* electrons are reaching the collector, for Langmuir has shown that there is present in these discharges a small number of electrons of energy a little less than the primaries, which differ from the primaries in having random velocities. He calls these the "secondary electrons," and suggests that they result from collisions of primary electrons with gas molecules.

In addition to establishing the fact that the primary electrons which reach a collector at a distance of 60 cm. come from the direction of the cathode, these data give some knowledge of the sort of path which they may follow. It has been pointed out that an electron which takes a path making an angle with the axis is not thereby removed from the primary current stream unless the angle is wide enough to give the electron a radial velocity sufficient to enable it to reach the wall. If it approaches the boundary of the glow at an angle of only 45°, it must have twice the energy, and at an angle of 30° with the boundary it must have four times the energy that it would need in order to reach the wall at normal incidence. If it lacks this energy, it will be reflected from the boundary first on one side of the tube and then on another side, and will follow a zigzag path down the tube.

The Back Collector curve in fig. 5 (*b*) (Curve B) passes through zero current at +36·5 volts; in this experiment the potential of the glow was approximately 75 volts.

Therefore, even under the conditions of this experiment, which were most unfavourable for a collector surface, if insulated, to acquire a high negative charge, we find that when the collector became equivalent to an insulated surface, its negative potential with respect to the glow amounted to −38·5 volts. Only electrons with energies corresponding to 77 volts or more could reach it if they approached it at an angle of 45°. The relative numbers of these electrons present in the primary current appear from the Front Collector curve (A) in the same diagram; they are the currents received at −2 volts and higher negative voltages. Since actually the wall is in a better position than a back collector to receive electrons that will give it a negative charge, its retarding field will be at least as strong as the field in this illustration. Consequently, electrons with energies that correspond to a fall through the anode potential, or less, cannot reach the wall if they strike the glow boundary at an angle of less than 45° with the boundary surface. There is therefore a wide variety of zigzag paths that these electrons may travel. However, it follows from the same argument that the electrons which travel these paths will not contribute to the primary current that is measured at high retarding potentials, for a 75-volt electron that approaches a collector at an angle of 20° with the normal cannot move against a retarding field of more than 66·2 volts.

Assumptions with regard to Velocities.—Since it is now known that the electrons collected at "0 volts" come in nearly straight paths from the cathode, and since their high energy makes it improbable that they have lost any energy by inelastic collisions on the way, it only remains to question whether reasonable assumptions can be made with regard to singling out electrons of the same velocity, before proceeding to use measurements of primary electron currents to determine the electron mean free path. Langmuir concludes from his experiments on the scattering of primary electrons that the scattering must be due to a direct effect of the primary electrons themselves, and one which is confined to the region actually traversed by them. In addition, the extent of the scattering depends on the magnitude of the primary current; and if this current is small there is no scattering. With the primary current from a filament emitting 5 m.a. (milliamperes) at 50 volts, there was no effect of this kind greater than would be expected as a result of the initial velocities of the electrons and the voltage drop along the filament. Unfortunately the current-voltage

curves taken with a collector at long distances from the cathode do not allow the magnitude of the complete primary current to be distinguished readily from the rest of the electron current, since the curves rise smoothly through the cathode potential with no distinguishing humps in that region. But conjecture shows that the primary current must become very small at increasing distances from the cathode, and is probably never large beyond a distance of 20 cm. away; and, in addition, some of the primary current flows directly to the grid without ever passing down the tube. In this case all the scattering will take place near the cathode, where by far the greatest current density is concentrated; and although the actual grid current is higher than Langmuir's (*i. e.* 20 m.a. or 30 m.a. compared to the 5 m.a. quoted above), the primary current at a moderate distance from the cathode will be no greater in a 20-m.a. discharge than Langmuir measured close to his cathode in a 5-m.a. discharge. On this theory the primary electrons, after passing a distance of a few cms. beyond the grid, will proceed along the tube with unchanged energy until they meet with an inelastic collision. With this assumption it is possible to interpret the current received by the collector *at a given voltage* when the collector is placed at different distances along the tube, as corresponding to a group of electrons of the same axial velocity. Obviously, only voltages lying in the range where primary electrons are the only electrons collected are suitable for these measurements.

The mean free path λ, that will be calculated from the values of the primary electron current at measured intervals along the tube, will be the mean path between collisions measured in an axial direction; and if any of the electrons in this current follow a zigzag path, λ will need to be increased by a small factor to give the true mean length of path. To estimate the magnitude of this factor, it will be recalled that an electron which describes a zigzag inclined at 20° with the axis will need to have about 9 volts more energy than axial electrons (with 60 to 70 volts energy) in order to be included in the same group with them. Since the electrons that are measured are already near the limit of high energy, the number with that much additional energy is comparatively scant, and, moreover, the path difference at an angle of 20° is only 6·4 per cent., so the factor by which these will alter the average must be small. It may be roughly estimated to be not more than 3 per cent. The path increase caused by the earth's magnetic field has been shown to be negligible.

Similar reasoning shows that this method of measuring λ does not necessarily detect the occurrence of all collisions of electrons with gas molecules. An electron which loses energy, or which is deflected through a small angle without loss of energy, is thereby removed to a group of lower axial velocity. It will therefore be absent from the current measured at the voltage corresponding to the group to which it originally belonged, and its absence will lower the current unless its place is taken by an electron transferred by a similar mechanism from a group with higher axial velocity. Since the supply of electrons with higher energy is low, the chance that such a place will be filled is comparatively small. The chance that it will be filled by an inelastic collision is very much less than that it will be filled by an elastic collision deflecting through a small angle, since the axial velocity change involved is so much less in the latter case. Therefore λ obtained by a method which depends on measuring the fraction of electrons that are missing from a given group at successive intervals along a tube, can be interpreted as meaning fairly closely the mean path of electrons which make no collisions with gas molecules. Since the measurements may, however, include some electrons which have been deflected through very small angles by elastic collisions, the calculated values of λ may be somewhat too high to be accurate values of the mean free path which an electron will describe between collisions *of any kind* with gas molecules.

Data on Mean Free Paths.

The method of obtaining the data was to plot the current-voltage curves for a collector placed at five different distances along the axis of the tube, under identical glow conditions for each of the five curves, and then measure on the graph the electron currents at 0 volts, +5 volts, and +10 volts.

Since λ is given by

$$\lambda = \frac{x_2 - x_1}{\ln \frac{i_1}{i_2}},$$

the logarithm of the electron currents was plotted against the distance in the manner illustrated in fig. 6. The points lie along straight lines when plotted in this way, and the values of λ calculated from the slopes are marked on each diagram.

Fig. 6 (*a*) shows that the points corresponding to 0 volts, +5 volts, and +10 volts lie along lines which have the same slope. This seems to be a justification of the assumptions

Fig. 6.

Plots of Logarithm of Electron Current against Distance from Grid.

(*a*) For collector at three voltages in same glow at 12°·4 C.

(*b*) For collector at 0 volts (cathode voltage) in glows at four pressures of Hg vapour.

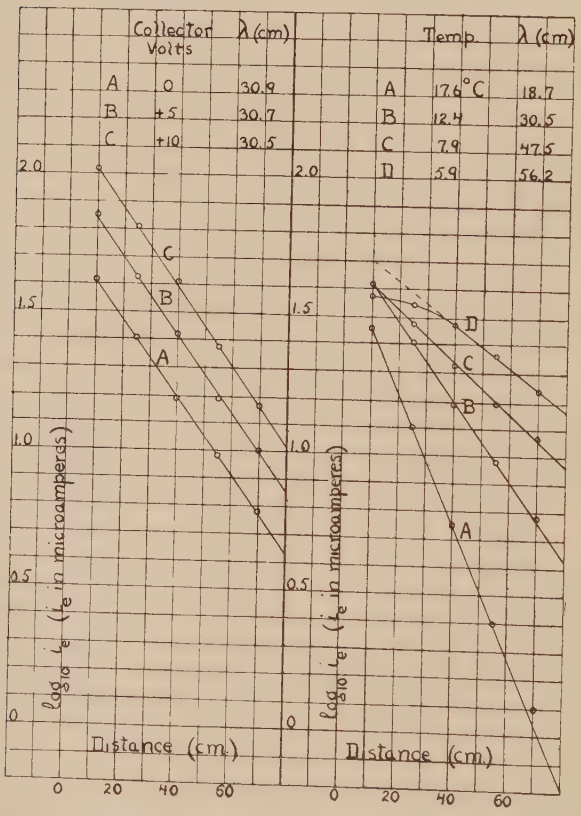

made with regard to scattering, since if the scattering process continued along the tube this relationship could hardly hold. The corresponding lines for each of the six sets of curves that were obtained show the three slopes equal in each case within 3 per cent. experimental error, except in the case of the curves at lowest pressure which will be described shortly.

Three sets of curves were taken at 12°·4 C. to determine

whether λ is affected by the intensity of ionization in the glow or by the voltage of the electrons. The values obtained are tabulated below.

TABLE II.

Grid current milliamps.	Grid volts.	$\lambda_{0\text{ volts}}$ cm.	$\lambda_{+5\text{ volts}}$ cm.	$\lambda_{+10\text{ volts}}$ cm.	λ. Mean.
20	60	30·5	30·8	31·4	30·9
20	80	30·0	30 0	29·7	29·9
30	60	30·9	30·7	30·5	30·7

The values of λ differ among themselves by no more than the experimental error, so that it may be definitely stated that within this range of voltage, and of ionization intensity, λ is determined only by the mercury-vapour pressure. This is in agreement with the observations of Ramsauer * and of Mayer † on other gases, who found that λ varied markedly with the voltage only for slow-speed electrons, corresponding to voltages from about 1 to 25 volts for argon. Experiments were not carried beyond the range given in Table II., as these showed that if changes in λ existed they could not be measured with any certainty without pushing conditions beyond the limit of what a tungsten filament will stand for the length of time required to take these runs. A feature which concerns only the theory of the mechanism of scattering appeared in these data, in the fact that the actual points obtained in the three different cases were so nearly the same that an attempt at plotting a graph of the three lines at 0 volts results in only a confused tangle.

The task of obtaining the curves at different pressures of mercury vapour was enormously facilitated by the knowledge that conditions in the glow, other than the pressure, were of no consequence; for the same glow conditions are not suited to measurements at all pressures, and at 17°·6 C. it was imperative to run the filament at 30 m.a. emission in order to obtain enough electrons to measure at the further end of the tube, whereas at 5°·9 C. this emission was too high. A curve from each set at different temperatures is shown in fig. 6 (*b*); the two at higher temperature were taken at 30 m.a., and the two at lower temperature at 20 m.a. grid current. All four were at 60 volts grid potential: this is the lowest value at which the glow can generally be forced

* Ramsauer, *Ann. d. Phys.* lxiv. p. 513 (1921), lxvi. p. 546 (1921), lxxii. p. 345 (1923).

† Mayer, *Ann. d. Phys.* lxiv. p. 451 (1921).

past a collector at 70 cm. distance so as to have the collector completely surrounded by the glow.

The four lines in fig. 6 (*b*) all correspond to a collector at 0 volts ; that is, connected directly to the negative end of the cathode. The three at higher temperatures are straight, with slopes corresponding to the pressure of saturated mercury vapour at these temperatures ; the line at 5°·9 C. curves toward lower values at the upper end. This is taken to mean that when this pressure is reached the primary current has increased to such a value that scattering is not completed close to the filament, but continues for some distance along the tube. This would have the effect of scattering more electrons into the class with velocities corresponding to 0 volts by the time the beam had travelled part way down the tube, than there were in this class when the beam passed a collector stationed at 10 cm. from the grid ; and the curve indicates that this may be just what takes place. Although a change of 2°·0 C. seems small to allow this effect to make its appearance between 7°·9 C. and 5° 9 C., the plots show that a considerable increase in primary current has been able to take place in just this range.

Values of λ *compared with Pressure of Mercury Vapour.*

Table III. gives the values of λ determined in the manner that has been described, with the corresponding pressures of mercury vapour, for the four temperatures that were investigated. The mercury-vapour pressures were calculated from Knudsen's * equation :

$$\log p = 10{\cdot}5724 - 0{\cdot}847 \log \mathrm{T} - \frac{3342{\cdot}26}{\mathrm{T}},$$

where p is measured in mm. of Hg. The majority of the determinations of mercury-vapour pressure at low temperatures made by Knudsen and other experimenters agree fairly closely with this formula. λ is in each case the mean of the values obtained at the three different collector potentials.

Table III.

Temp.	λ.	Pressure.	$p\lambda$.
5·9° C.	56·2 cm.	0·000329 mm.	0·0185
7·9	47·5	·000398	·0189
12·4	30·5	·000605	·0185
17·6	18·7	·000966	·0181

The fourth column shows that the product $p\lambda$ is nearly

* Knudsen, *Ann. d. Phys.* xxix. p. 179 (1909).

constant. From the mean value of $p\lambda$ we obtain a value for λ of 18·5 cm. at 0·001 mm. pressure. The estimated correction of 3 per cent. for zigzag paths would raise this λ to 19·1 cm.

The writer wishes to express her thanks to Sir Ernest Rutherford for his interest in this work, and to Mr. Stead, who set her to investigate the properties of long glows and gave her constantly the benefit of his experience. She is also indebted to Dr. Langmuir for important criticisms and suggestions in the course of writing this paper.

XV. *On the Explanation of Spectra of Metals of Group II.* —Part II.

By P. K. Kichlu *and* M. Saha, *D.Sc., F.R.S., University of Allahabad, Allahabad (India)**.

IN a previous paper one of us † has discussed the origin of the higher Rydberg sequence terms in the normal spectra of elements of group II. It is well known that besides these normal terms all these elements give a number of anomalous terms. They were noticed by Rydberg ‡ in 1894 in the spectra of Ca and Sr, and Popow § discovered similar groups in the spectra of Ba and Al in 1915. In 1921, Götze ‖ interpreted these groups as a transition between the normal p-group and another group which he called p' (sometimes also called $\bar{p}$, which notation we shall follow. That the $\bar{p}$-group was essentially of the same nature as the ordinary p was made clear from investigation of the Zeeman effect of these groups.

Since this time numerous groups of dashed (or barred) terms have been discovered in the spectra of elements of higher groups ; but the first indication of the origin of these terms was given by Russell and Saunders ¶, and independently by Wentzel **. Russell and Saunders discovered other groups of $p\bar{p}$ and $d\bar{d}$ combinations in spectra of Ca, Sr, and Ba. These $\bar{p}$ and $\bar{d}$ terms are sometimes negative, and the above-

* Communicated by the Authors.
† M. N. Saha, Phil. Mag., June 1927.
‡ Rydberg, *Wied. Ann.* lii. p. 119 (1891).
§ Popow, *Ann. der Physik*, Bd. xlv. p. 147 (1914).
‖ Götze, *Ann. der Physik*, Bd. lxvi. p. 285 (1921).
¶ Russell and Saunders, Astrophysical Journal, lxi. p. 38 (1925).
** Wentzel, *Phys. Zeits.* xxiv. p. 106 (1923) ; xxv. p. 182 (1924).

mentioned authors noted that if a certain number was added to these terms they formed approximately a Rydberg sequence. This number was approximately 13700 in the case of Ca, which is about the same as the difference between the values of the fundamental ^2S-term of Ca^+ and the next term in order of value, viz. ^2D. From this fact the above-mentioned authors concluded that the anomalous terms arise when the stationary electron of Ca is in the metastable M_3-level.

In this investigation it will be shown that the conclusion of these authors regarding the origin of $\bar{p}$-terms is correct in the case of Ca, Sr, and Ba; but from this it is not safe to draw any general conclusion regarding the nature of the dashed terms. As was pointed out in the note on the spectrum of Neon* by the senior author, whenever from any particular distribution of electrons in potential orbits F, D, P terms simultaneously arise, they must then have the same combinatory powers, so that if F and P are treated like ordinary terms, D must be dashed. But we can also dash F and P and treat D as an undashed term. It is purely a matter of convention, in which we have to be guided by our previous knowledge of the history of the spectrum of the element.

Origin of $P\bar{P}$-*Terms in the Spectrum of* Mg, Zn, Cd, *etc.*

As Bowen † and Millikan have pointed out, $P\bar{P}$-terms are known in the spectra of Mg, Zn, and Cd, for which the metastable level of the ionized element is not ^2D, but ^2P. Bowen and Millikan, by their hot-spark method, were able to discover $P\bar{P}$ groups in the spectra of Be, B^+, C^{++}, N^{+++}, O^{++++}, and in Al^+, Si^{++}, P^{+++}, S^{++++}, Cl^{+++++}, which have got a structure similar to that of Mg. They discovered the most interesting laws regarding the values of these $P\bar{P}$-groups, and showed theoretically as well as experimentally that the values of these $P\bar{P}$-groups were approximately the same as the value of the fundamental line ($^1S - {}^1P$) of these elements. Sawyer and Beese, in a note to 'Nature' of Dec. 26, 1925, however, find that in the case of Zn and Cd the values of $P\bar{P}$-groups are the mean between the values of (^1S—^1P) of the normal element and ^2S—^2P of the ionized element. We shall not dwell upon Bowen and Millikan's explanation of

* M. Saha, Phil. Mag.

† Millikan and Bowen, Phys. Rev. xxv. p. 150 (1925).

the origin of these terms at this place, as this will come out later on in the course of discussion.

All these facts, and the other details discovered by Russell and Saunders in the spectra of Ca, Sr, and Ba, receive a unitary explanation on the lines suggested in the former paper of the senior author* and in the note on the spectrum of Neon. We shall begin by writing down the structure diagram for Mg and Ca.

Structure Diagram for Mg (12).

K_1 2						
	L_1 2	L_2 6				
		M_1 2	M_2	M_3		
			N_1	N_2	N_3	N_4
				O_1	O_2	O_3

Structure Diagram for Ca (20)

K_1 2						
	L_1 2	L_2 6				
		M_1 2	M_2 6	M_3		
			N_1 2	N_2	N_3	N_4

The normal state of Mg is obtained by keeping both the electrons in M_1; in the case of Ca, both in N_1. For transitions to higher levels, one electron has to be kept at M_1 for Mg, and at N_1 for Ca; the other electron has to be successively shifted to all positions on the right. Terms arising from levels on the same vertical column will have approximately the same scale of values, while they will decrease progressively as we pass to further columns on the right. It is emphasized at this point that we assign the total quantum number 1 to those terms which have their origin in the undisturbed outermost level. Thus the term arising from the combination M_1 M_1, viz. $^1S_0$, has the total quantum number 1. As the electron is shifted to successive levels on the right, the total quantum number increases by one at each step. This method of fixing up the total quantum number for optical terms is evidently

* M. N. Saha, Phil. Mag. June 1927 and "Note on the Spectrum of Neon" (Phil. Mag. July 1927, p. 223).

more appropriate for expressing actual facts than Bohr's representation of terms by 3S (for Mg, M_{II}), 4S (for Ca, same as N_{II}), etc., though the latter method of representation has the merit of giving a unitary representation to the X-ray levels as well as optical levels.

The normal terms of Mg are therefore due to combinations :

(*a*) $M_1 M_1$ (both the electrons in M_1) giving $^1S_0$ only, as first pointed out by Pauli *.

$M_1 N_1$, $M_1 O_1$, $M_1 P_1$, ... will give higher Rydberg sequences of $^1S_0$-term, and a sequence of $^3S_1$-terms beginning with $2\,^3S_1$ (from $M_1 N_1$ in the case of Mg).

(*b*) $M_1 M_2$ (one electron is in M_1, the running electron is in M_2).

Terms obtained : ^1P, ^3P.

$M_1 N_1$, $M_1 O_2$, $M_1 P_2$, ... give higher Rydberg sequence terms to this set of singlet and triplet P's. The P-sequence begins with the total quantum number 2.

(*c*) $M_1 M_3$ (the running electron in M_3).

Terms obtained : ^1D, ^3D.

$M_1 N_3$, $M_1 O_3$, $M_1 P_3$, ... give the Rydberg sequence. The D-sequence will begin with the total quantum number 3.

In the case of Ca,

(*a*) $N_1 N_1$ ... give us $^1S_0$, and
$N_1 O_1$, $N_1 P_1$, ... give us the ^1S and ^3S series.

(*b*) $N_1 N_2$ give us the first ^1P and ^3P terms, and
$N_1 O_2$, $N_1 P_2$ the higher ^1P and ^3P Rydberg terms.

In the (*c*) combination the first combination is $N_1 M_3$, and not $N_1 N_3$. As the M_3-level has at least the same order of value as N_2, $N_1 M_3$ will give us ^1D and ^3D terms of the same order of value as the first ^1P and ^3P terms. This explains the occurrence of large D-terms in the spectrum of Ca, and *mutatis mutandis* in Sr and Ba. Thus in Ca, Sr, and Ba the D-sequence will begin with 2, and not with 3 as in Mg.

If we write out the structure diagrams for Zn and Cd, we see that the normal spectrum will be exactly like that of Mg. No D-terms comparable in value to the first P-terms will occur, and the sequence will begin with the total quantum number $n=3$.

* W. Pauli, Jun., *Zs. für Physik*, Bd. xxxi. p. 765 (1925).

Structure Diagram for Zn (30).

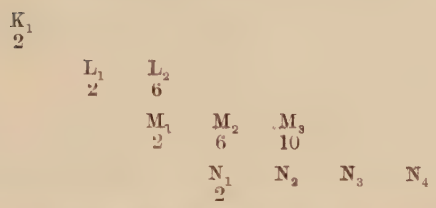

(Both electrons are in N_1. The next transition is horizontally from N_1 to N_2. M_3 is completely filled.) A number of anomalous terms is possible from the combination $9M_3 . 2N_1 N_2$, giving ^3F, $^3\bar{D}$, ^3P, $^1\bar{F}$, ^1D, ^1P, but it is not yet known whether they exist.

Structure Diagram for Cd (48).

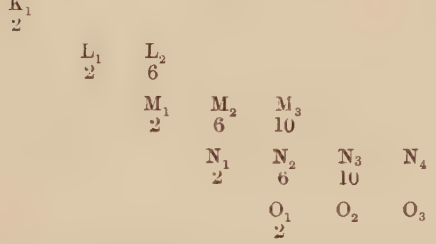

(In normal case other electrons are in O_1. Transition is horizontally from O_1 to O_2, giving $O_1 O_2$ as the next state. N_3 is completely filled up. Here also the $9N_3 . 2O_1 O_2$ combination is possible.)

In order to account for the anomalous terms, let us put one electron permanently in the next higher level and move the second electron through the next successive levels. In the case of Mg, Zn, and Cd there is no metastable level diagonally across the fundamental level. Thus, taking the case of Mg, the level M_1 will be kept entirely empty: one electron will be kept permanently at M_2, the second electron will be moved successively through the $M_2, M_3, N_1, N_2, N_3, \ldots$ levels. In Ca, however, the level next to the fundamental is M_3, so that the fixed electron will be always at M_3, and the running electron will move through the other possible levels, viz. $N_1, M_3, N_2, \ldots$. *For this reason the large* D*-terms which arise from the combination* $M_3 N_1$ *may be considered as the first of the anomalous terms in* Ca.

Anomalous Terms in Mg, Zn, Cd.

Let us now find out, by applying the combination rules of Pauli, Heisenberg, and Hund, the probable anomalous terms in the spectra of Mg, Zn, and Cd.

(*a*) $M_2 M_2$ give ${}^3\bar{P}_{0,1,2}$, ${}^1D_2$, ${}^1S_0$.

The P's will be dashed, because $M_1 M_2$ give us ${}^3P_{0,1,2}$, and transition is possible between $(M_1 M_2)$ and $(M_2 M_2)$.

Value of ${}^3\bar{P}_{0,1,2}$.

Let us consider the relative values of the following sequences for Mg :—

$M_1 M_2$	$M_1 N_2$	$M_1 O_2$	$M_1 P_2$	$M_1 Q_2$
$1\,{}^3P$	$2\,{}^3P$	$3\,{}^3P$	$4\,{}^3P$	$5\,{}^3P$
$M_2 M_2$	$M_2 N_2$	$M_2 O_2$	$M_2 P_2$	$M_2 Q_2$
$1\,{}^3\bar{P}$	$2\,{}^3\bar{P}$	$3\,{}^3\bar{P}$	$4\,{}^3\bar{P}$	$5\,{}^3P$

Taking corresponding pairs of higher Rydberg terms, say $5\,{}^3P$ and $5\,{}^3\bar{P}$, we find that the second electron is in both cases far out. The atomic residue will therefore exert, on the inner of the two valence electrons, approximately the same force in both cases. In other words, we can write symbolically

$$(5\,{}^3P \rightarrow 5\,{}^3\bar{P}) = (M_1 Q_2) \rightarrow (M_2 Q_2)$$
$$= (M_1 \rightarrow M_2)\, Q_2.$$

The symbol in the last step denotes that the energy of the electron in the Q_2 position has the same value in both cases because it is far out, hence $5\,{}^3P - 5\,{}^3P = (M_1 \rightarrow M_2)$ of the atomic residue. This atomic residue is, however, the Mg^+ electron, M_1 corresponds to the fundamental ${}^2S$ of Mg^+, and M_2 corresponds to the ${}^2P$ of Mg^+. We therefore arrive at the rule that for the higher terms

$$({}^3P - {}^3\bar{P}) \text{ of Mg} = ({}^2S - {}^2P) \text{ of } Mg^+.$$

When we pass on, however, to the lower terms like $2\,{}^3P - 2\,{}^3\bar{P}$, the influence of the atomic residue on the running electron can no longer be regarded as the same in both cases. Hence the above rule will not hold so well. Taking

$$1\,{}^3P - 1\,{}^3\bar{P} = (M_1 M_2 - M_2 M_2),$$

we find that the transition is obtained by moving one

electron from M_1 to M_2, the other electron always remaining at M_2, *i.e.*,

M_1	M_2	
1	1 . . .	^3P
→	1,1 . . .	$^3\overline{P}$.

The difference in energy may be assumed to be approximately the same as is required in the passage of the electron from $M_1 \rightarrow M_2$ from the $M_1 M_1$-stage :

M_1	M_2	
1,1	. . .	$^1S_0$
→	1 . . .	$^3P, ^1P$,

the difference being that in the first case the transition is with the stationary electron at M_2, in the second case it is with the stationary electron at M_1. Hence

$1\,^3P - 1\,^3\overline{P}$ is $> {}^1S - {}^1P$ of the metal . . . . (A)

and $< {}^2S - {}^2P$ of the ionized metal . (B)

Rule (A) is given (with = instead of >) by Bowen and Millikan *, whose arguments are almost the same as that given here : rule (B) is given by Sawyer and Beese, who make $^3P - ^3\overline{P}$ equal to the mean value of

$$(^1S - ^1P) \text{ of } M \quad \text{and} \quad (^2S - ^2P) \text{ of } M^+$$

for Zn and Cd. The validity of the above rules will be apparent from the following table :—

TABLE I.

Element.	Value of $P - \overline{P}$.	$^1S - {}^1P$ of M.	$^2S - {}^2P$ of M^+.
Mg	35982	35051	35669
Zn	47894	46745	48482
Cd	44088	43692	44135
Hg	?	54099	?
Al^+	56690	59845	53918
Si^{++}	76986	82878	71280
P^{+++}	97037	105190	88649
S^{++++}	116985	127144	105866
Cl^{+++++}	136928	148949	123001

The figures in Table I., as well as theoretical arguments, show that Sawyer and Beese's rule represents facts more accurately than Millikan and Bowen's rule. The $^1D_2$, and $^1S_0$-terms expected from $M_2 M_2$-combination has also been recently obtained by one of us in Mg.

* Bowen and Millikan, Phys. Rev. vol. xxv. p. 150 (1925).

Higher negative terms may be obtained by keeping the first electron at M_2, and allowing the other electron to run through the higher levels M_3.... Though they are not yet known, one typical example may be given :—

Combination $M_2\,M_3$ will give us

$$^3F \quad ^3\overline{D} \quad ^3P$$
$$^1F \quad ^1D \quad ^1P.$$

^3F will have the highest (*i. e.* lowest negative) value. They may be expected to have the value ^1D of Mg -35000, *i. e.* about -20000 for Mg. If they exist, they will combine with the ^1D, ^3D terms of Mg.

Origin of Anomalous Terms in Ca, Sr, *and* Ba.

Bowen and Millikan have pointed out that P $\overline{P}$-multiplets of the above description have not yet been discovered in the spectra of Ca, Sr, and Ba. The fact receives a clear explanation when we look at the structure diagrams of these elements.

Structure Diagram for Sr (38).

2 K				
8 L				
18 M				
	N_1 2	N_2 6	N_3	N_4
		O_1 2	O_2	O_3

(Normal terms are obtained by keeping one electron permanently at O_1 and allowing the other to run through O_1, O_2, N_3.... ; for anomalous terms, keep the electron at N_3 and let the other run through the levels O_1, N_3, O_2, etc.)

Structure Diagram for Ba (56).

2 K				
8 L				
18 M				
	N_1 2	N_2 6	N_3 10	N_4
		O_1 2	O_2 6	O_3
			P_1 2	P_2

(To get the normal terms, one of the two electrons is placed at P_1 and the other moves through P_1, N_4, O_3, P_2..... The N_1P_4 combination, which is expected to give a large ^1F and ^3F term, is not yet known with certainty.)

For Ca M_3 is the level next in value to N_1, and we keep the first electron in this level. The anomalous terms are then obtained by allowing the other electron to run through the other possible levels. We get the following combinations :—

(*a*) $M_3 M_3$.

Since both electrons are in M_3-orbit (Pauli's rule will apply), we obtain :

$$^3\overline{F},\ ^3\overline{P},\ ^1G_4,\ ^1D_2,\ ^1S_0.$$

State $(N_1 M_3)$ giving ^3D, ^1D will not combine with $M_3 M_3$, because $N_1 \rightarrow M_3$ is forbidden. Hence the D-terms arising from this combination will be of the same nature as the D-terms from $M_3 M_3$, *i. e.* they are not dashed. This enables us to fix the nature of the other terms. $M_3 N_3$, $M_3 O_3$.... will give us the higher members of the group :

$$\left|\begin{array}{ccccc} ^3G & ^3\overline{F} & ^3D & ^3\overline{P} & ^3S \\ ^1G & ^1\overline{F} & ^1D & ^1\overline{P} & ^1S \end{array}\right|.$$

(*b*) $M_3 N_2$.

This combination gives us

$$\begin{array}{ccc} 2\,^3F & 2\,^3\overline{D} & 2\,^3P \\ 2\,^1F & 2\,^1\overline{D} & 2\,^1P. \end{array}$$

$M_3 O_2$, $M_3 P_2$..... gives the higher members of the sequence.

(*c*) $M_3 O_1$.

This combination give us

$$3\,^3D,\quad 3\,^1D.$$

These terms will form higher Rydberg sequence of displaced type with the large ^3D and ^1D. Evidence of their existence has been obtained in the spectrum of Ba. For reasons stated before

$$1\,^3\overline{D} \text{ of Ca} = 1\,^3P \text{ of Ca} + (^1S - ^3D) \text{ of Ca} \quad . \quad . \quad (A)$$

$$\text{or} \qquad + (^1S - ^1D) \text{ of Ca} \quad . \quad . \quad (B)$$

Relation (A) will be approximately correct, but (B) indicates only an upper limit. The same argument will hold for Sr and Ba. The values of $^2S_1 - ^2D_3$ for Ca^+, Sr^+ and Ba^+,

and $^1S_1 - {}^3D_2$ and $^1S_1 - {}^1D_2$ for Ca, Sr and Ba are shown below :—

TABLE II.

	M.		M^+.
	$(^1S - {}^3D_2)$.	$(^1S - {}^1D_2)$.	$^2S_1 - {}^2D_2$.
Ca	20350	21850	13650
Sr	18219	20149	14557
Ba	9215	11395	4884

M = neutral element ; M^+ = ionized atom of the element.

TABLE III.

State.	Present notation.	Russell & Saunders' notation.	Term values.					
			Ca.		Sr.		Ba.	
(*a*) $M_3 M_3$	$^3\overline{F}_{4,3,2}$	...	.....		.....		19077·9 19510·1 19990·3	432·2 480·2
	$^3\overline{P}_{2,1,0}$	p'	10753·0 10839·8 10887·1	86·8 47·3	10250·7 10525·5 10731·8	247·8 206·3	18110·5 18549·3 18820·3	438·8 271·0
	$^1S_0$							
	$^1D_2$	X	8584·9		8964·9		9929·0	
	$^1G_4$							
(*b*) $M_3 N_2$	$^3F_{4,3,2}$	f''	13407·6 13485·9 13573·9	78·3 88·0	12006·0 12335·7 12658·5	329·7 322 8	18372·6 19082 1 19964 8	709·5 882 7
	$^3D_{3,2,1}$	d'	11045·3 11085·3 11112·0	40·0 26·7	9365·9 9543·4 9661·1	177·5 117·8	17049·8 17498·1 17837·6	448·3 339·5
	$^3P_{2,1,0}$	p''	9964·3 9969·1 9971·0	4·8 1·9	8588·5 8622·2 8633·0	33·7 10·8	16073·1 16325·5 16387·5	252·4 62 0
	$^1F_3$	Y	8767·0		9836·1		15213 4	
	$^1\overline{D}_2$							
	$^1P_1$		.....		.....		13475·2 *	
(*c*) $M_3 O_1$	$^3D_{3,2,1}$							
	$^1D_2$		.....		.....		4526 †	

* Identified by Russell and Saunders, *loc. cit.*

† We have for Ba, $^3\overline{D}_{3,2} - 4526 = 12523{\cdot}18$ (1), 12972·3 (8 *u*) ;
b $^3F - 4526 = 14556$ (6*r*).

In Barium we have followed Paschen's * identification of the D-term. According to Fowler † $^2S - ^2D$ for $Ba^+ = 11990$.

A preliminary comparision with the new terms obtained by Russell and Saunders shows that the above conclusions are well verified. The detailed identification is shown in Table III.

Table III. shows that Russell and Saunders' f'', p'', and d' terms can be identified with the ^3F, ^3P, and ^3D terms arising from the $M_3 N_2$ combination. In fact they observe that f'' and p'' are in all respects like ordinary f and p terms. They also follow the usual rule which has been brought to light by Hund ‡ and others, that when from the same combination F, D, and P terms arise, F is usually > D > P.

A number of singlet terms have been mentioned by Russell and Saunders, but their nature has not yet been clearly elucidated. We have therefore refrained from trying to identify them with singlet terms $^1F_3$, $^1D_2$, $^1P_1$. But in the case of Ca, we can hazard the identification mentioned in Table III. Of these, $Y = {}^1F_3$ seems to be pretty certain. X may be put $= {}^1D_2$, but it seems to be very difficult to fix up the nature of the "x." Back § finds from Zeeman-effect data that "x" is not a singlet term, but a triplet term, $^3F_2$. He has also given $^3F_3$, $^3F_4$. But he finds that the splitting factor g for Zeeman effect is different ($\frac{3}{4}$) in the case of $^3F_2$ from the value of g given by Landé's formula ($\frac{2}{3}$), and sees in this a justification of Landé's "Verzweigungs-prinzip." The nature of the large term W, or of Z also, cannot be fixed up from the present data. It may be added that Russell and Saunders have taken only those lines which are given by King from his furnace-spectra data. If the full list of arc lines is taken from Kayser and Konen's '*Handbuch der Spektroskopie*,' vol. vii., it is found that there are many lines yet to be classified.

Values of the Terms.

The identification is rendered more probable from the following theoretical considerations about their values :—

It will be seen that the Barium values of anomalous terms are much larger than Ca or Sr values. Further, the terms arising from $M_3 N_2$ combination have the same order of value as those arising from $M_3 N_3$ combination. Let us consider

* Paschen and Götze, 'Serienspektren,' Chap. on Barium.
† A. Fowler, 'Series in Line-Spectra, p. 137 (1922).
‡ F. Hund, *Zs. für Physik*, Bd. xxxiii. p. 841 (1925).
§ Back, *Zs. für Physik*, Bd. xxxiii. p. 584.

the sequence of terms arising from the following pairs of combinations :—

$M_3 N_2$	$M_3 O_2$	$M_3 P_2$	$M_3 Q_2$	$M_3 R_2$
$^1\bar{D}, ^3\bar{D}$	$2\,^1\bar{D}, 2\,^3\bar{D}$	$3\,^1\bar{D}, 3\,^3\bar{D}$	$4\,^1\bar{D}, 4\,\bar{D}$	$5\,^1D, 5\,^3\bar{D}$
$N_1 N_2$	$N_1 O_2$	$N_1 P_2$	$N_1 Q_2$	$N_1 R_2$
$^1P, ^3P$	$2\,^1P, 2\,^3P$	$3\,^1P, 3\,^3P$	$4\,^1P, 4\,^3P$	$5\,^1P, 5\,^3P$.

Of the set of terms arising from $M_3 X_2$ ..... we have taken only the D's. Compare the values of each corresponding pair in each vertical column.

Now,

$$M_3 R_2 \rightarrow N_1 R_2 = (M_3 \rightarrow N_1) R_2$$
$$= (M_3 - N_1) \text{ of } Ca^+ \text{ approximately}$$
$$= (^2S - ^2D) \text{ of } Ca^+.$$
$$\therefore 5\,^3\bar{D} \text{ of } Ca = 5\,^3P \text{ of } Ca - (^2S - ^2D) \text{ of } Ca^+. \quad . \quad . \quad . \quad . \quad (A)$$

The value of $^3\bar{D}$ and other terms like $f''(b^3F)$ arising from this level will therefore lie between the limits:

	$^3p_2-(^1S-^2D)$	$^3p_2-(^2S-^2D)$	Actual values. f''.	$^3\bar{D}$.
For Ca	12139	20338	13485	11085
Sr.....	10888	16480	12335	9543
Ba	17120	23631	19082	17498

$1\,^3\bar{D}$ values are thus seen to be slightly lower than the lower limit, and $b1^3F$ values higher than the lower limit. Higher Rydberg terms to the above set have not yet been obtained in sufficient number to enable us to make a satisfactory comparison and to see whether a member like

$$5\,^3\bar{D} = 5\,^3P - (^2S - ^2D) \text{ of } M^+$$

also follows the expected order.

Values of Terms arising from $M_3 M_3$*-levels.*

Compare, as before, the set of values arising from the combinations :

$M_3 M_3$	$M_3 N_3$	$M_3 O_3$	$M_3 P_3$	$M_3 Q_3$
$^1P\,^3P$	$2\,^1P, 2\,^3P$	$3\,^1\bar{P}, 3\,^3\bar{P}$	$4\,^1\bar{P}, 4\,^3\bar{P}$	$5\,^1\bar{P}, 5\,^3\bar{P}$
$N_1 M_3$	$N_1 N_3$	$N_1 O_3$	$N_1 P_3$	$N_1 Q_3$
$^1D, ^3D$	$2\,^1D, 2\,^3D$	$3\,^1D, 3\,^3D$	$4\,^1D, 4\,^3D$	$5\,^1D, 5\,^3D$

By the same argument as before the values of the higher terms like $5\,{}^3\bar{P}$ will approximately be equal to

$$5\,{}^3D-({}^2S-{}^2D) \text{ of } M^+,$$

while the value of $1\,{}^3\bar{P}$ will be between $1\,{}^3D-({}^1S-{}^1D)$ of M and $1\,{}^3D-({}^2S-{}^2D)$ of M^+. The following table shows the expected values of ${}^4\bar{P}$ compared to the limits calculated as above:—

	Limits.	${}^3\bar{P}$.
Ca.....	7106–15666	10839
Sr	7567–13159	10525
Ba.....	21419–27930	18549

The value of ${}^3\bar{P}$ in the case of Ca and Sr is approximately the mean of the limits. But the Ba value of ${}^3P$ is less than even the lower limit.

The above comparison explains a feature of the Barium spectrum. The anomalous terms are much larger than the corresponding terms in Ca and Sr. It is easily seen that it is due to the smaller value of the shift numbers ${}^1S-{}^1D$ and ${}^2S-{}^2D$ in the case of Ba. The value of the terms arising from X_3Y_2 and X_3X_3-levels are of the same order, since ${}^2P$ and ${}^3D$ terms have the same order of value. In Barium ${}^3D$ is much larger than ${}^3P$, and we therefore find that the terms arising from X_3X_3 are much larger than the terms arising from X_2Y_3.

The Rydberg Sequence of Anomalous Terms.

Rydberg sequence has been established satisfactorily up to the fifth term only in the case of Ca ${}^3\bar{P}$ terms. The comparison of values is given below :—

	$1\,{}^3\bar{P}$.	$2\,{}^3\bar{P}$.	$3\,{}^3\bar{P}$.	$4\,{}^3\bar{P}$.	$5\,{}^3\bar{P}$.
	10840	767	−4983	−8313	−10063
${}^3D-({}^2S-{}^2D)$	15306	−2097	−7090	−9359	−10649
${}^3D-({}^1S-{}^2D)$	7106				

Russell and Saunders find that if 13711 $({}^2S-{}^2D)$ be added to the sequence of ${}^3P$ terms, they form approximately a Rydberg sequence.

Existence of ${}^3\bar{F}$-terms.

The most important group of terms from the combination $M_2\,M_3$ is ${}^3\bar{F}$, which is expected to be larger than ${}^3\bar{P}$, identified with certainty with Russell and Saunders' p'. But these

terms have not yet been identified. The cause is to be traced to its combinatory properties. It can combine with

$$^3F \quad ^1F \quad ^3\overline{D} \quad ^1\overline{D}$$

arising from combination $(M_3\,M_2)$, and with the triplet F of the normal spectrum and also with the $N_1\,N_2$ terms (Ca). But the terms ^3F, ^1F, $^3\overline{D}$, $^1\overline{D}$ of combination $M_3\,N_2$ have values very nearly equal to $^3\overline{F}$, *i.e.* the difference $^3\overline{F}—^3F$ would be very small ; the lines, if they exist, would be in the far infra-red. Only in the case Ba can we expect ^3F to have a sufficiently large value. We have not yet been able to identify the $^3\overline{F}$ terms without ambiguity, but the following identification may be provisionally given :—

	$\overline{F}_2$ (480·2) 19990·3	$\overline{F}_3$ (432·2) 19510·1	$\overline{F}_4$ 19077·9
$3\,^3F_2$=7426·8	(1*u*) 12563·5		
$3\,^3F_3$=7412 8	?	(2) 12097·3	(1*r*) 11665·4
$3\,^3F_4$=7398·6		(1) 12112·0	(6*u*) 11679·3

The combination with ^3F of state $M_2\,M_3$ ought to give us strong lines, but they would be hopelessly in the infra-red if these values of $^3\overline{F}$ prove to be correct. But we can take the higher Rydberg sequence terms of this ^3F, for which Russell and Saunders give the values 4966·3, 4747·5, and 4558·6. We get the following multiplet :—

	$\overline{F}_2$ 19990·3	$\overline{F}_3$ 19510·1	$\overline{F}_4$ 19077·9
$2b\,^3F_2$=4966·3.....	(1) 15024·1	(1) 14543·2	
$2b\,^3F_3$=4747·5.....	?	(1) 14762·8	(1) 14330·5
$2b\,^3F_4$=4558·6.....		?	?

Probably the last term, viz. 4558, has not been correctly identified, for we have failed to establish it from other sources. The reality of the $^3\overline{F}$ for Ba here given is strengthened by

the following further combinations:—

$$19990{\cdot}3 - q_1 = 13305{\cdot}2\,(1u),$$
$$19510{\cdot}1 - 3^1F_3 = 13372{\cdot}0\,(2),\quad 19510{\cdot}1 - q_2 = 12270{\cdot}0\,(2),$$
$$19510{\cdot}1 - q_3 = 12311{\cdot}2\,(2),$$
$$19077{\cdot}9 - q_3 = 11880{\cdot}9\,(1u).$$

Though the existence of the $^3\overline{F}$ terms has not yet been established, except in the case of Ba, they form very prominent members in the spectra of Sc^+, Y^+, and La^+. Here $^2S - ^2D$ of M^+ (*i.e.* of Sc^{++}, Y^{++}, La^{++}) is negative, *i.e.* the ^2D-term is larger than ^2S; hence terms which arise when the stationary electron is at M_3 are much larger than the terms arising out of the combinations N_1X: in other words, though the elements have a structure similar to that of the alkaline earths, the spectrum is just reversed, the anomalous terms become normal terms, and the normal terms become anomalous. Thus in Sc^+ *, for which the structure diagram is the same as that for Ca, we have the following terms (since the absolute value is not known, the largest term is given the value 0; the values of the other terms are obtained by subtracting the number placed against each number from the value of the biggest term):—

Sc^+.

State.	Terms.	Term values.
$N_1\ M_3$	^3D	0, 67·6, 177·8
	^1D	?
$M_3\ M_3$.....	$^3\overline{F}$	4802, 4883, 4987
	$^3\overline{P}$	12073·8, 12101·3, 12154·1
$M_3\ N_2$	^3F	27440·9, 27602·7, 27841·4
	$^3\overline{D}$	27918·1, 28021·6, 28161·5
	^3P	?

Thus here $^3\overline{F}$ forms the second biggest set of terms. The same feature is observed in the spectra of Y^+ and La^+ †. The barium spectrum is intermediate in nature between the two groups, Ca and Sr on one hand, Sc^+, Y^+, L^+ on the other hand.

* S. Goudsmit, J. van der Mark, and P. Zeeman, Proc. Amst. vol. xxviii. p. 127.

† Y^+-spectrum: Meggers, Journ. Opt. Sci. Am. vol. xii. p. 418 (1926). La^+: Goudsmit, *loc. cit.* Goudsmit has apparently taken the terms in the reverse order.

XVI. *Note on the Motion of Fluid in a Curved Pipe.*

By W. R. Dean, *M.A., Imperial College of Science* *.

IN this paper the steady motion of incompressible fluid through a pipe of circular cross-section which is coiled in a circle is considered. It is found necessary to approximate by supposing that the curvature of the pipe is small, or that R, the radius of the circle in which the pipe is coiled, is large in comparison with a, the radius of the cross-section. The theory is in good qualitative agreement with experiments conducted by Prof. J. Eustice † on the stream-line motion of water in curved pipes. A quantitative comparison, however, requires a closer approximation than that of this paper; it is found that the theoretical results apply only if $n^2a/1440\,\mathrm{R}$, where n is the Reynolds' number, is small, while in all the experiments the value of this expression is greater than 1. It is probably for this reason that the interesting result established experimentally that at increased velocity of flow the curvature of the stream-lines is increased (so that they follow more nearly the line of the pipe) cannot be obtained from the theory at its present stage; however, an alternative explanation appears possible, and is given in § 13.

2. Fig. 1 shows the system of coordinates that has been found convenient in considering the motion of fluid through a pipe of circular cross-section coiled in the form of a circle. The surface of such a pipe is an anchor ring, of which OZ in fig. 1 is the axis. C is the centre of the section of the pipe by a plane that makes an angle θ with a fixed axial plane. CO, the perpendicular drawn from C upon OZ, is of the length R, so that R is the radius of the circle in which the pipe is coiled. The plane through O perpendicular to OZ will be called the "central plane" of the pipe, and the circle traced out by C its "central line." P, any point of the section drawn, is at distance r from C, while CP makes an angle ψ with a line through C parallel to OZ. The position of P is then specified by the orthogonal coordinates r, ψ, θ. The surface of the pipe is given by $r=a$, a being the radius of any section. The components of velocity corresponding to these coordinates are U, V, W; U is therefore in the direction CP, V perpendicular to U and in the plane of the cross-section, and W perpendicular to this plane. The general direction of flow will be taken to be the direction in which θ increases.

The motion of the fluid is supposed to be due to a fall in pressure along the pipe. There will be a fall in pressure if

* Communicated by Prof. S. Chapman, D.Sc., F.R.S.

† Proc. Roy. Soc. A, vol. lxxxv. p. 119 (1911).

fluid enters the pipe from a container at known pressure at one end and flows along the pipe to a container at lower pressure at the other end. Except near the ends, where

Fig. 1.

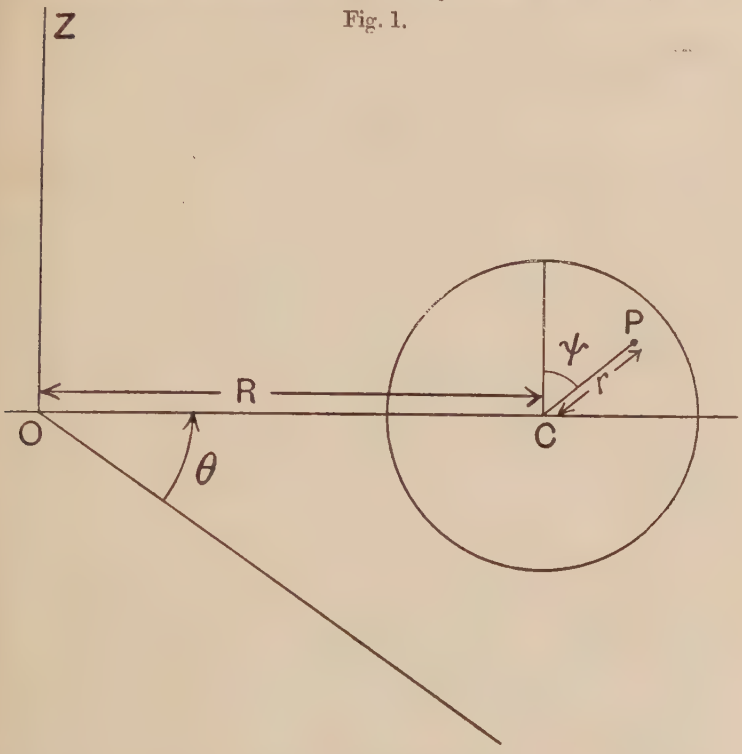

there is certain to be some irregularity of flow, we may expect a steady motion in which U, V, and W (but not P, the pressure) are independent of θ.

The equations for such a motion are these :

$$U\frac{\partial U}{\partial r}+\frac{V}{r}\frac{\partial U}{\partial \psi}-\frac{V^2}{r}-\frac{W^2\sin\psi}{R+r\sin\psi}$$
$$=-\frac{\partial}{\partial r}\left(\frac{P}{\rho}\right)-\nu\left[\left(\frac{1}{r}\frac{\partial}{\partial \psi}+\frac{\cos\psi}{R+r\sin\psi}\right)\left(\frac{\partial V}{\partial r}+\frac{V}{r}-\frac{1}{r}\frac{\partial U}{\partial \psi}\right)\right], \quad \ldots (1)$$

$$U\frac{\partial V}{\partial r}+\frac{V}{r}\frac{\partial V}{\partial \psi}+\frac{UV}{r}-\frac{W^2\cos\psi}{R+r\sin\psi}$$
$$=-\frac{1}{r}\frac{\partial}{\partial \psi}\left(\frac{P}{\rho}\right)+\nu\left(\frac{\partial}{\partial r}+\frac{\sin\psi}{R+r\sin\psi}\right)\left(\frac{\partial V}{\partial r}+\frac{V}{r}-\frac{1}{r}\frac{\partial U}{\partial \psi}\right), \quad \ldots (2)$$

and

$$U\frac{\partial W}{\partial r}+\frac{V}{r}\frac{\partial W}{\partial \psi}+\frac{UW\sin\psi}{R+r\sin\psi}+\frac{VW\cos\psi}{R+r\sin\psi}$$
$$=-\frac{1}{R+r\sin\psi}\frac{\partial}{\partial\theta}\left(\frac{P}{\rho}\right)+\nu\left[\left(\frac{\partial}{\partial r}+\frac{1}{r}\right)\left(\frac{\partial W}{\partial r}+\frac{W\sin\psi}{R+r\sin\psi}\right)\right.$$
$$\left.+\frac{1}{r}\frac{\partial}{\partial\psi}\left(\frac{1}{r}\frac{\partial W}{\partial\psi}+\frac{W\cos\psi}{R+r\sin\psi}\right)\right]. \quad . \quad . \quad (3)$$

The fluid is supposed incompressible, so that the equation of continuity is

$$\frac{\partial U}{\partial r}+\frac{U}{r}+\frac{U\sin\psi}{R+r\sin\psi}+\frac{1}{r}\frac{\partial V}{\partial\psi}+\frac{V\cos\psi}{R+r\sin\psi}=0. \quad . \quad (4)$$

These four equations reduce to equations for the corresponding motion in spherical polar coordinates if we write $R=0$, and to equations in cylindrical coordinates if we write $1/R=0$ and $\partial/R\partial\theta=\partial/\partial z$ *.

3. We now introduce the assumption that the curvature of the pipe is small : that is, that a/R is small. If the pipe were straight a/R would vanish, and the equations could be satisfied by

$$U=V=0, \quad W=A(a^2-r^2), \quad P/\rho=Cz,$$

where A and C are constants, and z is the distance (measured along the central line) of any section of the pipe from a fixed section. For the slightly curved pipe we assume

$$U=u, \quad V=v, \quad W=A(a^2-r^2)+w, \quad P/\rho=Cz+p/\rho, \quad . \quad (5)$$

where u, v, w, and p are all small and of order a/R.

If terms of order a^2/R^2 are ignored, the equation of continuity is

$$\frac{\partial u}{\partial r}+\frac{u}{r}+\frac{1}{r}\frac{\partial v}{\partial\psi}=0, \quad . \quad . \quad . \quad . \quad . \quad (6)$$

while the first two equations of motion become

$$-\frac{A^2(a^2-r^2)^2}{R}\sin\psi=-\frac{\partial}{\partial r}\left(\frac{p}{\rho}\right)-\frac{\nu}{r}\frac{\partial}{\partial\psi}\left(\frac{\partial v}{\partial r}+\frac{v}{r}-\frac{1}{r}\frac{\partial u}{\partial\psi}\right), \quad (7)$$

and

$$-\frac{A^2(a^2-r^2)^2}{R}\cos\psi=-\frac{1}{r}\frac{\partial}{\partial\psi}\left(\frac{p}{\rho}\right)+\nu\frac{\partial}{\partial r}\left(\frac{\partial v}{\partial r}+\frac{v}{r}-\frac{1}{r}\frac{\partial u}{\partial\psi}\right).$$
$$. \quad . \quad . \quad (8)$$

Writing, in conformity with (5), $\partial/R\partial\theta=\partial/\partial z$, we have

* If either substitution is made, the resulting equations are not, however, in the form in which they are usually quoted ; the expressions multiplied by ν in equations (1) to (3) are actually the components of $-\operatorname{curl}\operatorname{curl}\mathbf{v}$, where $\mathbf{v}$ is the velocity, but this vector is equal to $\nabla^2\mathbf{v}$ since $\operatorname{div}\mathbf{v}=0$.

from the third equation of motion

$$u(-2\mathrm{A}r) = -\left(1-\frac{r\sin\psi}{\mathrm{R}}\right)\frac{\partial}{\partial z}\left(\mathrm{C}z+\frac{p}{\rho}\right)$$
$$+\nu\left(\frac{\partial^2}{\partial r^2}+\frac{1}{r}\frac{\partial}{\partial r}+\frac{1}{r^2}\frac{\partial^2}{\partial\psi^2}\right)\{\mathrm{A}(a^2-r^2)+w\}$$
$$+\nu\left(\frac{\partial}{\partial r}+\frac{1}{r}\right)\left\{\frac{\mathrm{A}(a^2-r^2)\sin\psi}{\mathrm{R}}\right\}$$
$$+\frac{\nu}{r}\frac{\partial}{\partial\psi}\left\{\frac{\mathrm{A}(a^2-r^2)\cos\psi}{\mathrm{R}}\right\}.$$

The terms of this equation that are not small must vanish; these are $(-\mathrm{C}-4\nu\mathrm{A})$. We therefore have

$$\mathrm{C} = -4\nu\mathrm{A}, \quad . \quad . \quad . \quad . \quad . \quad . \quad . \quad . \quad . \quad (9)$$

which gives the relation between pressure gradient and rate of flow in a straight pipe of circular section *. We then have the equation

$$-2\mathrm{A}ru = -\frac{\partial}{\partial z}\left(\frac{p}{\rho}\right)-6\nu\mathrm{A}\frac{r\sin\psi}{\mathrm{R}}+\nu\left(\frac{\partial^2 w}{\partial r^2}+\frac{1}{r}\frac{\partial w}{\partial r}+\frac{1}{r^2}\frac{\partial^2 w}{\partial\psi^2}\right).$$
$$. \quad . \quad . \quad (10)$$

The four equations (6), (7), (8), and (10) determine the motion.

4. From equation (10) $\partial p/\partial z$ must be a function of r and ψ, so that p must be of the form $\mathrm{A}z+\mathrm{B}$, where A and B are functions of r and ψ. If, however, this expression for p is substituted in (7) and (8), it appears that A must be a constant; hence p may be taken to be a function of r and ψ only. If we now write

$$u = u'\sin\psi, \qquad v = v'\cos\psi,$$
$$w = w'\sin\psi, \quad p/\rho = p'\sin\psi,$$

where u', v', w', and p' are functions of r alone, the four fundamental equations become

$$\frac{du'}{dr}+\frac{u'}{r}-\frac{v'}{r} = 0, \quad . \quad . \quad . \quad . \quad . \quad . \quad . \quad . \quad . \quad . \quad (11)$$

$$-\frac{\mathrm{A}^2(a^2-r^2)^2}{\mathrm{R}} = -\frac{dp'}{dr}+\frac{\nu}{r}\left(\frac{dv'}{dr}+\frac{v'}{r}-\frac{u'}{r}\right), \quad . \quad . \quad . \quad (12)$$

$$-\frac{\mathrm{A}^2(a^2-r^2)^2}{\mathrm{R}} = -\frac{p'}{r}+\nu\frac{d}{dr}\left(\frac{dv'}{dr}+\frac{v'}{r}-\frac{u'}{r}\right), \quad . \quad . \quad (13)$$

and

$$-2\mathrm{A}ru' = -6\nu\mathrm{A}\frac{r}{\mathrm{R}}+\nu\left(\frac{d^2w'}{dr^2}+\frac{1}{r}\frac{dw'}{dr}-\frac{w'}{r^2}\right). \quad (14)$$

* H. Lamb, 'Hydrodynamics' (4th edition), § 331.

If p' is eliminated from (12) and (13), the following equation results :

$$4A^2r^2(a^2-r^2)/R\nu = \left(r\frac{d^2}{dr^2}+\frac{d}{dr}-\frac{1}{r}\right)\left(\frac{dv'}{dr}+\frac{v'}{r}-\frac{u'}{r}\right).$$

The solution of this, regarded as a differential equation for $dv'/dr+(v'-u')/r$, is

$$dv'/dr+(v'-u')/r = B/r+Cr+A^2r^3(3a^2-r^2)/6R\nu, \quad (15)$$

B and C being arbitrary constants. Substituting in equation (15) the value of v' given by (11), we have

$$r\frac{d^2u'}{dr^2}+3\frac{du'}{dr} = B/r+Cr+A^2r^3(3a^2-r^2)/6R\nu,$$

whence

$$u' = D+E/r^2+(B\log r)2+Cr^2/8+A^2r^4(6a^2-r^2)/288R\nu,$$

where D and E are arbitrary constants. It follows that

$$v' = D-E/r^2+B(1+\log r)/2+3Cr^2/8 + A^2r^4(30a^2-7r^2)/288R\nu.$$

We must have

$$B = E = 0 ;$$

otherwise the velocity of the fluid at points of the central line ($r=0$) will not be finite.

It is interesting to notice that another condition is automatically satisfied. When $r=0$ we must have

$$u' = v',$$

and this is the case since each of these expressions is equal to D. It appeared at first sight that the conditions

$$u' = v' = 0, \quad r = 0$$

were necessary, and it is the fact that the conditions

$$w' = p' = 0, \quad r = 0$$

are necessary for a solution of physical significance. For consider two points on the line OC (fig. 1) which are near to, but on opposite sides of, C. At one point $\psi=\pi/2$, $\sin\psi=1$, while at the other $\psi=3\pi/2$, $\sin\psi=-1$. There will therefore be a finite difference in pressure, for instance, at these two points, however close they may be together, unless at the centre $p'=0$. A similar consideration shows that w' must vanish at the centre. But the case of u' and v' is different. Let the component in the plane of the section of the velocity of the fluid at C be of the magnitude V_c and in the direction of the line $\psi=\psi_0$. At any point (r, ψ) in the immediate neighbourhood of C the velocity in the plane

of the section will be given approximately by

$$u = V_c \cos(\psi - \psi_0), \quad v = -V_c \sin(\psi - \psi_0).$$

The component velocities ($u' \sin\psi$, $v' \cos\psi$) found above are of this form only if $u' = v'$, and it has been found that this condition is satisfied. Moreover, it is clear that we must have $\psi_0 = \pi/2$: hence the velocity at the centre of the pipe is of magnitude D and in the direction of the line OC.

At the surface of the pipe, $r = a$, the velocity components u and v, and hence u' and v', must vanish. Consequently

$$D + Ca^2/8 + 5A^2a^6/288R\nu = 0$$

and

$$D + 3Ca^2/8 + 23A^2a^6/288R\nu = 0,$$

whence

$$C = -A^2a^4/4R\nu, \qquad D = A^2a^6/72R\nu.$$

The resulting expressions for the two velocity components are

$$u = A^2 \sin\psi (a^2 - r^2)^2 (4a^2 - r^2)/288R\nu \quad . \quad . \quad . \quad (17)$$

and

$$v = A^2 \cos\psi (a^2 - r^2)(4a^4 - 23a^2r^2 + 7r^4)/288R\nu. \quad (18)$$

5. Now that u' and v' are known, p', upon which depends the pressure, is determinate. Before the results of (17) and (18) can be accepted, it must be shown that p' and w' vanish when $r = 0$. From (13)

$$p'/r = A^2(a^2 - r^2)^2/R + \nu \frac{d}{dr}\left(\frac{dv'}{dr} + \frac{v'}{r} - \frac{u'}{r}\right),$$

and since it is clear that the terms on the right-hand side of this equation are finite when $r = 0$, it follows that $p' = 0$ when $r = 0$. From (14) and (17),

$$\frac{d^2w'}{dr^2} + \frac{1}{r}\frac{dw'}{dr} - \frac{w'}{r^2} = \frac{6Ar}{R} - \frac{A^3r}{144R\nu^2}(a^2 - r^2)^2(4a^2 - r^2).$$

The solution is

$$w' = F/r + Gr + 3Ar^3/4R - \frac{A^3}{1152R\nu^2}(4a^6r^3 - 3a^4r^5 + a^2r^7 - r^9/10).$$

F must vanish, and it is then evident that $w' = 0$ when $r = 0$. The necessary condition that w' and p should vanish at the central line is therefore fulfilled.

The boundary conditions require $w' = 0$, $r = a$; hence

$$w' = -\frac{3Ar}{4R}(a^2 - r^2) + \frac{A^3r}{1152R\nu^2}[4a^6(a^2 - r^2) - 3a^4(a^4 - r^4) + a^2(a^6 - r^6) - (a^8 - r^8)/10]. \quad (19)$$

6. The results of (17), (18), and (19) can be expressed in a more convenient form. Let W_0 be the value of W at the centre of the pipe; from (5) and (19),

$$W_0 = Aa^2, \quad . \quad . \quad . \quad . \quad . \quad . \quad (20)$$

and is therefore constant. Aa^3/ν, or aW_0/ν, is a non-dimensional constant, the value of which determines the nature of the flow; we write

$$n = Aa^3/\nu. \quad . \quad . \quad . \quad . \quad . \quad . \quad (21)$$

Finally let

$$r' = r/a. \quad . \quad . \quad . \quad . \quad . \quad . \quad . \quad (22)$$

Then

$$U/W_0 = na \sin\psi(1-r'^2)^2(4-r'^2)/288R, \quad . \quad . \quad . \quad (23)$$

$$V/W_0 = na \cos\psi(1-r'^2)(4-23r'^2+7r'^4)/288R, \quad (24)$$

and

$$W/W_0 = (1-r'^2)\left[1-\frac{3r\sin\psi}{4R}+\frac{n^2r\sin\psi}{11520R}\{19-21r'^2 + 9r'^4-r'^6\}\right]. \quad (25)$$

7. It is known* that to cause a given rate of flow a larger pressure gradient is required in a curved pipe than in a straight one, the difference being considerable even when the curvature is small. From this it was anticipated that the difference would be found to depend on the first power of a/R, but the preceding work shows that this is not the case. It is clear that when W is integrated over the whole cross-section the terms involving $\sin\psi$ disappear; the rate of flow is therefore $\pi a^4 A/2$. The pressure is not, of course, constant over a cross-section of the pipe; so that there is not a constant pressure gradient as there is in the case of flow through a straight pipe. But it is natural to define as the mean pressure gradient the space-rate of decrease in pressure along the central line of the pipe. Now, it has been pointed out that p, the part of the pressure that varies across the section, must vanish at the central line; the pressure at any point of this line is therefore $-4\nu Az$, and the mean pressure gradient $4\nu A$. The relation between this quantity and the rate of flow is therefore the same as if the pipe were straight. A closer approximation† than that of this

* This is stated by Eustice, *loc. cit.* p. 119; *cf.* also J. H. Grindley and A. H. Gibson, Proc. Roy. Soc. A, vol. lxxx. p. 114 (1908).

† *Note added.*—Work done since this paper was written has shown that it is necessary to retain the terms of order a^2/R^2.

paper is then required to find the relation between rate of flow and curvature for a given pressure gradient.

8. The motion of the fluid is of special simplicity in the central plane of the pipe. At any point on OC, ψ is either $\pi/2$ or $3\pi/2$; in either case $\cos\psi$, and with it V, vanishes. At any such point the direction of the velocity of the fluid lies in the central plane; hence a particle of the fluid once in this plane does not leave it in the subsequent motion. The motion in one half of the pipe is therefore quite distinct from that in the other.

The differential equation to the stream-lines in the central plane is

$$\frac{dr}{\mathrm{U}} = \frac{(\mathrm{R}\pm r)d\theta}{\mathrm{W}},$$

but with sufficient accuracy we can ignore r in comparison with R and write $\mathrm{A}(a^2-r^2)$ for W. We then have

$$\frac{dr}{\mathrm{R}d\theta} = \frac{\mathrm{U}}{\mathrm{W}_0(1-r'^2)}$$
$$= na(1-r'^2)(1-r'^2/4)/72\mathrm{R},$$

or

$$\frac{dr'}{d\theta} = n(1-r'^2)(1-r'^2/4)/72, \quad . \quad . \quad . \quad (26)$$

by substituting for U from (23) and writing $\sin\psi=+1$. This equation will give a first approximation to the stream-lines, but only to those parts of them on the outside of the central line. To get the other parts we must write $\sin\psi=-1$, and the sign of equation (26) must be reversed. Thus, while on the outside of the central line r' increases with θ, the contrary is the case on the inside; but on both sides the general motion of the fluid is the same, namely a continuous movement from the inner to the outer edge of the pipe. It is, in fact, clear from (23) that the direction of the velocity component along OC is the same at all points of OC. It follows from (26) that

$$\theta = \frac{24}{n}\log\left[\frac{(1+r')^2(1-r'/2)}{(1-r')^2(1+r'/2)}\right], \quad . \quad . \quad . \quad (27)$$

if θ is measured from the point where the stream-line crosses the central line $r'=0$. Evidently θ increases steadily with r', but since θ tends to infinity as the value of r' approaches 1, the stream-line never reaches the outer edge of the pipe. The same expression for θ as in (27), but with the sign reversed, gives the equation to the part of the stream-line on the inside of the central line.

For given r' the value of θ varies inversely as n, and hence inversely as the general velocity of flow. Consequently the angular distance in which a stream-line starting from the centre gets to within a given distance from the outer edge of the pipe is smaller the larger the mean velocity. The relation between θ and r' does not, however, involve a/R, and is therefore independent of the curvature of the pipe.

The table shows the relation between θ and r' on the assumption that θ, measured in degrees, is 50 times the logarithm to base 10 of the function of r' in equation (27). The corresponding value of n is 63·3 ; for a larger value n' the values of θ in the table must be reduced in the ratio $63{\cdot}3/n'$.

TABLE.—Relation between r' and θ.

r' $(=r/a)$	0	0·1	0·2	0·3	0·4	0·5	0·6	0·7	0·8	0·85	0·9
θ (degrees)	0	6·6	13·3	20·3	28·0	36·6	46·8	59·5	77·0	89·4	106·8

The form of the whole stream-line is shown in fig. 2, the direction of motion being indicated by the arrow. If the curve drawn is rotated as a whole about O through any angle the curve so obtained is another central stream-line, all these lines being of exactly the same form. In fig. 2 a/R has been assumed, for convenience, to have the large value 1/3; the r', θ relation is not, as has been seen, affected by the value of a/R, but the approximate results above would not, of course, apply to a pipe with such large curvature.

The figure shows plainly a steady motion of the fluid in the central plane from the inner to the outer edge of the pipe. Since the fluid is assumed incompressible, it is clear enough without further analysis that at a point near the central plane and on the outside of the central line the motion must be directed away from the central plane, while it must be towards the central plane at a point near this plane and inside the central line.

9. The differential equation to any stream-line is

$$\frac{dr}{\mathrm{U}} = \frac{r\,d\psi}{\mathrm{V}} = \frac{\mathrm{R}\,d\theta}{\mathrm{A}(a^2 - r^2)}, \quad . \quad . \quad . \quad . \quad . \quad (28)$$

the same approximation as before being made in the last ratio. What is of most interest is the variation in position with regard to the central line of a fluid element as it moves along the pipe ; this variation is given by the

relation between r and ψ. From the equality of the first two ratios in (28) we have

$$\frac{dr}{(1-r'^2)(4-r'^2)\sin\psi} = \frac{r\,d\psi}{(4-23r'^2+7r'^4)\cos\psi},$$

or

$$\tan\psi\,d\psi = \frac{4-23r'^2+7r'^4}{r'(1-r'^2)(4-r'^2)}\,dr'.$$

Fig. 2.

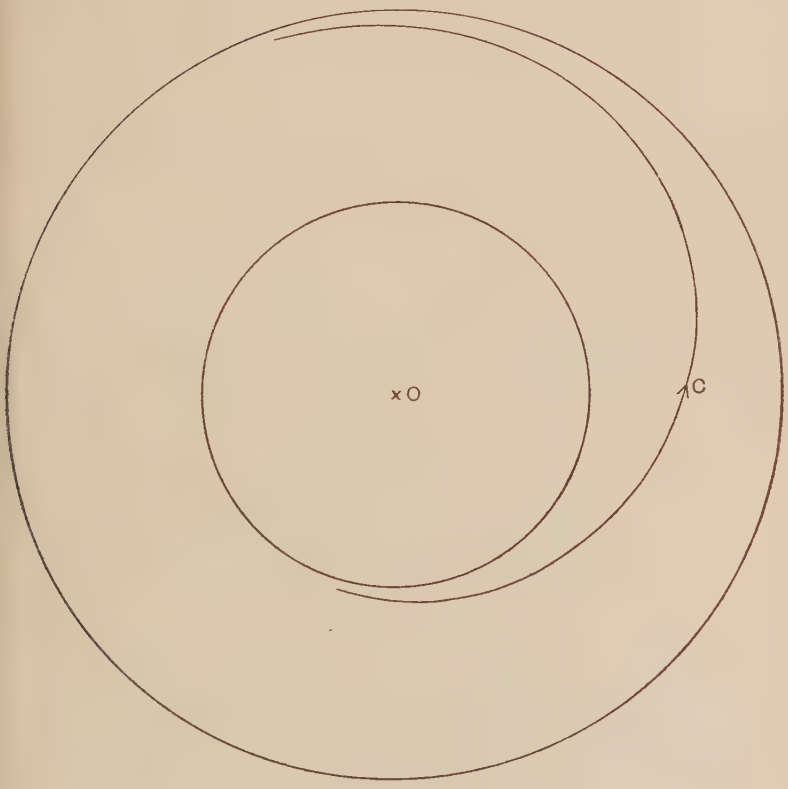

Stream-line in the central plane.

By integration,

$$\sec\psi = kr'(1-r'^2)^2(1-r'^2/4), \quad . \quad (29)$$

where k is an arbitrary constant.

The relation between r' and ψ therefore depends neither on a/R nor on n. For any value of k a closed (r', ψ) curve

is obtained. If k is positive, $\sec\psi$ is positive for all values of r' concerned, and the curve is in the upper half of the cross-section. For an equal and opposite value of k the closed curve obtained is the reflexion in OC of the previous curve: it has already been seen that the motions in the two parts into which the pipe is divided by the central plane are independent. A series of the curves is shown in fig. 3. They represent what may loosely be called the

Fig. 3.

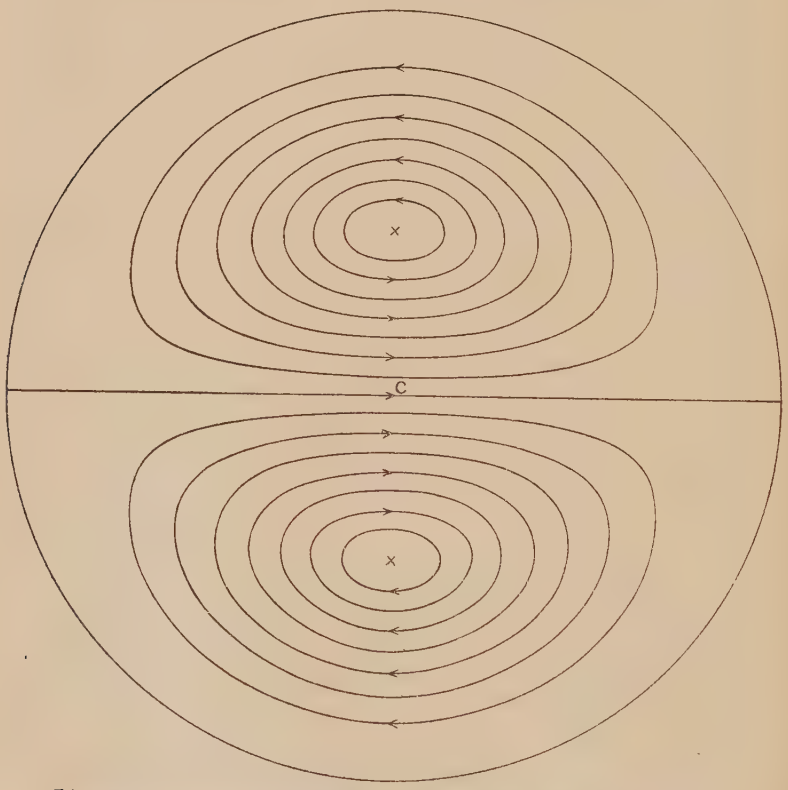

Lines showing the movement of fluid elements in the cross-section of the pipe.

projections of the paths of the fluid elements on the cross-section of the pipe; the direction of motion of the elements is shown by the arrows. On this motion is, of course, to be superposed the motion of the elements along the channel; the closed path of the projection corresponds to a helical motion of the fluid element.

From equation (24), V vanishes for all values of ψ when

$$7r'^4 - 23r'^2 + 4 = 0,$$

the only relevant solution of this equation being $r' = 0{\cdot}429$. At the points where $r' = 0{\cdot}429$ and ψ is 0 or π, both U and V vanish ; these are the points denoted by crosses in fig. 3. The two stream-lines through these points are clearly circles in planes parallel to, and equidistant from, the central plane. The motion of the fluid as a whole can be regarded as made up of what are roughly screw motions in opposite directions about these two circular stream-lines. The general nature of the motion suggested by the theory is now clear.

10. The precise relation between θ and the other variables is of little interest, for the angular distance (θ) in which the projection of a fluid element describes a closed path such as those of fig. 3 must tend to infinity as the minimum distance of the path from C tends to zero. This is clear from the motion of the fluid elements in the central plane, but may be shown directly as follows :—Part of a closed path that is at one point very near to, and above, C must practically coincide with the whole of the upper semicircle of the section of the pipe. θ can be found from the differential equation

$$d\theta = \frac{288r'\,d\psi}{n\cos\psi(4 - 23r'^2 + 7r'^4)}.$$

Normally the relation between r' and ψ must be known before θ can be found, but for points practically coincident with the boundary we can write $r' = 1$. Then

$$d\theta = -\frac{24}{n}\sec\psi\,d\psi,$$

and the angular distance in which a fluid element near the boundary goes from the point where $\psi = \alpha$ to that where $\psi = 0$ is proportional to $\log\tan\left(\frac{\pi}{4} + \frac{\alpha}{2}\right)$. This expression is large if α is nearly $\pi/2$.

The only point of interest is that for given r' and $d\psi$, $d\theta$ is inversely proportional to n, and therefore varies inversely with the mean velocity. It has been shown that the form of the closed curves of fig. 3 is independent of the velocity of the fluid, but on the other hand the angular distance in which they are completely described by the projection of a fluid element is inversely proportional to the mean velocity.

11. So far as the general nature of the motion is concerned, the theory is in complete agreement with the experiments of Eustice on the stream-line motion of water in curved pipes of circular cross-section. In the experiments the motion was made visible by the introduction into the stream at various points of dyed water, which was drawn out into thin coloured lines fixed relatively to the pipe. A coloured line in the central plane of the pipe was roughly of the form of the stream-line shown in fig. 2, showing that the fluid elements near the central plane moved steadily across from the inner to the outer edge of the pipe. But when such a line approached the outer edge, it was found to break up into two coloured bands, one of which went round the boundary of the pipe, above the central plane, to the inner edge, while the other described a similar path below the central plane. This is exactly the motion that the theory would suggest. What has been called a coloured line in the central plane consists, of course, of fluid elements both above the plane and below it; it is evident from fig. 3 that according to the theory the coloured matter of a line in the central plane should be divided into two parts. Again the theory accounts for the distinction implied by the above use of the word bands (as opposed to lines). Two fluid elements, both on the same side of the central plane and both near to it, describe (relatively to the section of the pipe) closed paths which are close together. But we have seen that the angular distance in which such a closed path is described tends to infinity (somewhat as a logarithm) as the minimum distance of the path from the central line tends to zero. Thus, if the distance from the central plane of one of the two fluid elements is twice that of the other, the ratio of the angular distances in which they describe their respective closed paths is likely to be in the neighbourhood of log 2. Though originally near together, two such elements will ultimately be far apart. The coloured matter originally concentrated begins therefore to be dispersed as soon as it approaches the outer edge of the pipe.

The motion described above continues: the bands which reach the inner edge then move to the outer edge, remaining near the central plane, and thence round the boundary to the inner edge again. Fig. 5 of Eustice's paper shows in a pipe of small radius of curvature (a/R approximately 1/7) a coloured line which twice approaches the outer edge and twice the inner edge in an angular distance of less than 2π. The dispersion of the coloured matter must however continue, and the theory suggests, what is found to be the fact, that

the "distinctive character of the colour filament is gradually lost" *.

On the other hand, experiment shows that a coloured line at a sufficient distance from the central plane and, say, above it, is in the form of a helix which is entirely confined to the upper part of the pipe, and that such a line is not dispersed into a band ; in both respects the theory agrees.

12. It is not possible to compare numerically the theory at its present stage with the experimental work. It is usually difficult to make a definite statement as to the limits within which a first approximation such as this is valid ; but a rough idea of the range of validity can be formed from the above expressions for the velocity components. It has been supposed throughout that w is small in comparison with the velocity component W of which it is a part, and therefore the term in the second bracket in the expression for W given by equation (25) must be nearly 1. The expression $r'(19-21r'^2+9r'^4-r'^6)$ is a maximum (for values of r' between 0 and 1) when r' is approximately 0·65, its value being then about 7·6. Hence $n^2a/1440\,\mathrm{R}$ must be small. Again, U and V have been supposed small in comparison with W. From (23) and (24) this supposition requires $na/72\,\mathrm{R}$ to be small, but except for relatively small values of n the former condition is the more stringent. But how small $n^2a/1440\,\mathrm{R}$ must be for a given order of accuracy to be attained it is difficult to say, for w is actually 0 at points of the central line, and what is of most importance is presumably the accuracy of the assumption so far as flow near the centre of the pipe is concerned.

In most of the experiments the values of $n^2a/1440\,\mathrm{R}$ are, however, greater than 1, so that the theory certainly cannot be applied numerically. The least value of a/R is ·005, for a pipe of 1 cm. diameter coiled in a circle of radius 100 cm. The least mean velocity of flow given for this pipe is 6·4 cm. per sec.; the corresponding value of n (the temperature of the water being 18° C.) is over 500, while that of $n^2a/1440\,\mathrm{R}$ is nearly unity.

13. After a good general agreement between theory and experiment, it is surprising to find what appears to be a complete discrepancy, even although a detailed comparison is out of the question. It is found experimentally that the effect of increasing the mean velocity is that the curvature of the coloured lines is increased : the angular distance in

* *Loc. cit.* p. 123.

which a coloured line in the central plane reaches the outer edge and divides into two bands is found to increase with the velocity. In the limited range wherein the theory applies, the contrary appears to be the case. In § 8 it has been seen that the angular distance in which a central stream-line passes over some given fraction of the radius of the pipe towards the outer edge varies inversely as the mean velocity. A similar result has been found in § 10 in the case of any stream-line*.

The figures in Prof. Eustice's paper make his conclusion quite clear. The most direct of the comparisons of flow in a given pipe at different velocities is that shown in fig. 3 (25) † of his paper, as in the case there illustrated the coloured lines that are compared start from exactly the same point of the cross-section. This figure shows the flow in a pipe of 1 cm. diameter bent in a circle of 25 cm. radius. When the mean velocity is 5·5 cm. per sec. a coloured line starting practically from a point of the central line twice reaches the outer edge and twice the inner edge in an angular distance of little more than $\pi/2$; at twice this velocity a coloured line starting from the same point reaches each edge once only in the same angular distance. The discrepancy may be due merely to the fact that no direct comparison between theory and experiment is possible; but there is another way in which the results might be reconciled. Both theory and experiment agree in that the coloured matter of a central filament is dispersed as soon as it approaches the outer edge of the pipe. Now the coloured matter originally at greatest distance from the central plane suffers the least dispersion, and it must be this matter which preserves the distinctive character of the pair of bands (into which the original single line is divided) after they have been once round the upper or lower half of the boundary. But the angular distance in which either of the bands describes its path from the outer to the inner edge is considerably affected by the distance of closest approach to the central plane of the coloured matter composing it; and this distance will be in effect the maximum distance of the coloured matter of the original filament from the central plane. The original cross-section of the coloured filament is therefore of fundamental importance in deciding how rapidly it will subsequently cross from one edge of the

* In the hope of elucidating this matter the writer has recently considered the flow of fluid through a sinuous channel, but also in this case the departure, in a given distance, of a stream-line from the central line of the channel is directly proportional to the velocity.

† *Loc. cit.* p. 122.

pipe to the other ; the smaller the cross-section the more slowly will the repeated crossings take place. The discrepancy between theory and experiment therefore disappears if it is the case that at increased velocity of flow the cross-sections of the original filaments are sufficiently reduced. In any case it is clear that a numerical comparison between theory and experiment, so far as a filament originally in the central plane is concerned, is impossible unless the cross-section of the filament before dispersion takes place is known.

XVII. *A Note on the Spectrum of Neon.* *By* MEGHNAD SAHA, *D.Sc., F.R.S., Professor of Physics, Allahabad University, Allahabad, India* *.

THOUGH the spectral lines of Neon have been completely grouped into series by Paschen, the nature of the series terms was not clearly understood, and a good deal of discussion has been devoted to it. Paschen † discovered

A set of four terms ($s_2\ s_3\ s_4\ s_5$)
of value ranging between 38040–39887 ;

a set of ten terms ($p_1 \ldots \ldots \ldots p_{10}$)
of value ranging between 20958–25671·65 ;

a set of 12 terms ($d_1\ d_1' \ldots \ldots \ldots d_6,\ s_1',\ s_1'' \ldots \ldots s''''$)
of value ranging from 11493–12419.

None of these terms, however, constitute the fundamental level of Neon, which must have a very large value corresponding to the observed ionization potential of 21 volts. This level was discovered by Hertz ‡, by means of his vacuum spectrograph. It gives rise to two lines $\lambda=735{\cdot}7$ and $\lambda=743{\cdot}5$, separated by a frequency interval of 1428, which is just the difference between the values of Paschen's s_2 and s_4 terms.

From these data, and from a discussion of data on the Zeeman effect of Neon-lines, Goudsmit § has proposed the following new designation of Paschen's terms. Goudsmit's

* Communicated by the Author.
† Paschen, *Ann. d. Physik*, vol. lx. and lxiii.
‡ Hertz, *Zs. für Physik*, vol. xxxii. p. 933.
§ See Goudsmit, *Zs. f. Physik.* vol. xxxii. and Back, vol. xxxvii. p. 197.

scheme explains the structure of the Neon spectrum far better than Landé's theory of Spectra of the Second Degree (Spektra der Zweiter Stufe) which he deduced from his 'Verzweigungsprinzip.'

Terms (Paschen's Notation).	Designation according to Goudsmit.	Observed g-factor.	Theoretical g-factor,
Hertz's fundamental level.	$^1S_0$	0/0	0/0
s_2	$^1P_1$	1	1
s_3	^3P	?	$\frac{0}{0}$
s_4	$^3P_1$	$\frac{3}{2}$	$\frac{3}{2}$
s_5	$^3P_2$	?	$\frac{3}{2}$
p_1	$^1S_0$		$\frac{0}{0}$
p_5	$^1\bar{P}_1$	1	1
p_8	$^1D_2$	1·137	1
p_{10}	$^3S_1$	2	2
p_3	$^3\bar{P}_0$	?	$\frac{0}{0}$
p_2	$^3\bar{P}_1$	$\frac{4}{3}$	$\frac{3}{2}$
p_4	$^3\bar{P}_2$	$\frac{4}{3}$	$\frac{3}{2}$
p_7	$^3D_1$	$\frac{2}{3}$	$\frac{1}{2}$
p_6	$^3D_2$	$\frac{7}{6}$	$\frac{7}{6}$
p_9	$^3D_3$	?	$\frac{4}{3}$

The nature of the next group of terms called d's and s's by Paschen has been fixed up by Hund, though their g-factor is yet unknown. Most of the lines arising from the combination of these terms with the p's lie in the extreme infra red, so that it would be very difficult to observe their Zeeman effect. It is, however, evident that they cannot all belong to the d group, for d_6 has the inner quantum number 4, and no triplet term up to d can have such a high inner quantum number. Higher terms like ^3F are clearly involved. In this note, the above facts discovered by Hund and Goudsmit are put in new symbols explained by the author in an earlier paper (Saha, Phil. Mag., June 1927).

The number below each term like M denotes the full number of electrons required to close the subgroup completely. A level like L_2 was subdivided into L_{21}, L_{22}, by Stoner with two and four electrons respectively, but this has been omitted.

Chart illustrating the Formation of Atoms.

H He	K_1 2				Transition I 21 Sc to 28 Ni	Group II 39 V to 46 Pa	Rare Earths 57 La to 70 Yb	Transition Group III 71 Lu to 78 Pt			
3 Li to 10 Ne		L_1 2	L_2 6								
11 Na to 18 A			M_1 2	M_2 6	M_3 10						
29 Cu to 36 Kr		19 K 20 Ca		N_1 2	N_2 6	N_3 10	N_4 14				
47 Ag to 54 Xe		37 Rb 38 Sr			O_1 2	O_2 6	O_3 10	O_4	O_5		
79 Au to 86 Nt		55 Cs 56 Ba				P_1 2	P_2 6	P_3	P_4	P_5	P_6

Advantage of this Method of Representation.

The first period Li to Ne .... is formed when the electrons are made to fill the L-levels. The second period (11) Na to (19) A when the M, and M_2 levels are filled up. It is now known, that if a fresh electron is now brought up, instead of going to M_3, it comes over to N_1, forming K and Ca.

The negative energy value of the electron in position N_1 is therefore larger than the value in position M_3. To represent this state of affairs, we have written N_1 below M_2 and not following M_3, as is usually the custom. We have followed this system all throughout. Thus roughly if by

(X) we represent the energy value of any level, then

$$(K_1) > L_1 > (L_2),\ (M_1)$$
$$> (M_2),\ (N_1)$$
$$> (M_3),\ (N_2),\ (O_1)$$
$$\text{etc., etc.}$$

Terms on the same vertical column like (L_2) (N_1) or (M_3) (N_2) (O_1) . . . . have the same order of energy value, though each preceding term is larger than the next.

The diagram makes clear the formation of the transitional groups, and rare earths, and persistence of the pair of alkali and alkaline earths throughout the whole system. After Argon, we have K and Ca formed in which the N_1-level is filled up. The next electron must go to the M_3-level. This happens till the M_3-level is completely filled up. Then with copper, a new group begins to be formed. In this way, we can explain the formation of pairs of alkalies and alkaline earth (O_1—Rb and Sr), (P_1—Cs and Ba), the successive transitional groups, and the rare earths.

Application to Spectroscopy.

But the scheme is more fruitful when we utilize it for the explanation of spectra :—

Taking Na, we again write out the structure diagram, but now with the higher levels unfilled :—

Spectrum of Sodium.

K_1	L_1	L_2	M_1	M_2	M_3	N_1	N_2	N_3	N_4
2	2	6	[1]	(1)	(1)	(1)	(1)	(1)	(1)
			^2S	^2P	$1\,^2D$	$2\,^2S$	$2\,^2P$	$2\,^2D$	$1\,^2F$

M_1 L denotes the normal level of the atom. It is the first term of the S-series, and may be written as 1^2S_1, using Russell and Saunders' notation. The electron, as it runs

through the higher levels denoted by (1), gives rise to the spectral terms written under that level. The diagram also gives a rough indication of the sequence of values of successive terms. Thus

$$1\,^2S_1 > 1\,^2P_{1,2},\ 2\,^2S$$
$$> 1\,^2D_{2,3},\ 2\,^2P_{1,2},\ 3\,^2S_1$$
$$> 1\,^2F_{3,4},\ 2\,^2D_{2,3},\ 3\,^2P_{1,2},\ 4\,^2S.$$

Of course these inequalities are only roughly obeyed.

In the construction of the spectra of alkaline earths, we have to keep one electron fixed at N_1, O_1 or P_1, as the case may be, and allow the other electron to run through the higher levels. The methods of working have already been discussed in a previous paper communicated to the Philosophical Magazine.

We shall now discuss the spectrum of Neon.

Explanation of the Spectrum of Neon.

K_1							
2							
L_1	L_2						
2	5, 1						
	M_1	M_2	M_3				
	(1)	(1)	(1)				
		N_1	N_2	N_3	N		
		(1)	(1)	(1)	(1)		
			O_1	O_2	O_3	O_4	
			(1)	(1)	(1)	(1)	

The normal state of Neon is obtained when all the six electrons are allowed to fill the L_2-level. It has got $I_k=0$, $I_r=0$, hence it is an $^1S_0$-term.

The higher orbits are produced when we keep 5 electrons in L_2 and allow the other to pass through the higher levels. The 5 electrons in L_2 give us a doublet P-level, so that we can construct the terms successively as follows:—

Running electron in M_1 } Combination of ^2P with $^2S_1$
$I_r=\frac{2}{2}, 0,\ I_k=|1+0|=1.$

Hence we get $^1P_1, {}^3P_{0,1,2}$ which are identified by Goudsmit with Paschen's s_2, s_3, s_4, s_5.

If the running electron is in N_1, O_1, P_1 ... ..., we shall get the higher Rydberg sequences of these terms.

Running electron in M_2 } Combination of ^2P with ^2P.
$I_k = |1+1| = 2, 1, 0.$

Hence we expect

$$c^1S_0 \qquad c^3S_1,$$
$$c^1\bar{P}_1 \qquad c^3\bar{P}_{0,1,2},$$
$$c^1D_2 \qquad c^3D_{1,2,3}.$$

These are the terms which have been obtained by Goudsmit by a similar process, and identified with Paschen's p's. Now it is quite evident that the p-terms arising from this process will be capable of combining with the previous p-terms (Paschen's s's). For the process simply means transition of the electron from $M_1 \rightarrow M_2$ and it is perfectly admissible. The present p-terms must therefore be dashed, while the s- and d-terms must remain undashed.

Since all these terms arise from the same level, they have approximately the same scale of values, as observed.

If the electron is in any one of the higher 2-levels, as N_2 or D_2, or P_2, they will give rise to the higher Rydberg sequences to the present set, having identical combinatory powers.

Running electron in M_3 } Combination of ^2P with ^2D.
We have $I_k = |2+1| = 3, 2, 1.$

Hence we expect

$$d^1P_1 \qquad d^3P_{0,1,2},$$
$$d^1\bar{D}_2 \qquad d^3\bar{D}_{1,2,3},$$
$$d^1F_3 \qquad d^3F_{2,3,4}.$$

We expect twelve terms.

Now Paschen has given exactly twelve terms with

$j = 0$, for $d_6 \quad \therefore d_6 = c^3P_0$.

$j = 1$, for $(d_2\ d_5\ s_1') = (c^1P_1, c^3P_1, c^3D_1)$,

$j = 2$, for $(d_1''\ d_3\ s_1''\ s_1'''') = (c^1\bar{D}_2, c^3P_2, c^3\bar{D}_2, c^3F_2)$,

$j = 3$, for $(d_1', d_4, s_1''') = (c'F_3, c^3\bar{D}_3, c^3F_3)$,

$j = 4$, for $d_4^1 = c^3F_4$.

The explanation of these terms is due to Hund, but detailed identification is difficult, and an attempt has been made by writing down the multiplets and comparing the intensities according to that to be expected from the

Sommerfel-Ornstein-Dorgelo scheme. Table I. shows the results of detailed identification.

TABLE I.

Spectal Term.	Term in Paschen's notation.	Term Values.	Inner Quantum Number.
$d\,^1P_1$	s_1'	11493·76	1
* $d\,^1D_2$	d_1''	12229·69	2
† $d\,^1F_3$	s_1'''	11519·27	3
$d\,^3P_0$	d_0	12419·90	0
$^3P_1$	d_3	12405·20	1
$^3P_2$	d_3	12322·24	2
$d\,^3D_1$	d_2	12292·98	1
* $d\,^3D_2$	s_1''	11509·52	2
$d\,^3D_3$	d_1'	12228·26	3
† $d\,^3F_2$	s_1''''	11520·80	2
$d\,^3F_3$	d_4	12337·35	3
$d\,^3F_4$	d_4'	12339·15	4

* The positions of these two terms may be interchanged.
† Positions interchangeable.

The identification is somewhat ambiguous in certain cases How far the intensity rules are followed will be seen from the following tables. Certain values like (d_1' d_1'') are so close to each other that the lines occurring from them cannot be separated from each other, and the intensity-data in these cases are open to certain amount of doubt. The values of all these terms are of the same order and approximately equal to $\frac{N}{3^2}$. Some of the multiplets with intensities are shown in the following tables.

TABLE II.

The $c\,^3D - d\,^3F$-multiplet.

$c=5L_2M_2$ / $d=5L_2M_3$	(p_7) $^3D_1$.	(p_6) $^3D_2$.	(p_9) $^0D_3$.
(s'''') $^3F_2$	8136·4 (7) 12287·0	8267·14 (3) 12092·7	
(d_4) $^3F_3$		8865·7 (3) 11276·3	8376·4 (1) 11934·9
(d_4') $^3F_4$			8377·63 (7) 11933·3

TABLE II. (*continued*).

The $c\ ^3D - g\ ^3P$-multiplet.

$b=5L_2M_2$ / $g=5L_2N_3$	(p_7) $^3D_1$.	(p_6) $^3D_2$.	(p_9) $^3D_3$.
$(d_6)\ ^3P_0$	5934·46 (7) 16846·0		
$(d_5)\ ^3P_1$	?	6000·95 (6) 16659·4	
$(d_3)\ ^3P_2$	5919·04 (2) 16889·9	5987·93 (8) 16695·6	5760·58 (7) 17354·5

The multiplet represents the combination of ^3D, and second Rydberg sequence of ^3P terms.

The $c\ ^3D - d\ ^3\bar{D}$-multiplet.

c / d	(p_7) $^3D_1$.	(p_6) $^3D_2$.	(p_9) $^3D_3$.
$(d_2)\ ^3\bar{D}_1$	8681·93 (3) 11515·0	8830·80 (0) 11320·9	
$(s_1'')\ ^3\bar{D}_2$	8128 95 (3) 12298·3	8259·39 (4) 12104·1	7833·12 (1) 12762·8
$(d_1')\ \bar{D}_3$		8780·63 (4) 11385·6	8300·34 (7) 12044·4

Singlet-Combinations.

c / d	p_{10} S_1.
$(s_1')\ ^1P_1$	7051·29 (5) 14177·9
$(d_6)\ ^3P_0$	7544·08 (6) 13251·8
$(d_5)\ ^3P_1$	7535·78 (8) 13266·4
$(d_3)\ ^3P_2$	7488·85 (9) 13349·5
$(d_2)\ ^3\bar{D}_1$	7472·42 (4) 13378·8

It will thus be seen that the complicated spectrum of Neon is very simply explained on the recent theories of complicated spectra. The theory accounts for not only the fundamental levels, but also for all the higher levels, the Rydberg sequences, and the order of values observed in each case. It also gives a very cogent explanation of the origin of the dashed terms, and explains such transitions as apparently break the selection principle, *e.g.* $\Delta K = 2$, or 3.

We can summarize the results as follows :—

	Position.	Term.	
(*a*)	$6L_2$,	$^1S_0$	
(*b*)	$5L_2$, M_1	$^1P_1$, $^3P_{0,1,2}$	
	N_1	Higher Rydberg sequence terms to the above.	
(*c*)	$5L_2$, M_2	$b\,^1S_0$	$b\,^3S_1$
		$b\,^1\overline{P}_1$	$b\,^3\overline{P}_{0,1,2}$
		$b\,^1\overline{D}_2$	$b\,^3D_{1,2,3}$
	$5L_2$, N_2, O_2	Same terms but of higher Rydberg sequence.	
(*d*)	$5L_2$, M_3	$c\,^1P_1$	$c\,^3P_{0,1,2}$
		$c\,^1\overline{D}_2$	$c\,^3\overline{D}_{1,2,3}$
		$c\,^1F_3$	$c\,^3F_{2,3,4}$
	$5L_2$, N_3, O_3	gives higher Rydberg sequence terms.	

Transitions take place between terms of groups

$$(a) \longrightarrow (b) \longrightarrow (c) \longrightarrow (d) \longrightarrow$$

Corresponding to the transition of the electron from

$$L_2 \longrightarrow M_1 \longrightarrow M_2 \longrightarrow M_3.$$

The scheme also explains that the fundamental term $^1S_0$ will be rather solitary, *i.e.* will not have terms of higher Rydberg sequence following it.

My thanks are due to Mr. K. Mazumder for drawing the charts.

XVIII. *On the paper "On the Reflecting Power of the Carbon Atom for High-frequency Rays"* (Phil. Mag. iii. 1927, p. 195).

To the Editors of the Philoophical Magazine.

GENTLEMEN,—

IN the paper mentioned above, the formula (6), which I gave on page 199, is only applicable to a pure and very compact powder. If we take the general case of a mixture of powders, of which the density in the briquet under X-rays is δ and which contains the substance to be studied, of density ρ, at the concentration n, one has (with the notations of the paper) :

$$\Delta\nu = \Delta V \cdot \frac{1}{n} \cdot \frac{\rho}{\delta}.$$

In the formula (6) we must therefore replace μ, absorption coefficient of the powder, by $\mu \cdot \frac{\rho}{n\delta}$ and

$$\frac{E}{I} = \nu \cdot \frac{a}{\pi D} \cdot \phi(\theta) \cdot \frac{1}{2\mu \frac{\rho}{n\delta}} (1 - e^{-2\mu s/\sin\theta}) \lambda^3 N^2 S^2 f^2 \text{ *}.$$

In the case of a pure powder (*cf.* Compton, 'X-Rays and Electrons,' p. 131), $\mu \frac{\rho}{\delta}$ is the absorption coefficient of a crystal of this substance : it is therefore useless to measure μ, if $e^{-2\mu s/\sin\theta}$ is negligible. But in the case of an impure powder (case of the diamond utilized, which contains a little iron) μ must be measured.

In my paper there is, of course, no correction to be made for relative measurements of f. For the "absolute" experiments, the corrections are, in this case, of little importance. For diamond ($\rho = 3{\cdot}5$), the sensitive method of analysis given on page 205 enables us to find n. The best values of $\frac{\mu}{\rho}$ for C are probably those of Allen, whose measurements give, for λKMo, KCu, KFe, $\frac{\mu}{\rho} = 0{\cdot}68$; $5{\cdot}2$; $9{\cdot}8$; for Fe, $\frac{\mu}{\rho} = 36{\cdot}9$; 330 ; 80. [The numbers on page 205, taken from Siegbahn, 'The Spectroscopy of X-Rays,' page 248, and Kaye, 'X-Rays,' 2nd ed. page 138, are far too low. *Cf.* Compton,

* In $\Phi(\theta)$, the polarization factor had been written inadvertently $1+\cos^2 2\theta$, instead of $\frac{1+\cos^2 2\theta}{2}$. Replace 4 by 8.

loc. cit.] We find in this way $n_C = 2{\cdot}2$ g. ; $n_{Fe} = {\cdot}034$ g. (corresponding absorptions, 2·7 ; 22·6 ; 24·4). The absorption of rock-salt is $\mu_{NaCl,\,KMo} = 17{\cdot}4$. The calculations, redone with these figures, give $f_{C(111)} = 2{\cdot}6$. n_C is known at about 10 per cent.: so the accuracy does not exceed 15 per cent. The conclusions are not modified. I hope to be able to repeat these experiments more accurately.

For naphthalene and anthracene the absorptions are, from $\left(\frac{\mu}{\rho}\right)_{C,\,KCu}$, 5·9 and 6·5. This gives for F_N and F_A 19·5 and 20, and f_C in these substances is 6·7 (Naph.) and 5·9 (Anth.), near 6. It may be pointed out that F may be calculated directly from $E/E_{NaCl_{(110)}}$, which is known, taking an absorption coefficient of 160 for NaCl (KCu), calculated from 17·4 (KMo) by means of the $\lambda^{2\cdot92}$ law. The results are the same.

Believe me yours truly,

30th May, 1927. M. Ponte.

XIX. *The Calculation of the Equivalent Conductivity of Strong Electrolytes.*—Part I. *Aqueous Solutions.* (ii.) *Application to Data at* 0°, 18°, *and* 25° *C. By* Allan Ferguson, *M.A., D.Sc., and* Israel Vogel, *M.Sc., D.I.C.**

IN Part I. of this series of investigations (Ferguson and Vogel, this Journal, 1925, vol. l. p. 971) the values of Λ_0 for some thirty-seven strong electrolytes were calculated, using a simple but reliable method for computing B and n in the equation

$$\Lambda_0 = \Lambda + BC^n.$$

Contrary to the usual assumption that n is independent of the nature of the electrolyte, it was shown that B and n vary in a regular manner with the nature of the electrolyte and their values are, therefore, important characteristics of each electrolyte. Further, the formula is applicable to uni-uni, uni-bi, and bi-bivalent electrolytes.

The assumption of the constancy of n is fundamental in certain new theories of strong electrolytes. Debye and Hückel, for instance, find that their theory (*Phys. Zeit.* 1923, xxiv. p. 305) leads directly to Kohlrausch's square root formula ("Gesetz")

$$\frac{\Lambda_0 - \Lambda}{\Lambda_0} = BC^{\frac{1}{2}},$$

where B is determined in terms of certain constants for the

* Communicated by the Authors.

substances concerned and *the exponent of* C *is independent of the nature of the electrolyte.* This is directly opposed to the results we have obtained, and we hope later to discuss this point at length.

The methods commonly employed for the determination of Λ_0 lead to markedly different values, and have been the subject of much comment and criticism.

(*a*) Certain methods such as that depending on the Ostwald–Bredig–Walden rule (Lorenz, *Z. anorg. Chem.* 1919, cviii. pp. 81, 191; 1920, cxii. p. 210) and that suggested by Randall (J. Amer. Chem. Soc. 1916, xxxviii. p. 788) are recognized as approximate methods.

(*b*) Methods have been proposed from time to time which have the Storch equation as basis. That used by Noyes (J. Amer. Chem. Soc. 1908, xxx. p. 335), which consists "in plotting the reciprocal of the equivalent conductance ($1/\Lambda$) at the various concentrations (C) against $(C\Lambda)^{n-1}$ and varying the value of n until a linear plot was obtained and then extrapolating for zero concentration," is cumbersome and at most very approximate (*cf.* Abbott and Bray, J. Amer. Chem. Soc. 1909, xxxi. p. 729). Bates (*ibid.* 1913, xxxv. p. 519) has described a procedure based on the assumption that the n of the Storch equation

$$(C\alpha)^n = KC(1-\alpha)$$

is variable and decreases with rising concentration (*cf.* also Noyes and Falk, J. Amer. Chem. Soc. 1912, xxxiv. p. 454, who find the same law of variation of n). This is directly contrary to our own experience, as we find from an examination of nineteen electrolytes of the most varied type that either n is independent of the concentration over a very wide range, or it may be put as equal to $a+bC$, where b is a *positive* constant in all the instances that we have examined.

(*c*) The methods which, directly or indirectly, make any assumptions concerning the validity or invalidity of the law of mass action (*cf.* Washburn, J. Amer. Chem. Soc. 1918, xl. pp. 122 & 150) are likely to lead to values of Λ_0 weighted by the assumptions made (*cf.* Ferguson and Vogel, this Journal, July 1927).

(*d*) Various methods have been proposed which are based on the theory of Hertz (*Ann. d. Physik,* 1912, xxxvii. p. 1). These have been chiefly employed by Lorenz and his coworkers (Lorenz, *Z. anorg. Chem.* 1920, cxiii. p. 135; 1921, cxviii. p. 209: Lorenz and Osswald, *ibid.* 1920, cxiv. p. 209: Lorenz and Neu, *ibid.* 1921, cxvi. p. 45: Lorenz and Michael, *ibid.* 1921, cxvi. p. 161: Lorenz and Voigt, *ibid.*

1925, cxlv. p. 277 : Lorenz and Westenberger, *ibid.* 1926, clv. p. 144). It cannot be said that the fundamental postulates of Hertz's theory are well established (*cf.* Auerbach, *Ergebnisse der exakten Naturwissenschaften*, 1922, iv. p. 233), nor have the chief deductions of Lorenz been experimentally verified. The different methods based on Hertz's theory do not, in a large number of cases, give concordant results—these will be referred to later—and the values, in most instances, differ from those deduced by the more generally accepted methods.

(*e*) By far the best known of the various methods employed are those which use some special form of the equation

$$\Lambda_0 = \Lambda + \mathrm{F}(\Lambda, \mathrm{C}).$$

Equations of this type have been used by Kohlrausch (*Das Leitvermögen der Elektrolyte*, p. 107 (1916)),

$$\Lambda_0 = \Lambda + b\mathrm{C}^{\frac{1}{3}}, \quad . \quad . \quad . \quad . \quad . \quad . \quad (\alpha)$$

$$\Lambda_0 = \Lambda + \mathrm{P}\mathrm{C}^{\frac{1}{2}}, \quad . \quad . \quad . \quad . \quad . \quad . \quad (\beta)$$

$$\Lambda_0 = \Lambda + k\Lambda^p\mathrm{C}^{\frac{1}{2}}, \quad . \quad . \quad . \quad . \quad . \quad (\gamma)$$

by Lorenz and by Walden (*Z. anorg. Chem.* 1919, cxcviii. p. 191; 1921, cxv. p. 49) who use

$$\Lambda_0 = \Lambda + m\mathrm{C}^{0{\cdot}45}, \quad . \quad . \quad . \quad . \quad . \quad (\delta)$$

and by the present writers, who employ

$$\Lambda_0 = \Lambda + \mathrm{B}\mathrm{C}^n. \quad . \quad . \quad . \quad . \quad . \quad . \quad (\epsilon)$$

Of these equations (β) has long been recognized as giving results of at least as high an order of reliability as those reached by the methods previously discussed. The present writers have shown *that n and* B *can not be assumed constant, but that they vary from electrolyte to electrolyte.* They feel, therefore, that the results computed with values of n and B characteristic of each electrolyte are likely to be more reliable than those based on equations (β) and (δ)—equations (α) and (γ) are generally recognized as of a lower order of reliability—and for this reason have extended their calculations to a wider range of experimental data.

The method has now been applied to experimental data at 0°, 18°, and 25°. The data at 0° are due to Walden and Ulich (*Z. phys. Chem.* 1923, cvi. p. 49) ; the conductivities at round concentrations were interpolated from a large scale Λ–C graph. The results are shown in full in Table I. below as the constancy of the values of Λ_0 over a given range of concentration forms an important feature of these investigations.

TABLE I.

	KCl.		NaCl.		KNO_3.	
*Concentration.	Λ.	Λ_0.	Λ.	Λ_0.	Λ.	Λ_0.
$2{\cdot}0\times10^{-4}$	—	—	—	—	—	—
$5{\cdot}0\times10^{-4}$	80·65	81·51	66·15	66·72	79 29	79·88
$1{\cdot}0\times10^{-3}$	80·27	81·51	65·80	66·69	78·95	79·89
$2{\cdot}0\times10^{-3}$	79·69	81·48	65·26	66·67	78·35	79·83
$5{\cdot}0\times10^{-3}$	78·50	81·41	64·07	66·64	77·07	79·76
$1{\cdot}0\times10^{-2}$	77·30	81·51	62·80	66·85	75·75	(80·00)

	KIO_3.		$KClO_4$.		$LiClO_4$.	
*Concentration.	Λ.	Λ_0.	Λ.	Λ_0.	Λ	Λ_0.
$2{\cdot}0\times10^{-4}$	—	—	—	—	54·19	54·31
$5{\cdot}0\times10^{-4}$	60·20	60·69	76·31	76·84	54·06	54·29
$1{\cdot}0\times10^{-3}$	59·90	60·70	76·00	76·86	53·85	54·30
$2{\cdot}0\times10^{-3}$	59·35	60·67	75·45	76·84	53·48	54·28
$5{\cdot}0\times10^{-3}$	58·10	60·63	74·15	76·80	52·55	54·25
$1{\cdot}0\times10^{-2}$	56·90	(61·06)	72·67	(76·97)	51·49	(54·50)

	K Picrate.	
Concentration.	Λ.	Λ_0.
$2{\cdot}0\times10^{-4}$	54·97	55·17
$5{\cdot}0\times10^{-4}$	54·75	55·14
$1{\cdot}0\times10^{-3}$	54·44	55·09
$2{\cdot}0\times10^{-3}$	53·91	55·00
$5{\cdot}0\times10^{-3}$	52·79	54·96
$1{\cdot}0\times10^{-2}$	51·76	(55·41)

* Throughout this series of papers C will be expressed in gram equivalents per litre.

Table II. below contains the mean values of Λ_0 at 0° C. together with the values of B and n for these seven electrolytes.

TABLE II.

Electrolyte.	Λ_0.	B.	n.
KCl	81·48	48·21	0·5296
NaCl	66·68	83·38	0·6569
KNO_3	79·85	87·51	0·6569
KIO_3	60·67	111·72	0·7146
$KClO_4$	76·84	108·75	0·7013
$LiClO_4$	54·29	134·04	0·8242
K Picrate ...	55·07	114·06	0·7476

In Tables III. and IV. are shown the results for some electrolytes at 18° C. ($LiClO_4$, K Picrate, Walden and Ulich, *Z. phys. Chem.* 1923, cvi. p. 49; $RaBr_2$, Kohlrausch and Henning, *Ges. Abh.* 1911, ii. p. 1108; $ZnSO_4$, Kohlrausch and Grüneisen, *ibid.* 1911, ii. p. 1078; CH_3COONa, Lorenz and Osswald, *Z. anorg. Chem.* 1920, cxiv. p. 202).

TABLE III.

	$LiClO_4$.		K Picrate.		$RaBr_2$.	
Concentration.	Λ.	Λ_0.	Λ.	Λ_0.	Λ.	Λ_0.
$1{\cdot}0\times10^{-4}$	—	—	—	—	123·7	126·8
$2{\cdot}0\times10^{-4}$	87·89	88·55	—	—	122·7	126·7
$5{\cdot}0\times10^{-4}$	87·54	88·37	88·10	89·74	120·9	126·6
$1{\cdot}0\times10^{-3}$	87·07	88·36	87·50	89·75	119·4	126·8
$2{\cdot}0\times10^{-3}$	86·31	88·31	86·65	89·74	117·1	126·7
$5{\cdot}0\times10^{-3}$	84·71	88·28	85·00	89·71	113·4	126·9
$1{\cdot}0\times10^{-2}$	83·07	(88·62)	83·31	89·79	110·0	(127·6)

	$ZnSO_4$.		CH_3COONa.	
Concentration.	Λ.	Λ_0.	Λ.	Λ_0.
$1{\cdot}0\times10^{-4}$	109·53	114·26	—	—
$2{\cdot}0\times10^{-4}$	107·46	114·27	—	—
$5{\cdot}0\times10^{-4}$	103·16	114·21	—	—
$1{\cdot}0\times10^{-3}$	98·39	114·31	74·90	75·98
$2{\cdot}0\times10^{-3}$	92·05	—	74·27	75·97
$5{\cdot}0\times10^{-3}$	81·76	—	72·82	75·90
$1{\cdot}0\times10^{-2}$	72·76	—	71·21	76·04

TABLE IV.

Electrolyte.	Λ_0.	B.	*n.*
$LiClO_4$	88·33	103·32	0·6351
K Picrate	89·74	53·81	0·4596
$RaBr_2$	126·8	100·9	0·3791
$ZnSO_4$	114·26	608·5	0·5274
CH_3COONa ...	75·96	95·88	0·6489

Practically the only accurate data for aqueous salt solutions at 25° seem to be those of Lorenz and Michael (*loc. cit.*). Here also the values of Λ at round concentrations were interpolated from a large scale Λ–C plot. The results are given in Tables V. and VI. below, and it will be seen that the consistency of the values of Λ_0 from the lowest concentration measured to about 0·01 N leaves little to be desired.

TABLE V.

	$KMnO_4$.		KCl.		NaCl.	
Concentration.	Λ.	Λ_0.	Λ.	Λ_0.	Λ.	Λ_0.
$5{\cdot}0\times10^{-4}$	134·16	136·84	148·86	152·28	125·42	128·08
$1{\cdot}0\times10^{-3}$	133·25	136·85	147·80	152·24	124·45	128·08
$2{\cdot}0\times10^{-3}$	132·00	136·82	146·55	152·30	123·37	128·06
$5{\cdot}0\times10^{-3}$	129·67	136·77	144·16	152·26	121·20	128·02
$1{\cdot}0\times10^{-2}$	127·30	136·82	141·73	152·23	118·95	128·00

	KBr.		NaBr.		CH_3COONa.	
Concentration.	Λ.	Λ_0.	Λ.	Λ_0.	Λ.	Λ_0.
$5{\cdot}0\times10^{-4}$	150·72	153·30	127·37	129·51	—	—
$1{\cdot}0\times10^{-3}$	149·79	153·28	126·55	129·51	88·22	89·49
$2{\cdot}0\times10^{-3}$	148·51	153·24	125·39	129·46	87·44	89·44
$5{\cdot}0\times10^{-3}$	146·15	153·22	123·24	129·47	85·70	89·35
$1{\cdot}0\times10^{-2}$	143·68	153·26	120·92	129·50	83·79	89·55

TABLE VI.

Electrolyte.	Λ_0.	B.	n.
KCl	152·26	58·82	0·3742
NaCl	128·05	59·50	0·4089
KBr	153·26	72·08	0·4382
NaBr	129·49	72·43	0·4631
$KMnO_4$	136·82	66·68	0·4227
CH_3COONa..	89·46	119·22	0·6578

For the sake of comparison the values of Λ_0 calculated for these electrolytes by Lorenz and his collaborators are included in Table VII.

TABLE VII.

	Authors.	* Lorenz and Michael.	‡ Lorenz and Voigt.
Electrolyte.	Λ_0.	Λ_0.	Λ_0.
$KMnO_4$	136·82	136·08	—
KCl	152·26	151·03	151·4577
NaCl	128·05	127·32	127·8405
KBr	153·26	152·92	—
NaBr	129·49	129·21	—
CH_3COONa.	89·46	† 90·05	91·3063

* Lorenz and Michael, *Z. anorg. Chem.* cxvi. p. 161 (1921).
† Lorenz and Osswald, *ibid.* cxiv. p. 209 (1920).
‡ Lorenz and Voigt, *ibid.* cxlv. p. 277 (1925).

It will be seen that the differences are very much greater than the experimental error involved in the determination of the conductivities. It is significant that although both the calculations of Lorenz and Michael and of Lorenz and Voigt are based on Hertz's theory, different values of Λ_0 are obtained. The results for sodium acetate are somewhat doubtful, as Lifschitz and Beck (*Helv. Chimica Acta*, 1919, ii. p. 133) appear to have exceeded the Λ_0 value here calculated at a dilution of 1024 litres. Mention may be made here of the fact that the results of Lifschitz and Beck are in agreement with the older observations of Ostwald and of Bredig.

The Effect of Temperature on the Constants B *and* n *in the Equation* $\Lambda_0 = \Lambda + BC^n$.

From the few results available it appears that the constant B varies irregularly with temperature while *n* appears to decrease with rise of temperature except in the case of potassium bromide and of sodium acetate.

Calculation of Mobilities at Infinite Dilution.

At 0° *C.*—The anion transport number of potassium chloride was taken as 0·505 (Walden, *Das Leitvermögen der Lösungen*, i. Teil, p. 236, 1924) and the values of the mobilities thereby computed are exhibited in Table VIII. below.

TABLE VIII.

Cation 0° C.		Anion 0° C.	
Ion.	$\Lambda_0 c^+$.	Ion.	$\Lambda_0 a^-$.
K^+	40·3	Cl^-	41·2
Na^+	25·5	NO_3^-	39·5
Li^+	17·8	IO_3^-	20·3
Cs^+	43·5	ClO_4^-	36·5
		Picrate$^-$ ...	14·7

At 18° *C.*—With the aid of the mobilities already calculated in Part I. (*loc. cit.*) Table IX. was constructed.

TABLE IX.

Cation 18° C.		Anion 18° C.	
Ion.	$\Lambda_0 c^+$.	Ion.	$\Lambda_0 a^-$.
$\frac{1}{2}Ra^{++}$	59·1	ClO_4^-	54·80
$\frac{1}{2}Zn^{++}$	46·01	CH_3COO^- ...	32·48
		Picrate$^-$	25·14

At 25° *C.*—Two methods were employed. The first depended on the assumption that the anion transport number of potassium chloride is 0·5030 (Noyes, J. Amer. Chem. Soc. 1912, xxxiv. p. 454). In the second method the mobility at infinite dilution of the permanganate at 25° was calculated from the mobilities at various concentrations experimentally determined by Lorenz and Neu (*Z. anorg. Chem. Soc.* 1921, cxvi. p. 45). It was found that an equation of the form $\mu_0=\mu+bC^d$, where μ is the mobility at concentration C, μ_0 the mobility at zero concentration, and b and d are constants, represents the relation between the mobility at the lowest measured concentration up to 0·005 N with an accuracy equal to that of the experimental data, and one can therefore extrapolate to zero concentration with some confidence. The results for the permanganate ion are presented in Table X.

Table X.

$$\mu_0=\mu+100{\cdot}83\ C^{0{\cdot}7578}.$$

C.	μ.	μ_0.
$5{\cdot}0\times10^{-4}$	60·91	61·23
$1{\cdot}0\times10^{-3}$	60·70	61·24
$2{\cdot}0\times10^{-3}$	60·31	61·22
$5{\cdot}0\times10^{-3}$	59·40	61·22
$1{\cdot}0\times10^{-2}$	58·35	(61·43)
Mean		61·23

Knowing μ_0 for the permanganate ion, the corresponding mobilities of the other ions can be easily calculated. In Table XI. are exhibited the values of μ_0 obtained by both methods, and it will be seen that the agreement is quite satisfactory. Attention must, however, be directed to the fact that the values of the mobilities here deduced differ from those calculated by other investigators: some results are given in Table XII. below.

Table XI.

μ.	*Method* 1.	*Method* 2.	*Mean.*
K^+	75·59	75·67	75·63
Na^+	51·38	51·46	51·42
Cl^-	76·67	76·59	76·63
Br^-	77·89	77·81	77·85
MnO_4^-	61·23	61·15	61·19

TABLE XII.

μ_0.	*Authors.*	*Lorenz and Michael.*	* *International Critical Tables.*
K^+	75·59	74·40	—
Na^+	51·38	50·69	—
Cl^-	76·67	76·63	75·10
Br^-	77·89	78·52	77·44
MnO_4^-	61·19	61·68	—

The values for the conductances at infinite dilution of the dichloracetate, trichloracetate, trichlorbutyrate, *ortho* nitrobenzoate, cyanacetate, 3 : 5 dinitrobenzoate and *ortho* chlorbenzoate deduced in Part I. (*loc. cit.*) are, the authors regret, subject to an error in calculation †; the corrected values are included in the complete table of mobilities given below.

TABLE XIII.

Cation 0° C.		Anion 0° C.	
Ion.	$\Lambda_0 c^+$.	Ion.	$\Lambda_0 a^-$.
K^+	40·3	Cl^-	41·2
Na^+	25·5	NO_3^-	39·5
Li^+	17·8	IO_3^-	20·3
Cs^+	43·5	ClO_4^-	36·5
		Picrate$^-$	14·7
Cation 18° C.		Anion 18° C.	
Ion.	$\Lambda_0 c^+$.	Ion.	$\Lambda_0 a^-$.
K^+	64·60	Cl^-	65·54
Na^+	43·48	NO_3^-	61·83
Li^+	33·53	IO_3^-	34·00
Tl^+	65·53	Br^-	67·70
Cs^+	67·53	I^-	66·06
Ag^+	54·36	F^-	46·77
$\frac{1}{2}Ca^{++}$	52·19	CNS^-	56·48
$\frac{1}{2}Sr^{++}$	51·66	ClO_3^-	54·97
$\frac{1}{2}Ba^{++}$	55·04	ClO_4^-	54·80
$\frac{1}{2}Ra^{++}$	59·1	CH_3COO^-	32·48
$\frac{1}{2}Pb^{++}$	61·61	Picrate$^-$	25·14
$\frac{1}{2}Mg^{++}$	45·78	$\frac{1}{2}SO_4^{--}$	68·25
$\frac{1}{2}Cd^{++}$	46·45	$\frac{1}{2}C_2O_4^{--}$	61·13
$\frac{1}{2}Zn^{++}$	46·01		
$\frac{1}{2}Cu^{++}$	45·91		

* Quoted by Bencowitz and Renshaw, J. Amer. Chem. Soc. xlviii. p. 2146 (1926).

† The mobility of the potassium ion at 18° was subtracted instead of that at 25°.

TABLE XIII. (*continued*).

Cation 25° C.		Anion 25° C.	
Ion.	$\Lambda_0 c^+$.	Ion.	$\Lambda_0 a^-$.
K^+	75·63	Cl^-	76·63
Na^+	51·42	Br^-	77·85
		MnO_4^-	61·19
		CH_3COO^-	38·04
		Dichloracetate$^-$	46·9
		Trichloracetate$^-$	43·4
		Trichlorbutyrate$^-$	30·9
		Ortho Nitrobenzoate$^-$	32·4
		Cyanacetate$^-$	41·5
		3 : 5 Dinitrobenzoate$^-$	28·3
		Ortho Chlorbenzoate$^-$	55·4

One of the authors (I. V.) wishes to thank the Trustees of the Dixon Fund for a grant with the aid of which part of the expenses of this investigation have been met.

East London College
(University of London).

The Imperial College of Science
and Technology, South Kensington.

XX. *The Loud-Speaker as a Source of Sound for Reverberation Work.*

To the Editors of the Philosophical Magazine.

GENTLEMEN,—

IN a letter published in the December, 1926, number of the Philosophical Magazine Mr. Hart criticises our recent paper* on "The Loud-Speaker as a Source of Sound for Reverberation Work," in so far as it concerns the question of Degradation of Acoustical Energy.

Such of our results as we considered reliable, namely, those obtained with the specially constructed condenser microphone, were consistent with the view that at a constant frequency the response of the microphone was proportional to the amplitude of the received sound, and that there was no viscous or similar degradation of sound energy between the loud-speaker and the microphone. Mr. Hart suggests

* Phil. Mag. ii. p. 51 (1926).

that degradation may have occurred, its effects being just counterbalanced by lack of proportionality in the response of the microphone. We do not regard this as probable. The width of air gap in our condenser transmitter is about 0·001 inch, and we estimate the maximum amplitude of vibration to be of the order of 0·000001 inch. We find it difficult to believe that with this type of instrument such small displacements could be so far outside the limits of proportionality as to obscure the considerable degradation effect which Mr. Hart appears to expect.

Moreover, Mallett and Dutton *, in experiments at frequencies above 400, kept the output from a source constant and, using a Rayleigh disk as measuring instrument, found the acoustic amplitudes at various distances from the source to obey the usual theory, there being no sign of "degradation."

These experiments relate to frequencies higher than that (100) for which Mr. Hart presents results, and this may explain to some extent why no appreciable degradation was noted. On the other hand, however, when we turn to Mr. Hart's paper †, we feel that the evidence is not altogether convincing. He states that, of the family of curves obtained: "only one, namely, that corresponding to a distance of 40 cms. from the source, can be drawn with certainty." He has drawn this curve and then calculated the curves which would be expected at other distances from the source if the inverse square law of sound intensity were obeyed. Mr. Hart found that "at the higher intensities the experimental points have a strong tendency to lie below these curves—*i. e.* to indicate unduly low intensities—for distances from the source greater than 40 cms." He concluded therefore that some of the sound energy has been lost from the fundamental frequencies in transmission between 40 cm. and the other distances at which readings were taken.

It appears to us, however, that a curve can be drawn with reasonable certainty through the experimental points obtained at a distance of 70 cm. from the source, and it has the advantage over the work at 40 cm. that results were recorded up to the highest activities at which the source was employed. Using this curve as basis, theoretical curves may be drawn for the various distances from the source by following Mr. Hart's procedure and using the microphone calibration revealed by Mr. Hart's own inverse square calculation. The experimental points then appear to us

* Journ. I. E. E. lxiii. pp. 502, 715 (1925).
† Roy. Soc. Proc. cv. p. 80 (1924).

to agree much more closely with these inverse square law curves, there being no regular deviation to suggest degradation.

In view of this position, therefore, we still feel we were justified in saying in our paper "it must be *assumed* that at this frequency, at any rate, there is no appreciable degradation."

Yours faithfully,

A. H. Davis,
N. Fleming.

March, 1927.

XXI. *The Calculation of Activity Coefficients from Conductivity Measurements.* *By* C. W. Davies, *M.Sc., University College of Wales, Aberystwyth* *.

THE object of this note is to show that the careful measurement of the conductivities of weak electrolytes provides a valuable means of studying the activity coefficients of ions.

If strong electrolytes may be regarded as completely dissociated in dilute solutions, the diminution in equivalent conductivity that they show with increase in concentration is entirely due to changes in the mobilities of the ions ; and in dilute solutions of a weak electrolyte the mobilities of the ions will be expected to show quite similar changes with respect to the total ionic concentration. The true degree of dissociation of a weak electrolyte, at concentration C, will then be given by the ratio Λ/Λ_x, where Λ_x is the sum of the mobilities of cation and anion at ion-concentration $\Lambda/\Lambda_x . C$. This leads to the revised form of the dilution law :

$$\frac{\Lambda^2 . C . f_c . f_a}{\Lambda_x . (\Lambda_x - \Lambda) . f_u} = K, \quad . \quad . \quad . \quad . \quad . \quad (1)$$

where f_c, f_a, are the activity coefficients of cation and anion respectively, and f_u—the activity coefficient of the undissociated molecules—probably does not differ materially from one in dilute solutions.

In a previous paper † this equation was tested for several organic acids. In the absence of activity data for these acids the activities were calculated by an approximate formula which is not strictly true. More recently the same

* Communicated by the Author.
† J. Phys. Chem. xxix. p. 977 (1925).

equation has been put forward by Sherrill and Noyes * and by MacInnes †, who, however, employed the Debye and Hückel expression ‡ :

$$\log \gamma = -0{\cdot}5 \sqrt{C_i},$$

for computing the activity coefficients, where $\gamma = \sqrt{f_c \cdot f_a}$, and C_i is the ion-concentration.

Both these methods of calculating activity coefficients may introduce considerable errors §, and moreover are unnecessary ; for if accurate conductivity data are available the ratio :

$$\frac{\Lambda^2 \cdot C}{\Lambda_x \cdot (\Lambda_x - \Lambda)} = \frac{K}{f_c \cdot f_a} = K' \quad . \quad . \quad . \quad . \quad (2)$$

can be calculated, and will normally be found to increase regularly with increasing concentration. Now for all electrolytes hitherto investigated the mean activity coefficient and the concentration are connected by the limiting law :

$$\log \gamma = -A \sqrt{C_i}, \quad . \quad . \quad . \quad . \quad . \quad (3)$$

which holds to an ion-concentration of 0·01 N.

From (2) and (3) it follows that

$$\log K' - \log K = 2A \sqrt{C_i}, \quad . \quad . \quad . \quad . \quad (4)$$

so that by plotting $\log K'$ against $\sqrt{C_i}$ a straight line is obtained whose slope determines the constant A, and which can be produced to evaluate K, the true dissociation constant. Furthermore, regular deviations from a straight line are found to serve as sensitive indications of abnormal behaviour on the part of the solute.

The value of Λ_x may either (*a*) be calculated from the empirical formula ‖ :

$$\Lambda_x = \Lambda_\infty - K : \sqrt{C_i} \cdot (\sqrt{\Lambda^{\cdot}_\infty} + \sqrt{\Lambda'_\infty}),$$

where $\Lambda^{\cdot}_\infty$, Λ'_∞ are the mobilities of cation and anion ; or, (*b*), if the data are available, the method of Sherrill and

* J. Amer. Chem. Soc. vol. xlviii. p. 1861 (1926).

† *Ibid.* p. 2068 (1926).

‡ *Physik. Zeit.* vol. xxiv. p. 185 (1923).

§ The value of the constant is 0·39, not 0·5, for HCl (Randall and Vanselow, J. Amer. Chem Soc. vol. xlvi. p. 2435 (1924) ; Nonhebel, Phil. Mag. [7] ii. p. 1085 (1926)).

‖ J. Phys. Chem. xxix. p. 473 (1925). The value of K is 5·24 at 18° C. A rough estimate of the effect of temperature on K gave the value 5·61 at 25°, but the figure K = 5·74 at 25° is now adopted. This is based on the actual measurements at 25° of Lorenz, Osswald and Michael (*Z. anory. Chem.* vol. cxiv. p. 209 ; vol. cxvi. p. 161) and of Parker (J. Amer. Chem. Soc. vol. xlv. p. 2017, 1923).

Noyes and of MacInnes can be used. This depends on the principle that the conductivities of strong electrolytes are additive in dilute solutions so that, for example, Λ_x for acetic acid at the ionic concentration 0·001 is given by $\Lambda_{\cdot 001\ HCl} + \Lambda_{\cdot 001\ NaAc} - \Lambda_{\cdot 001\ NaCl}$.

The latter method has the greater range, for conductivities can be regarded as additive up to a concentration of 0·01 N,

Fig. 1.

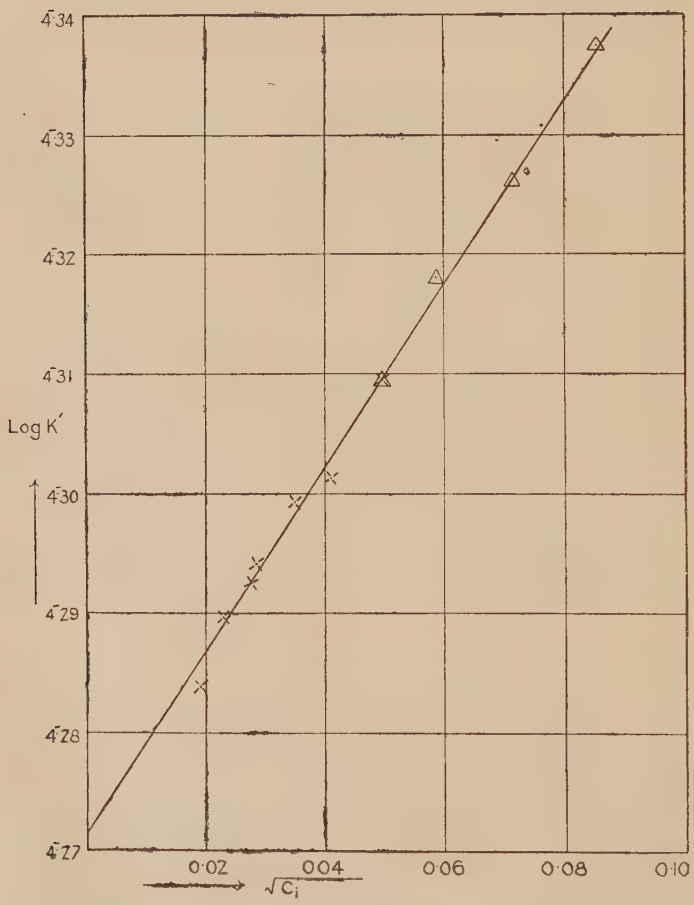

whereas the former method only applies to the range C = 0 to C = 0·002 : within which, of course, both methods should, and do, lead to the same result.

Application to existing data.

There are available only a few series of conductivity measurements with weak electrolytes which claim any great accuracy. Auerbach and Zeglin* have measured sodium formate and formic acid at 18°, and their results yield the data plotted in fig. 1. Triangles are used to show the points obtained by using method (*b*) described above, for calculating Λ_x. The remaining points were obtained by method (*a*), the value $\Lambda_\infty = 363{\cdot}5$ being taken for formic acid. The two methods give values in complete agreement, and it is evident that the curve enables the constant A to be evaluated with considerable precision.

The data used are given in Table I., which shows the value of A obtained from the curve, and the values of K, the true dissociation constant, which are obtained when this value of A is introduced into equation (4). Had "A" been given the Debye-Hückel value, K would have shown a regular trend from $0{\cdot}1785 \,.\, 10^{-4}$ in the most concentrated solution to $0{\cdot}1848 \,.\, 10^{-4}$.

Table I.

Formic acid at 18°. A = 0·383.

C.	Λ.	K . 10^3.
0·2534	10·16	0·1869
·1266	14·20	·1868
·06022	20·31	·1875
·03208	27·36	·1868
·01595	37·93	·1861
·008809	50·07	·1872
·004161	70·21	·1872
·003855	72·51	·1866
·001923	97·92	·1871
·001052	124·9	·1859

The only other suitable data on which much reliance can be placed are those of Kendall †. The results obtained fron these are summarized in Table II. ‡

* *Z. phys. Chem.* vol. ciii. p. 191 (1922).

† J. Chem. Soc. vol. ci. p. 1285 (1912).

‡ In compiling this table the values of K′ calculated by MacInnes (*loc. cit.*) were used.

TABLE II.

Cyanoacetic acid at 25°. A = 0·372.

C.	Λ.	K . 10^3.
0·05946	88·0	·3541
0·02972	117·0	·3561
0·01487	152·5	·3556
0·007435	193·9	·3557
0·003716	238·7	·3562
0·001858	282·6	·3578
0·0009290	320·0	·359
0·0004645	347·1	·350

o-Nitrobenzoic acid at 25°. A = 0·381.

C.	Λ.	K . 10^2.
0·03125	139·7	·6039
0·01562	179·0	·6095
0·007812	221·9	·6096
0·003906	265·0	·6094
0·001953	303·6	·615
0·0009765	333·5	·603

o-Chlorobenzoic acid at 25°. A = 0·351.

C.	Λ.	K . 10^2.
0·006662	134·6	·1230
0·003331	174·0	·1237
0·001666	218·0	·1236
0·0008327	262·6	·1234

3·5-Dinitrobenzoic acid at 25° A = 0·440.

C.	Λ.	K . 10^2.
0·003929	175·7	·1508
0·001965	219·0	·1505
0·0009824	262·7	·1508
0·0004912	301·5	·151

At concentrations below 0·001 N most conductivity measurements with acids are unreliable, owing, probably, to the use of glass cells *. At the higher concentrations, too, irregularities may be expected, since with increasing viscosity of the solution Λ/Λ_x no longer represents the true degree of dissociation. The effect of both these factors can be seen in Table II., but there is an intermediate region in which A can be determined accurately. Where few measurements have been made within this region, as in the case of dinitrobenzoic acid, less reliance can be placed on the result.

Finally, the data of Kendall for acetic acid are shown in Table III. In this case the uncorrected data fail to give a constant value for A, but if Λ is replaced by the "viscosity corrected" value, $\Lambda \cdot \eta/\eta_0$, a linear curve is obtained in this case also, and A has the value 0·393. The reason for the great importance of the viscosity correction in this case is, of course, that acetic acid is very much weaker than the other acids considered ; so that a much greater change in total concentration—and consequently in viscosity— accompanies a given change in ion concentration.

* Kraus and Parker, J. Amer. Chem. Soc. vol. xliv. p. 2429 (1922).

TABLE III.

Acetic acid at 25°. A = 0·393.

C	0·07369	0·03685	0·01842	0·009212	0·004608	0·002303
Λ	6·086	8·591	12·091	16·98	23·81	33·22
[K . 10^4].	·1756	·1768	·1778	·1778	·1784	·1788
Λ . η/η_0...	6·138	8·628	12·12	17·00	23·82	33·22
K . 10^4 ...	·1784	·1786	·1782	·1784	·1785	·1788

The method has also been applied to some of the earlier data of Ostwald, Bethmann and Ebersbach *, but with these the points obtained were so scattered as to indicate little except that the acids probably show normal behaviour. Schaller † has measured the conductivity of o-Nitrobenzoic acid between 25° and 90° C. Between these temperatures Λ_∞ increases from 382 to 708, and K decreases from 0·0061 to 0·0014. "A" was found to change from 0·5 at 25° to 0·7 at 90°, but this variation is almost covered by the probable error. According to the theories of Milner ‡ and of Debye and Hückel, the increase in A should be about 12 per cent.

Conclusions.

For the acids considered, the constant A varies from 0·35 to 0·44, but until further data are obtained it is impossible to say whether this variability is real. The most reliable series of measurements give: Formic acid, 0·382; Acetic acid, 0·393; Cyanoacetic acid, 0·372: and having regard to the possible sources of error the value $A = 0·38 \pm ·01$ may be accepted for all the acids investigated.

With this may be compared the value for Hydrochloric acid. Randall and Vanselow find 0·393 from freezing-point measurements; Nonhebel gives 0·39 as the most probable value yielded by E.M.F. measurements at 25°. The divergence of this figure from that required by Debye and Hückel's theory—0·5—is considerable, and Nonhebel has pointed out that it lends support to the Milner theory which requires the value 0·37.

The results obtained in this paper afford further evidence for this view. They may, however, be interpreted in another way, if A is considered not to be constant for all electrolytes but to depend upon the nature of the ions involved. Then

* Kohlrausch-Holborn, 'Leitvermögen der Elektrolyte.'

† *Z. phys. Chem.* vol. xxv. p. 515 (1898).

‡ Phil. Mag. xxiii. p. 551 (1912).

the fact that for these acids A has almost constant values, and ones that are lower than those usually accepted for the uni-univalent salts, will be attributed to the influence of the hydrogen ion which is common to them all and which may show an especially small decrease in activity coefficient with rising concentration.

The Edward Davies Chemical
Laboratories, Aberysthwyth.
April 3, 1927.

XXII. *Notices respecting New Books.*

Atoms and Molecules. By R. M. Caven, D.Sc. (London), F.I.C. (Blackie & Son Ltd. London & Glasgow. 7*s.*)

THIS work by Prof. Caven of Glasgow provides a very suitable introduction for first and second year students to the modern theories of Atomic Physics. It begins with an outline of the older Atomic and Molecular theories, and with the older views of valency and chemical constitution. A brief account of the classification of the elements is also given.

After this review of the classical ideas Prof. Caven goes on to give an introduction to the modern ideas of Atomic Physics, and an important chapter is devoted to the Colloidal State.

The treatment in the volume under review is necessarily rather slight, but it can be recommended as providing a satisfactory introduction for the University student.

The Absolute Differential Calculus. By T. Levi-Civita. (Blackie & Son. Price 21*s.*)

The present volume contains a complete translation from the Italian text of Levi-Civita's important work issued in Rome in 1925. It also contains two new chapters which are concerned with the fundamental principles of Einstein's General Theory of Relativity—including, as a limiting case, the so-called Special or Restricted Theory—as an application of the Absolute Calculus.

In this work Levi-Civita has taken the classical laws of mechanics as the starting-point, and he then investigates inductively all the modifications which must be introduced in order to take account of Einstein's ideas. This method is, of course, diametrically opposed to the procedure followed by many writers, who enunciate the postulates of mechanics in tensor form. But the method in this work has its own advantages.

The present work can be heartily recommended and will undoubtedly be very valuable indeed to the large number of students of Relativity who have not been able to read the work

in the original, and the translator, Miss Marjorie Long, formerly Scholar of Girton College, Cambridge, is to be congratulated on the excellence of the translation.

A Concise Geometrical Conics. By C. V. Durell. (Macmillan & Co. Price 4*s.*)

The present book contains the companion volume to Mr. Durell's volume on Projective Geometry, and it will, no doubt, turn out to be equally useful. It is a feature of the book that a large number of examples and riders have been included, and it will be very valuable to the teacher to have sufficient riders of a more difficult character to draw upon. It is also convenient that Mr. Durell has included alternative methods of proof (by means of projection) of certain theorems in an appendix.

XXIII. *Proceedings of Learned Societies.*

GEOLOGICAL SOCIETY.

[Continued from vol. iii. p. 1350.]

March 23rd, 1927.—Dr. F. A. Bather, M.A., F.R.S., President, in the Chair.

THE following communication was read:—

'The Stratigraphy and Geological Structure of the Cambrian Area of Comley (Shropshire).' By Edgar Sterling Cobbold, F.G.S.

The object of this paper is to place on record the exact positions of the excavations made by the author since 1906, and to describe the stratigraphy and tectonics as revealed by them and by the surface-features.

After a shortened historical account of research the author gives an index-list of the excavations, references to their positions, to the appropriate Reports made to the British Association for the Advancement of Science, and to the faunal horizons seen at each spot. Notes upon some recent excavations and field-work are appended.

Under the heading of stratigraphy, he discusses the sequence and general lithographical characters of the horizons as previously defined, Q. J. G. S. vol. lxxvi (1920) p. 326.

Under the heading of tectonics, evidence is adduced to show that the folding and faulting of the Cambrian fall naturally into four groups: (1) post-Mesonacidian and pre-Paradoxidean,

general direction unknown; (2) post-Paradoxidean and pre-Caradocian, general direction north-north-west to south-south-east; (3) post-Caradocian and pre-Silurian, general direction north-east to south-west, all the result of compressive forces; and (4) post-Silurian, tensional stresses responsible for the Church Stretton Fault. Certain faults affecting the Cambrian are traced up to the Caradocian, but do not affect its outcrop; others affect the Cambrian profoundly, but show slight signs of posthumous movement in post-Ordovician times; and yet others are seen which are regarded as due to the post-Silurian tension.

The facts detailed in the paper enable us to form a fairly consecutive series of views of the deposition and deformation of the Comley Cambrian deposits. These are briefly summarized under fourteen or fifteen headings, and indicate seven diastrophic phases of various intensities. As Prof. Charles Lapworth once said of the bottom of the Cambrian Sea, 'it kept coming up again'.

Special attention is given to the complicated Dairy Hill portion of the area, where recent study and some fresh excavation in 1926 have fully substantiated the inference previously drawn from the Comley Breccia-Bed, that a peak or promontory of Lower Cambrian sandstone remained above water during the accumulations of some 300 feet or more of strata of the *Paradoxides-groomi* Zone.

The paper is illustrated by a geological map of the area on the 6-inch scale, a reproduction of the Dairy Hill portion on the 25-inch scale, an ideal section of the *Paradoxides* Beds while still horizontal, and a sheet of six parallel sections across the area.

April 6th.—Dr. F. A. Bather, M.A., F.R.S., President, in the Chair.

The following communication was read:—

'The Kateruk Series and Associated Rocks of the Northern Suk Hills (Kenya Colony).' By Vincent G. Glenday, M.A., F.G.S., and John Parkinson, M.A., Sc.D., F.G.S.

The paper describes a series of completely metamorphosed sediments which crop out on or near the Kateruk River, an eastward-flowing tributary of the Turkwal River, situated about 35° 15′ long. E. and 2° 37′ lat. N., in the north-western part of Kenya Colony. The rocks consist of the metamorphosed representatives of various sedimentary deposits, ashes being included. The constituents indicate a somewhat lower grade of metamorphism than those of the Turoka Series of the south, and it is considered that, although closely related to the latter, the Kateruk Series may eventually prove to be slightly younger. Gabbros, considerably altered, are intrusive in these rocks, and are believed to pass into certain hornblende-schists. On the other hand, some of the latter are thought to be ashes.

April 27th.—Dr. F. A. Bather, M.A., F.R.S., President, in the Chair.

The following communication was read:—

'The Serpentines of the Shetland Islands, and the Associated Rocks and Minerals.' By Frank Coles Phillips, M.A.

The Shetland Islands consist mainly of a series of schists and paragneisses, with a strike over the greater part of the area of about north 10° east, and a steep westward dip. Around the eastern and western margins of Mainland occur patches of Old Red Sandstone sediments, and in the north an extensive development of igneous products of that age. A series of older intrusions, ranging from ultrabasic to acid, is found among the metamorphic rocks.

The most basic of these earlier intrusions, chiefly developed in the northernmost islands of Unst and Fetlar, was a dunite, now almost entirely serpentinized. This is found mainly around the western and northern margins of the Unst intrusion, and is succeeded on the east by varieties containing rhombic pyroxene and by peridotite. A constant accessory in these rocks is a chrome-spinel, and in places this becomes concentrated as workable deposits of chromite. The ores are of two main types: banded chromite-serpentine and lenticles of massive chromite-rock. Investigation of thin slices shows that the chromite was the earliest-separated constituent from the magma, followed by the silicates, crystallization being in part contemporaneous. The present distribution of the deposits is the result of partial attainment of concentration by aggregation and sinking, complicated by later crushing and faulting. The serpentine is intersected by veins of pyroxenite, largely converted to antigoritic serpentine.

The gabbro, succeeding on the east, is extensively altered, the original pyroxene being uralitized and the felspar converted to a saussuritic aggregate. In Balta and Huney the gabbro is cut by veins of pegmatoid gabbro and albite-zoisite-rock. These changes of serpentinization, uralitization, and saussuritization are referred to autometamorphism effected by late-magmatic juvenile water.

Later mineralogical and chemical changes have been brought about by dynamic metamorphism and low-temperature weathering. Extensive carbonation has given rise to segregation-veins of magnesia-lime-iron carbonates, often in well-developed crystals. Talcose schists, the Shetland 'soapstones', are typical products of dynamic metamorphism, the talc being accompanied by magnesian carbonates, representing the excess of magnesia over silica in the original ultrabasic rock compared with that required for the formation of talc. Kämmererite and uvarovite may owe their origin to hydrothermal action; an anthophyllite-schist has been formed, apparently with the introduction of silica. Chrysotile and hornblende-asbestos occur in veins.

May 25th.—Dr. F. A. Bather, M.A., F.R.S., President.

President, in the Chair.

The following communication was read :—

'The Old Red Sandstone of the Bristol District.' By Frederick Stretton Wallis, M.Sc., Ph.D., F.G.S.

The Old Red Sandstone sediments in the immediate neighbourhood of Bristol have been examined and the results recorded from stratigraphical, petrographical, and palæontological standpoints.

Although the total thickness of these deposits is now estimated at 3000 feet, the faunal contents give evidence of the presence of beds of Upper Old Red Sandstone age only, and no apparent unconformity in the strata or mineralogical break has been detected.

Every gradation of deposit between the following types can be found :—Coarse- and fine-grained sandstones, conglomeratic sandstones, siltstones, quartzites, cornstones, pure limestones, and conglomerates. True marls and shales are absent.

It is shown that the material was derived from a pre-Cambrian massif consisting of gneisses, mica- and quartz-schists with abundant quartz augen and volcanic or intrusive rocks, together with a sedimentary series of arenaceous and calcareous (largely silicified) types.

This source was situated north-west of Bristol, and its rocks are shown to have been similar in character to those of the Mona Complex, and especially to the Gwna Beds of that formation. It is not, however, necessary to postulate that the material came from 'Anglesey' of the present day. Unfortunately, we do not know even the approximate dimensions of the original complex, and the material may have come from some part of it exposed in Old Red Sandstone times, but now covered by later deposits.

The sediments were transported by a great river, which, flowing through a country affected by heavy seasonal or spasmodic rainfalls, finally reached the sea by a broad delta in the neighbourhood of the Bristol district. Lagoons also formed important physiographical features near the coast.

June 15th.—Dr. F. A. Bather, M.A., F.R.S., President, in the Chair.

The following communications were read:—

1. 'The Structural Relations of the Mourne Granites (Ireland).' By James Ernest Richey, M.C., B.A., F.R.S.E., F.G.S.

The Mourne Mountains are some 13 miles long by about 5 miles wide, and include many peaks of more than 2000 feet in height. The granite-massif of inferred Tertiary age is intruded into Silurian shales, and truncates a north-westerly basic dyke-swarm, of which fact Sir Richard Griffiths was aware in 1835.

The massif is found to consist of at least four distinct intrusions, composed of different granite varieties. The granites all have well-marked, fine-grained intrusive margins, whether in contact with shales or with older granite. Three of these granites form the eastern half of the massif, while the fourth occurs on the west. Eastern and western portions are in contact, but only for about 2 miles, so that the massif as a whole is of hour-glass shape. Exposures are usually good, except where the eastern and western portions join. There is, however, some evidence of the Western Granite being later than the others.

The Western Granite, as shown by the Geological Survey mapping, carried out by Traill in 1870–73, extends outwards on all sides below a slightly domed roof of shales, cappings of which rest upon the granite.

The Eastern Granites are deeply eroded enough to show bounding walls as well as roofs. Floors are nowhere seen. These Eastern Granites are arranged one within the other, with a marked excentricity towards one side. The outermost granite is the oldest, the innermost the youngest. Relations between the individual roofs and walls are remarkably similar. In each case, a slightly dome-shaped roof turns abruptly into a wall, which is either vertical or steeply inclined outwards. The forms of the granites, so far as seen at the present denudation-levels, are therefore essentially steep-sided, truncated cones, or cylinders, with slightly dome-shaped tops.

Features observed by Traill are that granite-margins transgress the bedding of the Silurian shales, and that the direction of the dip of the shales is unaffected by the intrusion of the granites. The absence of xenoliths, except at actual margins, and the plane surfaces of contacts, are other noteworthy features. The country-rocks have not been pushed to one side, or upwards, as in laccolithic intrusion, nor does overhead stoping appear to have played any part, at least at the present level of observation. It is inferred that the spaces occupied by the various granites have been provided by subterranean cauldron-subsidence of the pre-existing rocks. The intrusion of the Eastern Granites successively one within the other may be then explained by assuming renewed subsidence of the first-subsided block.

2. 'The Stratigraphy of the Valentian Rocks of Shropshire: the Main Outcrop.' By Walter Frederick Whittard, Ph.D., B.Sc., D.I.C., F.G.S.

The Valentian rocks of Shropshire are found in three disconnected outcrops, namely:—

(i) the Main Outcrop,
(ii) the Longmynd-Shelve Outcrop,
(iii) the Breidden Outcrop.

It is the first of these that is described in this paper.

The threefold classification of Salter & Aveline has been adopted,

but their nomenclature has been modified: the rocks are subdivided as follows:—

	Thickness in feet.
(3) Purple Shales	0–400
(2) *Pentamerus* Beds	0–500
(1) Arenaceous Beds	0–200

The Arenaceous Beds extend from near Cardington north-eastwards to the Wrekin, and they consist essentially of conglomerates, grits, and sandstones. Evidence is given for a southerly derivation of the pebbles comprising these beds, and a north-easterly longshore drift is postulated. The Arenaceous Beds attain their maximum development in the Kenley, Church Preen district, and there is reason to suppose that they were partly deposited in an embayment limited by these localities.

The *Pentamerus* Beds are well exposed in several dingles, and detailed descriptions are given of those sections from which graptolites have been collected. The presence of a conglomerate which is restricted to the Wrekin area indicates that the Uriconian rocks were probably exposed here at this time.

The Purple Shales consist almost entirely of purple, maroon, or green mudstones or shales; shelly limestones and calcareous sandstones occur irrespective of horizon. The Onny section is described in detail, and faunal evidence is produced to show that only Purple Shales are exposed in the river-bank. A thin calcareous conglomerate has yielded fossils characteristic of three faunas, of which the Purple Shales fauna alone is indigenous.

The age of the Buildwas Beds is given as the Zone of *Cyrtograptus murchisoni*, a conclusion based on a graptolite assemblage obtained from the Onny River.

The Valentian rocks are displaced by a series of dip-faults, but no folding, other than that caused by slip, has been detected. The unconformable relation of the Silurian rocks to older sediments is fully described, and it is suggested that post-Silurian movements have occurred along the Severn Valley at the region where it is crossed by the Silurian outcrop.

Evidence based on field-data is produced which suggests that the Valentian rocks of the main outcrop were deposited in partly isolated or protected waters.

The few graptolites so far obtained show that only Upper Valentian rocks are exposed; there is no evidence of beds younger than the Zone of *Monograptus crispus*, and most probably the higher zones of the Gala were overlapped by the Wenlock Shales. The rocks of the main outcrop are correlated with the Woolhope and May Hill successions, in which only the highest Valentian rocks are developed.

[*The Editors do not hold themselves responsible for the views expressed by their correspondents.*]

Fig. 2.

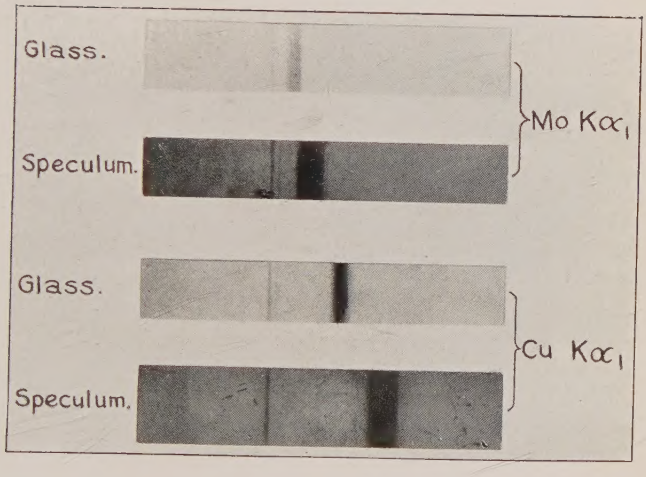

FIG. 1.

FIG. 3.

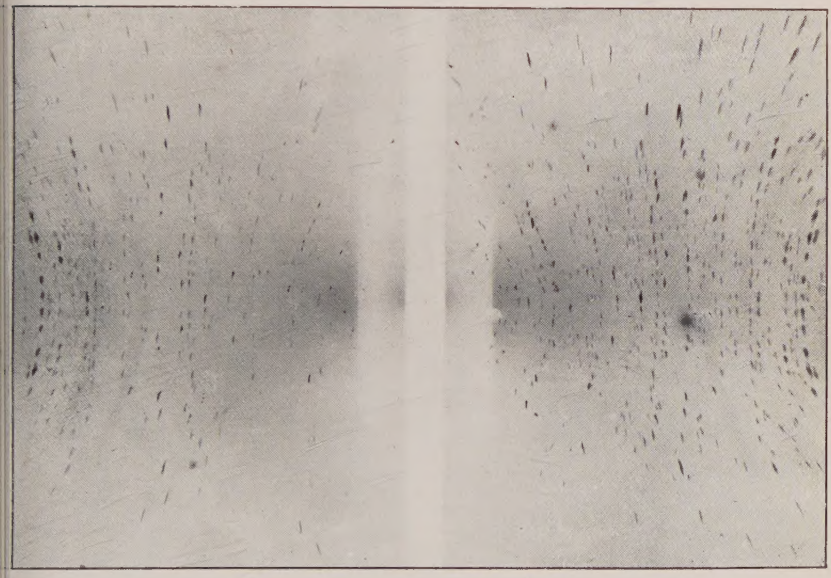

FIG. 4.